

Electronic Thesis and Dissertation Repository

---

4-18-2023 11:30 AM

## Genetic Tools Towards A Synthetic Biology Approach For Whole Mitochondrial Genome Engineering

Ryan R. Cochrane, *Western University*

Supervisor: Karas, Bogumil J., *The University of Western Ontario*

Co-Supervisor: Edgell, David R., *The University of Western Ontario*

A thesis submitted in partial fulfillment of the requirements for the Doctor of Philosophy degree in Biochemistry

© Ryan R. Cochrane 2023

Follow this and additional works at: <https://ir.lib.uwo.ca/etd>



Part of the [Biotechnology Commons](#)

---

### Recommended Citation

Cochrane, Ryan R., "Genetic Tools Towards A Synthetic Biology Approach For Whole Mitochondrial Genome Engineering" (2023). *Electronic Thesis and Dissertation Repository*. 9294.  
<https://ir.lib.uwo.ca/etd/9294>

This Dissertation/Thesis is brought to you for free and open access by Scholarship@Western. It has been accepted for inclusion in Electronic Thesis and Dissertation Repository by an authorized administrator of Scholarship@Western. For more information, please contact [wlsadmin@uwo.ca](mailto:wlsadmin@uwo.ca).

## Abstract

Synthetic biology is an interdisciplinary research field that standardizes and repurposes biological components to better understand life, solve complex problems and produce superlative organisms for industry. As synthetic biology has developed, the goal has become to generate fully controllable systems through whole genome engineering (WGE), the cumulation of standardized genome engineering protocols, and DNA delivery methods. In eukaryotes, genetic tools for WGE are limited to the nucleus and present a need to expand to include mitochondria, which maintain their own unique genome and produce energy for the cell. The work presented here begins developing the resources needed to enable whole mitochondrial genome engineering.

First, to standardize mitochondrial genome engineering protocols, I cloned the mitochondrial genomes of two diatomaceous algae, *Phaeodactylum tricornutum* and *Thalassiosira pseudonana*, as plasmids in *Escherichia coli* and *Saccharomyces cerevisiae* using PCR-based and transformation-associated recombination cloning methods. Next, a PCR-based engineering method was optimized to generate derivative algal mitochondrial genomes cheaper than the cost of DNA synthesis in approximately ten days. Additionally, minimal host burden and plasmid instability was detected for the mitochondrial plasmids making them suitable cargo for delivery experiments.

After, I sought to adapt an entirely *in vivo* DNA delivery method, bacterial conjugation, for mitochondrial transformation. Two approaches have been envisioned for bacterial conjugation to mitochondria, cell fusion of a bacteria containing a mitochondrial plasmid followed by intra-cellular bacterial conjugation, and engineering key conjugative proteins with the addition of a mitochondrial localization signal. In either scenario, DNA transfer rates will likely decrease beyond the rate of detection. Therefore, I first looked to improve DNA transfer to eukaryotes by generating and screening a deletion plasmid library for the broad-host range conjugative plasmid, pTA-Mob 2.0. From this data, pSC5 was created that improved DNA delivery to yeast. The utility of pSC5's superior DNA delivery was demonstrated by creating the pSC5-toxic plasmids, which contained genes toxic or partially toxic to yeast. The pSC5-toxic plasmids effectively killed yeast and established a

novel first-in-the-world conjugation-based antifungal. Together these resources for mitochondrial genome engineering and improved DNA delivery should improve the feasibility of future endeavors in whole mitochondrial genome engineering.

**Keywords:** *Phaeodactylum tricornutum*, *Thalassiosira pseudonana*, *Metschnikowia*, *Candida*, yeast, algae, bacterial conjugation, antifungal, mitochondrial plasmid, mitochondrial genome engineering

## Lay Summary

Cells can be viewed as microscopic machines, such as a computer. Like a software program, their DNA encodes instructions, which the operating system interprets as commands based on various inputs, similar to a cell sensing its environment. A cell's complete set of instructions is referred to as a genome, and scientists can modify genomes to alter how and what the cell does, including producing medicines or storing carbon, for instance. However, with current technologies in most cells, typically, only a few edits to a genome can be made at a time, making the process tedious and labor-intensive.

Recently, technologies that enable researchers to modify entire genomes simultaneously have become available. These technologies are referred to in their entirety as whole genome engineering (WGE). WGE is accomplished by writing a new desired genome and building it from scratch using chemical methods called DNA synthesis. The synthetic genome's instructions are verified and then delivered into a cell lacking DNA. These technologies have been developed for relatively simple bacteria; however, more complex cells lack WGE methods and can each contain 1–3 different genomes that could be modified. The main limiting factors are an absence of standardized methods for modifying entire genomes of more complex cell types and difficulties delivering them where they need to go.

This thesis develops foundational technologies required to enable future WGE of the genome located within a cellular compartment called the mitochondria, widely known for its role in energy production. Specifically, I developed standardized methods for modifying mitochondrial genomes in approximately ten days at a fraction of the cost of DNA synthesis. After, I sought to improve DNA delivery to complex cells using a method called bacterial conjugation. I improved this DNA delivery method to fungi 23-fold and showed it could be used as an antifungal. Future research should attempt to adapt this DNA delivery method's specificity in complex cells, from indiscriminate DNA delivery anywhere inside the cell to specifically their mitochondrial compartment. Now, WGE of mitochondria requires developing innovative ways to identify what cells have successfully received a genome and deciding what to make them do.

## Co-Authorship Statement

For the work presented in Chapters 2–4, R. R. Cochrane and B. J. Karas conceived the experiments. R. R. Cochrane performed the experiments, and R. R. Cochrane and B. J. Karas analyzed the results. R. R. Cochrane created the figures and wrote the manuscripts with input from B. J. Karas. Exceptions and additional contributions for each Chapter are noted below.

In regard to Chapter 2:

S. Hamadache performed analysis of sequencing data used in Table 2-2 and Supplementary Table B-2, and created plasmid maps used in Figure 2-2A). M. P. M. Soltysiak assembled and screened the plasmids pPT-PCR C2-1 and C2-2 used in Figure 2-2 C, D), and Tables 2-1 and 2-2. S. L. Brumwell performed growth experiments, analyzed data, and created figures for Figure 2-3C, D). P. Janakirama of Designer Microbes Inc. assembled the plasmids pPT-PCR C1 and C2.

In regard to Chapter 3:

S. Hamadache performed analysis of sequencing data and generated Table 3-2 and Supplementary Table C-2, and created plasmid maps used in Figures 3-1A, B), 3-4 A, C), and Supplementary Figure C-2. S. L. Brumwell performed growth experiments, analyzed data, and created Figure 3-2. A. Shrestha analyzed data and created Figure 3-3, and performed RNA extraction for Supplementary Tables C-3 and C-4. D. J. Giguere generated and analyzed the RNA sequencing data in Supplementary Tables C-3 and C-4.

In regard to Chapter 4:

R. S. Shapiro contributed to conception of experiments involving *Candida* species and assisted in the writing of the manuscript. M. A. Lachance provided yeast strains listed in Section 4.4.2. B. J. Karas created the graphics of Figures 4-1, 4-3, 4-4A), 4-6A), 4-7A). S. L. Brumwell created the plasmids pAGE1.0, pAGE2.0.T, and pAGE2.0-i listed in Table 4-1. H. H. Say sequenced all previously unpublished plasmids listed in Table 4-1. A. Shrestha performed, analyzed data, and created Figures 4-2, 4-4 B) (Note: for *E. coli*, data analysis only), 4-5, and 4-7, and Supplementary Figures D-3, D-4, D-6, and D-7; and created Supplementary Tables D-2, D-5, D-6, and D-10. C. Tong assisted in the generation of data

for Figures 4-2, 4-4B), 4-5B, C), and 4-7, Supplementary Figures D-6 and D-7, and Supplementary Tables D-3, D-5, D-6, and D-10. K. Van Belois assisted in the generation of data for Figures 4-2 and 4-7, and Supplementary Table D-3. E. J. L. Walker generated the data for Figure 4-3, and designed, built, and screened pSC5-toxic2. J. S. Meaney performed *E. coli*-to-*E. coli* bacterial conjugation for Figure 4-4B), and Supplementary Table D-5. M. Agyare-Tabbi performed and analyzed data pertaining to the bacterial conjugation of plasmids to *Candida* species and created figures for Figure 4-5A), and Supplementary Figure D-4. D. P. Nucifora designed, built, and screened pSC5-toxic1. M. M. S. De Almeida created and screened many plasmids of Supplemental Table D-3. S. Hamadache performed analysis of sequencing data M3C1 and M3C2 only, and generated Supplementary Table D-4.

## Dedication

This thesis is dedicated to my parents Joseph Bruce Cochrane and Gail Allen whose logical worldview, relentless work ethic and self-sacrifice have offered me every opportunity to succeed in life. You have cultivated an unshakeable self-confidence in my mind and heart that anything is achievable with discipline and kindness. Thank you.

“Quit, don’t quit... Noodles, don’t noodles... You are too concerned with what was and what will be. There is a saying: Yesterday is history, tomorrow is a mystery, but **today is a gift.** That is why it is called the present.”

— Grand Master Oogway

## Acknowledgments

**My family.** As a mischievous child, too clever and bored for his own good, the old adage, “... it takes a village,” could not be more accurate. A massive thank you to all the kin who raised me, “... by valor and exertion” – Cochrane Clan. A special thanks to aunts Cindy Cochrane, Meg Keller, Nancy Allen, Lana Allen, and Connie Popov, and uncles Scott Keller, Robert Cochrane, Bill Cochrane, Roy Allen, and Bobby Allen. You all shaped my character and nurtured my resolve. My cousins and lifelong best friends, Mason Ross, Corey Keller, and Cole Bullas, I could not have asked for better role models. Mason, in hardship, I have never met such a kindhearted person. Thank you for keeping me soft and compassionate. Lara Cochrane, my sister, you are among the most intelligent humans I have ever met. Your inner strength and perseverance are a constant source of inspiration for me to keep going. I love you always, and your existence blesses the world. Ben, Gabriele, and Peter Hanke, you adopted me long before graduate school. Thank you for understanding how badly I needed to succeed. Your encouragement often restored my tired spirits! Becky Hanke, I could not have done this without you, you have gotten me through my weakest moments, and dreams of our future have pushed me forward. Your love for life, eye for beauty, and balance have complemented my compulsion to overwork and enriched my life and graduate school experience far beyond my greatest dreams. I love you.

**My peers.** To the cohort before me, Sam Slattery, Thomas A. McMurrugh, Sander Roy, Jeremy Lant, Matthew Berg, Aisha Freeman, Karen Dunkerley, and Ryan Grainger, you gracefully guided me and many others through the hoops of graduate school, thank you. To my cohort, I’ve enjoyed every opportunity to collaborate! Our constant “one-upmanship” and frequent friendly challenges motivated me to work and think harder. To my lab mates, thank you for indulging my extreme skepticism, cynicism, and critical nature concerning our science and results; it was probably annoying sometimes. However, it was always from a place of pure curiosity and appreciation. Samir Hamadache, you make the best butter chicken I have ever tasted! Jordyn Meaney, you are a force best not to be reckoned with when you have an objective in mind. Emma J. Walker, your research and writing are thoughtful, thorough, and creative! Mark Pampuch, thank you for talking deeply and honestly about science and life with me on many occasions. Daniel Nucifora, your ambition has been contagious. To my students Jennifer Davis, Emily Carvalhais, and Jiayi Wang, you were



godsent. Your dedication to the Karas Lab and your projects made leaps and bounds forward. I wish you all the best in your future endeavors. Finally, I could not be luckier to have had the privilege to work with and learn from incredible post-doctoral fellows in our lab—specifically, Drs. Preetam Janakirama, Mariana M. Severo de Almeida, and Arina Shrestha, you treated me with respect and patience, and I am grateful! Stephanie Brumwell, you are my best friend, and I wish you the absolute best! You were a positive role model, a stellar graduate student, and taught me how to approach difficulties with grace and clarity. We brought out the best in each other inside the lab and out!

**My sage guides.** Dr. David Edgell, you were the first to provide me with the opportunity to enter the academic arena. Since the beginning, you urged me to make mistakes and read more; both have paid massive dividends. Thank you for introducing me to Dr. Bogumil Karas, constantly pushing me to find alignment between my projects and their purpose, and challenging my thinking throughout graduate school. Dr. Bogumil Karas, you are the life of the scientific party. Thank you for making science so enticing; your enthusiasm will inspire many future synthetic biologists, including myself. While aware of the strategic maneuvering required for self-growth, you taught me the tactical requirements of day-to-day, week-to-week, and month-to-month goal setting required to ensure superior progress. I love to hate that Gantt Chart, but you must respect it! “Karas Lab, we solve problems here.” – Karas Lab. My advisory committee, Drs. Murray Junop and Krzysztof Szczyglowski, thank you for believing in me, supporting my projects, and managing my expectations! Dr. Brian Shilton, thank you for demonstrating how to interact with students during teaching assistantships and as graduate student chair for providing thoughtful insights and a conducive space to work through the challenges of graduate school.

**The Organizations.** A special thanks to the support staff Barbara L. Green, Kyle Pollard, Lindsay Ralph, Boun Thai, Glenda C. Ogilvie, Megan Luckovitch, Neiven Timothaws, and Dr. Lynn Weir, who logistically made life so much more straightforward throughout graduate school. The Rotary-, RotarACT-, and InterACT clubs of London for helping me develop leadership skills and providing a chance to serve my community.

## Table of Contents

Abstract.....	ii
Lay Summary.....	iv
Co-Authorship Statement.....	v
Dedication.....	vii
Acknowledgments.....	viii
Table of Contents.....	x
List of Tables.....	xv
List of Figures.....	xvi
List of Appendices.....	xvii
List of Abbreviations and Symbols.....	xviii
Chapter 1.....	1
1 Introduction.....	1
1.1 Synthetic biology.....	1
1.2 Organelles.....	2
1.2.1 Endosymbiont theory – Origin of the mitochondria.....	2
1.2.2 The mitochondria.....	3
1.3 Mitochondrial genome engineering.....	4
1.4 Mitochondrial genome cloning.....	6
1.4.1 Cloning methods.....	6
1.4.2 Host organisms.....	9
1.5 Mitochondrial transformation.....	10
1.5.1 Biolistic-mediated DNA delivery.....	10
1.5.2 Bacterial conjugation.....	13
1.6 Emerging and existing platforms.....	13

1.6.1	<i>S. cerevisiae</i> .....	16
1.6.2	<i>C. reinhardtii</i> .....	16
1.6.3	Diatoms and unconventional yeasts.....	17
1.7	Scope of this thesis.....	18
1.8	References.....	20
Chapter 2.....		38
2	Rapid method for generating designer algal mitochondrial genomes.....	38
2.1	Introduction.....	38
2.2	Results and Discussion .....	40
2.2.1	Design-build-test cycle to enable rapid engineering of organelle genomes .....	40
2.2.2	Cloning of the <i>P. tricornutum</i> mitochondrial genome.....	42
2.2.3	Sequence analysis of cloned <i>P. tricornutum</i> mitochondrial genomes .....	45
2.2.4	Maintenance of <i>P. tricornutum</i> mitochondrial plasmids in host organisms .....	47
2.3	Conclusions.....	51
2.4	Materials and Methods.....	51
2.4.1	Strains and growth conditions.....	51
2.4.2	DNA preparation.....	52
2.4.3	DNA fragment preparation for PCR-based cloning.....	53
2.4.4	DNA fragment preparation for transformation-associated recombination (TAR) cloning.....	54
2.4.5	Yeast spheroplast transformation protocol .....	55
2.4.6	<i>E. coli</i> transformation.....	55
2.4.7	Screening strategy.....	56
2.4.8	Evaluation of growth phenotypes of host strains.....	57
2.5	References.....	59

Chapter 3.....	64
3 Cloning of <i>Thalassiosira pseudonana</i> 's mitochondrial genome in <i>Saccharomyces cerevisiae</i> and <i>Escherichia coli</i> .....	64
3.1 Introduction.....	64
3.2 Results.....	66
3.2.1 Cloning of <i>T. pseudonana</i> 's mitochondrial genome.....	66
3.2.2 Sequence analysis of cloned <i>T. pseudonana</i> mitochondrial genomes .....	69
3.2.3 Maintenance of <i>T. pseudonana</i> 's mitochondrial genome in host organisms .....	69
3.2.4 Assessing the expression of <i>T. pseudonana</i> and <i>P. tricornutum</i> mitochondrial genes in <i>E. coli</i> .....	75
3.3 Discussion.....	75
3.4 Conclusions.....	77
3.5 Materials and Methods.....	78
3.5.1 Strains and growth conditions.....	78
3.5.2 Total DNA isolation by modified alkaline lysis .....	78
3.5.3 DNA fragment preparation for PCR-based cloning.....	78
3.5.4 Yeast spheroplast transformation protocol .....	80
3.5.5 <i>E. coli</i> transformation.....	80
3.5.6 Screening strategy.....	81
3.5.7 Evaluation of growth phenotypes of host strains .....	81
3.5.8 Bacterial RNA extraction.....	82
3.5.9 RNA sequencing .....	83
3.5.10 Plasmid stability assay .....	83
3.5.11 Statistical analyses .....	85
3.6 References.....	85
Chapter 4.....	90

4 Superior conjugative plasmids delivered by bacteria to diverse fungi .....	90
4.1 Introduction.....	90
4.2 Results.....	92
4.2.1 Development of streamlined conjugation plasmids .....	92
4.2.2 Creation of the superior conjugative plasmid pSC5 .....	98
4.2.3 Bacterial conjugation to diverse yeast species.....	100
4.2.4 Domestication of pSC5 for Golden Gate assembly .....	103
4.2.5 Proof of concept for bacterial conjugation-mediated delivery as an antifungal .....	103
4.3 Discussion.....	105
4.4 Material and Methods .....	108
4.4.1 Experimental design.....	108
4.4.2 Microbial strains and growth conditions.....	108
4.4.3 Plasmid construction.....	109
4.4.4 Plasmid analysis.....	111
4.4.5 Bacterial conjugation .....	112
4.4.6 RNA isolation and quantitative reverse transcriptase-polymerase chain reaction.....	113
4.4.7 Statistical analysis.....	114
4.5 References.....	114
Chapter 5.....	122
5 General Discussion .....	122
5.1 Design-build-test: Mitochondrial genome cloning and engineering .....	122
5.2 Mitochondrial plasmid stability and host burden.....	123
5.3 Improving bacterial conjugation.....	124
5.3.1 Improved bacterial conjugation efficiency to eukaryotes.....	126

5.3.2 Modulating bacterial conjugation specificity for mitochondrial DNA-delivery .....	127
5.4 Whole mitochondrial genome engineering.....	129
5.5 Conclusion .....	130
5.6 References.....	131
Appendices.....	138
Curriculum Vitae .....	181

## List of Tables

Table 2-1: Cloning of the <i>P. tricornutum</i> mitochondrial genome in the host organisms <i>S. cerevisiae</i> and <i>E. coli</i> .....	44
Table 2-2: Summary of mutations identified in the cloned <i>P. tricornutum</i> mitochondrial plasmids .....	46
Table 2-3. Doubling time of host organisms harboring either a mitochondrial genome or control plasmid.....	50
Table 3-1. Cloning of the <i>T. pseudonana</i> full and reduced mitochondrial genomes in the host organisms <i>S. cerevisiae</i> and <i>E. coli</i> .....	68
Table 3-2. Summary of mutations identified in the cloned <i>T. pseudonana</i> mitochondrial genomes .....	70
Table 4-1. Plasmids used in this study .....	95

## List of Figures

Figure 1-1. Overview of strategies used to clone mitochondrial genomes .....	7
Figure 1-2. Hierarchical strategy for building and cloning mitochondrial genomes <i>de novo</i> using synthetic oligonucleotide.....	8
Figure 1-3. Transformation and bacterial conjugation of isolated mitochondria .....	11
Figure 1-4. Biolistic-mediated DNA delivery .....	12
Figure 1-5. Strategies for mitochondrial DNA-delivery by bacterial conjugation .....	14
Figure 2-1: Design-build-test cycle for the rapid engineering of mitochondrial genomes.....	41
Figure 2-2. Design, amplification, and analyses of cloned <i>P. tricornutum</i> mitochondrial genomes .....	43
Figure 2-3. Analysis of growth of <i>S. cerevisiae</i> and <i>E. coli</i> strains harboring cloned <i>P. tricornutum</i> mitochondrial genomes on solid media and in liquid media .....	49
Figure 3-1. Design, amplification, and analysis of cloned <i>T. pseudonana</i> mitochondrial genomes .....	67
Figure 3-2. Growth of host strains harboring cloned <i>T. pseudonana</i> mitochondrial genomes in liquid media .....	72
Figure 3-3. Growth phenotypes of <i>S. cerevisiae</i> and <i>E. coli</i> harboring a cloned <i>T. pseudonana</i> mitochondrial genome .....	73
Figure 3-4. Plasmid stability assay of cloned <i>T. pseudonana</i> and <i>P. tricornutum</i> mitochondrial genomes over 60 generations .....	74
Figure 4-1. Experimental Design.....	92
Figure 4-2 Transfer of minimized plasmids from <i>E. coli</i> to <i>S. cerevisiae</i> via bacterial conjugation.....	95
Figure 4-3 Identification of mutations in M3C1 responsible for improved bacterial conjugation to <i>S. cerevisiae</i> .....	96
Figure 4-4 Creation and analysis of the pSC5 conjugative plasmid.....	98
Figure 4-5 Bacterial conjugation of pSC5 to wild yeast strains .....	100
Figure 4-6 Development of a pSC5 plasmid compatible with GG assembly .....	101
Figure 4-7 Conjugation-based antifungal .....	103



## **List of Appendices**

Appendix A: Copyright Permissions .....	136
Appendix B: Supplemental Information for Chapter 2 .....	140
Appendix C: Supplemental Information for Chapter 3 .....	142
Appendix D: Supplemental Information for Chapter 4 .....	153

## List of Abbreviations and Symbols

$\Omega$	ohm
~	approximately
<	lesser than
>	to
+	plus
±	plus-minus
=	equals
%	percent
°C	degrees Celsius
-HIS	synthetic complete media lacking histidine
-TRP	synthetic complete media lacking tryptophan
$\alpha$	alpha
$\beta$	beta
$\mu$ E	microeinstein
$\mu$ F	microfarad
$\mu$ g	microgram
$\mu$ L	microliter
$\mu$ M	micromolar
<i>aacC1</i>	aminoglycoside-(3)- <i>N</i> -acetyltransferase
<i>ACT1</i>	yeast actin
<i>ade2</i>	phosphoribosylaminoimidazole carboxylase
Ala	alanine
<i>aphA</i>	aminoglycoside 3'-phosphotransferase
Arg	arginine
<i>ARG8<sup>m</sup></i>	acetylornithine aminotransferase encoded with translation table 3
<i>ARSH4</i>	autonomous replication sequence
Asn	asparagine
Asp	aspartic acid
AT	adenine and thymine
ATCC	American Type Culture Collection
<i>atp</i>	mitochondrial ATP synthase (Complex V)
<i>bla</i>	beta-lactamase
bp	base pair
C	clone
Ca	<i>Candida auris</i>
Cas9	CRISPR-associated protein 9
<i>cat</i>	chloramphenicol acetyltransferase
Cbe	<i>Candida aff. bentonensis</i>
Cbr	<i>Candida bromeliacearum</i>
CCAP	Culture Collection of Algae and Protozoa
CCIB	Computational and Integrative Biology
cDNA	complementary DNA
<i>CEN6</i>	<i>Saccharomyces cerevisiae</i> chromosome 6 centromere
CFU	colony forming unit

<i>cir</i> <sup>0</sup>	lacking 2μ plasmid
CM	chloramphenicol
<i>cob</i>	mitochondrial cytochrome b (Complex III)
<i>cox</i>	mitochondrial cytochrome c oxidase (Complex IV)
CRISPR	clustered regularly interspaced palindromic repeats
Ct	<i>Candida tolerans</i>
Cub	<i>Candida ubatubensis</i>
<i>cysG</i>	siroheme synthase
D	directly
DNA	deoxyribonucleic acid
<i>d-nat</i>	<i>N</i> -acetyltransferase encoded for diatoms
<i>dum</i>	dark uniparental minus
EDTA	ethylenediaminetetraacetic acid
F	forward
<i>fcpD</i>	fucoxanthin chlorophyll a/c binding protein D
<i>fiw</i>	fertility inhibition of incW plasmids gene
fmol	femtomole
<i>FUM</i> <sup>m</sup>	fumarase protein encoded with translation table 3
g	gram
G0	generation zero
G60	generation sixty
G+C	guanine plus cytosine
gDNA	genomic DNA
<i>GFP</i>	green fluorescent protein
<i>GFP</i> <sup>m</sup>	green fluorescent protein encoded with translation table 3
GG	Golden Gate
Gln	glutamine
Glu	glutamic acid
Gly	glycine
GXL	<b>GC</b> -rich templates, <b>excess</b> template, and <b>long</b> amplicons
h	hour
HCA	<i>HIS3-CEN6-ARSH4</i>
HF	high fidelity
His	histidine
<i>HIS3</i>	imidazoleglycerol-phosphate dehydratase
I	induced
ID	indirectly
Ile	isoleucine
Inc.	incorporated
IQR	interquartile range
IR	inverted repeat
<i>ist</i>	insertion sequence transposition function gene
kbp	kilobase pairs
<i>kfr</i>	<i>korF</i> -regulated function gene
<i>Kil</i>	host-killing function when depressed gene
<i>kla</i>	KilA phenotype gene
<i>kle</i>	KilE phenotype gene
<i>kor</i>	host killing override/gene regulation gene

kV	kilovolt
L	liter
L1	synthetic seawater
LB	lysogeny broth
LBmc	lysogeny broth supplemented with magnesium sulfate and calcium chloride
Leu	leucine
Lys	lysine
<i>lys2</i>	L-2-aminoadipate reductase
m	meter
M	molar
<i>MAT<math>\alpha</math></i>	mating type alpha
Mb	<i>Metschnikowia borealis</i>
Mbp	megabase pairs
Met	methionine
<i>met14</i>	adenylyl-sulfate kinase
mg	milligram
Mg	<i>Metschnikowia gruessi</i>
min	minute
mL	milliliter
MI	<i>Metschnikowia lunata</i>
mm	millimeter
mM	millimolar
Mp	<i>Metschnikowia pulcherrima</i>
MPX	multiplex
<i>mrfp</i>	monomeric Red Fluorescent Protein
mRNA	messenger RNA
Mt	mitochondrial
n	sample size
N	nourseothricin resistance gene
<i>nad</i>	mitochondrial NADH dehydrogenase (Complex I)
<i>nat</i>	<i>N</i> -acetyltransferase gene
NEB	New England Biolabs
ng	nanogram
OD	optical density
ORF	open reading frame
<i>oriT</i>	origin of transfer
<i>p</i>	p-value
P	primer
<i>par</i>	plasmid partitioning gene
PCR	polymerase chain reaction
pDNA	plasmid DNA
pH	potential of hydrogen
Phe	phenylalanine
PMSF	phenylmethylsulfonyl fluoride
Pro	proline
pSC5	pSuperCon5
psi	essential translation termination factor protein – Sup35p
R	reverse

R <sup>-</sup>	restriction minus
RCF	relative centrifugal force
rDNA	recombinant DNA
RecA	recombinase
<i>rep</i>	origin of replication
Rep	replicate
<i>rho</i> <sup>0</sup>	absent mitochondrial DNA
<i>rho</i> <sup>-</sup>	mutated mitochondrial DNA
<i>RIP1</i> <sup>m</sup>	Rieske FeS protein encoded with translation table 3
RNA	ribonucleic acid
<i>rpl</i>	mitochondrial ribosomal protein for large subunit
RPM	revolutions per minute
<i>rps</i>	mitochondrial ribosomal protein for small subunit
rRNA	ribosomal RNA
<i>rrnL</i>	genes for large subunit of ribosomal RNA
<i>rrnS</i>	genes for small subunit of ribosomal RNA
<i>rrsA</i>	16S ribosomal RNA
RT	room temperature
qRT-PCR	quantitative reverse transcriptase-polymerase chain reaction
s	second
Sc	<i>Saccharomyces cerevisiae</i>
sddH <sub>2</sub> O	sterile double-distilled water
Ser	serine
<i>Sh ble</i>	bleomycin resistance protein from <i>Streptoalloteichus hindustanus</i>
SOC	super optimal broth with catabolite repression
SPEM	sorbitol-EDTA-sodium phosphate dibasic heptahydrate-sodium phosphate
SSB	single stranded DNA-binding protein
STOP	stop codon
T	thousand units per gram
TAE	tris-acetic acid-EDTA
TAR	transformation-associated recombination
<i>tat</i>	mitochondrial twin-arginine protein translocation system gene
td	doubling time
TE	tris-EDTA
Thr	threonine
tmtc	too many to count
To	<i>traJ</i> ORF mutation
Tp	<i>traJ</i> promoter mutation
<i>tra</i>	transfer function A gene (Tra1)
Tra1	transfer operon 1 – mobilization proteins
Tra2	transfer operon 2 – mating-pair formation proteins
TraA–G	primase operon
TraC	DNA primase and single-stranded DNA binding protein
TraF	peptidyl transferase
TraG	coupling protein of <i>tra</i> and <i>trb</i> functions
TraH	relaxosome protein
TraH–J	relaxase operon
TraI	relaxase

TraJ	<i>oriT</i> recognizing protein
TraK	<i>oriT</i> binding protein
TraK–M	leader operon
<i>trb</i>	transfer function B gene (Tra2)
TrbC	pilin protein
<i>trf</i>	trans-acting replication function gene
<i>trn</i>	tRNA gene
<i>TRP1</i>	N-(5'-phosphoribosyl)anthranilate isomerase
Tyr	tyrosine
UGA	uracil-guanine-adenine
UI	uninduced
<i>upf</i>	unknown plasmid function gene
<i>URA3</i>	orotidine 5-phosphate decarboxylase
V	volt
Val	valine
<i>w/v</i>	weight by volume
WGE	whole genome engineering
x	times
<i>y-nat</i>	<i>N</i> -acetyltransferase encoded for yeasts
YKO	Yeast Knockout Collection
YPD	yeast extract-peptone-dextrose
YPDA	yeast extract-peptone-dextrose-adenine

## Chapter 1

### 1 Introduction

#### 1.1 Synthetic biology

Synthetic biology is a contemporary field of study that characterizes life by combining multiple scientific disciplines. It is a vast field that standardizes and repurposes biological components such as DNA, RNA, proteins, metabolic processes, and lipid membranes [1–6]. In research, the reconstruction of cellular processes from their component parts highlights the limitations of current knowledge and informs subsequent inquiries. In industry, life engineered with synthetic properties can improve society and solve complex problems. The emergence of synthetic biology followed the development of three enabling technologies: 1) DNA sequencing, 2) DNA synthesis, and 3) DNA editing. It is now possible to combine these technologies to generate novel synthetic DNA molecules (DNA synthesis), introduce them into living organisms (DNA editing), and rapidly confirm their genotypes (DNA sequencing). It is the role of the synthetic biologist to combine these three technologies to engineer lifeforms effectively and efficiently with unique and valuable characteristics.

The power of synthetic biology is its ability to introduce many modifications to a genome simultaneously. As the field of synthetic biology develops, the goal has become to generate fully controllable systems through whole genome engineering (WGE) [7–17]. This has been realized in the prokaryotes *Mycoplasma genitalium*, *Mycoplasma mycoides*, and *Escherichia coli* by the total synthesis and assembly of entire genomes [9,13–15,17] and has begun in eukaryotes by The Synthetic Yeast Genome Project (*Saccharomyces cerevisiae* 2.0) that is building an entirely customizable synthetic version of the yeast genome, which is more stable than the wild-type strains [16,18–20]. The power of these models is apparent and is being applied gradually to other organisms [10–12]. However, while these systems offer total control over the nuclear genome in eukaryotes, the nucleus is only part of the equation. To enable full control and completely

harness the power of eukaryotes for synthetic biology, it will be necessary to apply the same approach of WGE to their organelles.

## **1.2 Organelles**

Organelles are subcellular structures that have specific roles inside eukaryotic cells. Examples of organelles include the ribosome, endoplasmic reticulum, Golgi apparatus, chloroplast, and mitochondria. Compartmentalization within membrane-bound organelles enables specialized metabolisms within the cell, like complex coordination of energy production and storage. The mitochondria and chloroplast are unique organelles arising from an endosymbiotic relationship resulting in the integration of a bacterium into a host cell that persisted and became specialized.

### **1.2.1 Endosymbiont theory – Origin of the mitochondria**

Symbiosis is a mutually beneficial relationship between two organisms that live in a close physical association. Endosymbiosis is a unique form of symbiosis where one of the symbiotic organisms resides within the other. Endosymbiont theory asserts that the emergence of mitochondria resulted from endosymbiosis and attempts to describe the conditions of eukaryogenesis, the progression of events toward eukaryotic life. There are two contending endosymbiotic models for the emergence of mitochondria: phagotrophy and syntrophy also referred to as mitochondria-late and mitochondria-early models, respectively [21–35].

Briefly, one version of the endosymbiotic theory is the hydrogen hypothesis [27]. It proposes an anaerobic syntrophy between a strictly hydrogen-dependent autotrophic archaeobacterium host [36–48] and a heterotrophic facultatively anaerobic bacterium endosymbiont [40,47–55], which are both supported by phylogenetic studies. The symbiosis was progressively strengthened by the extension of the host cell membrane around the bacterium, increasing surface area for the exchange of metabolites and leading



to eventual encapsulation [27,29,31,32,34,36,37,56–58]. Furthermore, the persistence of the intracellular bacterium initiated the conditions for the evolution of the endomembrane system within the archaeal host [24,29,59]. Once internalized, an entire bacterial genome's worth of genes were donated from the endosymbiont to the host genome through endosymbiont gene transfer [55,60–64]. The endosymbiont gene transfer of bacterial genes reinforced the intra-cellular symbiosis [61], replaced many archaeal pathways in the host generating a composite host genome [61,63–65], and resulted in genome reduction of the endosymbiont into the mitochondrial genomes observed today [60,61,64]. The result was a primitive eukaryote with defining traits, including cytoskeleton, separation of transcription and translation spatiotemporally, increased cell size relative to prokaryotes, mosaic linear chromosomes, and, importantly, membrane-bound compartments such as the mitochondria.

### **1.2.2 The mitochondria**

The exact number of mitochondria in a cell differs between species, but in single-celled eukaryotes, there are typically 1–10 mitochondria [66–71]. All mitochondria are composed of an outer and inner membrane. The inner membrane forms infoldings, called cristae, that increase surface area for aerobic respiration and shape the boundary of the mitochondrial matrix where its metabolisms are performed [72–75]. Although mitochondria are commonly represented as bean-like structures, they come in many shapes and sizes and form highly dynamic networks that undergo binary fission and fusion [66,71,72,76].

Mitochondria are widely known as the “powerhouse of the cell” for their integral role in adenosine triphosphate production by oxidative phosphorylation [64,73,77]. However, it also performs many other essential metabolisms for the cell, including pyruvate metabolism, tricarboxylic acid cycle, fatty-acid biosynthesis and  $\beta$ -oxidation, branched-chain amino acid degradation, and the biosynthesis of ubiquinone, biotin, and iron-sulfur clusters [55,73–75,78–84]. Mitochondrial proteomes typically contain 100–1000's of proteins mainly encoded in the nucleus [60,70,81,82]. Mitochondrial proteins

expressed from the nucleus are identified by an N-terminal leader-peptide sequence that signals transport to the mitochondrial translocase of the outer membrane protein [73,85]. The unfolded protein is fed through the mitochondrial translocase of the outer membrane protein and, subsequently, the translocase of the inner membrane protein [73,85], where the leader-peptide sequence is cleaved off, and the protein assumes its mature conformation [73,85]. A small minority of the mitochondrial proteome is encoded in the mitochondrial genome. Mitochondria maintain a core set of genes, including machinery for DNA replication and expression, the electron transport chain, protein import, and protein maturation [55,63,64,86–88]. The mitochondrion usually contains 10–1000 copies of its genome, which is small, compact, and circular [64,71,79,87,89]. However, in some organisms, the genome can be linear [71,79,87,89,90], mini- and maxi-circles [87,91], or completely absent [63,64].

The presence of mitochondrial genomes offers an opportunity for synthetic biologists to engineer eukaryotic life far beyond the capabilities of prokaryotes or the eukaryotic nuclear genome alone. The mitochondria host a diversity of metabolisms with the potential for engineering and offer a sequestered location to express transgenic pathways. Metabolic specialization and compartmentalization of membrane-bound organelles are vital features that need to be exploited to harness the full potential of eukaryotic platforms. However, WGE strategies for mitochondria are required.

### **1.3 Mitochondrial genome engineering**

Genetic manipulations to alter the mitochondrial compartment's function can be targeted to either the nuclear or mitochondrial genomes. Nuclear genome engineering is typically used because of its ease of transformation and extensive genetic toolbox relative to the mitochondria, which lacks genome engineering techniques in many species [92–94]. Native mitochondrial proteins encoded in the nuclear genome are common targets for genetic engineering or the study of mitochondria [95–97]. Alternatively, chimeric proteins can be constructed with transit peptides to localize transgenic proteins or pathways to mitochondria [94,96–102]. However, these methods are limited in the size

and type of proteins that correctly localize within the mitochondria, restricting the diversity of proteins and pathways that can be imported [103–106]. Also, these methods do not enable modifications of the mitochondrial genome directly.

There are several advantages to engineering a mitochondrial genome as opposed to a nuclear genome, including a lack of positional effects [1,6,107,108], RNA interference [6,109], and gene silencing [6,109,110] that are common to the nucleus. The ploidy of mitochondrial genomes increases the copy number of transgenic cassettes resulting in high protein accumulation, and its polycistronic gene organization simplifies recombinant DNA (rDNA) design [87,111]. The mitochondrial compartment enables the localization of synthetic genetic pathways “hidden” from the rest of the cell and the expression of unique proteins containing oxygen-sensitive metal clusters [73,75,112]. Moreover, the expression of protein pathways in the mitochondria can compartmentalize toxic intermediates, increase local concentrations, and minimize competing reactions from the rest of the cell, ultimately increasing product yields [21,96,97,99,100,102,113]. Finally, mitochondrial engineering offers improved control of carbon flux and energetics of eukaryotic cells as the primary site of cellular energy metabolism and regulation [100].

Synthetic biology aspires to facilitate whole mitochondrial genome engineering approaches that enable complete genetic control of eukaryotes. Efficient whole mitochondrial genome engineering requires methods for the rapid generation and testing of derivative mitochondrial genomes with multiple genetic changes. Creation of these methods requires: 1) mitochondrial genomes to be cloned into a host organism for simplified handling and manipulation of DNA, 2) rapid genetic engineering protocols, and 3) robust methods of DNA delivery. Many mitochondrial genomes have been successfully cloned into host organisms; however, robust methods of engineering and transforming whole mitochondrial genomes into mitochondria are lacking.

## 1.4 Mitochondrial genome cloning

### 1.4.1 Cloning methods

Molecular cloning is the replication of DNA to produce a population of cells with identical DNA molecules. It is achieved by assembling rDNA containing vector DNA (i.e., from the host for DNA maintenance) and source DNA (i.e., from the organism of interest). The vector DNA minimally includes a selection marker, a promoter and terminator to drive selection marker expression, and an origin of replication (Figure 1-1A) [114–120]. For mitochondrial genome engineering, the source DNA consists of a mitochondrial genome created from either biological (Figure 1-1B) [114,115,119,121–130] or synthetic DNA (Figure 1-2) [131]. While rDNA can be assembled *in vitro*, it requires a living host organism to prevent DNA damage by shearing forces, maintain the cloned DNA, and expand the population of rDNA molecules.

Mitochondrial genomes cloned from biological sources can be captured indirectly or directly using PCR-based [123–126] or transformation-associated recombination (TAR) cloning methods [119,120,125], respectively (Figure 1-1B). The vector DNA for either cloning method is designed with overlapping sequence homology at its termini to the mitochondrial genome for integration during DNA assembly. In PCR-based cloning, the source DNA is indirectly amplified in pieces with overlapping sequence homology [123–126]. Alternatively, in TAR cloning, source DNA is directly isolated from the organism of interest and linearized using a restriction enzyme with a single cut site [119,120,125]. In both methods, the rDNA can be assembled either by homology-directed repair within a host organism or *in vitro* and subsequently transformed into a host organism. The presence of correctly cloned rDNA is confirmed through *in vitro* diagnostic tests such as PCR screens, restriction enzyme digestion, and DNA sequencing. Alternatively, mitochondrial genomes can be cloned *de novo* by DNA synthesis. Typically, a hierarchical assembly of DNA is used that progressively builds larger molecules until a complete genome is achieved (Figure 1-2) [12,13,15,16,123,131]. For example, the mouse mitochondrial genome has been assembled from completely synthetic DNA oligos [131]. In all cases, the mitochondrial genome must be stored *in*

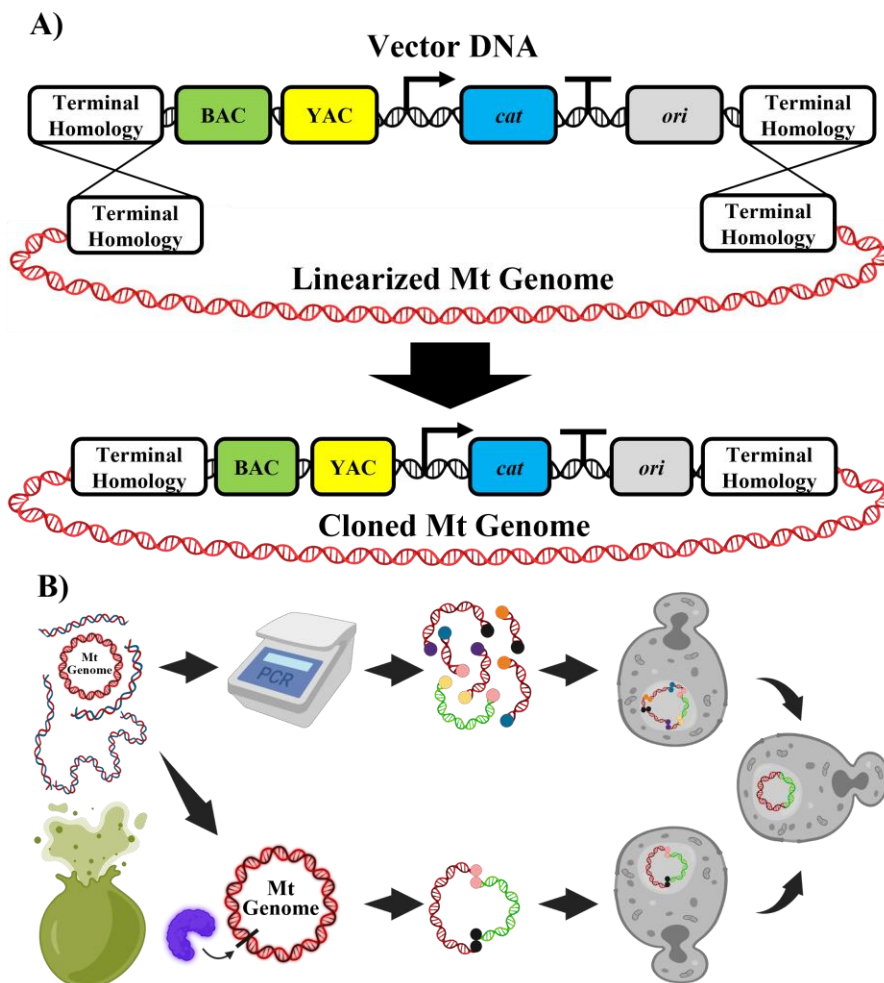


**Figure 1-1. Overview of strategies used to clone mitochondrial genomes. A)** Schematic of a generic cloning vector (black) containing all the genetic elements required for selection and stable propagation in bacteria (green; BAC – bacterial artificial chromosome), yeast (yellow; YAC – yeast artificial chromosome), and a hypothetical organism of interest (blue and grey; *cat* – chloramphenicol acetyltransferase, and *ori* – origin of replication). At their termini, both the vector DNA and mitochondrial genome (red; Mt – mitochondrial) contain sequence homology (white) to each other. The mitochondrial genome becomes cloned following integration of the vector DNA by homology-directed repair (bottom) and stable maintenance in a host organism. **B)** Schematic of the PCR-based (top) and transformation-associated recombination (bottom; TAR) cloning methods used to clone mitochondrial genomes in yeast. In both methods, total DNA (i.e., nuclear and organellar DNA) is isolated from cells. In PCR-based cloning, the mitochondrial genome (red) and a cloning vector (green) are PCR-amplified with sequence homology to adjacent fragments. In TAR cloning, a mitochondrial genome is linearized by a restriction enzyme (purple) and a cloning vector is PCR-amplified with terminal sequence homology. In both methods, the fragments are pooled and transformed into yeast to generate a cloned mitochondrial genome. Figure created with BioRender.com.

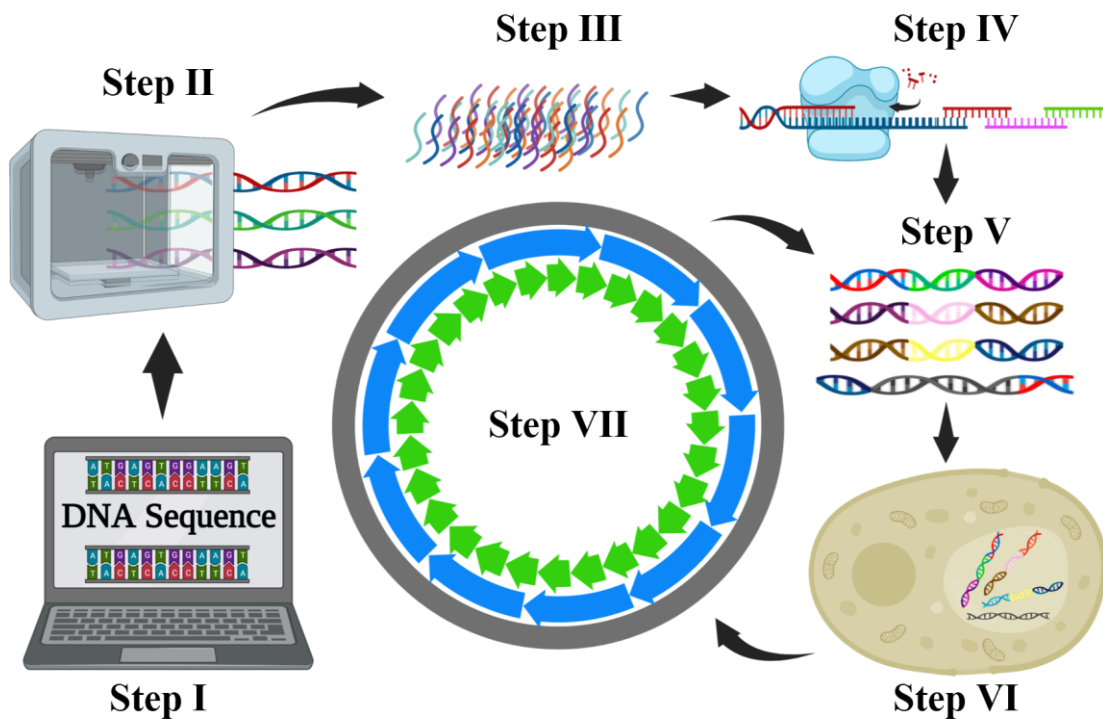


**Figure 1-2. Hierarchical strategy for building and cloning mitochondrial genomes *de novo* using synthetic oligonucleotides.** A mitochondrial genome is designed and fragmented into short overlapping oligonucleotides *in silico* (Step I), and generated by DNA synthesis (Step II). The short oligonucleotides are pooled (Step III) and joined by PCR-stitching into long overlapping oligonucleotides (Step IV). Many long oligonucleotides and a cloning vector are pooled (Step V) and transformed into yeast (Step VI), which assembles a plasmid that harbors a small ~1 kbp fragment of the mitochondrial genome. In the first cycle, the genome is cloned as small fragments across many plasmids (green; Step VII). The genome is iteratively cloned (Steps V–VII) into progressively fewer fragments by assembling larger fragments from many smaller previously cloned fragments (blue; Step VII). The cycle repeats until a single yeast strain assembles an entire genome (grey; Step VII). Figure created with BioRender.com.

*vivo* in a host organism, typically *E. coli* or *S. cerevisiae*, to protect and expand the population of cloned DNA.

### 1.4.2 Host organisms

Many potential organisms can be used as hosts for rDNA, but the most widely used are *E. coli* and *S. cerevisiae* [7]. Innate characteristics of rDNA can often cause unexpected effects on host organisms, such as decreased host cell viability or plasmid stability due to polymerase stalling in repetitive regions of DNA [116,132,133] or aberrant gene expression [114,116,122,134–136] that can drain the host cell's energy stores. This is especially true of mitochondrial genomes that have historically been troublesome to clone and maintain in bacteria [114,115,119,122,124,126,129,135,137]. The likelihood of shared genetic elements between a host genome and rDNA can initially be estimated by the similarity of the G+C%-content of their DNA [1,7,116,122]. For instance, it is more likely that origins of replication, promoters, and terminators will be recognized or occur spontaneously when prokaryotic hosts are used to clone mitochondrial genomes due to their similarity in G+C%-content and prokaryotic ancestry.

Many challenges can be overcome using a eukaryotic host such as *S. cerevisiae*, which has evolved different expression and translation machinery that do not recognize conjugation the prokaryotic genetic elements [7,119,126,138]. However, it may be beneficial to use prokaryote hosts for specific circumstances, such as cell fusion experiments or bacterial conjugation (*in vivo* DNA delivery). Therefore, it is essential to test host burden and plasmid stability before storage in any host organism. Typically, host burden is measured by comparing the growth of strains harboring rDNA to wild-type on plates or in liquid media. Most often, the growth rate will decrease as the plasmid copy number increases [134,139,140]. Whereas, as plasmid size increases, the growth rates are unaffected, but maximum culture cell density decreases [140]. Plasmid stability is tested by isolating plasmids before and after propagation and confirming their integrity by sequencing or enzymatic digestion [114,117,124,126]. If problems are identified, the

causative DNA sequences can be modified or removed to resolve the issue, or a low copy number plasmid vector can be used to reduce metabolic load [114,116,119,122,124].

## 1.5 Mitochondrial transformation

The introduction of rDNA into a cell is accomplished in three ways: 1) transduction, 2) transformation and 3) bacterial conjugation [112]. Examples of these methods include agrobacterium-mediated DNA transfer, glass bead agitation, biolistic-mediated DNA delivery, electroporation, and cell-penetrating peptides. Many DNA delivery methods have been attempted on model organisms such as, *S. cerevisiae* and *Chlamydomonas reinhardtii*, but only a handful of techniques have successfully introduced rDNA into a mitochondrion [93,141–143]. While electroporation [93,114,144,145] and bacterial conjugation [93,145] have been used to deliver DNA to isolated mammalian mitochondria (Figure 1-3), only biolistic-mediated DNA delivery has transformed intact mitochondria within whole cells [89,141,146–157].

### 1.5.1 Biolistic-mediated DNA delivery

The biolistic transformation method has been shown to deliver DNA to all cellular compartments, including the nucleus and organelles [6,107,108,150,151,154]. This method accelerates particles coated with DNA toward a cell culture that mechanically passes through the cell membranes, delivering DNA to all cellular compartments (Figure 1-4) [6,149,150,154]. The mechanical shear forces applied to the DNA as it passes the cell membrane and cytoplasm create an inverse relationship between the size of DNA and the success in delivering DNA to the cell. In all eukaryotes (i.e., fungal, mammalian, and plant), this delivery method results in extensive cellular damage killing a vast majority of transformable cells and for mitochondrial transformation is currently limited to cells containing a protective cell wall, such as fungi or algae, that can mitigate much of the cellular damage caused [149,158,159].



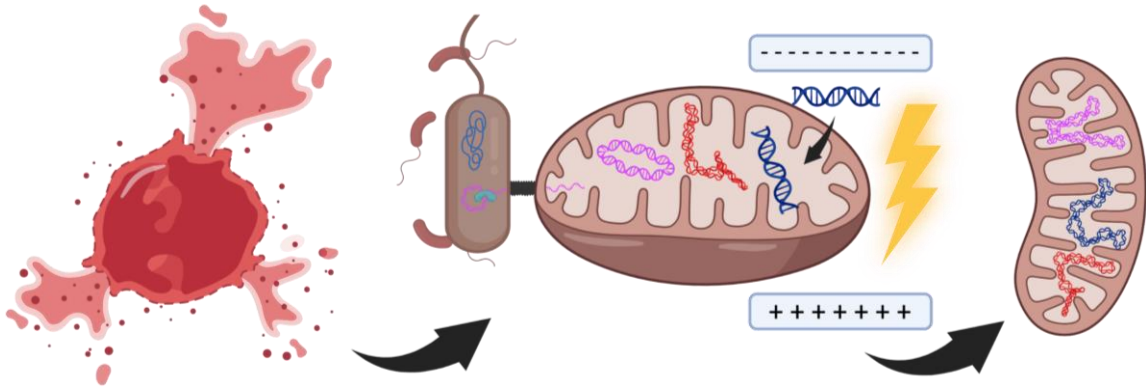


**Figure 1-3. Transformation and bacterial conjugation of isolated mitochondria.**

Functional and structurally intact mitochondria are isolated from cells (left). Extracted mitochondria can be genetically altered using bacterial conjugation or electroporation (middle). The schematic depicts three different DNA molecules from left to right: 1) plasmid DNA (pink), 2) native mitochondrial genome (red), and 3) linear DNA (dark blue). The transformed mitochondria persist transiently and can be studied (right). Figure created with BioRender.com.

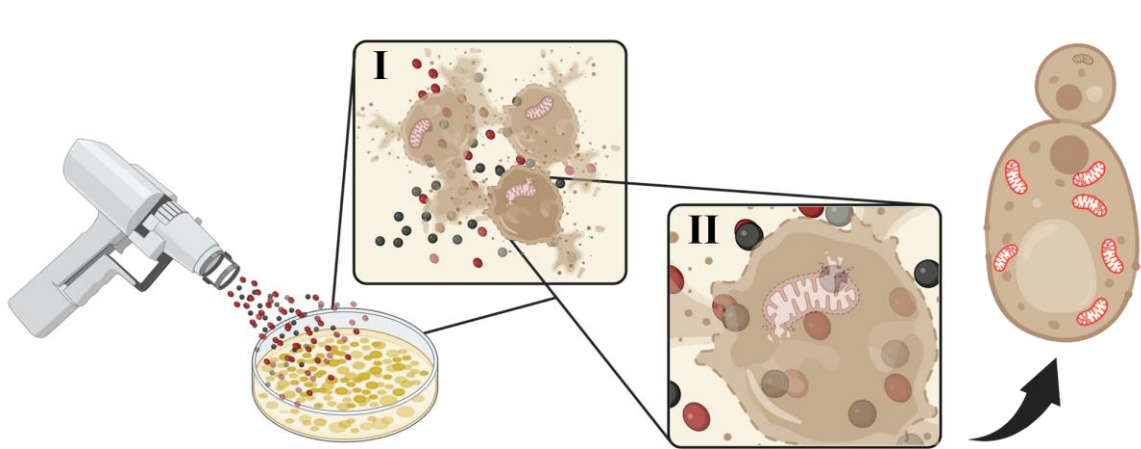


**Figure 1-4. Biolistic-mediated DNA delivery.** Particles coated with DNA for delivery (red and black) are accelerated by a gene gun (left) towards a petri dish containing densely grown cells. In the first window (I), particles puncture the cell wall and a proportion of organelle compartments, including mitochondria (pink). In the second window (II), a black particle ruptured a mitochondrion and successfully deposited DNA in a now-damaged organelle. A minority of cells successfully repair their cell wall and organelle membranes and re-constitute a cell with transformed mitochondria (red; right). Figure created with BioRender.com.

## 1.5.2 Bacterial conjugation

Bacterial conjugation is a natural process by which bacteria physically exchange genetic material (bp–Mbp in size). Bacterial donors harbor a conjugative plasmid encoding all the structural and mobilization components of the bacterial conjugation process [160,161]. The structural proteins form a pilus that transverses the donor and recipient cells [160,162–164]. The mobilization proteins recognize and bind the plasmid DNA (pDNA) and actively co-transport it through the pilus to the recipient cell cytoplasm as single-stranded DNA [160,165–171]. Bacterial conjugation has become an established method of *in vivo* DNA delivery to eukaryotes such as yeasts and algae and has previously been shown to deliver DNA to isolated mammalian mitochondria [117,118,145,172–175].

These promising data have encouraged attempts to redirect DNA delivery by bacterial conjugation from the nucleus to the mitochondria as an alternative to the biolistic-mediated DNA delivery method. Bacterial conjugation is an appealing alternative method for development because the DNA is transferred entirely *in vivo*, avoiding DNA damage by shearing that commonly occurs *in vitro* [93,145]. Mitochondria-specific DNA delivery by bacterial conjugation is being explored using 1) cell fusion accompanied by intra-cellular bacterial conjugation [93,112,176,177] and 2) engineering conjugative mobilization proteins with mitochondrial localization signals (Figure 1-5) [93,178,179]. In either scenario, altering bacterial conjugation for efficient mitochondrial DNA delivery will require seizing the host's mitochondrial protein translocation machinery to import foreign bacterial proteins and DNA.

## 1.6 Emerging and existing platforms

Many eukaryotic platforms are used for synthetic biology, such as plants, fungi, algae, and animal cell lines [1–5,92,180]. Microalgae and yeast are increasingly used eukaryotic systems for synthetic biology because, unlike animals or plants, they are single-celled

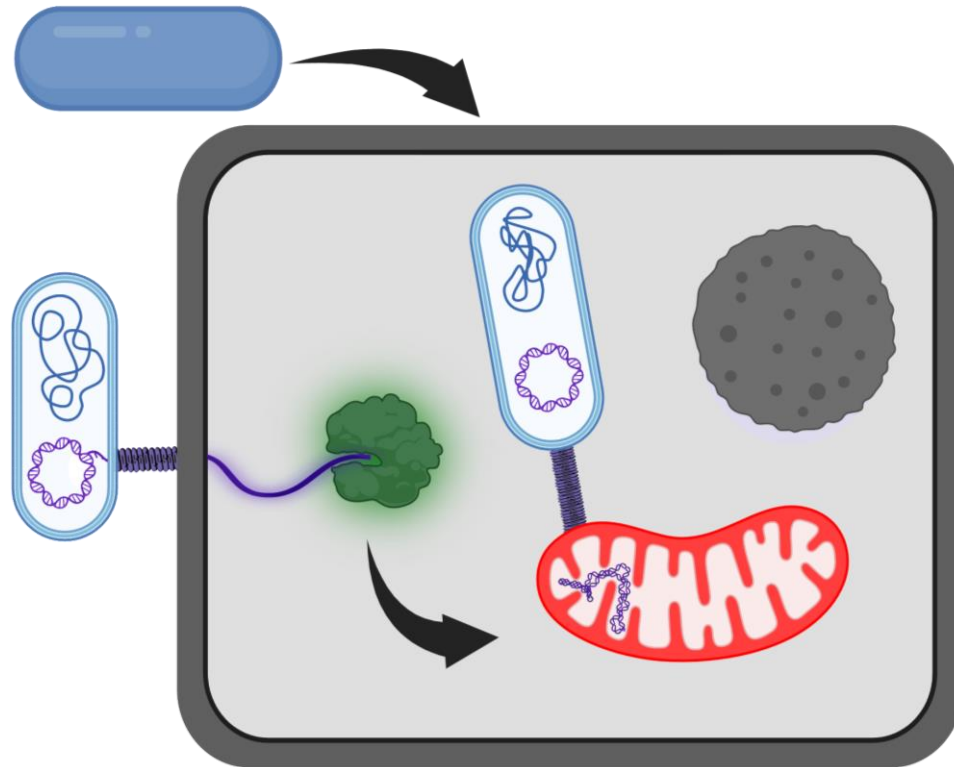


**Figure 1-5. Strategies for mitochondrial DNA-delivery by bacterial conjugation.**

Two approaches for mitochondria-specific DNA delivery are cell fusion accompanied by intra-cellular bacterial conjugation (top) and engineering of key conjugative mobilization proteins with mitochondrial localization signals (bottom). In the first approach, a bacterium (blue) is fused with a eukaryote and preferentially delivers DNA (purple) to mitochondria (red) instead of the nucleus (black). In the second approach, a relaxase engineered with a mitochondrial localization signal (green), transits to the mitochondria, and delivers DNA to the mitochondrial matrix. Figure created with BioRender.com.

organisms that divide rapidly and can be scaled up in bioreactors [1,92,180,181]. Microalgae are attractive due to their genetic diversity, range of metabolic processes, and physical characteristics [1,6,92,182]. Yeasts are appealing due to their hardiness in diverse environments and relevance to human health and industry [180,183–190]. To fully harness these systems for biotechnology, a synthetic biology approach, including mitochondrial genome cloning and delivery, is required. Mitochondrial genomes must first be cloned, which has been completed for several species, including human, mouse, fungi, plants, and algae [114,115,119,121,123–131]. However, methods for DNA delivery to the mitochondria of unicellular eukaryotes have been reported for only a few species: *S. cerevisiae* [146,149–154,157,191], *C. reinhardtii* [147,148,154–156,192,193], and *Candida glabrata* [194].

In each case of successful mitochondrial DNA transformation, the minimal requirement was the identification of respiratory deficient mutants that display a recoverable phenotype [147,149–151,153–155]. These mutants can be identified from spontaneous mutations or generated by random mutagenesis using ethidium bromide or acroflavin [89,152,156,195,196]. In the case of *S. cerevisiae* and *C. glabrata*, these were the petite mutants, which only grow on fermentable media, and in *C. reinhardtii*, the *dum* mutants that can only grow in the presence of light [154]. Respiratory-deficient mutants harbor either a large deletion (*rho*<sup>-</sup>/*dum*), point mutations (*dum*) [89,148,154,156,196], or lack a mitochondrial genome entirely (*rho*<sup>0</sup>) [149,151,154]. Phenotypically, most *dum* mutants have lost the ability to grow under heterotrophic conditions; however, some with altered *nad* genes can grow in the dark but more slowly than wild-type [196,197]. The result is the availability of a collection of transformable mitochondrial mutants for yeast and algae.

Petite and *dum* mutants have many properties that make them essential models for mitochondrial transformation [71,149,154]. First, these mutants survive without functional mitochondria (*rho*<sup>-</sup>/*rho*<sup>0</sup>/*dum*) [149,151,154]. Both the yeast and algae mitochondria perform active homologous recombination allowing for directed DNA modifications based on sequence similarities [89,149,150,154]. Further, *rho*<sup>0</sup> mutants can be transformed with bacterial plasmids and do not require an origin of replication to be

maintained, drastically simplifying engineering efforts [149–151,154]. Finally, the sexual mating of *S. cerevisiae* mitochondrial transformant strains results in homoplasmic cells harboring a mutation of interest [71,149,151,152,154].

### 1.6.1 *S. cerevisiae*

*S. cerevisiae* is the most intensively studied model organism for eukaryotic systems, with an extensive genetic toolbox and sequenced genomes [7,102,184,198,199]. Mitochondrial transformation is performed using biolistic-mediated DNA delivery with a transformation efficiency ranging from 0.1–1.3 transformants/ $\mu\text{g}$  of DNA [149–151]. The experiment typically co-transforms two DNA molecules, one with nuclear selection and the other with a portion of wild-type mitochondrial DNA [149–154,157]. Following bombardment, the cells are plated on primary selection for the nuclear marker and incubated for 4–5 days [149,151,154,157]. Selection for mitochondrial transformants is performed among the nuclear transformants by mating with a non-respiring tester strain, which results in respiring diploids [149–152,154,157]. Selection markers, such as *URA3* or *TRP1*, when used in the mitochondria, escape to the nucleus at a high frequency [154,200,201], whereas the markers *ARG8<sup>m</sup>* [152,154], *RIP1<sup>m</sup>* [153,154], *FUM<sup>m</sup>* [154], and *GFP<sup>m</sup>* [146,154,157] have been re-coded for expression in the mitochondria and are stably maintained. *S. cerevisiae* is the most developed system for mitochondrial transformation and offers foundational knowledge and methodologies for developing other eukaryotes for mitochondrial genome engineering.

### 1.6.2 *C. reinhardtii*

The only algal species where mitochondrial transformation has been achieved is *C. reinhardtii*. Mitochondrial transformation is performed using biolistic-mediated DNA delivery with efficiencies ranging from 100–250 transformants/ $\mu\text{g}$  of DNA [154,155]. DNA constructs are designed for *dum* mutants that recover their respiratory competency [89,155,156,192]. Following bombardment, colonies are grown in the dark for 4–8

weeks, and then transformants are confirmed by diagnostic PCR [89,147,148,154–156,192,193]. In addition to recovering a heterotrophic phenotype, variants of *C. reinhardtii*'s *cob* gene were identified that confer antibiotic resistance to myxothiazol [202], enabling the transformation of a mutant with intact telomeres [154,155]. Other selection markers, such as *Sh ble* [154,192] and *GFP* [147,154], have since been successfully used. *C. reinhardtii* represents a crucial first step in the mitochondrial transformation of algae and a systematic approach to developing methods in other algae.

### 1.6.3 Diatoms and unconventional yeasts

Developing interest in algae and yeasts for synthetic biology applications and basic biology research has resulted in efforts to repurpose the existing mitochondrial transformation methods in *S. cerevisiae* and *C. reinhardtii* to additional yeast and algae species. Diatoms are one group of algae that are of particular interest for generating high-value molecules, such as precursors for biofuel, and they are important contributors to the global carbon and silica cycles [1,6,182,203,204]. Despite there being little success of mitochondrial genome engineering in algae species other than *C. reinhardtii* to date, interest is mounting, as demonstrated by the SynDiatom Project, which seeks to create diatomaceous algae composed of synthetic nuclear, chloroplast and mitochondrial genomes [10].

In yeast, the progress made with *S. cerevisiae* presents powerful tools for mitochondrial genome engineering, such as multiple selection markers, transformable knockout strains, maintenance of bacterial plasmids, and mating protocols that generate mitochondrial homoplasmy. Significantly, the occurrence of petite mutants extends to many species beyond *S. cerevisiae*, including *C. glabrata*, *C. albicans*, *Kluyveromyces lactis*, *Saccharomyces castellii*, and others [71,194]. Recently, *C. glabrata*, a closely related species to *S. cerevisiae*, was reported to have undergone successful mitochondrial transformation using the *ARG8<sup>m</sup>* marker [194]. Although mitochondrial homoplasmy was not obtained, heteroplasmic transformants were confirmed by PCR, quantitative PCR, and Southern blotting and were stable in the absence of arginine.

Before mitochondrial transformation in diatoms and unconventional yeasts is possible, their mitochondria require proteomic and genetic characterization. Genetic mutations of the mitochondrial genome that produce viable organisms with either antibiotic resistance or recoverable respiratory deficiencies need to be identified and characterized. Standardized selection markers and transformation protocols must be reproduced for multiple algae and yeasts that enable reliable selection of transformants and generation of mitochondrial homoplasmy.

## **1.7 Scope of this thesis**

The foundation of this thesis is to progress the fields of synthetic biology and organelle engineering by improving and standardizing methods for mitochondrial genome engineering and DNA delivery. Synthetic biology seeks total genetic control over biological systems through WGE, which includes the mitochondrial and chloroplast genomes in eukaryotes. However, the development of WGE tools for genome-scale manipulation of DNA is limited to the nucleus. Genetic tools that enable the creation and delivery of designer genomes to any compartment in microbes will empower researchers with potential opportunities, including increasing biosafety and containment of laboratory microbes, producing lucrative biomolecules, and better understanding the origins of eukaryotic life.

The completion of WGE technologies for all eukaryotic genomes will be an unprecedented milestone for synthetic biology and provide a platform to engineer life in astonishing ways yet to be imagined. With WGE tools, the genetic code of microbes can be altered or expanded to form an effective barrier between laboratory and environmental microbes, whereby the genetic code of either species would be misinterpreted by the other. The expression of biosynthetic pathways in mitochondria supports the production of diverse biomolecules by offering an alternative intracellular environment that maintains differing redox potentials or oxygen concentrations. Finally, installing “ancestral-like” mitochondrial genomes will provide insights into how eukaryotic life began and eukaryogenesis evolved into extant eukaryotic species observed today.



Expanding WGE technologies to mitochondrial genomes is vital to harness the potential of eukaryotic platforms for synthetic biology.

Previously, mitochondrial genomes have been cloned in yeast and bacteria with varying degrees of adversity, but few strategies or tools for genome-scale engineering of mitochondrial genomes have been developed and demonstrated. Furthermore, despite progress in cloning and manipulating mitochondrial genomes, methods for delivering DNA to mitochondria are exclusive to three microbes using biolistic-mediated gene gun delivery, which is highly destructive and inefficient. As an alternative, *in vivo* methods of DNA delivery, such as bacterial conjugation, are being adapted for mitochondrial DNA delivery. Previous groups have attempted to improve DNA delivery to eukaryotes using bacterial conjugation by screening the genetic background of donor and recipient cells and optimizing bacterial conjugation parameters. The genetic tools this thesis presents move the field forward by enabling the rapid engineering of entire diatom mitochondrial genomes and improving DNA delivery to eukaryotic cells by bacterial conjugation.

In Chapters 2 and 3, I developed a whole mitochondrial genome engineering platform for two diatoms, *P. tricornutum* and *T. pseudonana*. Each genome was cloned into both *S. cerevisiae* and *E. coli* using PCR-based and TAR cloning methods. I characterized the mutation rate of each cloning method and performed a cycle of engineering on a mitochondrial genome to demonstrate the speed and ease of introducing genetic modifications. I assessed the host burden of *S. cerevisiae* and *E. coli* harboring these genomes via growth rates and plasmid stability in *E. coli*. Finally, gene expression from the mitochondrial plasmids in *E. coli* was analyzed using RNA sequencing.

Then I focused my attention on improving DNA delivery methods to eukaryotic cells via bacterial conjugation in Chapter 4. I aimed to enhance bacterial conjugation rates to establish a practicable *in vivo* DNA delivery method more amenable to mobilization protein engineering efforts. Using the pTA-Mob 2.0 conjugative plasmid, I developed a deletion plasmid library containing 55 deletions and tested each plasmid for DNA delivery to bacterial and eukaryotic cells. Deletions were combined into cluster deletions to generate progressively smaller conjugative plasmids, and a superior

conjugative plasmid was created: pSuperCon5 (pSC5). I showed that the improved conjugative ability of pSC5 was donor independent by using *Sinorhizobium meliloti* as a donor rather than *E. coli*. My colleagues and I repurposed bacterial conjugation by “loading” pSC5 with toxic genes for killing yeasts as a proof-of-principle for a novel antifungal. More importantly, we demonstrated that bacterial conjugation with pSC5 could deliver DNA to unconventional yeasts, including *C. auris* and *Metschnikowia* species, which had not previously been reported. Together these resources for mitochondrial genome engineering and improved DNA delivery should improve the feasibility of future endeavors in whole mitochondrial genome engineering.

## 1.8 References

1. Scaife MA and Smith AG. Towards developing algal synthetic biology. *Biochem Soc Trans.* 2016;44:716–722. doi:10.1042/BST20160061
2. Martella A, Pollard SM, Dai J, and Cai Y. Mammalian synthetic biology: Time for big MACs. *ACS Synth Biol.* 2016;5:1040–1049. doi:10.1021/acssynbio.6b00074
3. Kis Z, Pereira HS, Homma T, Pedrigi RM, and Krams R. Mammalian synthetic biology: Emerging medical applications. *J R Soc Interface.* 2015;12:20141000. doi:10.1098/rsif.2014.1000
4. Fesenko E and Edwards R. Plant synthetic biology: A new platform for industrial biotechnology. *J Exp Bot.* 2014;65:1927–1937. doi:10.1093/jxb/eru070
5. Barnum CR, Endelman BJ, and Shih PM. Utilizing plant synthetic biology to improve human health and wellness. *Front Plant Sci.* 2021;12:691462. doi:10.3389/fpls.2021.691462
6. Kselíková V, Singh A, Bialevich V, Čížková M, and Bišová K. Improving microalgae for biotechnology — From genetics to synthetic biology – Moving forward but not there yet. *Biotechnol Adv.* 2022;58:107885. doi:10.1016/j.biotechadv.2021.107885
7. Karas BJ, Suzuki Y, and Weyman PD. Strategies for cloning and manipulating natural and synthetic chromosomes. *Chromosom Res.* 2015;23:57–68. doi:10.1007/s10577-014-9455-3

8. Ostrov N, Beal J, Ellis T, Gordon DB, Karas BJ, Lee HH, et al. Technological challenges and milestones for writing genomes. *Science*. 2019;366:310–312. doi:10.1126/science.aay0339
9. Fredens J, Wang K, de la Torre D, Funke LFH, Robertson WE, Christova Y, et al. Total synthesis of *Escherichia coli* with a recoded genome. *Nature*. 2019;569:514–518. doi:10.1038/s41586-019-1192-5
10. Pampuch M, Walker EJJ, and Karas BJ. Towards synthetic diatoms: The *Phaeodactylum tricornutum* Pt-syn 1.0 project. *Curr Opin Green Sustain Chem*. 2022;35:100611. doi:10.1016/j.cogsc.2022.100611
11. Boeke JD, Church G, Hessel A, Kelley NJ, Arkin A, Cai Y, et al. The genome project-write. *Science*. 2016;353:126–127. doi:10.1126/science.aaf6850
12. Wang Y, Shen Y, Gu Y, Zhu S, and Yin Y. Genome writing: Current progress and related applications. *Genom Proteom Bioinf*. 2018;16:10–16. doi:10.1016/j.gpb.2018.02.001
13. Hutchison CA, Chuang R-Y, Noskov VN, Assad-Garcia N, Deerinck TJ, Ellisman MH, et al. Design and synthesis of a minimal bacterial genome. *Science*. 2016;351:aad6253. doi:10.1126/science.aad6253
14. Lartigue C, Glass JI, Alperovich N, Pieper R, Parmar PP, Hutchison CA, et al. Genome transplantation in bacteria: Changing one species to another. *Science*. 2007;317:632–638. doi:10.1126/science.1144622
15. Gibson DG, Glass JI, Lartigue C, Noskov VN, Chuang R-Y, Algire MA, et al. Creation of a bacterial cell controlled by a chemically synthesized genome. *Science*. 2010;329:52–56. doi:10.1126/science.1190719
16. Richardson SM, Mitchell LA, Stracquadanio G, Yang K, Dymond JS, DiCarlo JE, et al. Design of a synthetic yeast genome. *Science*. 2017;355:1040–1044. doi:10.1126/science.aaf4557
17. Ostrov N, Landon M, Guell M, Kuznetsov G, Teramoto J, Cervantes N, et al. Design, synthesis, and testing toward a 57-codon genome. *Science*. 2016;353:819–822. doi:10.1126/science.aaf3639
18. Dai J, Boeke JD, Luo Z, Jiang S, and Cai Y. Sc3.0: Revamping and minimizing the yeast genome. *Genome Biol*. 2020;21:1–4. doi:10.1186/s13059-020-02130-z
19. Zhang W, Zhao G, Luo Z, Lin Y, Wang L, Guo Y, et al. Engineering the ribosomal DNA in a megabase synthetic chromosome. *Science*. 2017;355:eaf3981. doi:10.1126/science.aaf3981

20. Dymond JS, Richardson SM, Coombes CE, Babatz T, Muller H, Annaluru N, et al. Synthetic chromosome arms function in yeast and generate phenotypic diversity by design. *Nature*. 2011;477:471–476. doi:10.1038/nature10403
21. Cavalier-Smith T. The phagotrophic origin of eukaryotes and phylogenetic classification of *Protozoa*. *Int J Syst Evol Microbiol*. 2002;52:297–354. doi:10.1099/00207713-52-2-297
22. Sagan L. On the origin of mitosing cells. *J Theor Biol*. 1967;14:225–274. doi:10.1016/0022-5193(67)90079-3
23. Vellai T and Vida G. The origin of eukaryotes: The difference between prokaryotic and eukaryotic cells. *Proc R Soc London Ser B Biol Sci*. 1999;266:1571–1577. doi:10.1098/rspb.1999.0817
24. López-García P and Moreira D. Selective forces for the origin of the eukaryotic nucleus. *BioEssays*. 2006;28:525–533. doi:10.1002/bies.20413
25. Gray MW. The pre-endosymbiont hypothesis: A new perspective on the origin and evolution of mitochondria. *Cold Spring Harb Perspect Biol*. 2014;6:a016097. doi:10.1101/cshperspect.a016097
26. Speijer D. Alternating terminal electron-acceptors at the basis of symbiogenesis: How oxygen ignited eukaryotic evolution. *BioEssays*. 2017;39:1600174. doi:10.1002/bies.201600174
27. Martin W and Müller M. The hydrogen hypothesis for the first eukaryote. *Nature*. 1998;392:37–41. doi:10.1038/32096
28. Taylor FJR. Implications and extensions of the serial endosymbiosis theory of the origin of eukaryotes. *Taxon*. 1974;23:229–258. doi:10.2307/1218702
29. Baum DA and Baum B. An inside-out origin for the eukaryotic cell. *BMC Biol*. 2014;12:1–22. doi:10.1186/s12915-014-0076-2
30. Forterre P. A new fusion hypothesis for the origin of Eukarya: Better than previous ones, but probably also wrong. *Res Microbiol*. 2011;162:77–91. doi:10.1016/j.resmic.2010.10.005
31. Moreira D and López-García P. Symbiosis between methanogenic Archaea and  $\delta$ -proteobacteria as the origin of eukaryotes: The syntrophic hypothesis. *J Mol Evol*. 1998;47:517–530. doi:10.1007/PL00006408
32. Imachi H, Nobu MK, Nakahara N, Morono Y, Ogawara M, Takaki Y, et al. Isolation of an archaeon at the prokaryote–eukaryote interface. *Nature*. 2020;577:519–525. doi:10.1038/s41586-019-1916-6

33. Poole AM and Neumann N. Reconciling an archaeal origin of eukaryotes with engulfment: A biologically plausible update of the Eocyte hypothesis. *Res Microbiol.* 2011;162:71–76. doi:10.1016/j.resmic.2010.10.002
34. Spang A, Stairs CW, Dombrowski N, Eme L, Lombard J, Caceres EF, et al. Proposal of the reverse flow model for the origin of the eukaryotic cell based on comparative analyses of Asgard archaeal metabolism. *Nat Microbiol.* 2019;4:1138–1148. doi:10.1038/s41564-019-0406-9
35. John P and Whatley FR. *Paracoccus denitrificans* and the evolutionary origin of the mitochondrion. *Nature.* 1975;254:495–498. doi:10.1038/255428c0
36. Martijn J and Ettema TJG. From archaeon to eukaryote: The evolutionary dark ages of the eukaryotic cell. *Biochem Soc Trans.* 2013;41:451–457. doi:10.1042/BST20120292
37. Yutin N, Wolf MY, Wolf YI, and Koonin EV. The origins of phagocytosis and eukaryogenesis. *Biol Direct.* 2009;4:1–26. doi:10.1186/1745-6150-4-9
38. Williams TA, Foster PG, Nye TMW, Cox CJ, and Embley TM. A congruent phylogenomic signal places eukaryotes within the *Archaea*. *Proc R Soc B Biol Sci.* 2012;279:4870–4879. doi:10.1098/rspb.2012.1795
39. Kelly S, Wickstead B, and Gull K. Archaeal phylogenomics provides evidence in support of a methanogenic origin of the Archaea and a thaumarchaeal origin for the eukaryotes. *Proc R Soc B Biol Sci.* 2011;278:1009–1018. doi:10.1098/rspb.2010.1427
40. Pisani D, Cotton JA, and McInerney JO. Supertrees disentangle the chimerical origin of eukaryotic genomes. *Mol Biol Evol.* 2007;24:1752–1760. doi:10.1093/molbev/msm095
41. Foster PG, Cox CJ, and Embley TM. The primary divisions of life: A phylogenomic approach employing composition-heterogeneous methods. *Philos Trans R Soc B Biol Sci.* 2009;364:2197–2207. doi:10.1098/rstb.2009.0034
42. Williams TA and Embley TM. Archaeal “dark matter” and the origin of eukaryotes. *Genome Biol Evol.* 2014;6:474–481. doi:10.1093/gbe/evu031
43. Cox CJ, Foster PG, Hirt RP, Harris SR, and Embley TM. The archaeobacterial origin of eukaryotes. *Proc Natl Acad Sci U.S.A.* 2008;105:20356–20361. doi:10.1073/pnas.0810647105
44. Guy L, Saw JH, and Ettema TJG. The archaeal legacy of eukaryotes: A phylogenomic perspective. *Cold Spring Harb Perspect Biol.* 2014;6:a016022. doi:10.1101/cshperspect.a016022

45. Zaremba-Niedzwiedzka K, Caceres EF, Saw JH, Bäckström D, Juzokaite L, Vancaester E, et al. Asgard archaea illuminate the origin of eukaryotic cellular complexity. *Nature*. 2017;541:353–358. doi:10.1038/nature21031
46. Guy L and Ettema TJG. The archaeal ‘TACK’ superphylum and the origin of eukaryotes. *Trends Microbiol*. 2011;19:580–587. doi:10.1016/j.tim.2011.09.002
47. Thiergart T, Landan G, Schenk M, Dagan T, and Martin WF. An evolutionary network of genes present in the eukaryote common ancestor polls genomes on eukaryotic and mitochondrial origin. *Genome Biol Evol*. 2012;4:466–485. doi:10.1093/gbe/evs018
48. Rivera MC and Lake JA. The ring of life provides evidence for a genome fusion origin of eukaryotes. *Nature*. 2004;431:152–155. doi:10.1038/nature02848
49. Esser C, Ahmadinejad N, Wiegand C, Rotte C, Sebastiani F, Gelius-Dietrich G, et al. A genome phylogeny for mitochondria among  $\alpha$ -proteobacteria and a predominantly eubacterial ancestry of yeast nuclear genes. *Mol Biol Evol*. 2004;21:1643–1660. doi:10.1093/molbev/msh160
50. Fitzpatrick DA, Creevey CJ, and McInerney JO. Genome phylogenies indicate a meaningful  $\alpha$ -proteobacterial phylogeny and support a grouping of the mitochondria with the Rickettsiales. *Mol Biol Evol*. 2006;23:74–85. doi:10.1093/molbev/msj009
51. Brindefalk B, Ettema TJG, Viklund J, Tholleson M, and Andersson SGE. A phylometagenomic exploration of oceanic alphaproteobacteria reveals mitochondrial relatives unrelated to the SAR11 clade. *PLoS One*. 2011;6:e24457. doi:10.1371/journal.pone.0024457
52. Andersson SGE, Zomorodipour A, Andersson JO, Sicheritz-Pontén T, Alsmark UCM, Podowski RM, et al. The genome sequence of *Rickettsia prowazekii* and the origin of mitochondria. *Nature*. 1998;396:133–140. doi:10.1038/24094
53. Rodríguez-Ezpeleta N and Embley TM. The SAR11 group of alpha-proteobacteria is not related to the origin of mitochondria. *PLoS One*. 2012;7:e30520. doi:10.1371/journal.pone.0030520
54. Thrash JC, Boyd A, Huggett MJ, Grote J, Carini P, Yoder RJ, et al. Phylogenomic evidence for a common ancestor of mitochondria and the SAR11 clade. *Sci Rep*. 2011;1:13. doi:10.1038/srep00013
55. Gray MW. Mitochondrial evolution. *Cold Spring Harb Perspect Biol*. 2012;4:a011403. doi:10.1101/cshperspect.a011403

56. Baker BJ, Tyson GW, Webb RI, Flanagan J, Hugenholtz P, Allen EE, et al. Lineages of acidophilic Archaea revealed by community genomic analysis. *Science*. 2006;314:1933–1935. doi:10.1126/science.1132690
57. Jochimsen B, Peinemann-Simon S, Völker H, Stüben D, Botz R, Stoffers P, et al. *Stetteria hydrogenophila*, gen. nov. and sp. nov., a novel mixotrophic sulfur-dependent *crenarchaeote* isolated from Milos, Greece. *Extremophiles*. 1997;1:67–73. doi:10.1007/s007920050016
58. Mills DB. The origin of phagocytosis in Earth history. *Interface Focus*. 2020;10:20200019. doi:10.1098/rsfs.2020.0019
59. Martin W and Koonin EV. Introns and the origin of nucleus–cytosol compartmentalization. *Nature*. 2006;440:41–45. doi:10.1038/nature04531
60. Timmis JN, Ayliffe MA, Huang CY, and Martin W. Endosymbiotic gene transfer: Organelle genomes forge eukaryotic chromosomes. *Nat Rev Genet*. 2004;5:123–135. doi:10.1038/nrg1271
61. Doolittle WF. You are what you eat: A gene transfer ratchet could account for bacterial genes in eukaryotic nuclear genomes. *Trends Genet*. 1998;14:307–311. doi:10.1016/S0168-9525(98)01494-2
62. Brown JR. Ancient horizontal gene transfer. *Nat Rev Genet*. 2003;4:121–132. doi:10.1038/nrg1000
63. Adams KL and Palmer JD. Evolution of mitochondrial gene content: Gene loss and transfer to the nucleus. *Mol Phylogenet Evol*. 2003;29:380–395. doi:10.1016/S1055-7903(03)00194-5
64. Burger G, Gray MW, and Lang BF. Mitochondrial genomes: Anything goes. *Trends Genet*. 2003;19:709–716. doi:10.1016/j.tig.2003.10.012
65. Rivera MC, Jain R, Moore JE, and Lake JA. Genomic evidence for two functionally distinct gene classes. *Proc Natl Acad Sci*. 1998;95:6239–6244. doi:10.1073/pnas.95.11.6239
66. Visser W, van Spronsen EA, Nanninga N, Pronk JT, Kuenen JG, and van Dijken JP. Effects of growth conditions on mitochondrial morphology in *Saccharomyces cerevisiae*. *Antonie Van Leeuwenhoek*. 1995;67:243–253. doi:10.1007/BF00873688
67. Cole LW. The evolution of per-cell organelle number. *Front Cell Dev Biol*. 2016;4:1–7. doi:10.3389/fcell.2016.00085
68. Okie JG, Smith VH, and Martin-Cereceda M. Major evolutionary transitions of life, metabolic scaling and the number and size of mitochondria and chloroplasts. *Proc R Soc B Biol Sci*. 2016;283:20160611. doi:10.1098/rspb.2016.0611

69. Borowitzka MA and Volcani BE. The polymorphic diatom *Phaeodactylum tricornutum*: Ultrastructure of its morphotypes. *J Phycol.* 1978;14:10–21. doi:10.1111/j.1529-8817.1978.tb00625.x
70. Schober AF, Río Bartulos C, Bischoff A, Lepetit B, Gruber A, and Kroth PG. Organelle studies and proteome analyses of mitochondria and plastids fractions from the diatom *Thalassiosira pseudonana*. *Plant Cell Physiol.* 2019;60:1811–1828. doi:10.1093/pcp/pcz097
71. Solieri L. Mitochondrial inheritance in budding yeasts: Towards an integrated understanding. *Trends Microbiol.* 2010;18:521–530. doi:10.1016/j.tim.2010.08.001
72. Cogliati S, Enriquez JA, and Scorrano L. Mitochondrial cristae: Where beauty meets functionality. *Trends Biochem Sci.* 2016;41:261–273. doi:10.1016/j.tibs.2016.01.001
73. Malina C, Larsson C, and Nielsen J. Yeast mitochondria: An overview of mitochondrial biology and the potential of mitochondrial systems biology. *FEMS Yeast Res.* 2018;18:1–17. doi:10.1093/femsyr/foy040
74. Pronk JT, Yde Steensma H, and Van Dijken JP. Pyruvate metabolism in *Saccharomyces cerevisiae*. *Yeast.* 1996;12:1607–1633. doi:10.1002/(SICI)1097-0061(199612)12:16<1607::AID-YEA70>3.0.CO;2-4
75. Mühlenhoff U and Lill R. Biogenesis of iron–sulfur proteins in eukaryotes: A novel task of mitochondria that is inherited from bacteria. *Biochim Biophys Acta Bioenerg.* 2000;1459:370–382. doi:10.1016/S0005-2728(00)00174-2
76. Di Bartolomeo F, Malina C, Campbell K, Mormino M, Fuchs J, Vorontsov E, et al. Absolute yeast mitochondrial proteome quantification reveals trade-off between biosynthesis and energy generation during diauxic shift. *Proc Natl Acad Sci.* 2020;117:7524–7535. doi:10.1073/pnas.1918216117
77. McBride HM, Neuspiel M, and Wasiak S. Mitochondria: More than just a powerhouse. *Curr Biol.* 2006;16:R551–R560. doi:10.1016/j.cub.2006.06.054
78. Hock MB and Kralli A. Transcriptional control of mitochondrial biogenesis and function. *Annu Rev Physiol.* 2009;71:177–203. doi:10.1146/annurev.physiol.010908.163119
79. Burger G, Forget L, Zhu Y, Gray MW, and Lang BF. Unique mitochondrial genome architecture in unicellular relatives of animals. *Proc Natl Acad Sci.* 2003;100:892–897. doi:10.1073/pnas.0336115100



80. Gruber A and Kroth PG. Intracellular metabolic pathway distribution in diatoms and tools for genome-enabled experimental diatom research. *Philos Trans R Soc B Biol Sci.* 2017;372:20160402. doi:10.1098/rstb.2016.0402
81. Gonczarowska-Jorge H, Zahedi RP, and Sickmann A. The proteome of baker's yeast mitochondria. *Mitochondrion.* 2017;33:15–21. doi:10.1016/j.mito.2016.08.007
82. Morgenstern M, Stiller SB, Lübbert P, Peikert CD, Dannenmaier S, Drepper F, et al. Definition of a high-confidence mitochondrial proteome at quantitative scale. *Cell Rep.* 2017;19:2836–2852. doi:10.1016/j.celrep.2017.06.014
83. Pierrel F, Hamelin O, Douki T, Kieffer-Jaquinod S, Mühlhoff U, Ozeir M, et al. Involvement of mitochondrial ferredoxin and para-aminobenzoic acid in yeast coenzyme Q biosynthesis. *Chem Biol.* 2010;17:449–459. doi:10.1016/j.chembiol.2010.03.014
84. Hiltunen JK, Autio KJ, Schonauer MS, Kursu VAS, Dieckmann CL, and Kastaniotis AJ. Mitochondrial fatty acid synthesis and respiration. *Biochim Biophys Acta Bioenerg.* 2010;1797:1195–1202. doi:10.1016/j.bbabi.2010.03.006
85. Herrmann JM. Converting bacteria to organelles: Evolution of mitochondrial protein sorting. *Trends Microbiol.* 2003;11:74–79. doi:10.1016/S0966-842X(02)00033-1
86. Allen JF. The function of genomes in bioenergetic organelles. *Philos Trans R Soc London Ser B Biol Sci.* 2003;358:19–38. doi:10.1098/rstb.2002.1191
87. Gray MW, Lang BF, and Burger G. Mitochondria of protists. *Annu Rev Genet.* 2004;38:477–524. doi:10.1146/annurev.genet.37.110801.142526
88. Gray MW, Lang BF, Cedergren R, Golding GB, Lemieux C, Sankoff D, et al. Genome structure and gene content in protist mitochondrial DNAs. *Nucleic Acids Res.* 1998;26:865–878. doi:10.1093/nar/26.4.865
89. Boynton JE and Gillham NW. Genetics and transformation of mitochondria in the green alga *Chlamydomonas*. In *Methods in Enzymology*; 1996; Vol. 264, pp. 279–296.
90. Nosek J, Tomáška L, Fukuhara H, Suyama Y, and Kováč L. Linear mitochondrial genomes: 30 years down the line. *Trends Genet.* 1998;14:184–188. doi:10.1016/S0168-9525(98)01443-7
91. Watanabe KI, Bessho Y, Kawasaki M, and Hori H. Mitochondrial genes are found on minicircle DNA molecules in the mesozoan animal *Dicyema*. *J Mol Biol.* 1999;286:645–650. doi:10.1006/jmbi.1998.2523

92. Brasil B dos SAF, de Siqueira FG, Salum TFC, Zanette CM, and Spier MR. Microalgae and cyanobacteria as enzyme biofactories. *Algal Res.* 2017;25:76–89. doi:10.1016/j.algal.2017.04.035
93. Yoon YG, Koob MD, and Yoo YH. Re-engineering the mitochondrial genomes in mammalian cells. *Anat Cell Biol.* 2010;43:97–109. doi:10.5115/acb.2010.43.2.97
94. Gammage PA, Moraes CT, and Minczuk M. Mitochondrial genome engineering: The revolution may not be CRISPR-ized. *Trends Genet.* 2018;34:101–110. doi:10.1016/j.tig.2017.11.001
95. Sabharwal A, Campbell JM, Schwab TL, WareJoncas Z, Wishman MD, Ata H, et al. A primer genetic toolkit for exploring mitochondrial biology and disease using zebrafish. *Genes.* 2022;13:1317. doi:10.3390/genes13081317
96. Avalos JL, Fink GR, and Stephanopoulos G. Compartmentalization of metabolic pathways in yeast mitochondria improves the production of branched-chain alcohols. *Nat Biotechnol.* 2013;31:335–341. doi:10.1038/nbt.2509
97. Lv X, Wang F, Zhou P, Ye L, Xie W, Xu H, et al. Dual regulation of cytoplasmic and mitochondrial acetyl-CoA utilization for improved isoprene production in *Saccharomyces cerevisiae*. *Nat Commun.* 2016;7:12851. doi:10.1038/ncomms12851
98. Yoon YG and Koob MD. Selection by drug resistance proteins located in the mitochondria of mammalian cells. *Mitochondrion.* 2008;8:345–351. doi:10.1016/j.mito.2008.07.004
99. Yee DA, DeNicola AB, Billingsley JM, Creso JG, Subrahmanyam V, and Tang Y. Engineered mitochondrial production of monoterpenes in *Saccharomyces cerevisiae*. *Metab Eng.* 2019;55:76–84. doi:10.1016/j.ymben.2019.06.004
100. Yuan J and Ching C-B. Mitochondrial acetyl-CoA utilization pathway for terpenoid productions. *Metab Eng.* 2016;38:303–309. doi:10.1016/j.ymben.2016.07.008
101. Farhi M, Marhevka E, Masci T, Marcos E, Eyal Y, Ovadis M, et al. Harnessing yeast subcellular compartments for the production of plant terpenoids. *Metab Eng.* 2011;13:474–481. doi:10.1016/j.ymben.2011.05.001
102. Besada-Lombana PB, McTaggart TL, and Da Silva NA. Molecular tools for pathway engineering in *Saccharomyces cerevisiae*. *Curr Opin Biotechnol.* 2018;53:39–49. doi:10.1016/j.copbio.2017.12.002
103. Claros MG, Perea J, Shu Y, Samatey FA, Popot J, and Jacq C. Limitations to *in vivo* import of hydrophobic proteins into yeast mitochondria. *Eur J Biochem.* 1995;228:762–771. doi:10.1111/j.1432-1033.1995.0762m.x

104. Curatti L and Rubio LM. Challenges to develop nitrogen-fixing cereals by direct *nif*-gene transfer. *Plant Sci.* 2014;225:130–137. doi:10.1016/j.plantsci.2014.06.003
105. von Heijne G. Why mitochondria need a genome. *FEBS Lett.* 1986;198:1–4. doi:10.1016/0014-5793(86)81172-3
106. Xiang N, Guo C, Liu J, Xu H, Dixon R, Yang J, et al. Using synthetic biology to overcome barriers to stable expression of nitrogenase in eukaryotic organelles. *Proc Natl Acad Sci.* 2020;117:16537–16545. doi:10.1073/pnas.2002307117
107. Apt KE, Kroth-Pancic PG, and Grossman AR. Stable nuclear transformation of the diatom *Phaeodactylum tricornutum*. *MGG Mol Gen Genet.* 1996;252:572–579. doi:10.1007/s004380050264
108. Falciatore A, Casotti R, Leblanc C, Abrescia C, and Bowler C. Transformation of nonselectable reporter genes in marine diatoms. *Mar Biotechnol.* 1999;1:239–251. doi:10.1007/PL00011773
109. Yamasaki T, Miyasaka H, and Ohama T. Unstable RNAi effects through epigenetic silencing of an inverted repeat transgene in *Chlamydomonas reinhardtii*. *Genetics.* 2008;180:1927–1944. doi:10.1534/genetics.108.092395
110. Neupert J, Gallaher SD, Lu Y, Strenkert D, Segal N, Barahimipour R, et al. An epigenetic gene silencing pathway selectively acting on transgenic DNA in the green alga *Chlamydomonas*. *Nat Commun.* 2020;11:6269. doi:10.1038/s41467-020-19983-4
111. Ojala D, Montoya J, and Attardi G. tRNA punctuation model of RNA processing in human mitochondria. *Nature.* 1981;290:470–474. doi:10.1038/290470a0
112. Pallen MJ. Time to recognise that mitochondria are bacteria? *Trends Microbiol.* 2011;19:58–64. doi:10.1016/j.tim.2010.11.001
113. Jaramillo-Madrid AC, Lacchini E, and Goossens A. Within and beyond organelle engineering: Strategies for increased terpene production in yeasts and plants. *Curr Opin Green Sustain Chem.* 2022;33:100572. doi:10.1016/j.cogsc.2021.100572
114. Yoon YG and Koob MD. Efficient cloning and engineering of entire mitochondrial genomes in *Escherichia coli* and transfer into transcriptionally active mitochondria. *Nucleic Acids Res.* 2003;31:1407–1415. doi:10.1093/nar/gkg228
115. Drouin J. Cloning of human mitochondrial DNA in *Escherichia coli*. *J Mol Biol.* 1980;140:15–34. doi:10.1016/0022-2836(80)90354-X
116. Godiska R, Patterson M, Schoenfeld T, and Mead DA. Beyond pUC: Vectors for cloning unstable DNA. *Optim DNA Seq Process.* 2005;1:55–76.

117. Brumwell SL, MacLeod MR, Huang T, Cochrane RR, Meaney RS, Zamani M, et al. Designer *Sinorhizobium meliloti* strains and multi-functional vectors enable direct inter-kingdom DNA transfer. PLoS One. 2019;14:e0206781. doi:10.1371/journal.pone.0206781
118. Karas BJ, Diner RE, Lefebvre SC, McQuaid J, Phillips APR, Noddings CM, et al. Designer diatom episomes delivered by bacterial conjugation. Nat Commun. 2015;6:6925. doi:10.1038/ncomms7925
119. Bigger BW, Liao A-Y, Sergijenko A, and Coutelle C. Trial and error: How the unclonable human mitochondrial genome was cloned in yeast. Pharm Res. 2011;28:2863–2870. doi:10.1007/s11095-011-0527-1
120. Kouprina N and Larionov V. Transformation-associated recombination (TAR) cloning for genomics studies and synthetic biology. Chromosoma. 2016;125:621–632. doi:10.1007/s00412-016-0588-3
121. Kessler U and Zetsche K. Physical map and gene organization of the mitochondrial genome from the unicellular green alga *Platymonas (Tetraselmis) subcordiformis (Prasinophyceae)*. Plant Mol Biol. 1995;29:1081–1086. doi:10.1007/BF00014979
122. Kearsey SE, Flanagan JG, and Craig IW. Cloning of mouse mitochondrial DNA in *E. coli* affects bacterial viability. Gene. 1980;12:249–255. doi:10.1016/0378-1119(80)90107-9
123. Itaya M, Fujita K, Kuroki A, and Tsuge K. Bottom-up genome assembly using the *Bacillus subtilis* genome vector. Nat Methods. 2008;5:41–43. doi:10.1038/nmeth1143
124. Yoon YG, Yang Y-W, and Koob MD. PCR-based cloning of the complete mouse mitochondrial genome and stable engineering in *Escherichia coli*. Biotechnol Lett. 2009;31:1671–1676. doi:10.1007/s10529-009-0063-9
125. Cochrane RR, Brumwell SL, Soltysiak MPM, Hamadache S, Davis JG, Wang J, et al. Rapid method for generating designer algal mitochondrial genomes. Algal Res. 2020;50:102014. doi:10.1016/j.algal.2020.102014
126. Cochrane RR, Brumwell SL, Shrestha A, Giguere DJ, Hamadache S, Gloor GB, et al. Cloning of *Thalassiosira pseudonana*'s mitochondrial genome in *Saccharomyces cerevisiae* and *Escherichia coli*. Biology. 2020;9:358. doi:10.3390/biology9110358
127. Moulinier T, Barroso G, and Labarère J. The mitochondrial genome of the basidiomycete *Agrocybe aegerita*: Molecular cloning, physical mapping and gene location. Curr Genet. 1992;21:499–505. doi:10.1007/BF00351660

128. Taylor JW and Smolich BD. Molecular cloning and physical mapping of the *Neurospora crassa* 74-OR23-1A mitochondrial genome. *Curr Genet*. 1985;9:597–603. doi:10.1007/BF00381173
129. Bartnik E, Biderman AW, Hahn U, Küntzel H, and Stpień PP. The cloning of *Aspergillus nidulans* mitochondrial DNA in *Escherichia coli* on plasmid pBR322. *Mol Gen Genet MGG*. 1981;182:332–335. doi:10.1007/BF00269679
130. Klein M, Eckert-Ossenkopp U, Schmiedeberg I, Brandt P, Unseld M, Brennicke A, et al. Physical mapping of the mitochondrial genome of *Arabidopsis thaliana* by cosmid and YAC clones. *Plant J*. 1994;6:447–455. doi:10.1046/j.1365-313X.1994.06030447.x
131. Gibson DG, Smith HO, Hutchison CA, Venter JC, and Merryman C. Chemical synthesis of the mouse mitochondrial genome. *Nat Methods*. 2010;7:901–903. doi:10.1038/nmeth.1515
132. Kaushal S and Freudenreich CH. The role of fork stalling and DNA structures in causing chromosome fragility. *Genes Chromosom Cancer*. 2019;58:270–283. doi:10.1002/gcc.22721
133. Bierne H and Michel B. When replication forks stop. *Mol Microbiol*. 1994;13:17–23. doi:10.1111/j.1365-2958.1994.tb00398.x
134. Silva F, Queiroz JA, and Domingues FC. Evaluating metabolic stress and plasmid stability in plasmid DNA production by *Escherichia coli*. *Biotechnol Adv*. 2012;30:691–708. doi:10.1016/j.biotechadv.2011.12.005
135. Mita S, Monnat RJ, and Loeb LA. Direct selection of mutations in the human mitochondrial tRNA<sup>Thr</sup> gene: Reversion of an ‘uncloneable’ phenotype. *Mutat Res Mol Mech Mutagen*. 1988;199:183–190. doi:10.1016/0027-5107(88)90244-8
136. Sorek R, Zhu Y, Creevey CJ, Francino MP, Bork P, and Rubin EM. Genome-wide experimental determination of barriers to horizontal gene transfer. *Science*. 2007;318:1449–1452. doi:10.1126/science.1147112
137. Berg PE, Lewin A, Christianson T, and Rabinowitz M. Propagation of restriction fragments from the mitochondrial DNA of *Saccharomyces cerevisiae* in *E. coli* by means of plasmid vectors. *Nucleic Acids Res*. 1979;6:2133–2150. doi:10.1093/nar/6.6.2133
138. Bigger B, Tolmachov O, Collombet J-M, and Coutelle C. Introduction of chloramphenicol resistance into the modified mouse mitochondrial genome: Cloning of unstable sequences by passage through yeast. *Anal Biochem*. 2000;277:236–242. doi:10.1006/abio.1999.4382

139. Flores S, de Anda-Herrera R, Gosset G, and Bolívar FG. Growth-rate recovery of *Escherichia coli* cultures carrying a multicopy plasmid, by engineering of the pentose-phosphate pathway. *Biotechnol Bioeng.* 2004;87:485–494. doi:10.1002/bit.20137
140. Ow DS-W, Nissom PM, Philp R, Oh SK-W, and Yap MG-S. Global transcriptional analysis of metabolic burden due to plasmid maintenance in *Escherichia coli* DH5 $\alpha$  during batch fermentation. *Enzyme Microb Technol.* 2006;39:391–398. doi:10.1016/j.enzmictec.2005.11.048
141. Lightowers RN. Mitochondrial transformation: Time for concerted action. *EMBO Rep.* 2011;12:480–481. doi:10.1038/embor.2011.93
142. Koulintchenko MV, Dietrich A, and Konstantinov YM. Mitochondrial genetic transformation via biotechnological approaches or natural competence mechanism: Do we have a choice? *Biopolym Cell.* 2012;28:261–266. doi:10.7124/bc.000058
143. Patananan AN, Wu T-H, Chiou P-Y, and Teitell MA. Modifying the mitochondrial genome. *Cell Metab.* 2016;23:785–796. doi:10.1016/j.cmet.2016.04.004
144. Collombet J-M, Wheeler VC, Vogel F, and Coutelle C. Introduction of plasmid DNA into isolated mitochondria by electroporation. *J Biol Chem.* 1997;272:5342–5347. doi:10.1074/jbc.272.8.5342
145. Yoon YG and Koob MD. Transformation of isolated mammalian mitochondria by bacterial conjugation. *Nucleic Acids Res.* 2005;33:e139–e139. doi:10.1093/nar/gni140
146. Cohen JS and Fox TD. Expression of green fluorescent protein from a recoded gene inserted into *Saccharomyces cerevisiae* mitochondrial DNA. *Mitochondrion.* 2001;1:181–189. doi:10.1016/S1567-7249(01)00012-5
147. Hu Z, Zhao Z, Wu Z, Fan Z, Chen J, Wu J, et al. Successful expression of heterologous *egfp* gene in the mitochondria of a photosynthetic eukaryote *Chlamydomonas reinhardtii*. *Mitochondrion.* 2011;11:716–721. doi:10.1016/j.mito.2011.05.012
148. Randolph-Anderson BL, Boynton JE, Gillham NW, Harris EH, Johnson AM, Dorthu M-P, et al. Further characterization of the respiratory deficient *dum-1* mutation of *Chlamydomonas reinhardtii* and its use as a recipient for mitochondrial transformation. *Mol Gen Genet MGG.* 1993;236:235–244. doi:10.1007/BF00277118

149. Bonnefoy N and Fox TD. Directed alteration of *Saccharomyces cerevisiae* mitochondrial DNA by biolistic transformation and homologous recombination. In *Methods molecular biology*; 2007; Vol. 372, pp. 153–166 ISBN 6176321972.
150. Johnston SA, Anziano PQ, Shark K, Sanford JC, and Butow RA. Mitochondrial transformation in yeast by bombardment with microprojectiles. *Science*. 1988;240:1538–1541. doi:10.1126/science.2836954
151. Fox TD, Sanford JC, and McMullin TW. Plasmids can stably transform yeast mitochondria lacking endogenous mtDNA. *Proc Natl Acad Sci*. 1988;85:7288–7292. doi:10.1073/pnas.85.19.7288
152. Steele DF, Butler CA, and Fox TD. Expression of a recoded nuclear gene inserted into yeast mitochondrial DNA is limited by mRNA-specific translational activation. *Proc Natl Acad Sci*. 1996;93:5253–5257. doi:10.1073/pnas.93.11.5253
153. Golik P, Bonnefoy N, Szczepanek T, Saint-Georges Y, and Lazowska J. The Rieske FeS protein encoded and synthesized within mitochondria complements a deficiency in the nuclear gene. *Proc Natl Acad Sci*. 2003;100:8844–8849. doi:10.1073/pnas.1432907100
154. Bonnefoy N and Remacle C. Biolistic transformation of *Chlamydomonas reinhardtii* and *Saccharomyces cerevisiae* mitochondria. *Methods Mol Biol*. 2022;1–19.
155. Remacle C, Cardol P, Coosemans N, Gaisne M, and Bonnefoy N. High-efficiency biolistic transformation of *Chlamydomonas* mitochondria can be used to insert mutations in complex I genes. *Proc Natl Acad Sci*. 2006;103:4771–4776. doi:10.1073/pnas.0509501103
156. Yamasaki T, Kurokawa S, Watanabe KI, Ikuta K, and Ohama T. Shared molecular characteristics of successfully transformed mitochondrial genomes in *Chlamydomonas reinhardtii*. *Plant Mol Biol*. 2005;58:515–527. doi:10.1007/s11103-005-7081-3
157. Suhm T, Habernig L, Rzepka M, Kaimal JM, Andréasson C, Buettner S, et al. A novel system to monitor mitochondrial translation in yeast. *Microb Cell*. 2018;5:158–164. doi:10.15698/mic2018.03.621
158. O’Brien JA and Lummis SCR. Nano-biolistics: A method of biolistic transfection of cells and tissues using a gene gun with novel nanometer-sized projectiles. *BMC Biotechnol*. 2011;11:66. doi:10.1186/1472-6750-11-66
159. O’Brien JA, Holt M, Whiteside G, Lummis SCR, and Hastings MH. Modifications to the hand-held gene gun: Improvements for *in vitro* biolistic transfection of organotypic neuronal tissue. *J Neurosci Methods*. 2001;112:57–64. doi:10.1016/S0165-0270(01)00457-5

160. Waters VL. Conjugative transfer in the dissemination of beta-lactam and aminoglycoside resistance. *Front Biosci.* 1999;4:d433-456. doi:10.2741/Waters
161. Pansegrau W, Lanka E, Barth PT, Figurski DH, Guiney DG, Haas D, et al. Complete nucleotide sequence of Birmingham IncP $\alpha$  plasmids. *J Mol Biol.* 1994;239:623–663. doi:10.1006/jmbi.1994.1404
162. Grahn AM, Haase J, Bamford DH, and Lanka E. Components of the RP4 conjugative transfer apparatus form an envelope structure bridging inner and outer membranes of donor cells: Implications for related macromolecule transport systems. *J Bacteriol.* 2000;182:1564–1574. doi:10.1128/JB.182.6.1564-1574.2000
163. Eisenbrandt R, Kalkum M, Lurz R, and Lanka E. Maturation of IncP pilin precursors resembles the catalytic dyad-like mechanism of leader peptidases. *J Bacteriol.* 2000;182:6751–6761. doi:10.1128/JB.182.23.6751-6761.2000
164. Eisenbrandt R, Kalkum M, Lai E-M, Lurz R, Kado CI, and Lanka E. Conjugative pili of IncP plasmids, and the Ti plasmid T pilus are composed of cyclic subunits. *J Biol Chem.* 1999;274:22548–22555. doi:10.1074/jbc.274.32.22548
165. Ziegelin G, Fürste JP, and Lanka E. TraJ protein of plasmid RP4 binds to a 19-base pair invert sequence repetition within the transfer origin. *J Biol Chem.* 1989;264:11989–11994. doi:10.1016/S0021-9258(18)80164-8
166. Fürste JP, Pansegrau W, Ziegelin G, Kröger M, and Lanka E. Conjugative transfer of promiscuous IncP plasmids: Interaction of plasmid-encoded products with the transfer origin. *Proc Natl Acad Sci.* 1989;86:1771–1775. doi:10.1073/pnas.86.6.1771
167. Pansegrau W, Balzer D, Kruff V, Lurz R, and Lanka E. *In vitro* assembly of relaxosomes at the transfer origin of plasmid RP4. *Proc Natl Acad Sci.* 1990;87:6555–6559. doi:10.1073/pnas.87.17.6555
168. Pansegrau W, Schröder W, and Lanka E. Relaxase (TraI) of IncP $\alpha$  plasmid RP4 catalyzes a site-specific cleaving-joining reaction of single-stranded DNA. *Proc Natl Acad Sci.* 1993;90:2925–2929. doi:10.1073/pnas.90.7.2925
169. Pansegrau W and Lanka E. Mechanisms of initiation and termination reactions in conjugative DNA processing. *J Biol Chem.* 1996;271:13068–13076. doi:10.1074/jbc.271.22.13068
170. Rees CED and Wilkins BM. Protein transfer into the recipient cell during bacterial conjugation: Studies with F and RP4. *Mol Microbiol.* 1990;4:1199–1205. doi:10.1111/j.1365-2958.1990.tb00695.x



171. Ziegelin G, Pansegrau W, Lurz R, and Lanka E. TraK protein of conjugative plasmid RP4 forms a specialized nucleoprotein complex with the transfer origin. *J Biol Chem.* 1992;267:17279–17286. doi:10.1016/S0021-9258(18)41923-0
172. Heinemann JA and Sprague GF. Bacterial conjugative plasmids mobilize DNA transfer between bacteria and yeast. *Nature.* 1989;340:205–209. doi:10.1038/340205a0
173. Piers KL, Heath JD, Liang X, Stephens KM, and Nester EW. *Agrobacterium tumefaciens*-mediated transformation of yeast. *Proc Natl Acad Sci.* 1996;93:1613–1618. doi:10.1073/pnas.93.4.1613
174. Nishikawa M and Yoshida K. Trans-kingdom conjugation offers a powerful gene targeting tool in yeast. *Genet Anal Biomol Eng.* 1998;14:65–73. doi:10.1016/S1050-3862(97)10003-1
175. Hayman GT and Bolen PL. Movement of shuttle plasmids from *Escherichia coli* into yeasts other than *Saccharomyces cerevisiae* using trans-kingdom conjugation. *Plasmid.* 1993;30:251–257. doi:10.1006/plas.1993.1056
176. Lim YM, de Groof AJC, Bhattacharjee MK, Figurski DH, and Schon EA. Bacterial conjugation in the cytoplasm of mouse cells. *Infect Immun.* 2008;76:5110–5119. doi:10.1128/IAI.00445-08
177. Yoon YG and Koob MD. Nonreplicating intracellular bacterial vector for conjugative DNA transfer into mitochondria. *Pharm Res.* 2012;29:1040–1045. doi:10.1007/s11095-012-0701-0
178. Vestweber D and Schatz G. DNA-protein conjugates can enter mitochondria via the protein import pathway. *Nature.* 1989;338:170–172. doi:10.1038/338170a0
179. Seibel P, Trappe J, Villani G, Klopstock T, Papa S, and Reichmann H. Transfection of mitochondria: Strategy towards a gene therapy of mitochondrial DNA diseases. *Nucleic Acids Res.* 1995;23:10–17. doi:10.1093/nar/23.1.10
180. Hyde KD, Xu J, Rapior S, Jeewon R, Lumyong S, Niego AGT, et al. The amazing potential of fungi: 50 ways we can exploit fungi industrially. *Fungal Divers.* 2019;97:1–136. doi:10.1007/s13225-019-00430-9
181. Fabris M, Abbriano RM, Pernice M, Sutherland DL, Commault AS, Hall CC, et al. Emerging technologies in algal biotechnology: Toward the establishment of a sustainable, algae-based bioeconomy. *Front Plant Sci.* 2020;11:1–22. doi:10.3389/fpls.2020.00279
182. Adarme-Vega TC, Lim DKY, Timmins M, Vernen F, Li Y, and Schenk PM. Microalgal biofactories: A promising approach towards sustainable omega-3 fatty acid production. *Microb Cell Fact.* 2012;11:1–10. doi:10.1186/1475-2859-11-96

183. Buzzini P, Turchetti B, and Yurkov A. Extremophilic yeasts: The toughest yeasts around? *Yeast*. 2018;35:487–497. doi:10.1002/yea.3314
184. Goffeau A, Barrell BG, Bussey H, Davis RW, Dujon B, Feldmann H, et al. Life with 6000 genes. *Science*. 1996;274:546–567. doi:10.1126/science.274.5287.546
185. Fisher MC, Gurr SJ, Cuomo CA, Blehert DS, Jin H, Stukenbrock EH, et al. Threats posed by the fungal kingdom to humans, wildlife, and agriculture. *MBio*. 2020;11:e00449-20. doi:10.1128/mBio.00449-20
186. Limon JJ, Tang J, Li D, Wolf AJ, Michelsen KS, Funari V, et al. *Malassezia* is associated with Crohn’s disease and exacerbates colitis in mouse models. *Cell Host Microbe*. 2019;25:377–388. doi:10.1016/j.chom.2019.01.007
187. Pappas PG, Lionakis MS, Arendrup MC, Ostrosky-Zeichner L, and Kullberg BJ. Invasive candidiasis. *Nat Rev Dis Prim*. 2018;4:1–20. doi:10.1038/nrdp.2018.26
188. Everard A, Matamoros S, Geurts L, Delzenne NM, and Cani PD. *Saccharomyces boulardii* administration changes gut microbiota and reduces hepatic steatosis, low-grade inflammation, and fat mass in obese and type 2 diabetic db/db mice. *MBio*. 2014;5:e01011-14. doi:10.1128/mBio.01011-14
189. Parapouli M, Vasileiadi A, Afendra A-S, and Hatziloukas E. *Saccharomyces cerevisiae* and its industrial applications. *AIMS Microbiol*. 2020;6:1–31. doi:10.3934/microbiol.2020001
190. Segal-Kischinevzky C, Romero-Aguilar L, Alcaraz LD, López-Ortiz G, Martínez-Castillo B, Torres-Ramírez N, et al. Yeasts inhabiting extreme environments and their biotechnological applications. *Microorganisms*. 2022;10:794. doi:10.3390/microorganisms10040794
191. Mireau H, Arnal N, and Fox TD. Expression of Barstar as a selectable marker in yeast mitochondria. *Mol Genet Genomics*. 2003;270:1–8. doi:10.1007/s00438-003-0879-2
192. Hu Z, Fan Z, Zhao Z, Chen J, and Li J. Stable expression of antibiotic-resistant gene *ble* from *Streptoalloteichus hindustanus* in the mitochondria of *Chlamydomonas reinhardtii*. *PLoS One*. 2012;7:e35542. doi:10.1371/journal.pone.0035542
193. Larosa V, Coosemans N, Motte P, Bonnefoy N, and Remacle C. Reconstruction of a human mitochondrial complex I mutation in the unicellular green alga *Chlamydomonas*. *Plant J*. 2012;70:759–768. doi:10.1111/j.1365-313X.2012.04912.x

194. Zhou J, Liu L, and Chen J. Mitochondrial DNA heteroplasmy in *Candida glabrata* after mitochondrial transformation. *Eukaryot Cell*. 2010;9:806–814. doi:10.1128/EC.00349-09
195. Nass MMK. Abnormal DNA patterns in animal mitochondria: Ethidium bromide-induced breakdown of closed circular DNA and conditions leading to oligomer accumulation. *Proc Natl Acad Sci*. 1970;67:1926–1933. doi:10.1073/pnas.67.4.1926
196. Matagne RF, Michel-Wolwertz MR, Munaut C, Duyckaerts C, and Sluse F. Induction and characterization of mitochondrial DNA mutants in *Chlamydomonas reinhardtii*. *J Cell Biol*. 1989;108:1221–1226. doi:10.1083/jcb.108.4.1221
197. Remacle C, Baurain D, Cardol P, and Matagne RF. Mutants of *Chlamydomonas reinhardtii* deficient in mitochondrial complex I: Characterization of two mutations affecting the *ndl* coding sequence. *Genetics*. 2001;158:1051–1060. doi:10.1093/genetics/158.3.1051
198. Foury F, Roganti T, Lecrenier N, and Purnelle B. The complete sequence of the mitochondrial genome of *Saccharomyces cerevisiae*. *FEBS Lett*. 1998;440:325–331. doi:10.1016/S0014-5793(98)01467-7
199. Vanderwaeren L, Dok R, Voordeckers K, Nuyts S, and Verstrepen KJ. *Saccharomyces cerevisiae* as a model system for eukaryotic cell biology, from cell cycle control to DNA damage response. *Int J Mol Sci*. 2022;23:11665. doi:10.3390/ijms231911665
200. Thorsness PE and Fox TD. Escape of DNA from mitochondria to the nucleus in *Saccharomyces cerevisiae*. *Nature*. 1990;346:376–379. doi:10.1038/346376a0
201. Shafer KS, Hanekamp T, White KH, and Thorsness PE. Mechanisms of mitochondrial DNA escape to the nucleus in the yeast *Saccharomyces cerevisiae*. *Curr Genet*. 1999;36:183–194. doi:10.1007/s002940050489
202. Bennoun P, Delosme M, and Kück U. Mitochondrial genetics of *Chlamydomonas reinhardtii*: Resistance mutations marking the cytochrome *b* gene. *Genetics*. 1991;127:335–343. doi:10.1093/genetics/127.2.335
203. Nelson DM, Tréguer P, Brzezinski MA, Leynaert A, and Quéguiner B. Production and dissolution of biogenic silica in the ocean: Revised global estimates, comparison with regional data and relationship to biogenic sedimentation. *Global Biogeochem Cycles*. 1995;9:359–372. doi:10.1029/95GB01070
204. Tréguer P, Nelson DM, Van Bennekom AJ, DeMaster DJ, Leynaert A, and Quéguiner B. The silica balance in the world ocean: A reestimate. *Science*. 1995;268:375–379. doi:10.1126/science.268.5209.375

## Chapter 2

### 2 Rapid method for generating designer algal mitochondrial genomes

The work presented in this chapter is adapted from:

Cochrane, RR, Brumwell, SL, Soltysiak, PM, Hamadache, S, Davis, JG, Wang, J, Tholl, SQ, Janakirama, P, Edgell, DR, & Karas, BJ (2020). Rapid method for generating designer algal mitochondrial genomes. *Algal Research*, 50, 102014.

#### 2.1 Introduction

Pressing challenges in agriculture, medicine, and energy can be addressed using designer organisms with engineered traits. The promise of synthetic biology lies in the ability to build, deliver, install, and test synthetic genomes and biosynthetic pathways in specialized hosts. *Phaeodactylum tricorutum* is a model diatom algal species that is an attractive candidate for synthetic biology applications [1–5]. For example, *P. tricorutum* is a popular candidate for biofuel production due to its natural propensity for lipid storage [6]. Due to the industrial and academic interest in this algal species, nuclear, mitochondrial, and plastid genomes were sequenced [7–9]. The availability of genome sequences has allowed for the development of genetic tools and DNA delivery methods such as biolistic-mediated transformation [10,11], electroporation [12–14], and bacterial conjugation [15,16]. Additional tools for *P. tricorutum* include a method for cloning whole chromosomes in yeast and *Escherichia coli* [17], characterized centromeres for maintaining episomal DNA [18], and genome-editing technologies [19–22]. We now have a powerful arsenal of tools for engineering algal nuclear genomes; however, tools for engineering and delivering organelle genomes are still lacking.

There are several advantages to engineering organelle genomes and installing synthetic DNA in these compartments rather than the nucleus. First, the polycistronic gene organization, lack of transgene silencing, and reduced positional effects in

organellar DNA simplify genome engineering relative to the nucleus. Second, organelles allow for the compartmentalization of biosynthetic pathways, which confines toxic intermediates, increases the metabolic flux, and minimizes competing reactions from the rest of the cell [23]. To exploit these benefits, scientists have cloned whole organelle genomes from various organisms, including human, mouse, maize, rice, and some algae [24–29]. Yet, a rapid method for whole organelle genome engineering for eukaryotic algae has not been established.

The first obstacle is the need for a fast and inexpensive method for synthesizing, assembling, and storing synthetic organelle genomes. While processes for synthesizing and replacing nuclear genomes have been established for some prokaryotes [30–34] and eukaryotes [35], genome-scale engineering and delivery are still very challenging [36]. The large, repetitive elements and AT-rich sequences of organelle genomes complicate the synthesis and cloning processes. Spurious expression of cloned genomes can be toxic to host organisms, including *Saccharomyces cerevisiae* and *E. coli* [37]. Importantly, the targeted delivery of whole organelle genomes to the appropriate cellular compartment in eukaryotic algal cells is still not possible.

Here, we report a rapid protocol for cloning designer *P. tricornutum* mitochondrial genomes with sizes ranging from ~60–95 kbp and demonstrate their maintenance in eukaryotic and prokaryotic host strains as the first step of a platform for robust, genome-scale mitochondrial genome engineering. We used TAR cloning to capture the wild-type mitochondrial genome of *P. tricornutum* and developed a PCR-based approach to clone modified versions of the genome. We then demonstrated the maintenance of wild-type and modified mitochondrial genomes in *S. cerevisiae* and *E. coli*.

## 2.2 Results and Discussion

### 2.2.1 Design-build-test cycle to enable rapid engineering of organelle genomes

Currently, there are no established methods for replacing whole eukaryotic algal organelle genomes. To address this need and enable full use of the organelle compartment for installing synthetic genomes, we are developing a design-build-test cycle for efficient capture, manipulation, delivery, and installation of organelle genomes (Figure 2-1A).

In one iteration of the design and build stages of the cycle, we cloned a whole mitochondrial genome and a reduced version with a repetitive region removed. To capture the whole mitochondrial genome, TAR cloning was used (Figure 2-1B). For TAR cloning, total algal DNA was captured in agarose plugs to obtain isolated, intact organelle genomes. Next, the mitochondrial DNA was linearized by a restriction enzyme that recognizes a single cut-site in the targeted mitochondrial genome. If there are no unique restriction enzyme cut-sites available, it is possible to select a restriction enzyme that cuts in multiple locations and perform a partial digest to obtain a proportion of genomes with a single cut at the desired location. If the cut site resides within an essential gene, a modified version (lacking the restriction enzyme cut site) of the gene can be added to the plasmid backbone. Alternatively, once the genome is cloned in yeast, the plasmid backbone can be moved to a different location by co-transforming a plasmid containing homology hooks to the new location and another fragment that will delete the plasmid in the original location and restore the interrupted gene. Finally, a clustered regularly interspaced palindromic repeats/CRISPR-associated protein 9 (CRISPR/Cas9) system can be devised to produce appropriate cut-sites at the desired location [39,40].

The linearized algal mitochondrial genome was captured by transforming it into *S. cerevisiae* along with a PCR-amplified plasmid backbone containing homology on each end to the mitochondrial genome regions flanking the cut-site. Although the process is more time-consuming, an entire organellar genome can be cloned. In PCR-based cloning

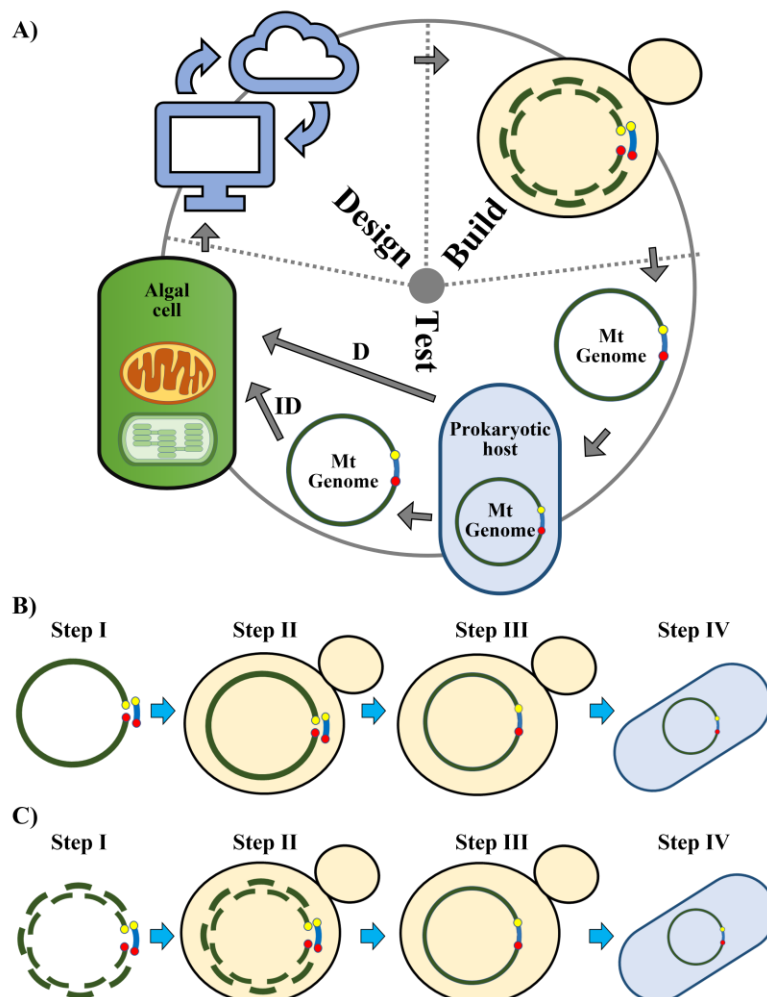


**Figure 2-1: Design-build-test cycle for the rapid engineering of mitochondrial genomes.** **A)** Genomes will be designed based on existing knowledge and discoveries from previous cycles; in the build stage, genomes will be synthesized, then assembled and cloned in yeast; in the test stage, genomes will be isolated from yeast, moved to an intermediate prokaryotic host and delivered directly (**D**) (e.g., bacterial conjugation, cell fusion) or indirectly (**ID**) (e.g., electroporation, biolistic-mediated transformation) to the mitochondria to test for viability, function, and localization. Mt – mitochondrial. **B–C)** Schematic of the approaches used to clone the mitochondrial genomes of *P. tricornutum*. **B)** Transformation-associated recombination (TAR) cloning method; **C)** PCR-based cloning method. Step I differs between the PCR-based and TAR cloning methods where, for the PCR-based cloning method, multiple overlapping fragments (green) are amplified, while for the TAR cloning method, the mitochondrial genome is linearized at a specific location. For both methods, the plasmid backbone (blue) contains homology overlaps (yellow and red) to the appropriate fragments or location in the genome. Steps II–IV are the same for both methods including DNA transformation (Step II), assembly in *S. cerevisiae* via homologous recombination (Step III), and transfer of cloned genomes into *E. coli* (Step IV).

(Figure 2-1C), the mitochondrial genome was cloned indirectly by amplifying fragments from total algal DNA with homologous DNA overhangs to adjacent fragments, followed by transformation into *S. cerevisiae* with the plasmid backbone. This process has allowed for the fast assembly of large plasmids [41]. However, it also has some drawbacks, including the risk of introducing unwanted point mutations and difficulty amplifying larger repetitive elements, which could limit the practicality and versatility of this approach. In both methods, elements required for replication in yeast (e.g., *CEN6-ARSH4-HIS3*) and *E. coli* (e.g., the origin of replication and selectable marker) must be provided as one or multiple plasmid backbone fragments containing appropriate homologous overhangs.

### **2.2.2 Cloning of the *P. tricornutum* mitochondrial genome**

Using the PCR-based approach, we cloned a reduced version of the *P. tricornutum* mitochondrial genome (Figure 2-2A). The wild-type genome was PCR-amplified in eight overlapping fragments that excluded a 35 kbp region of direct repeats [8]. In place of this repeat region, two fragments with genetic elements required for replication and selection in *S. cerevisiae*, *E. coli*, and algae (nuclear localization) were amplified from the multi-host shuttle plasmid pAGE3.0 [16]. In total, 10 DNA fragments were amplified (Figure 2-2B) and assembled following transformation and homologous recombination in *S. cerevisiae* spheroplasts, yielding 5023 transformed yeast colonies (Table 2-1). After moving the assembled plasmids to *E. coli*, two clones, pPT-PCR C1 and C2, were validated by multiplex (MPX) PCR and restriction digests (Figure 2-2C, D) were sequenced and analyzed for mutations (Section 2.2.3).

Importantly, we wanted to assess the fidelity of the PCR-based cloning method by comparing cloned sequences to their parental reference. However, the amplified fragments initially used in this iteration were derived from a potentially heterogenic population of mitochondrial genomes, which may differ from the published sequence. Therefore, to directly determine the mutation rate of the cloning method, the



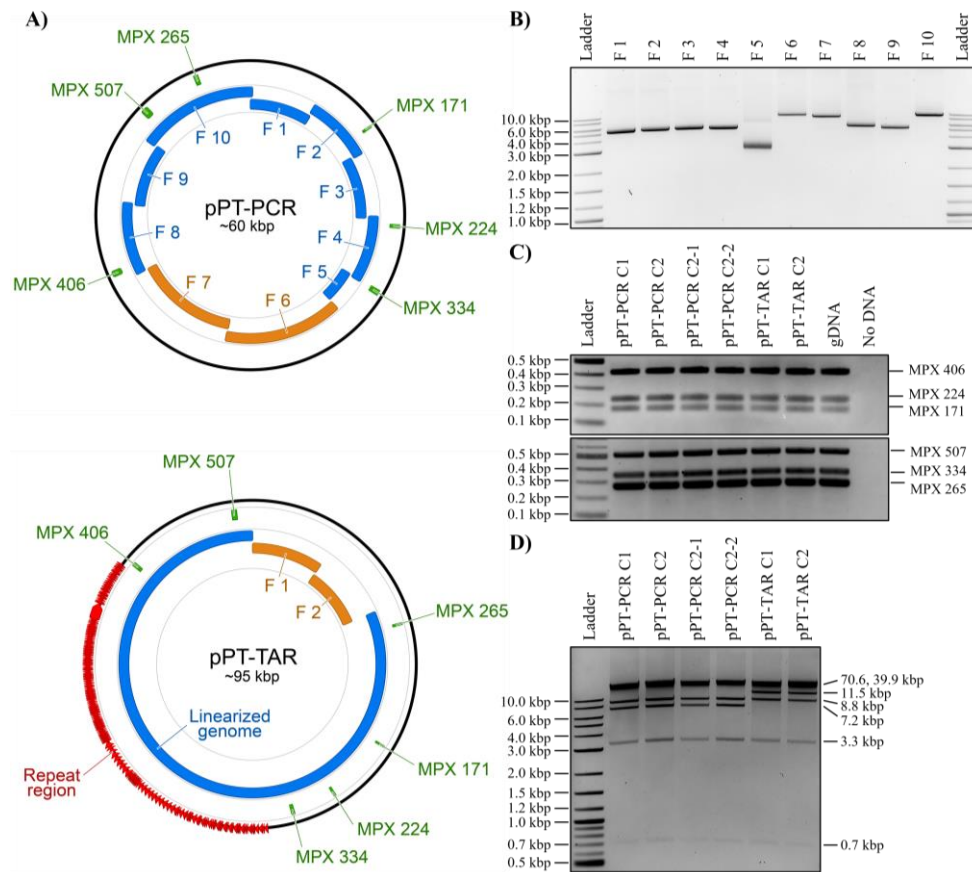


**Figure 2-2. Design, amplification, and analyses of cloned *P. tricornutum* mitochondrial genomes.** **A)** Plasmid maps of the *P. tricornutum* mitochondrial genomes cloned using PCR-based cloning (top) or transformation-associated recombination (TAR) cloning (bottom). For the PCR-based cloning method, the relative sizes and positions of the eight mitochondrial fragments (blue) and the two plasmid backbone fragments (orange) are shown. For the TAR cloning method, the relative sizes and positions of the linearized genome (blue) and the two plasmid backbone fragments (orange) are shown. In addition, the six MPX PCR amplicons used for diagnostic screening are indicated (green). These images were generated using Geneious version 2020.0, created by Biomatters. **B)** Agarose gel electrophoresis of the 8 PCR-amplified fragments of the *P. tricornutum* mitochondrial genome (fragments 1–5 and 8–10) and the pAGE3.0 backbone (fragments 6 and 7) for PCR-based cloning. The resulting amplicon sizes for fragments 1–10 are 5217-, 5190-, 5197-, 5175-, 2765-, 9124-, 8571-, 5605-, 5299-, and 9264-bp, respectively. **C)** MPX PCR screen of six cloned algal mitochondrial genomes isolated from *E. coli*. The expected size for each MPX amplicon is indicated by its name (in bp). **D)** Diagnostic restriction enzyme digest of six cloned algal mitochondrial genomes using *SrfI* and *SacII*. For the pPT-PCR clones, the expected band sizes are 39,925-, 8758-, 7177-, 3276-, and 707-bp; and for the pPT-TAR clones, the expected band sizes are 70,647-, 11,506-, 8758-, 3276-, and 707-bp. Notes: 1) There was no observable size difference between the 70.6 kbp and 39.9 kbp fragments, which is most likely due to the electrophoresis conditions (1% agarose gel, 100 V for 90 min); 2) The 707-bp band is present but very faint. For all gels, we used NEB 2-log ladder.

**Table 2-1: Cloning of the *P. tricornutum* mitochondrial genome in the host organisms *S. cerevisiae* and *E. coli*.** Two PCR-based cloning assemblies and one transformation-associated recombination (TAR) cloning assembly were performed. For the *E. coli* selection media, CM indicates chloramphenicol antibiotic. For the *S. cerevisiae* selection media, -HIS indicates synthetic complete media lacking histidine.

Design	<i>S. cerevisiae</i>			<i>E. coli</i>			
	Selection media	Colony count	MPX PCR screen	Selection media	Selected yeast colony: <i>E. coli</i> colony count	MPX PCR screen	Final genomes selected for analysis
Reduced genome PCR – 10 fragments Total DNA	-HIS	5023	20/20	CM	Yeast colony C1: 30 Yeast colony C2: 18	C1 = 8/8 C2 = 8/8	pPT-PCR C1 pPT-PCR C2
Reduced genome PCR – 10 fragments Clone pPT-PCR C2	-HIS	4880	20/20	CM	N/D	C2-1 = 5/5 C2-2 = 5/5	pPT-PCR C2-1 pPT-PCR C2-2
Full genome TAR – 3 fragments Digested total DNA	-HIS	608	2/204	CM	Yeast colony C1: 119 Yeast colony C2: 46	C1 = 1/1 C2 = 2/2	pPT-TAR C1 pPT-TAR C2

mitochondrial genome was re-amplified using DNA isolated from an isogenic culture of *E. coli* carrying pPT-PCR C2. The 10 fragments were assembled using the same method, with similar results as the first assembly (Table 2-1, Section 2.2.3). Two additional clones, pPT-PCR C2-1, and C2-2, were selected for further analysis.

We used the TAR cloning-based approach to clone the complete, repeat-containing genome (Figure 2-2A). Total *P. tricornutum* DNA was digested with the restriction enzyme PvuI, which cuts the mitochondrial genome at a single site. We amplified the plasmid backbone from pAGE3.0 as two fragments with end homology to each other and the sequences flanking the mitochondrial PvuI cut site. Transforming both PCR-amplified plasmid backbone fragments and the linearized genome into *S. cerevisiae* spheroplasts yielded 604 colonies (Table 2-1), from which 204 were screened and two clones, pPT-TAR C1, and C2, were identified as positive for the presence of the mitochondrial genome using MPX PCR. We then transferred these genomes to *E. coli* and reanalyzed them with MPX PCR and diagnostic restriction digest (Figure 2-2C, D). Although the build stage using the TAR cloning approach was successful, it was time-consuming and labor-intensive due to the requirement of obtaining high-quality DNA and screening a larger number of colonies. Nonetheless, this iteration can act as a good template for future design-build cycles, particularly for cloning large organellar genomes that are difficult to amplify by PCR.

### **2.2.3 Sequence analysis of cloned *P. tricornutum* mitochondrial genomes**

The six selected *P. tricornutum* mitochondrial clones were sequenced and analyzed for mutations. Sequences obtained for the original PCR-cloned (pPT-PCR C1 and pPT-PCR C2) and TAR cloned (pPT-TAR C1 and pPT-TAR C2) plasmids were aligned to reference sequences based on the published sequences [8,16]. The reassembled PCR-cloned plasmids (pPT-PCR C2-1 and pPT-PCR C2-2) were aligned to the sequence of their parent clone, pPT-PCR C2. Upon analyzing pPT-PCR C1 and C2, an average of 7 mutations per 60 kbp was found (Table 2-2), corresponding to 1 mutation per 8.6 kbp.

**Table 2-2: Summary of mutations identified in the cloned *P. tricornutum* mitochondrial plasmids.** Identified mutations are categorized as point mutations (synonymous, missense, nonsense, and those found in non-coding regions) or gap mutations (insertions and deletions, either non-coding or coding).

Clone	Point mutations				Gap mutations				Total
	Synonymous	Missense	Nonsense	Non-coding	Non-coding		Coding		
					Insertions	Deletions	Insertions	Deletions	
pPT-PCR C1	0	4	0	2	1	1	1	0	9
pPT-PCR C2	0	3	1	0	0	1	0	0	5
pPT-PCR C2-1	0	3	0	2	0	0	0	0	5
pPT-PCR C2-2	0	1	0	0	0	0	0	0	1
pPT-TAR C1	1	0	0	0	0	0	0	0	1
pPT-TAR C2	0	0	0	7	1	8	0	0	16

The two reassembled clones, pPT-PCR C2-1 and C2-2, acquired an average of 3 mutations per 60 kbp (Table 2-2), corresponding to 1 mutation per 20 kbp. See Supplementary Table B-2 for additional information about specific mutations. pPT-TAR C1 had only a single synonymous substitution (Table 2-2). However, the other clone generated using this method, pPT-TAR C2, contained a series of deletions in the repetitive region of the *P. tricornutum* mitochondrial genome (Table 2-2). This clone also carried eight single nucleotide substitutions, albeit all in non-coding regions of the plasmid except a synonymous mutation in the *cox3* gene. The difference in mutation rate between these two plasmids could be the result of recombination of the highly repetitive region of the mitochondrial genome during TAR cloning or an artifact of the sequencing method used as resolving large repetitive regions may require the use of long-read sequencing technologies.

Genetic changes found using both cloning methods could have occurred during the cloning process of each mitochondrial plasmid or during propagation in the host organisms harboring the plasmids. It is also plausible that some of these variants could naturally exist in the population of *P. tricornutum* mitochondrial genomes. If desired, identified mutations could be fixed through additional iterations of the design-build-test cycle. If necessary individual fragments would be cloned, and the sequence confirmed before being used in yeast assembly.

#### **2.2.4 Maintenance of *P. tricornutum* mitochondrial plasmids in host organisms**

*S. cerevisiae* and *E. coli* were used as host organisms to capture and store the *P. tricornutum* mitochondrial genome. *S. cerevisiae* was chosen because it is currently the best organism for assembling large DNA molecules due to its highly efficient homologous recombination machinery and demonstrated ability to maintain a wide range of genomes without adverse effects [42]. However, when using standard protocols for isolating pDNA, the yields from *S. cerevisiae* tend to be low. To overcome this problem, after assembly in *S. cerevisiae*, the cloned mitochondrial plasmids were transformed into

*E. coli*. In *E. coli*, the mitochondrial plasmids, which contain an arabinose-inducible origin of replication, can be induced to a higher copy number to generate increased DNA yields. Importantly, propagating genomes in *E. coli* allows for the development of direct transfer methods, such as bacterial conjugation, to deliver the plasmids to the desired destination organism. At the same time, because mitochondrial genomes are hypothesized to be of prokaryotic origin, there is a chance that a prokaryotic host would express functional proteins that might have adverse or toxic effects [32,43].

We sought to examine the burden of propagating the cloned mitochondrial genomes in eukaryotic and prokaryotic host strains. Colony formation on selective plates and growth rates in liquid media for both *S. cerevisiae* and *E. coli* strains carrying these plasmids were evaluated. If a plasmid causes cellular stress, it can decrease the growth rate and form smaller or fewer colonies on the plate. In *S. cerevisiae*, there was no observable decrease in colony size when strains harboring cloned mitochondrial genomes were dilution spot plated, compared with control plasmids with the same backbone, pAGE3.0 and pPtGE31 [19] (Figure 2-3A). Next, we compared growth in liquid media by using a 96-well plate reader. Interestingly, the strains carrying the mitochondrial genomes grew faster in liquid compared to the pAGE3.0 control but at a similar rate to the pPtGE31 control (Figure 2-3C and Table 2-3). Overall, this indicates that the maintenance of *P. tricornutum* mitochondrial genome plasmids do not have an adverse effect on yeast growth. In *E. coli*, we did not observe any substantial negative effects on growth rates of cells harboring *P. tricornutum* mitochondrial genomes compared to the control plasmids (Figure 2-3B, D, and Table 2-3). In addition, there was no substantial effect on growth rates when the cells were induced to have a high copy number of mitochondrial genomes. In future studies, additional experiments should be performed to evaluate the expression of all mitochondrial genes in *S. cerevisiae* and *E. coli*.

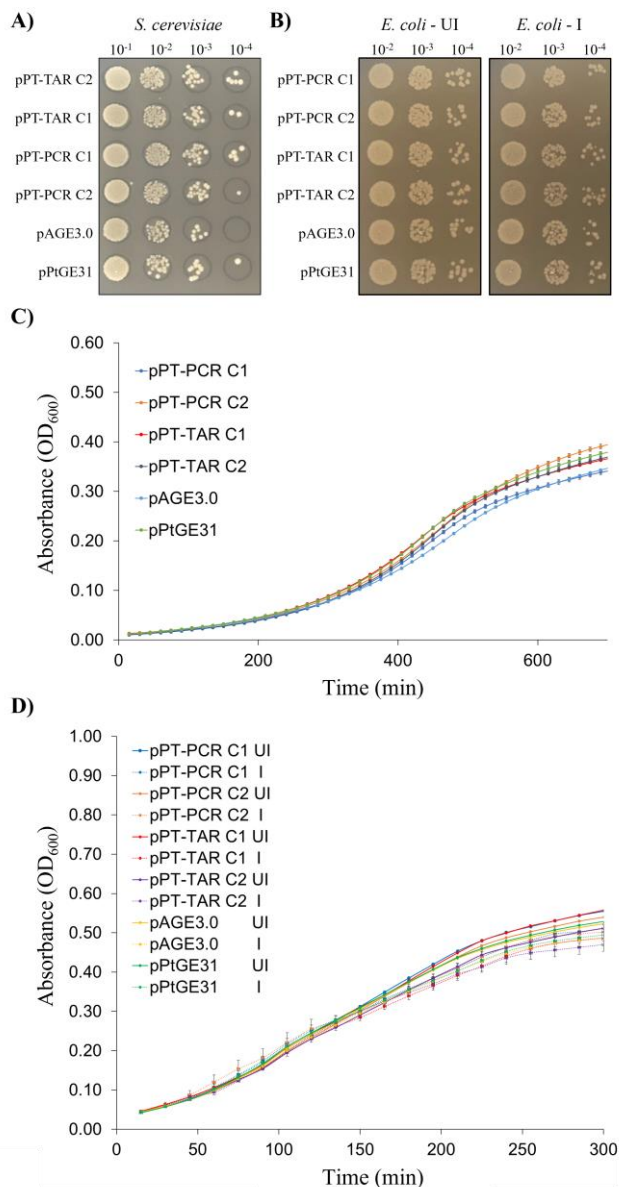


**Figure 2-3. Analysis of growth of *S. cerevisiae* and *E. coli* strains harboring cloned *P. tricornutum* mitochondrial genomes on solid media and in liquid media. A)** Dilutions ( $10^{-1}$ – $10^{-4}$ ) of *S. cerevisiae* strains plated on solid synthetic complete media lacking histidine supplemented with adenine ( $60 \text{ mg L}^{-1}$ ). **B)** Dilutions ( $10^{-2}$ – $10^{-4}$ ) of *E. coli* strains plated on solid LB media supplemented with chloramphenicol only (UI - uninduced) or with chloramphenicol and arabinose (I - induced) to increase plasmid copy number. **C)** Growth curves of *S. cerevisiae* strains grown in liquid synthetic complete media lacking histidine supplemented with adenine ( $60 \text{ mg L}^{-1}$ ). For each strain ( $n = 4$ ) and error bars represent the standard error of the mean. **D)** Growth curves of *E. coli* grown in liquid LB media supplemented with chloramphenicol only (UI) or with chloramphenicol and arabinose (I). For each strain ( $n = 8$ ) and error bars represent the standard error of the mean. td: doubling time.

**Table 2-3. Doubling time of host organisms harboring either a mitochondrial genome or control plasmid.** Doubling times of plasmid-containing *S. cerevisiae* strains were grown in synthetic complete yeast media lacking histidine at 30 °C with continuous, double orbital shaking. Doubling times of plasmid-containing *E. coli* strains were grown in either LB media supplemented with chloramphenicol (15 µg mL<sup>-1</sup>; Uninduced) or LB media supplemented with chloramphenicol (15 µg mL<sup>-1</sup>) and arabinose (100 µg mL<sup>-1</sup>; Induced) at 37 °C with continuous, double orbital shaking.

Sample	Doubling Time (min)		
	<i>S. cerevisiae</i>	<i>E. coli</i>	
		Uninduced	Induced
pPT-PCR C1	71	37	40
pPT-PCR C2	76	38	40
pPT-TAR C1	72	39	41
pPT-TAR C2	71	39	39
pAGE3.0	82	37	37
pPtGE31	72	37	38



## 2.3 Conclusions

The biotechnological potential of organelle engineering is held back by the need for more reliable methods to replace organellar genomes. Towards the goal of establishing a design-build-test cycle for genome-scale organelle engineering, we have developed two adaptable methods for cloning and manipulating eukaryotic mitochondrial genomes ranging in sizes from ~60–95 kbp. With a PCR-based cloning approach, we cloned a variant of the *P. tricornutum* mitochondrial genome lacking its 35 kbp repeat region, and with a TAR-based cloning approach, we captured the complete genome. The former had a mutation rate ranging from 1 mutation per 8.6–20 kbp, while the latter allowed us to identify one clone with only a single mutation. The cloned genomes imposed no substantial growth burden on *S. cerevisiae* and *E. coli* when these host organisms were used to propagate the plasmids. In this study, we completed the first step in developing a reproducible set of methods for cloning, manipulating, and installing synthetic organelle genomes.

## 2.4 Materials and Methods

### 2.4.1 Strains and growth conditions

*Phaeodactylum tricornutum* (Culture Collection of Algae and Protozoa CCAP 1055/1) was grown in synthetic seawater (L1 media) without silica at 18 °C under cool white fluorescent lights ( $75 \mu\text{E m}^{-2} \text{s}^{-1}$ ) and a photoperiod of 16 h light: 8 h dark. L1 media was made as previously described [15]. *Saccharomyces cerevisiae* VL6–48 (ATCC MYA-3666: *MAT $\alpha$* , *his3- $\Delta$ 200*, *trp1- $\Delta$ 1*, *ura3-52*, *lys2*, *ade2-101*, *met14*, *psi<sup>+</sup>*, *cir<sup>0</sup>*) was grown at 30 °C in rich yeast media (2 x YPDA: 20 g L<sup>-1</sup> yeast extract, 40 g L<sup>-1</sup> peptone, 40 g L<sup>-1</sup> glucose, and 200 mg L<sup>-1</sup> adenine hemisulfate), or synthetic complete media lacking histidine supplemented with adenine (60 mg L<sup>-1</sup>). Solid yeast media contained 2% agar. After spheroplast transformation, all complete minimal media used contained 1 M sorbitol [38]. *Escherichia coli* (Epi300, Lucigen) was grown at 37 °C in Lysogeny Broth (LB) supplemented with chloramphenicol (15  $\mu\text{g mL}^{-1}$ ).

## 2.4.2 DNA preparation

### 2.4.2.1 Isolations of *P. tricornutum* DNA in agarose plugs

For TAR cloning, total DNA was isolated from *P. tricornutum* in agarose plugs. *P. tricornutum* ( $1.0 \times 10^7$  cells mL<sup>-1</sup>) was plated and grown on 1% agarose L1 plates for four days. Next, 1 mL of 1 M sorbitol was used to scrape algal cells from each plate. Next, the combined cell suspension was centrifuged at 2000 x RCF for 2 min in a 15 mL conical Falcon tube, followed by 3000 x RCF for 1 min. Then, the supernatant was removed, and the cell pellet was resuspended in 2 mL of SPEM solution (1 M sorbitol, 10 mM EDTA (pH 7.5), Na<sub>2</sub>HPO<sub>4</sub>·7 H<sub>2</sub>O (2.08 g L<sup>-1</sup>), NaH<sub>2</sub>PO<sub>4</sub>·1 H<sub>2</sub>O (0.32 g L<sup>-1</sup>)) and incubated for 1 min at 37 °C. Next, the resuspended cells were incubated for 5 min at 50 °C and then mixed with an equal volume of 2.2% low-melting point agarose in TAE buffer (40 mM Tris, 20 mM acetic acid, and 1 mM EDTA), which was also kept at 50 °C. Aliquots of 100 µL were transferred into plug molds and allowed to solidify for 10 min at 4 °C. Once solidified, the plugs were removed from the molds and transferred into 50 mL conical Falcon tubes containing 5 mL of protoplasting solution ((8.5 mL of SPEM solution, 500 µL zymolyase-20 T solution (50 mg mL<sup>-1</sup>), 500 µL lysozyme (25 mg mL<sup>-1</sup>), 500 µL hemicellulase (25 mg mL<sup>-1</sup>), 50 µL β-mercaptoethanol (14.3 M)) and incubated for 30 min at 37 °C to digest algal cell walls. After, the protoplasting solution was removed, and the plugs were incubated with 5 mL of Proteinase K solution (100 mM EDTA (pH 8.0), 0.2% sodium deoxycholate, 1% sodium lauroyl sarcosine, and 1 mg mL<sup>-1</sup> Proteinase K) for 24 h at 50 °C. Then, the plugs were washed four times as follows: twice with 25 mL of wash buffer (20 mM Tris and 50 mM EDTA (pH 8.0)) for 2 h each at room temperature (RT), once with 25 mL of wash buffer containing 1 mM phenylmethylsulfonyl fluoride (PMSF) for 2 h at RT, and a final wash with 25 mL of wash buffer for 2 h.

For PvuI restriction digestion, the plugs were placed in 1.5 mL microcentrifuge tubes and washed with 1 mL of 0.1 x wash buffer for 1 h at RT, followed by a 5 h wash in 1.0 x NEBuffer 3.1 restriction buffer at RT. Finally, each plug was incubated with 50 units mL<sup>-1</sup> of PvuI restriction enzyme in 1 mL of 1.0 x NEBuffer 3.1 restriction buffer for 4 h at 37 °C. Following the digest, the plugs were washed for 1 h in 1 mL of TE buffer

(pH 8). Next, the TE buffer was removed, a fresh 100  $\mu\text{L}$  of TE buffer (pH 8) was added, and plugs were melted for 10 min at 65  $^{\circ}\text{C}$ . The solution was then equilibrated to 42  $^{\circ}\text{C}$  for 10 min before adding 2  $\mu\text{L}$  (2 units) of  $\beta$ -agarase. Finally, the solution was incubated at 42  $^{\circ}\text{C}$  for 1 h to allow the agarose to be digested. On average, each plug yielded a DNA concentration of 300  $\text{ng } \mu\text{L}^{-1}$ .

#### **2.4.2.2 DNA isolation by modified alkaline lysis**

Total DNA from *E. coli*, *S. cerevisiae*, and algae were isolated as previously described [15]. Before isolating DNA from *E. coli* for diagnostic restriction digests or sequencing, cells were induced with arabinose. For plasmid induction, 5 mL of *E. coli* overnight cultures grown in LB media supplemented with chloramphenicol (15  $\mu\text{g mL}^{-1}$ ) were diluted 1:50 into 50 mL of LB media supplemented with chloramphenicol (15  $\mu\text{g mL}^{-1}$ ) and arabinose (100  $\mu\text{g mL}^{-1}$ ) and grown for 8 h at 37  $^{\circ}\text{C}$ .

#### **2.4.3 DNA fragment preparation for PCR-based cloning**

PCR amplification of mitochondrial fragments was performed using *P. tricornutum* total DNA (first iteration) or *P. tricornutum* mitochondrial DNA cloned on a plasmid and isolated from *E. coli* as described in Section 2.4.2.2 (second iteration) as template DNA. The mitochondrial genome was amplified as eight overlapping fragments (primers: BK 141–144F/R, 145F/250R, 247F/146R, 147F/R, and 148F/140R, listed in Supplementary Table B-1), as well as two additional fragments (primers: BK 88F/245R and 251F/88R, listed in Supplementary Table B-1) to amplify the pAGE3.0 plasmid [16]. The pAGE3.0 plasmid contains all the genetic elements required for selection and stable propagation in host organisms *S. cerevisiae*, *P. tricornutum* (nuclear localization), *E. coli*, and *Sinorhizobium meliloti*. In addition, this plasmid contains an origin of transfer (*oriT*) to allow for plasmid transfer using bacterial conjugation. All primers were manually designed. Forward and reverse primers for fragments 1–4, 9–10, the forward primer for fragment 5, and the reverse primer for fragment 8 were designed to be 40 bp long.

Primers 80 bp in length were designed for fragments 6 and 7, the reverse primer for fragment 5, and forward primer for fragment 8. Overlaps between fragments were between 68 and 200 bp to allow for efficient yeast assembly.

Each fragment was individually amplified in a 25  $\mu\text{L}$  PCR reaction using 1  $\mu\text{L}$  of PrimeSTAR GXL polymerase, 1  $\mu\text{L}$  of template DNA (10–100  $\text{ng } \mu\text{L}^{-1}$  isolated total DNA from either *P. tricornutum* or *E. coli*), and the respective forward and reverse primers each at a final concentration of 0.2  $\mu\text{M}$ . The thermocycler was programmed as follows: five cycles of 98  $^{\circ}\text{C}$  for 10 s, 50  $^{\circ}\text{C}$  for 15 s, and 68  $^{\circ}\text{C}$  for 480 s, followed by 25 cycles of 98  $^{\circ}\text{C}$  for 10 s, 55  $^{\circ}\text{C}$  for 15 s, and 68  $^{\circ}\text{C}$  for 480 s, and one cycle of 68  $^{\circ}\text{C}$  for 600 s, finishing with an infinite hold at 12  $^{\circ}\text{C}$ . PCR product amplification was confirmed by performing agarose gel electrophoresis with 2  $\mu\text{L}$  of PCR product on a 1.4% agarose (*w/v*) gel.

To eliminate plasmid template DNA, PCR products were treated with 10 units (0.5  $\mu\text{L}$ ) of DpnI restriction endonuclease, incubated at 37  $^{\circ}\text{C}$  for 30 min, and deactivated for 20 min at 80  $^{\circ}\text{C}$ . Fragments were then purified using the EZ-10 Spin Column PCR Products Purification Kit and were combined into a single 1.5 mL microcentrifuge tube to equimolar concentrations ( $\sim 200$  ng of each fragment) and a total volume of  $\sim 30$   $\mu\text{L}$ .

#### **2.4.4 DNA fragment preparation for transformation-associated recombination (TAR) cloning**

*P. tricornutum*'s total DNA was digested with PvuI restriction enzyme, as described in Section 2.4.2.1. The pAGE3.0 plasmid was amplified as two fragments (primers: BK 88F/93R & 92F/88R, listed in Supplementary Table B-1). Each fragment was individually amplified in a 20  $\mu\text{L}$  PCR reaction using 0.8  $\mu\text{L}$  PrimeSTAR GXL polymerase, 0.8  $\mu\text{L}$  of template DNA (10  $\text{ng } \mu\text{L}^{-1}$  of plasmid template DNA isolated from *E. coli*), and the respective forward and reverse primers at a final concentration of 0.2  $\mu\text{M}$ . The thermocycler conditions used were as follows: 30 cycles of 98  $^{\circ}\text{C}$  for 10 s, 62  $^{\circ}\text{C}$  for 15 s, and 68  $^{\circ}\text{C}$  for 150 s, one cycle of 68  $^{\circ}\text{C}$  for 600 s, and an infinite hold at 12

°C. PCR product amplification was confirmed by performing agarose gel electrophoresis with 1  $\mu\text{L}$  of PCR product on a 1.4% agarose ( $w/v$ ) gel.

To eliminate the template DNA from the PCR products, DpnI treatment, and purification were performed as described in Section 2.4.3. Then, the fragments were combined into a single 1.5 mL microcentrifuge tube in the following proportions: 10  $\mu\text{L}$  linearized genome ( $\sim 300 \text{ ng } \mu\text{L}^{-1}$ ) and 7  $\mu\text{L}$  for each plasmid backbone fragment ( $\sim 300\text{--}500 \text{ ng } \mu\text{L}^{-1}$ ) prior to yeast transformation.

### **2.4.5 Yeast spheroplast transformation protocol**

Yeast spheroplasts were prepared as previously described [38], with the modification that mixtures of DNA fragments were used rather than bacterial culture. After transformation and recovery, the 1 mL of yeast cells was split into 300  $\mu\text{L}$  and 700  $\mu\text{L}$ . Each aliquot was added to a 15 mL conical Falcon tube containing 8 mL of melted 2% agar yeast synthetic complete media lacking histidine supplemented with adenine ( $60 \text{ mg L}^{-1}$ ) and 1 M sorbitol, which had been equilibrated at 50 °C. After 4–6 gentle inversions, the mixture was poured on top of an agar plate containing 10 mL of 2% agar yeast synthetic complete media lacking histidine supplemented with adenine ( $60 \text{ mg L}^{-1}$ ) and 1 M sorbitol. The plate was then incubated at 30 °C for 3–5 days until yeast colonies emerged for screening.

### **2.4.6 *E. coli* transformation**

TransforMax Epi300 electrocompetent *E. coli* cells were thawed on ice for 20 min. Then, 20  $\mu\text{L}$  aliquots of *E. coli* cells were transferred to sterile 1.5 mL microcentrifuge tubes and mixed with 1  $\mu\text{L}$  of total DNA extracted from a single yeast colony [37]. A Gene Pulser Xcell Electroporation System was set to 25  $\mu\text{F}$  capacitance, 200  $\Omega$  resistance, and 2.5 kV voltage. The DNA mixture and *E. coli* was then transferred to an ice-cold 2 mm cuvette and electroporated. Immediately, 1 mL of super optimal broth with catabolite

repression (SOC; 20 g L<sup>-1</sup> tryptone, 5 g L<sup>-1</sup> yeast extract, 0.5 g L<sup>-1</sup> NaCl, 10 mL of 250 mM KCl, 5 mL of 2 M MgCl<sub>2</sub>, and 20 mL of 1 M glucose) media was added to the cuvette, which was then incubated at 37 °C for 30 min, without shaking. Next, the mixture was transferred to a sterile 1.5 mL microcentrifuge tube and incubated for 1 h at 37 °C, shaking at 225 RPM. Finally, 100 µL of transformed cells were plated on selective LB 1.5% agar media supplemented with chloramphenicol (15 µg mL<sup>-1</sup>) and incubated overnight at 37 °C.

## **2.4.7 Screening strategy**

### **2.4.7.1 Screening yeast colonies**

To identify positive clones generated using the PCR-based and TAR cloning methods, all individual yeast colonies were struck onto selective 2% agar plates containing synthetic complete media lacking histidine supplemented with adenine (60 mg L<sup>-1</sup>) and grown overnight at 30 °C. Next, each streak was passed onto a second selective 2% agar plate and grown overnight at 30 °C. For TAR cloning, approximately 10 yeast colonies were pooled, to create 20 pools in total, by picking up a small amount of each colony and resuspending them together in 100 µL of TE buffer in 200 µL PCR tubes. For PCR-based cloning, the same protocol was followed except that cells from 20 individual colonies were used for each reaction. Subsequently, for both TAR cloning and PCR-based cloning methods, the resuspended cells were incubated at 95 °C for 15 min to lyse the cells. The tubes were then centrifuged for ~30 s using a mini centrifuge. Next, 1 µL of the supernatant was used as the DNA template for diagnostic MPX PCR.

MPX primer pairs were designed to have an optimal melting temperature of 60 °C using the online tool Primer3 (<http://bioinfo.ut.ee/primer3-0.4.0/>). MPX PCR was performed according to the Qiagen Multiplex PCR Handbook. To test potential pPT-TAR and pPT-PCR clones, two sets of MPX PCR were run, each yielding three amplicons. The first primer set, BK901, 904, and 906 F/R, generated amplicons of 265-, 334-, and 507-bp sizes, respectively. The second primer set, BK 902, 903, and 905 F/R, generated

171-, 224-, and 405-bp amplicons, respectively. Then, 2  $\mu\text{L}$  of the PCR products were loaded onto a 2% agarose gel for electrophoresis and analyzed. Next, DNA was isolated as described in Section 2.4.2.2 from selected positive clones and transformed into *E. coli* as described in Section 2.4.6.

### **2.4.7.2 Screening *E. coli* colonies**

First, a range of one to eight *E. coli* colonies transformed with DNA from positive yeast clones were screened using the same MPX PCR method as described in Section 2.4.7.1. The selected positive colonies were subsequently screened by diagnostic restriction enzyme digestion. To perform diagnostic restriction enzyme digestion, DNA was isolated from *E. coli* as described in Section 2.4.2.2, and the concentration of total isolated DNA was obtained using the DeNovix Inc. DS-11 FX+ Spectrophotometer. DNA preparations were  $\sim 5000 \text{ ng } \mu\text{L}^{-1}$  before digestion. Digestion reactions were generated using 5  $\mu\text{L}$  of DNA, 2  $\mu\text{L}$  of NEBuffer 3.1 restriction buffer, 0.2  $\mu\text{L}$  of SrfI, 0.2  $\mu\text{L}$  of SacII, and 12.6  $\mu\text{L}$  of water. Reaction mixtures were incubated at 37 °C for 60 min, and then 10  $\mu\text{L}$  was loaded onto a 1% agarose gel for electrophoresis.

For further confirmation, the isolated pDNA was submitted to the CCIB DNA Core at Massachusetts General Hospital for whole plasmid sequencing and reference mapping. Sequences obtained were aligned with their respective references using the algorithm built into Geneious version 2020.0. Alignment disagreements were identified as mutations, and each mutation was individually analyzed to curate a list of mutations (Supplemental Table B-2).

## **2.4.8 Evaluation of growth phenotypes of host strains**

### **2.4.8.1 *E. coli* growth in liquid media**

*E. coli* strains harboring plasmids with cloned mitochondrial genomes pPT-PCR C1 and C2, pPT-TAR C1 and C2, and control plasmids pAGE3.0 and pPtGE31 (lacking a

mitochondrial genome) were inoculated and grown overnight in 5 mL of LB media supplemented with chloramphenicol ( $15 \mu\text{g mL}^{-1}$ ) at  $37^\circ\text{C}$  with shaking at 225 RPM. The saturated cultures were diluted 100-fold into 5 mL of the same media and grown for 2 h in 50-mL conical Falcon tubes under the same conditions. The cultures were placed on ice and diluted to an  $\text{OD}_{600}$  of 0.1 in LB media supplemented with chloramphenicol ( $15 \mu\text{g mL}^{-1}$ ; uninduced) or LB media supplemented with chloramphenicol ( $15 \mu\text{g mL}^{-1}$ ) and arabinose ( $100 \mu\text{g mL}^{-1}$ ; induced). In quadruplicate, 200  $\mu\text{L}$  of each uninduced and induced culture was aliquoted into a 96-well plate. Once loaded, the 96-well plate was placed in a 96-well plate reader, Epoch 2. While in the plate reader, the strains were incubated at  $37^\circ\text{C}$  with continuous, double-orbital shaking.  $\text{OD}_{600}$  measurements were taken every 15 min for 5 h, for a total of 20 readings using Gen5 data analysis software version 3.08. This experiment was performed twice; therefore, eight measurements were obtained and averaged for each strain, and the standard error of the mean was calculated. The doubling time (td) of each strain was determined.

#### **2.4.8.2 *S. cerevisiae* growth in liquid media**

*S. cerevisiae* strains harboring pPT-PCR C1 and C2, pPT-TAR C1 and C2, and pAGE3.0 and pPtGE31 control plasmids (lacking a mitochondrial genome), were inoculated and grown overnight in 5 mL of synthetic complete yeast media lacking histidine supplemented with adenine ( $60 \text{ mg L}^{-1}$ ) at  $30^\circ\text{C}$  with shaking at 225 RPM. The saturated cultures were diluted 100-fold into 5 mL of the same media and allowed to grow for 2 h in a 50 mL conical Falcon tube under the same conditions. The cultures were diluted to an  $\text{OD}_{600}$  of 0.1 in the same media, and 200  $\mu\text{L}$  of each culture was aliquoted into a 96-well plate in quadruplicate. Once loaded, the 96-well plate was placed in a 96-well plate reader, Epoch 2. While in the plate reader, the strains were incubated at  $30^\circ\text{C}$  with continuous, double orbital shaking.  $\text{OD}_{600}$  measurements were taken every 15 min for 12 h for a total of 49 readings using Gen5 data analysis software version 3.08. Four measurements were obtained and averaged for each strain, and the standard error of the mean was calculated. The td of each strain was determined.



### 2.4.8.3 *E. coli* and *S. cerevisiae* growth on solid media

*E. coli* and *S. cerevisiae* strains harboring pPT-PCR C1 and C2, pPT-TAR C1 and C2, and pAGE3.0 and pPtGE31 control plasmids (lacking a mitochondrial genome), were inoculated and grown overnight in LB media supplemented with chloramphenicol (15  $\mu\text{g mL}^{-1}$ ) at 37 °C, and synthetic complete yeast media lacking histidine supplemented with adenine (60  $\text{mg L}^{-1}$ ) at 30 °C, respectively. The saturated cultures were diluted 100-fold in their corresponding media and grown for 2 h. The cultures were diluted to an OD<sub>600</sub> of 0.1, which was used to generate a range of dilutions for *E. coli* and *S. cerevisiae*. The dilution series was plated in 5  $\mu\text{L}$  aliquots onto their corresponding selection plates: 1.5% agar LB plates supplemented with chloramphenicol (15  $\mu\text{g mL}^{-1}$ ; uninduced) or with chloramphenicol (15  $\mu\text{g mL}^{-1}$ ) and arabinose (100  $\mu\text{g mL}^{-1}$ ; induced) for *E. coli*, and 2% agar plates containing synthetic complete yeast media lacking histidine supplemented with adenine (60  $\text{mg L}^{-1}$ ) for *S. cerevisiae*. Dilution plates for *E. coli* strains were grown overnight at 37 °C, and dilution plates for *S. cerevisiae* strains were grown for two days at 30 °C.

## 2.5 References

1. Scaife MA and Smith AG. Towards developing algal synthetic biology. *Biochem Soc Trans.* 2016;44:716–722. doi:10.1042/BST20160061
2. Adarme-Vega TC, Lim DKY, Timmins M, Vernen F, Li Y, and Schenk PM. Microalgal biofactories: A promising approach towards sustainable omega-3 fatty acid production. *Microb Cell Factories.* 2012;11:96. doi:10.1186/1475-2859-11-96
3. Brasil B dos SAF, de Siqueira FG, Salum TFC, Zanette CM, and Spier MR. Microalgae and cyanobacteria as enzyme biofactories. *Algal Res.* 2017;25:76–89. doi:10.1016/j.algal.2017.04.035
4. Hlavova M, Turoczy Z, and Bisova K. Improving microalgae for biotechnology – From genetics to synthetic biology. *Biotechnol Adv.* 2015;33:1194–1203. doi:10.1016/j.biotechadv.2015.01.009

5. Rosales-Mendoza S, Angulo C, and Meza B. Food-grade organisms as vaccine biofactories and oral delivery vehicles. *Trends Biotechnol.* 2016;34:124–136. doi:10.1016/j.tibtech.2015.11.007
6. Yongmanitchai W and Ward OP. Growth of and omega-3 fatty acid production by *Phaeodactylum tricorutum* under different culture conditions. *Appl Environ Microbiol.* 1991;57:419–425. doi:10.1128/aem.57.2.419-425.1991
7. Bowler C, Allen AE, Badger JH, Grimwood J, Jabbari K, Kuo A, et al. The *Phaeodactylum* genome reveals the evolutionary history of diatom genomes. *Nature.* 2008;456:239–244. doi:10.1038/nature07410
8. Oudot-Le Secq MP and Green BR. Complex repeat structures and novel features in the mitochondrial genomes of the diatoms *Phaeodactylum tricorutum* and *Thalassiosira pseudonana*. *Gene.* 2011;476:20–26. doi:10.1016/j.gene.2011.02.001
9. Oudot-Le Secq MP, Grimwood J, Shapiro H, Armbrust EV, Bowler C, and Green BR. Chloroplast genomes of the diatoms *Phaeodactylum tricorutum* and *Thalassiosira pseudonana*: Comparison with other plastid genomes of the red lineage. *Mol Gen Genomics.* 2007;277:427–439. doi:10.1007/s00438-006-0199-4
10. Apt KE, Kroth-Pancic PG, and Grossman AR. Stable nuclear transformation of the diatom *Phaeodactylum tricorutum*. *Mol Gen Genet.* 1996;252:572–579. doi:10.1007/s004380050264
11. Falciatore A, Casotti R, Leblanc C, Abrescia C, and Bowler C. Transformation of nonselectable reporter genes in marine diatoms. *Mar Biotechnol.* 1999;1:239–251. doi:10.1007/PL00011773
12. Zhang C and Hu H. High-efficiency nuclear transformation of the diatom *Phaeodactylum tricorutum* by electroporation. *Mar Genomics.* 2014;16:63–66. doi:10.1016/j.margen.2013.10.003
13. Miyahara M, Aoi M, Inoue-Kashino N, Kashino Y, and Ifuku K. Highly efficient transformation of the diatom *Phaeodactylum tricorutum* by multi-pulse electroporation. *Biosci Biotechnol Biochem.* 2013;77:874–876. doi:10.1271/bbb.120936
14. Miyagawa A, Okami T, Kira N, Yamaguchi H, Ohnishi K, and Adachi M. Research note: High efficiency transformation of the diatom *Phaeodactylum tricorutum* with a promoter from the diatom *Cylindrotheca fusiformis*. *Phycol Res.* 2009;57:142–146. doi:10.1111/j.1440-1835.2009.00531.x
15. Karas BJ, Diner RE, Lefebvre SC, McQuaid J, Phillips APR, Noddings CM, et al. Designer diatom episomes delivered by bacterial conjugation. *Nat Commun.* 2015;6:6925. doi:10.1038/ncomms7925

16. Brumwell SL, MacLeod MR, Huang T, Cochrane RR, Meaney RS, Zamani M, et al. Designer *Sinorhizobium meliloti* strains and multi-functional vectors enable. PLoS One. 2019;14:e0206781. doi:10.1371/journal.pone.0206781
17. Karas BJ, Molparia B, Jablanovic J, Hermann WJ, Lin YC, Dupont CL, et al. Assembly of eukaryotic algal chromosomes in yeast. J Biol Eng. 2013;7:30. doi:10.1186/1754-1611-7-30
18. Diner RE, Noddings CM, Lian NC, Kang AK, McQuaid JB, Jablanovic J, et al. Diatom centromeres suggest a mechanism for nuclear DNA acquisition. Proc Natl Acad Sci U.S.A. 2017;114:E6015–E6024. doi:10.1073/pnas.1700764114
19. Slattery SS, Diamond A, Wang H, Therrien JA, Lant JT, Jazey T, et al. An expanded plasmid-based genetic toolbox enables Cas9 genome editing and stable maintenance of synthetic pathways in *Phaeodactylum tricorutum*. ACS Synth Biol. 2018;7:328–338. doi:10.1021/acssynbio.7b00191
20. Wang H, Slattery S, Karas B, and Edgell DR. Delivery of the Cas9 or TevCas9 system into *Phaeodactylum tricorutum* via conjugation of plasmids from a bacterial donor. Bio Protoc. 2018;8:e2974. doi:10.21769/bioprotoc.2974
21. Weyman PD, Beeri K, Lefebvre SC, Rivera J, Mccarthy JK, Heuberger AL, et al. Inactivation of *Phaeodactylum tricorutum* urease gene using transcription activator-like effector nuclease-based targeted mutagenesis. Plant Biotechnol J. 2015;13:460–470. doi:10.1111/pbi.12254
22. Siaut M, Heijde M, Mangogna M, Montsant A, Coesel S, Allen A, et al. Molecular toolbox for studying diatom biology in *Phaeodactylum tricorutum*. Gene. 2007;406:23–35. doi:10.1016/j.gene.2007.05.022
23. Avalos JL, Fink GR, and Stephanopoulos G. Compartmentalization of metabolic pathways in yeast mitochondria improves the production of branched-chain alcohols. Nat Biotechnol. 2013;31:335–341. doi:10.1038/nbt.2509
24. Bigger BW, Liao AY, Sergijenko A, and Coutelle C. Trial and error: How the unclonable human mitochondrial genome was cloned in yeast. Pharm Res. 2011;28:2863–2870. doi:10.1007/s11095-011-0527-1
25. Yoon YG and Koob MD. Efficient cloning and engineering of entire mitochondrial genomes in *Escherichia coli* and transfer into transcriptionally active mitochondria. Nucleic Acids Res. 2003;31:1407–1415. doi:10.1093/nar/gkg228
26. Gibson DG, Smith HO, Hutchison CA, Venter JC, and Merryman C. Chemical synthesis of the mouse mitochondrial genome. Nat Methods. 2010;7:901–903. doi:10.1038/nmeth.1515

27. Gupta M and Hoo B. Entire maize chloroplast genome is stably maintained in a yeast artificial chromosome. *Plant Mol Biol*. 1991;17:361–369. doi:10.1007/BF00040631
28. Itaya M, Fujita K, Kuroki A, and Tsuge K. Bottom-up genome assembly using the *Bacillus subtilis* genome vector. *Nat Methods*. 2008;5:41–43. doi:10.1038/nmeth1143
29. O’Neill BM, Mikkelsen KL, Gutierrez NM, Cunningham JL, Wolff KL, Szyjka SJ, et al. An exogenous chloroplast genome for complex sequence manipulation in algae. *Nucleic Acids Res*. 2012;40:2782–2792. doi:10.1093/nar/gkr1008
30. Ostrov N, Landon M, Guell M, Kuznetsov G, Teramoto J, Cervantes N, et al. Design, synthesis, and testing toward a 57-codon genome. *Science*. 2016;353:819–822. doi:10.1126/science.aaf3639
31. Fredens J, Wang K, de la Torre D, Funke LFH, Robertson WE, Christova Y, et al. Total synthesis of *Escherichia coli* with a recoded genome. *Nature*. 2019;569:514–518. doi:10.1038/s41586-019-1192-5
32. Gibson DG, Glass JI, Lartigue C, Noskov VN, Chuang RY, Algire MA, et al. Creation of a bacterial cell controlled by a chemically synthesized genome. *Science*. 2010;329:52–56. doi:10.1126/science.1190719
33. Lartigue C, Glass JI, Alperovich N, Pieper R, Parmar PP, Hutchison CA, et al. Genome transplantation in bacteria: Changing one species to another. *Science*. 2007;317:632–638. doi:10.1126/science.1144622
34. Hutchison CA, Chuang RY, Noskov VN, Assad-Garcia N, Deerinck TJ, Ellisman MH, et al. Design and synthesis of a minimal bacterial genome. *Science*. 2016;351:aad6253. doi:10.1126/science.aad6253
35. Richardson SM, Mitchell LA, Stracquadanio G, Yang K, Dymond JS, DiCarlo JE, et al. Design of a synthetic yeast genome. *Science*. 2017;355:1040–1044. doi:10.1126/science.aaf4557
36. Ostrov N, Beal J, Ellis T, Gordon DB, Karas BJ, Lee HH, et al. Technological challenges and milestones for writing genomes. *Science*. 2019;366:310–312. doi:10.1126/science.aay0339
37. Karas BJ, Tagwerker C, Yonemoto IT, Hutchison CA, and Smith HO. Cloning the *Acholeplasma laidlawii* PG-8A genome in *Saccharomyces cerevisiae* as a yeast centromeric plasmid. *ACS Synth Biol*. 2012;1:22–28. doi:10.1021/sb200013j

38. Karas BJ, Jablanovic J, Sun L, Ma L, Goldgof GM, Stam J, et al. Direct transfer of whole genomes from bacteria to yeast. *Nat Methods*. 2013;10:410–412. doi:10.1038/nmeth.2433
39. Lee NCO, Larionov V, and Kouprina N. Highly efficient CRISPR/Cas9-mediated TAR cloning of genes and chromosomal loci from complex genomes in yeast. *Nucleic Acids Res*. 2015;43:e55. doi:10.1093/nar/gkv112
40. Ruiz E, Talenton V, Dubrana MP, Guesdon G, Lluch-Senar M, Salin F, et al. CReasPy-cloning: A method for simultaneous cloning and engineering of megabase-sized genomes in yeast using the CRISPR-Cas9 system. *ACS Synth Biol*. 2019;8:2547–2557. doi:10.1021/acssynbio.9b00224
41. Soltysiak MPM, Meaney RS, Hamadache S, Janakirama P, Edgell DR, and Karas BJ. Trans-kingdom conjugation within solid media from *Escherichia coli* to *Saccharomyces cerevisiae*. *Int J Mol Sci*. 2019;20:5212. doi:10.3390/ijms20205212
42. Karas BJ, Suzuki Y, and Weyman PD. Strategies for cloning and manipulating natural and synthetic chromosomes. *Chromosom Res*. 2015;23:57–68. doi:10.1007/s10577-014-9455-3
43. Sorek R, Zhu Y, Creevey CJ, Francino MP, Bork P, and Rubin EM. Genome-wide experimental determination of barriers to horizontal gene transfer. *Science*. 2007;318:1449–1452. doi:10.1126/science.1147112

## Chapter 3

### 3 Cloning of *Thalassiosira pseudonana*'s mitochondrial genome in *Saccharomyces cerevisiae* and *Escherichia coli*

The work presented in this chapter is adapted from:

Cochrane, RR, Brumwell, SL, Shrestha, A, Giguere, DJ, Hamadache, S, Gloor, GB, Edgell, DR, & Karas, BJ (2020). Cloning of *Thalassiosira pseudonana*'s mitochondrial genome in *Saccharomyces cerevisiae* and *Escherichia coli*. *Biology*, 9(11), 358.

#### 3.1 Introduction

Recent advancements in DNA sequencing and synthesis resulted in the development of a powerful set of biotechnology tools that can help to address global challenges in food and water sustainability, medicine production, and eco-friendly energies. Many potential organisms are under investigation for desirable properties useful for biotechnology applications. One attractive candidate is *Thalassiosira pseudonana*. This model-centric diatom is naturally found in oceanic water and plays a significant role in global carbon cycling and combatting climate change [1,2]. In addition, its silica frustule encasement is suitable for nanotechnologies and drug delivery [3,4]. Due to the growing interest in *T. pseudonana*, its nuclear, mitochondrial, and plastid genomes were sequenced [5–7], enabling the development of genetic tools and DNA delivery methods, such as bacterial conjugation and microparticle bombardment [8,9]. Additional genetic tools for *T. pseudonana* include selectable markers [9,10], promoters [9], transformation vectors [9], inducible protein expression [9], RNA interference [11,12], and CRISPR/Cas9 [10,13,14]. Finally, methods for isolating *T. pseudonana*'s chloroplast and mitochondria have been developed, and proteomic data made available [15]. Most of the described genetic tools allow the engineering of *T. pseudonana*'s nuclear genome; however, engineering its organelle genomes is still undeveloped. There are several advantages to engineering organelle genomes, including polycistronic gene organization, the lack of transgene silencing, reduced positional gene expression effects, and the

compartmentalization of biosynthetic pathways, each of which simplifies engineering [16]. In preparation for exploiting these qualities, organelle genomes from multiple species have been cloned [17–23].

We demonstrated the cloning of the mitochondrial genome of *P. tricornutum*, a model diatom algae species, in baker's yeast, *S. cerevisiae*, and *E. coli* [23]. *S. cerevisiae* has proven to be an excellent host for cloning large DNA fragments or whole genomes [19,24–27], and it was also demonstrated that chromosomes up to ~500 kbp could be cloned in *E. coli* [28]. To test the versatility and robustness of this method when applied to other algal species, we selected *T. pseudonana* because of the unique characteristics of its mitochondrial genome. First, the *T. pseudonana* mitochondrial genome is compact (~44 kbp), harboring a relatively small repeat region (~5 kbp) compared to the repeat region of *P. tricornutum* (~35 kbp). Second, *T. pseudonana* has a lower G+C%-content mitochondrial genome (30%) than *P. tricornutum* (35%). Third, *T. pseudonana*'s mitochondrial genome uses an alternative genetic code, which substitutes a typical stop codon (UGA) for a tryptophan residue [6]. This alternative genetic code could be beneficial during the development of a whole-genome delivery method, as any engineered selection markers integrated into this genome would only function when delivered to the mitochondrial compartment, eliminating the need to screen against nuclear transformants [29].

Here, we report the successful cloning of *T. pseudonana*'s mitochondrial genome in yeast and demonstrate that it can also be propagated in *E. coli*. In the first iteration (Design 1), the mitochondrial genome was cloned in its entirety (~44 kbp; ~58 kbp including pPtGE31 plasmid backbone); in the second iteration (Design 2), ~3.8 kbp of the ~5 kbp repetitive region was excluded (~40 kbp; ~58 kbp including pAGE3.0 plasmid backbone). Growth experiments performed on yeast in liquid media revealed that yeast strains carrying plasmids with cloned mitochondrial genomes had a slightly increased growth rate; however, after 24 h, the yeast strains grew to the same (Design 1) or slightly lower (Design 2) end-point densities compared to control strains. When these genomes were propagated in *E. coli* on a low copy number plasmid, they had the same growth rate and end-point densities as the control strains. However, when grown with arabinose to

increase the copy number of these genomes, all samples grew to significantly lower end-point densities after 11.5 h. Also, analysis of plasmids containing mitochondrial genomes following propagation in *E. coli* over 60 generations showed that about 17% of *T. pseudonana* mitochondrial genomes were mutated compared to 0% identified for equivalent experiments conducted using the *P. tricornutum* mitochondrial genome. Finally, RNA sequencing performed on *E. coli* harboring either alga's mitochondrial genome found that gene expression can be detected for *T. pseudonana* and *P. tricornutum* mitochondrial genes.

## 3.2 Results

### 3.2.1 Cloning of *T. pseudonana*'s mitochondrial genome

Using a PCR-based approach, we cloned *T. pseudonana*'s mitochondrial genome in its entirety (Design 1: 57,641 bp; composed of a 43,827 bp mitochondrial genome, 11,742 bp pPtGE31 plasmid backbone, and 2072 bp *URA3* additional selection marker for *S. cerevisiae*) as well as a reduced version lacking 3.8 kbp of the ~5.0 kbp repetitive sequence (Design 2: 57,557 bp; composed of a 40,034 bp mitochondrial genome and a 17,523 bp pAGE3.0 plasmid backbone) (Figure 3-1). For Design 1, the complete genome was PCR-amplified in eight overlapping fragments from total *T. pseudonana* DNA. Four additional overlapping fragments were amplified, including an *S. cerevisiae* selection marker *URA3* (Fragment 5) and the pPtGE31 plasmid backbone (Fragments 10–12) [30], which contains all the genetic elements required for plasmid propagation in yeast and *E. coli*. In total, 12 DNA fragments were amplified (Figure 3-1C) and assembled following transformation and homologous recombination in *S. cerevisiae*, yielding 187 yeast colonies (Table 3-1). For Design 2, the genome was PCR-amplified in seven overlapping fragments that excluded a 3.8 kbp repeat region. The pAGE3.0 plasmid [31] backbone was amplified as two additional fragments (Fragments 7–8) to provide all the genetic elements required for propagation in yeast and *E. coli*. In total, nine DNA fragments were amplified (Figure 3-1D) and assembled in yeast, yielding 680 colonies (Table 3-1). For each design of the mitochondrial genome, two clones identified as correct in yeast by



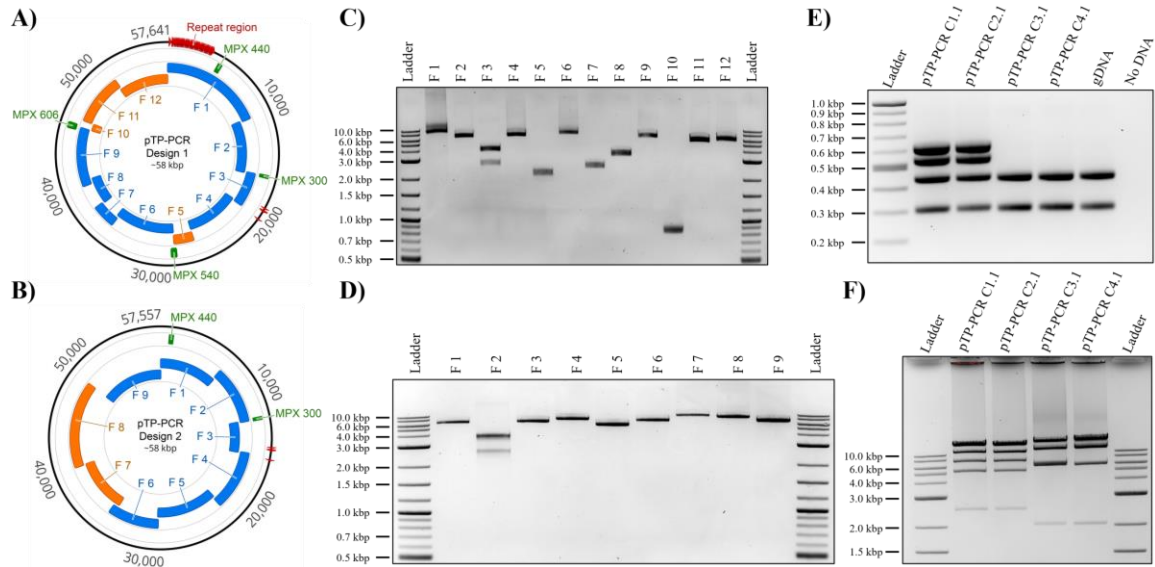


**Figure 3-1. Design, amplification, and analysis of cloned *T. pseudonana* mitochondrial genomes.** **A, B)** Plasmid maps of *T. pseudonana* mitochondrial genomes cloned with the repeat region (**A**—Design 1) or without (**B**—Design 2). The relative sizes and positions of the mitochondrial genome fragments (blue) and plasmid backbone fragments (orange) are shown. In addition, the four MPX PCR amplicons used for diagnostic screening and their sizes in bp are indicated (green). These images were generated using Geneious version 2020.2.4, created by Biomatters. **C)** Agarose gel electrophoresis of the 12 PCR-amplified fragments used to assemble plasmids as specified in Design 1. The resulting amplicon sizes for fragments 1–12 are 10,735-, 6092-, 3610-, 6274-, 2152-, 7035-, 2512-, 3250-, 6216-, 859-, 5367-, and 5870-bp, respectively. Note: Fragment 3 had a nonspecific amplicon but did not prevent the correct assembly. **D)** Agarose gel electrophoresis of the nine PCR-amplified fragments used to assemble plasmids as specified in Design 2. The resulting amplicon sizes for fragments 1–9 are 6092-, 3610-, 6254-, 7174-, 5417-, 6372-, 9136-, 8441-, and 6810-bp, respectively. Note: Fragment 2 had a nonspecific amplicon but did not prevent the correct assembly. **E)** MPX PCR screen of four cloned algal mitochondrial genomes isolated from *E. coli* with expected amplicon sizes of 300-, 440-, 540-, and 606-bp. Note: MPX amplicons 540- and 606-bp can only be amplified from Design 1 genomes. **F)** Diagnostic restriction digest of the four cloned algal mitochondrial genomes. For Design 1 genomes (pTP-PCR C1.1/2.1), after PvuI restriction enzyme digestion, the expected band sizes are 6-, 2454-, 4862-, 6262-, 12,903-, 15,405-, and 15,749-bp. For Design 2 genomes (pTP-PCR C3.1/4.1), after PmeI and BamHI restriction enzymes digestion, expected band sizes are 2031-, 5693-, 12,012-, 16,721-, and 20,960-bp.

**Table 3-1. Cloning of the *T. pseudonana* full and reduced mitochondrial genomes in the host organisms *S. cerevisiae* and *E. coli*.** Two PCR-based cloning assemblies were performed in *S. cerevisiae*. Correct genomes identified by MPX PCR were subsequently transformed into *E. coli*. The diagnostic MPX PCR was repeated on *E. coli* clones, and the final genomes were selected. For the *E. coli* media, CM indicates chloramphenicol antibiotic. For the *S. cerevisiae* selection media, -HIS indicates synthetic complete media lacking histidine. Four-amplicon MPX PCR, as shown in Figure 3-1E), was used.

Genome design Assembly type	<i>S. cerevisiae</i>			<i>E. coli</i>			
	Selection media	Colony count	MPX PCR screen	Selection media	Selected yeast colony: <i>E. coli</i> colony count	MPX PCR screen	Final genomes selected for analysis
1 – Full genome PCR – 12 fragments	-HIS -Uracil	187	15/20	CM	Yeast colony C1: 11 Yeast colony C2: 1137	C1 = 8/8 C2 = 4/4	pTP-PCR C1.1 pTP-PCR C2.1
2 – Reduced genome PCR – 9 fragments	-HIS	680	18/20	CM	Yeast colony C1: 4366 Yeast colony C2: 3530	C1 = 5/5 C2 = 5/5	pTP-PCR C3.1 pTP-PCR C4.1

diagnostic MPX PCR were selected and transformed into *E. coli*. After moving the assembled plasmids to *E. coli*, they were validated by diagnostic MPX PCR and restriction enzyme digest (Figure 3-1E, F). For Design 1, the two selected clones were named pTP-PCR C1.1/C2.1, and, for Design 2, pTP-PCR C3.1/C4.1. All four clones were sequenced and analyzed for mutations.

### **3.2.2 Sequence analysis of cloned *T. pseudonana* mitochondrial genomes**

Sequences obtained for the pTP-PCR plasmids were aligned to reference sequences, and upon analyzing mutations, pTP-PCR C1.1, C2.1, C3.1, and C4.1 had an average of 18 mutations per mitochondrial genome (Table 3-2, Supplementary Table C-2). We observed approximately twice the number of mutations in clones for Design 1; however, most of these mutations mapped to the repetitive region (Supplementary Table C-2), which could be due to sequencing errors. Mutations could have also occurred during the cloning process (PCR amplification of fragments) or propagation in the host organisms. It is also plausible that some of these variants could naturally exist in the population of *T. pseudonana* mitochondrial genomes or be variations between our strain and the sequenced genome. If desired, individual fragments could be cloned and confirmed by sequencing before use in yeast assembly.

### **3.2.3 Maintenance of *T. pseudonana*'s mitochondrial genome in host organisms**

We sought to examine the burden of propagating the cloned mitochondrial genomes in eukaryotic and prokaryotic host strains. *S. cerevisiae* and *E. coli* were used as host organisms to clone and store the *T. pseudonana* mitochondrial genome. We measured the growth of *E. coli* and *S. cerevisiae* strains in liquid media using a 96-well plate reader. Growth experiments performed for *S. cerevisiae* revealed that strains carrying plasmids with cloned mitochondrial genomes had a slightly increased growth rate; however, after

**Table 3-2. Summary of mutations identified in the cloned *T. pesudonana* mitochondrial genomes.** Identified mutations are categorized as point mutations (synonymous, missense, nonsense, and those found in non-coding regions) or gap mutations (insertions and deletions, either non-coding or coding).

Clone	Point mutations				Gap mutations				Total
	Synonymous	Missense	Nonsense	Non-coding	Non-coding		Coding		
					Insertion	Deletion	Insertion	Deletion	
pTP-PCR C1.1	1	6	0	8	0	6	0	3	24
pTP-PCR C2.1	1	3	0	7	2	8	0	2	23
pTP-PCR C3.1	0	5	0	0	0	1	2	4	12
pTP-PCR C4.1	1	5	0	3	0	1	0	2	12

24 h, the yeast strains grew to the same (Design 1) or slightly lower (Design 2) end-point densities as compared to control strains (Figure 3-2A and Figure 3-3A–D). For propagation in *E. coli*, we tested conditions where plasmids with mitochondrial genomes were maintained either as low or high (induced with arabinose) copy number. When these genomes were propagated in *E. coli* without arabinose induction to high plasmid copy number, there was no significant difference in the growth rate compared to the control strain (Figure 3-2B and Figure 3-3E, F). When grown with arabinose, all samples grew to a significantly lower end-point density than the uninduced strains (Figure 3-2B and Figure 3-3G, H); however, there were no significant differences between the control plasmid and plasmids harboring a mitochondrial genome within each growth condition (Figure 3-3G, H).

Additionally, when propagated in *E. coli* for an extended time (greater than 50 generations), we observed that a small fraction of genomes were mutated, as was evident by an absent PCR amplicon when clones were evaluated with MPX PCR (data not shown). To further investigate this, we evaluated one cloned mitochondrial genome (pTP-PCR C2.1) directly after transferring from yeast to *E. coli* (“G0”) or after ~60 generations (“G60”). Since we did not observe similar mutations in our previous work cloning the *P. tricornutum* mitochondrial genome, we used our cloned *P. tricornutum* mitochondrial genome (pPT-TAR C1) as a control [23]. In total, 30 colonies for both *T. pseudonana* (from clone pTP-PCR C2.1) and *P. tricornutum* (from clone pPT-TAR C1) were evaluated at G0 and G60 using a higher resolution MPX PCR screen with six amplicons.

At G0, all 30 *E. coli* clones harboring either plasmid showed successful amplification of all six amplicons. At G60, all 30 *E. coli* clones harboring pPT-TAR C1 had a complete genome as analyzed by MPX PCR, suggesting that, over 60 generations, this plasmid is stably maintained. However, only 25 of 30 *E. coli* clones containing pTP-PCR C2.1 had complete genomes at G60, as analyzed by MPX PCR (Figure 3-4). These 5 clones were further analyzed by restriction enzyme digest (Supplementary Figure C-1). Four of these plasmids showed aberrant restriction enzyme banding patterns, suggesting a

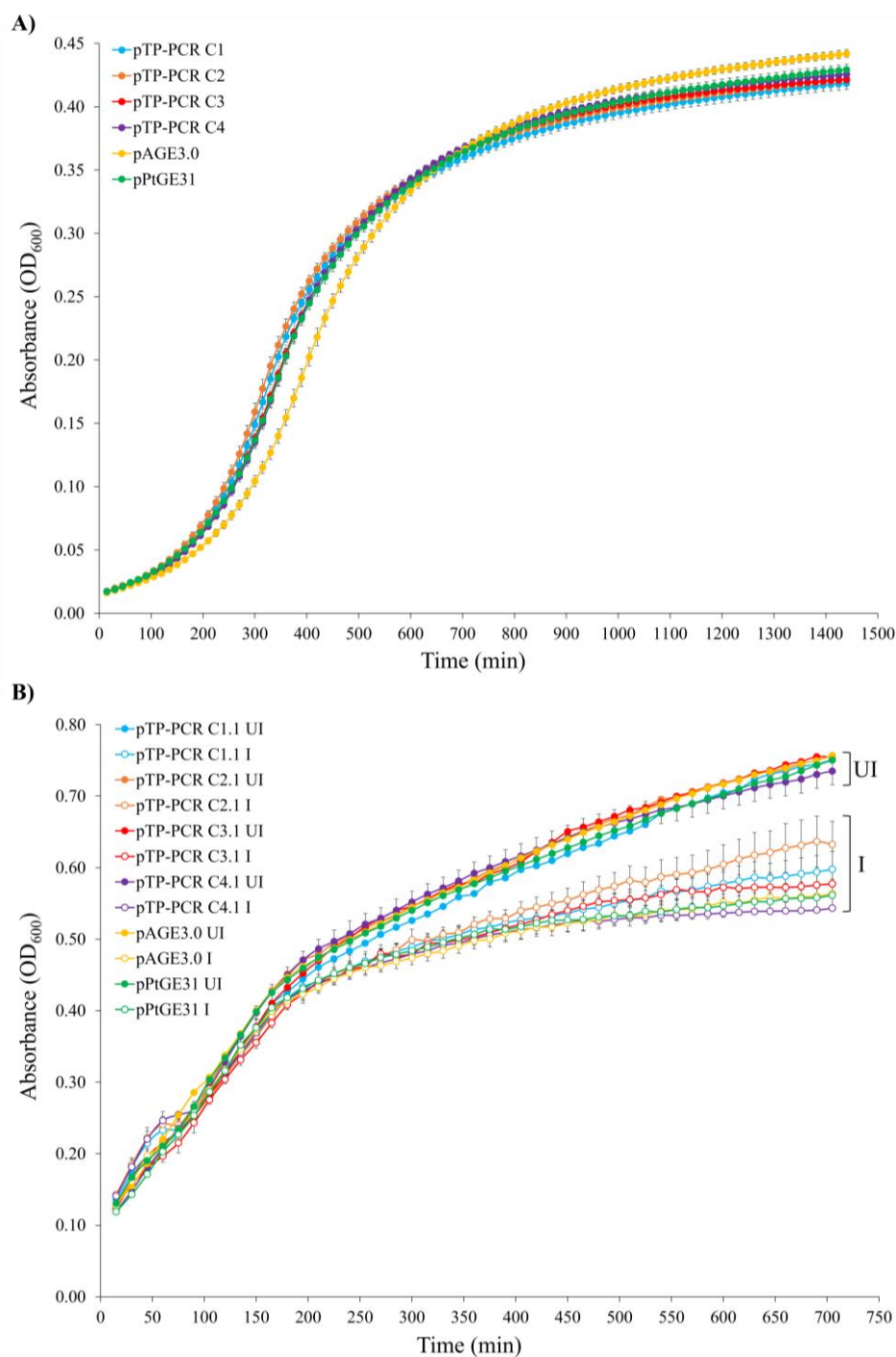


**Figure 3-2. Growth of host strains harboring cloned *T. pseudonana* mitochondrial genomes in liquid media. A)** Growth curves of *S. cerevisiae* strains grown in liquid synthetic complete media lacking histidine. **B)** Growth curves of *E. coli* strains grown in liquid LB media supplemented with chloramphenicol only (UI—un-induced) or with chloramphenicol and arabinose (I—induced). Each time point is the average of three biological replicates, each with four technical replicates and error bars representing the standard error of the mean.

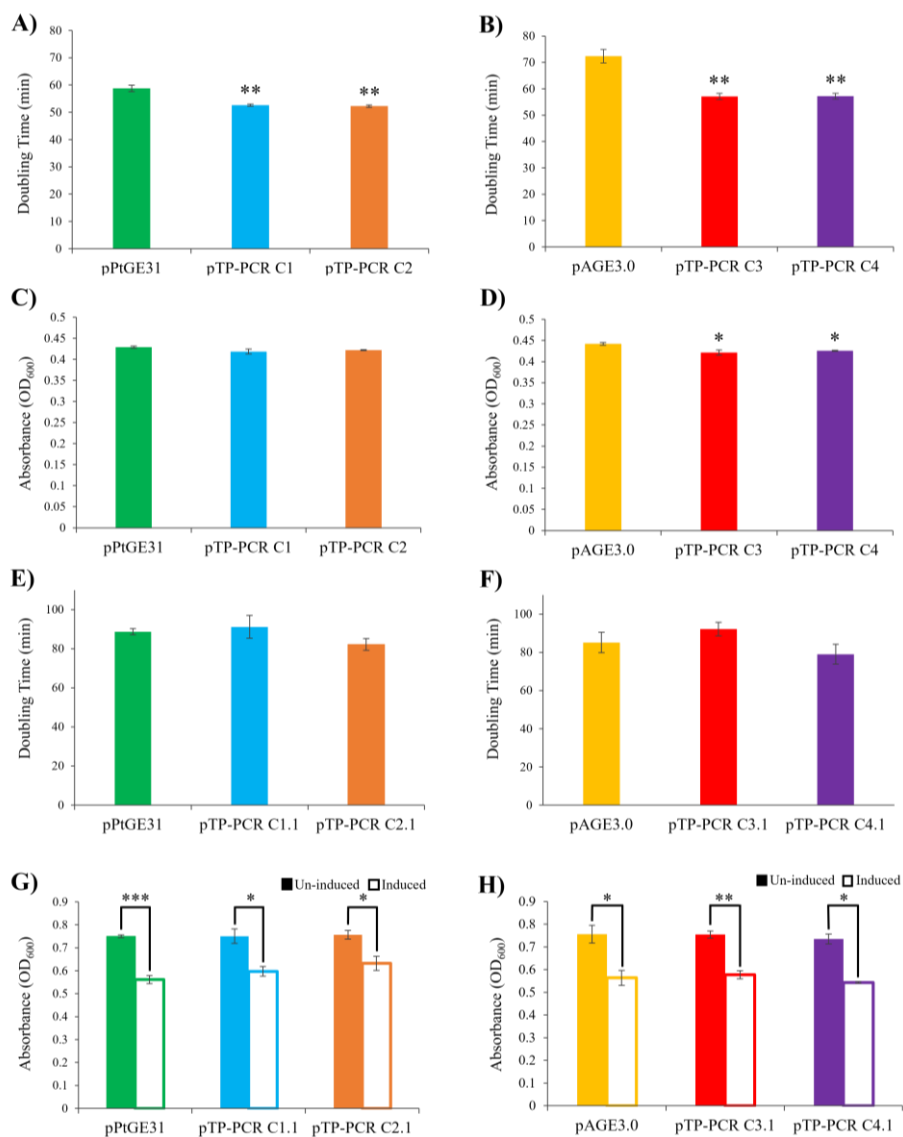


**Figure 3-3. Growth phenotypes of *S. cerevisiae* and *E. coli* harboring a cloned *T. pseudonana* mitochondrial genome. A–B)** The growth rate of *S. cerevisiae* harboring the full (A) and reduced (B) mitochondrial genome of *T. pseudonana* compared to control plasmids pPtGE31 and pAGE3.0, respectively. C–D) The maximum cell density reached by *S. cerevisiae* harboring the full (C) and reduced (D) mitochondrial genome compared to control plasmids. E–F) The growth rate of *E. coli* harboring the full (E) and reduced (F) mitochondrial genome, compared to control plasmids (uninduced conditions). G–H) Maximum cell density reached by *E. coli* harboring the full (G) and reduced (H) mitochondrial genome compared to control plasmids. Maximum density was compared in uninduced and arabinose-induced conditions. Note: Solid bars represent uninduced, and outlined bars represent induced conditions. Three biological replicates, each with four technical replicates, were used for data analysis. The scores represent means  $\pm$  standard error of the mean. Asterisks represent a significant difference from control plasmid (A–F) and/or between uninduced and induced *E. coli* harboring the same plasmid (G–H) (Student’s *t*-test: \*  $p < 0.05$ , \*\*  $p < 0.01$ ; \*\*\*  $p < 0.001$ ).

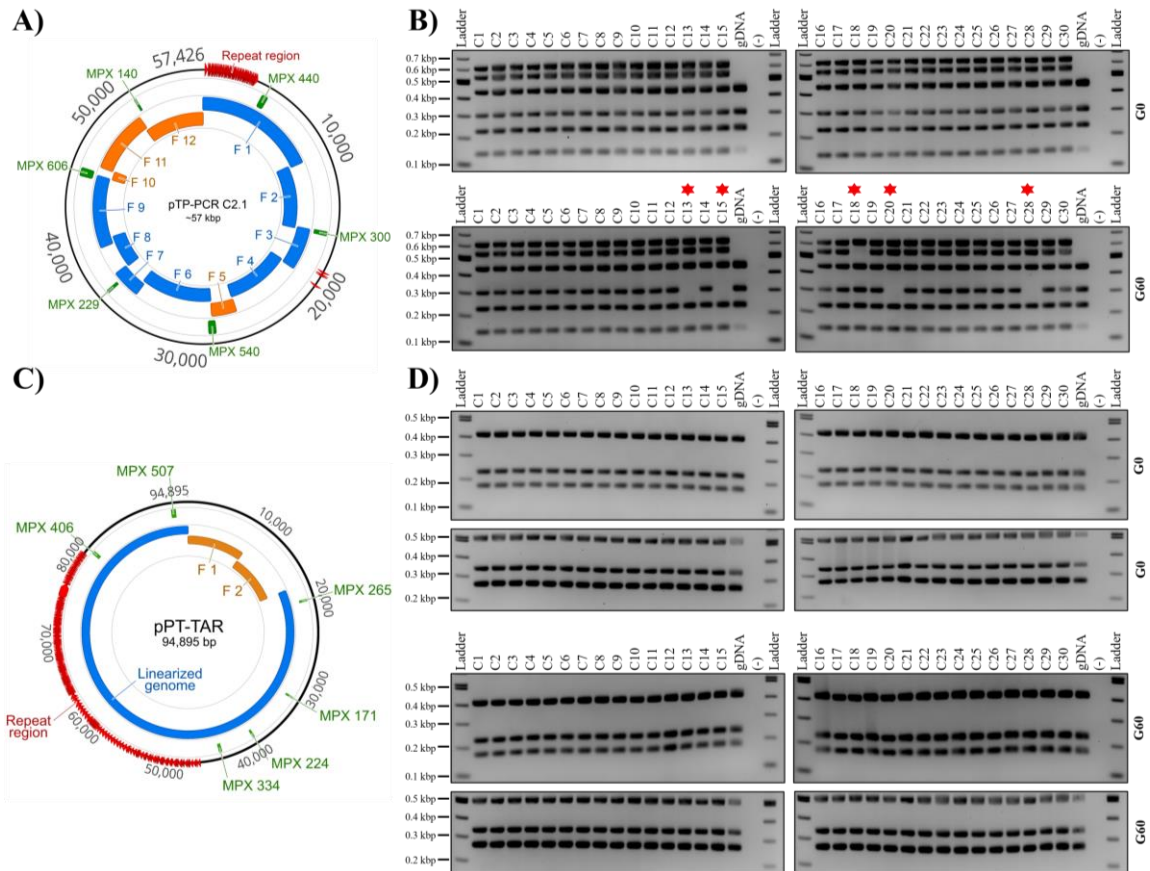


**Figure 3-4. Plasmid stability assay of cloned *T. pseudonana* and *P. tricornutum* mitochondrial genomes over 60 generations.** Thirty single colonies of either pTP-PCR C2.1 (A, B) or pPT-TAR C1 (C, D) were assayed by MPX PCR after transfer from yeast to *E. coli* (G0), and after ~60 generations (G60) in liquid LB media supplemented with chloramphenicol ( $15 \mu\text{g mL}^{-1}$ ). Notes: 1—in B), G60 colonies 13, 15, 18, 20, and 28 (red asterisk) are missing one PCR amplicon; 2—for *T. pseudonana* genomic DNA (gDNA), only the three fragments were expected to amplify, 229-, 300-, and 440-bp, but a small nonspecific band is also visible around 150 bp.



deletion or rearrangement. Three of these plasmids were sequenced, which confirmed that the absent MPX amplicon resulted from deletion events (Supplementary Figure C-2).

### **3.2.4 Assessing the expression of *T. pseudonona* and *P. tricornutum* mitochondrial genes in *E. coli***

RNA expression of mitochondrial genes was confirmed for pTP-PCR C2.1 and pPT-PCR C2.1 in *E. coli* with three biological replicates. Read counts were compared against pPtGE31 (lacking the mitochondrial genome). As expected, no reads from pPtGE31 mapped against the algal mitochondrial genomes, while genes from the pTP-PCR C2.1 and pPT-PCR C2.1 samples showed low read coverage. Low coverage of the mitochondrial genomes was likely obtained because the rRNA depletion kit selected failed to deplete the *E. coli* host's rRNA. The bacterial selection marker *cat* (providing resistance to chloramphenicol) was detected in all samples as expected; however, low read coverage was obtained for many of the genes on the pTP-PCR C2.1 and pPT-PCR C2.1 mitochondrial genomes (Supplementary Tables C-3 and C-4). The genes with the most mapped reads from the mitochondrial genome plasmids were rRNA and *cox1* genes. Although low read coverage was obtained, the counts confirm the expression of many of the mitochondrial genes from plasmids propagated in the *E. coli* hosts.

## **3.3 Discussion**

The biotechnological potential of organelle engineering is constrained by the lack of reliable methods to clone and deliver organelle genomes to the corresponding compartment. Toward this goal, we developed a method for cloning and manipulating *P. tricornutum* mitochondrial genomes in host organisms [23]. Here, we demonstrated that this method could be adapted to another microalga, *T. pseudonana*. As for *P. tricornutum*, we observed similar growth rates between host strains carrying empty plasmids and those with cloned *T. pseudonana* mitochondrial genomes. RNA expression analysis showed that many of the genes from plasmids harbouring *P. tricornutum* or *T.*

*pseudonana*'s mitochondrial genome are expressed in *E. coli*. Interestingly, mitochondrial gene expression in the host did not affect genome stability for *P. tricornutum*'s mitochondrial genome. Plasmids with *T. pseudonana*'s mitochondrial genomes were less stable with continued propagation in *E. coli*; after 60 generations, 17% of genomes were mutated.

It has been observed previously that cloning low G+C%-content DNA into bacteria can be problematic. As the G+C%-content decreases, the probability of any sequence producing a spontaneous promoter or origin of replication becomes more likely, which can result in plasmid toxicity and instability [36]. The addition of a second origin of replication can stall the replication fork, leading to plasmid rearrangements [37]. Challenges arise with G+C%-contents as low as 35–40%; however, it was shown that this DNA could be stably maintained at a low copy number [36]. Additionally, it has been shown that by engineering the vector backbone to be more accommodating, low G+C%-content genomes such as *Lactobacillus helveticus* (35%) could be cloned [36]. A future investigation could focus on optimizing the pTP-PCR plasmids for stability.

Although we can confirm that most of the mitochondrial genes on the pTP-PCR C2.1 and pPT-PCR C2.1 plasmids are expressed in *E. coli* hosts, the low read coverage obtained prevented us from performing a reliable differential expression analysis. However, the data does demonstrate that genes of the algal mitochondrial genomes are expressed in the *E. coli* hosts. To determine what genes of the mitochondrial genomes are more strongly expressed in the *E. coli* hosts, we will need to obtain higher coverage of the mitochondrial genome by successfully depleting the host's rRNA in a future experiment.

Now that two algal mitochondrial genomes have been cloned in host strains, we better understand potential hurdles that can be encountered when applying this method to other species. As a next step, a robust method for delivering these genomes to mitochondria will need to be developed. First, the mitochondrial genomes must be engineered with mitochondria-specific selectable markers. Using antibiotics targeting organelle-specific processes, previous studies have demonstrated an increased efficacy of

antibiotic resistance proteins when localized to the organelle compartment [38,39]. Further, two promising antibiotic selection markers, zeocin and chloramphenicol have been described for use in the mitochondria of *Chlamydomonas reinhardtii* [40] and the chloroplast of *P. tricornutum* [41], respectively. Additionally, any selection markers generated for *T. pseudonana*'s mitochondria will be designed using an alternative genetic code (UGA will be translated as a tryptophan instead of a stop codon), allowing proper antibiotic-resistance proteins to be expressed only in the mitochondrial compartment. This design feature will generate a powerful system for developing the genetic tools required for mitochondrial DNA delivery in *T. pseudonana*.

### 3.4 Conclusions

We have demonstrated that a previously developed method for cloning and manipulating mitochondrial genomes can be applied to additional microalga. With a PCR-based approach, we cloned the mitochondrial genome of *T. pseudonana* in its entirety (~44 and; ~58 kbp including the pPtGE31 plasmid backbone) or lacking a repetitive region (~40; ~58 kbp including the pAGE3.0 plasmid backbone). The cloned genomes imposed no substantial growth burden on *S. cerevisiae* and *E. coli* when these host organisms were used to propagate the plasmids. In *E. coli*, some plasmid instability was observed after 60 generations, likely attributable to the low G+C%-content of the mitochondrial genome. RNA sequencing was performed, and it was found that mitochondrial genes were being expressed from the plasmids harbored in *E. coli*. In this study, we replicated the previous methods for cloning and manipulating algal mitochondrial genomes using *T. pseudonana*. Subsequent work should focus on developing the technologies required for efficient mitochondrial DNA delivery.

## 3.5 Materials and Methods

### 3.5.1 Strains and growth conditions

*Thalassiosira pseudonana* (Culture Collection of Algae and Protozoa CCAP 1085/12) was grown in L1 media supplemented with 200  $\mu\text{M}$  of sodium silicate ( $\text{Na}_2\text{SiO}_3 \cdot 9 \text{H}_2\text{O}$ ) at 18 °C under cool white fluorescent lights ( $75 \mu\text{E m}^{-2} \text{s}^{-1}$ ) and a photoperiod of 16 h light: 8 h dark. L1 media was made as previously described [8]. *Saccharomyces cerevisiae* VL6-48 (ATCC MYA-3666: *MAT $\alpha$* , *his3- $\Delta$ 200*, *trp1- $\Delta$ 1*, *ura3-52*, *lys2*, *ade2-101*, *met14*, *psi*<sup>+</sup>, *cir*<sup>0</sup>) was grown at 30 °C in rich yeast media (2 x YPDA), or synthetic complete media lacking either histidine or both uracil and histidine. After yeast spheroplast transformation, all synthetic complete media used contained 1 M sorbitol [27]. *Escherichia coli* (Epi300, Lucigen) was grown at 37 °C in either LB media alone or supplemented with chloramphenicol (15  $\mu\text{g mL}^{-1}$ ).

### 3.5.2 Total DNA isolation by modified alkaline lysis

DNA from *E. coli*, *S. cerevisiae*, and algae were isolated as previously described in Section 2.4.2.2.

### 3.5.3 DNA fragment preparation for PCR-based cloning

#### 3.5.3.1 Design 1—full genome (pTP-PCR C1 and C2)

Mitochondrial genomes were cloned using the previously described method [23]. PCR amplification of mitochondrial fragments was performed using *T. pseudonana* total DNA. The mitochondrial genome was amplified as eight overlapping fragments (primers: P 1–4F/R and 6–8F/R, listed in Supplementary Table C-1), as well as four additional fragments (primers: P 5F/R and 10–12F/R, listed in Supplementary Table C-1) to amplify the *URA3* yeast selection marker and pPtGE31 plasmid backbone [30]. The pPtGE31 plasmid contains all the genetic elements required for selection and stable propagation in *S. cerevisiae*, *E. coli*, and *P. tricornutum*. In addition, this plasmid contains an *oriT* to allow for plasmid transfer using bacterial conjugation. All primers were manually

designed. Forward and reverse primers for fragments 2–3, 7–8, and the reverse primer of fragment 1 were designed to be 40 bp in length. Primers 60 bp in length were designed for fragments 4–6, 9–12, and the forward primer of fragment 1. Overlapping homology between fragments was between 80 and 635 bp to allow for efficient yeast assembly.

Each fragment was individually amplified in a 50  $\mu$ L PCR reaction using 1  $\mu$ L of PrimeSTAR GXL polymerase, 1  $\mu$ L of template DNA (1–100 ng  $\mu$ L<sup>-1</sup> isolated total DNA from either *T. pseudonana* or *E. coli*), and the respective forward and reverse primers each at a final concentration of 0.2  $\mu$ M. The thermocycler conditions for fragments 2, 4–9, and 11–12 was as follows: 25 cycles of 98 °C for 10 s, 60 °C for 15 s, and 68 °C for 600 s, and one cycle of 68 °C for 600 s, finishing with an infinite hold at 12 °C. The thermocycler for fragment 1 was programmed as follows: 5 cycles of 98 °C for 10 s, 50 °C for 15 s, and 68 °C for 420 s, followed by 20 cycles of 98 °C for 10 s, 60 °C for 15 s, and 68 °C for 420 s, and one cycle of 68 °C for 600 s, finishing with an infinite hold at 12 °C. The thermocycler for fragment 3 was programmed as follows: 25 cycles of 98 °C for 10 s, 50 °C for 15 s, and 68 °C for 660 s, and one cycle of 68 °C for 600 s, finishing with an infinite hold at 12 °C. The thermocycler for fragment 10 was programmed as follows: 25 cycles of 98 °C for 10 s, 55 °C for 15 s, and 68 °C for 60 s, and one cycle of 68 °C for 600 s, finishing with an infinite hold at 12 °C. PCR product amplification was confirmed by performing agarose gel electrophoresis with 2  $\mu$ L of PCR product on a 1.4% agarose (w/v) gel. To eliminate plasmid template DNA, PCR products were treated with DpnI restriction enzyme as previously described in Section 2.4.3.

### **3.5.3.2 Design 2—reduced genome lacking repetitive region (pTP-PCR C3 and C4)**

PCR amplification of mitochondrial fragments was performed using isolated *T. pseudonana* total DNA as the template DNA. The mitochondrial genome was amplified as seven overlapping fragments (primers: P 1R, 2–3F/R, 4F, 6R, 8R, 13–14F/R, and 17–18F, listed in Supplementary Table C-1), as well as two additional fragments (primers: P15–16F/R, listed in Supplementary Table C-1) to amplify the pAGE3.0 plasmid with

homology to sequence directly flanking the repeat region. The pAGE3.0 plasmid is a derivation of pPtGE31 providing additional elements for selection and stable propagation in *Sinorhizobium meliloti* [31]. All primers were manually designed. Forward and reverse primers for fragments 1–2, 5, the forward primer for fragments 4 and 6, and the reverse primer for fragments 3 and 9 were designed to be 40 bp long. Primers 60 bp in length were designed for the forward primer of fragment 3 and the reverse primer of fragment 4. The reverse primer of fragment 6, forward primer of fragment 9, and primers of fragments 7–8 were 80 bp in length. Overlapping homology between fragments was between 80 and 635 bp to allow for efficient yeast assembly.

Each fragment was individually amplified in a 50  $\mu$ L PCR reaction using 1  $\mu$ L of PrimeSTAR GXL polymerase, 1  $\mu$ L of template DNA (1–100 ng  $\mu$ L<sup>-1</sup> isolated total DNA from either *T. pseudonana* or *E. coli*), and the respective forward and reverse primers each at a final concentration of 0.2  $\mu$ M. The thermocycler for fragments 1, 3–5, and 7–9 was programmed as follows: 25 cycles of 98 °C for 10 s, 60 °C for 15 s, and 68 °C for 600 s, and one cycle of 68 °C for 600 s, finishing with an infinite hold at 12 °C. The thermocycler for fragments 2 and 6 was programmed as follows: 30 cycles of 98 °C for 10 s, 50 °C for 15 s, and 68 °C for 660 s, followed by one cycle of 68 °C for 600 s, finishing with an infinite hold at 12 °C. PCR product amplification was confirmed by performing agarose gel electrophoresis with 2  $\mu$ L of PCR product on a 1.4% agarose (w/v) gel. To eliminate plasmid template DNA, PCR products were treated with DpnI restriction enzyme as described previously in Section 2.4.3.

### **3.5.4 Yeast spheroplast transformation protocol**

Yeast spheroplast transformation was performed as previously described in Section 2.4.5.

### **3.5.5 *E. coli* transformation**

*E. coli* transformation was performed as previously described in Section 2.4.6.

### **3.5.6 Screening strategy**

#### **3.5.6.1 Screening Yeast Colonies**

To identify positive clones, individual yeast colonies were screened as previously described in Section 2.4.7.1, using selective 2% agar plates containing synthetic complete media lacking either histidine and uracil for pTP-PCR C1/2 or histidine for pTP-PCR C3/4. MPX primers used for screening yeast colonies differ from the original protocol and are listed in Supplementary Table C-1.

#### **3.5.6.2 Screening *E. coli* Colonies**

To identify positive clones, individual *E. coli* colonies were screened as previously described in Section 2.4.7.2 with the following modifications to the restriction enzyme digestion reactions. For pTP-PCR C1.1/2.1, digestion reactions were generated using 7  $\mu\text{L}$  of DNA ( $\sim 5000 \text{ ng } \mu\text{L}^{-1}$ ), 2  $\mu\text{L}$  of NEBuffer 3.1 restriction buffer, 0.4  $\mu\text{L}$  PvuI, and 10.6  $\mu\text{L}$  of water. For pTP-PCR C3.1/4.1, digestion reactions were generated using 7  $\mu\text{L}$  of DNA ( $\sim 5000 \text{ ng } \mu\text{L}^{-1}$ ), 2  $\mu\text{L}$  of CutSmart Buffer, 0.4  $\mu\text{L}$  PmeI, 0.4  $\mu\text{L}$  BamHI-HF, and 10.2  $\mu\text{L}$  of water. Reaction mixtures were transferred to a Bio-Rad thermocycler and incubated either at 37 °C for 90 min or 37 °C for 90 min, followed by 65 °C for 20 min for pTP-PCR C1.1/2.1 and C3.1/4.1, respectively. After confirmation by MPX PCR and diagnostic restriction enzyme digestion, the four plasmids underwent next-generation whole plasmid sequencing at CCIB DNA Core at Massachusetts General Hospital.

### **3.5.7 Evaluation of growth phenotypes of host strains**

#### **3.5.7.1 *S. cerevisiae* growth in liquid media**

Growth rates were evaluated for *S. cerevisiae* strains harboring pTP-PCR C1, C2, C3, and C4 plasmids, or pPtGE31 and pAGE3.0 control plasmids (lacking a mitochondrial genome), as previously described in Section 2.4.8.2, with absorbance ( $\text{OD}_{600}$ ) measurements taken every 15 min for 24 h. This experiment was performed with three

biological replicates, each with four technical replicates; therefore, 12 readings were obtained and averaged for each strain, the standard error of the mean was calculated, and the curves were plotted. End-point densities at 1440 min were averaged for each strain, and the standard error of the mean was calculated. The td of each replicate was determined using the R package Growthcurver (<http://github.com/sprouffske/growthcurver>) [32]. The td was averaged from the 12 replicates for each strain, and the standard error of the mean was calculated.

### **3.5.7.2 *E. coli* growth in liquid media**

Growth rates were evaluated for *E. coli* strains harboring pTP-PCR C1.1, C2.1, C3.1, and C4.1 plasmids or pPtGE31 and pAGE3.0 control plasmids (lacking a mitochondrial genome), as previously described in Section 2.4.8.1, except the samples were not placed on ice and absorbance (OD<sub>600</sub>) measurements were taken every 15 min for 11.5 h. This experiment was performed with three biological replicates, each with four technical replicates; therefore, 12 readings were obtained and averaged for each strain, the standard error of the mean was calculated, and the curves were plotted. End-point densities at 705 min were averaged for each strain, and the standard error of the mean was calculated. The td of each replicate was determined using the R package Growthcurver (<http://github.com/sprouffske/growthcurver>) [32]. The td was averaged from the 12 replicates for each strain, and the standard error of the mean was calculated. Replicates shown to be major outliers were removed from the dataset (Supplementary Note C-1).

### **3.5.8 Bacterial RNA extraction**

*E. coli* harboring the pTP-PCR C2.1, pPT-PCR C2.1 [23], or pPtGE31 plasmid (lacking a mitochondrial genome) were inoculated overnight in LB media supplemented with chloramphenicol (15 µg mL<sup>-1</sup>) from frozen strain stocks. In the morning, 1 mL of cells was diluted into 25 mL of LB media supplemented with chloramphenicol (15 µg mL<sup>-1</sup>) and grown for 120 min at 37 °C until absorbance (OD<sub>600</sub>) reached 1. Subsequently, the



RNA stabilization of the culture was performed using RNAProtect Bacteria Reagent. Briefly, 400  $\mu\text{L}$  ( $2 \times 10^8$  cells) of culture was transferred to a 15 mL Falcon tube containing 800  $\mu\text{L}$  of RNAProtect Bacteria Reagent, and the suspension was vortexed for 5 s and incubated at RT for 5 min. Total RNA was isolated using the RNeasy Mini Kit according to the manufacturer's instructions. Following treatment with DNase using RNase-free DNase Set, the RNA concentration was determined using DeNovix, and the integrity was verified by running 400 ng of RNA on a 1% agarose (*w/v*) gel. RNA samples were stored at  $-80\text{ }^\circ\text{C}$  until use.

### **3.5.9 RNA sequencing**

The quality of isolated RNA (Section 3.5.8) was validated using the Agilent Bioanalyzer 2100. The RNA library was created and sequenced using the NextSeq 550 platform (single end 150 mid-output), with rRNA depleted using the NEB bacterial rRNA depletion kit. Read quality was evaluated using FastQC v0.11.9, and the reads were trimmed using Trimmomatic v0.39 in single-end mode using the parameters AVGQUAL:25 CROP:150 MINLEN:100 [33–35]. Reads for the pTP-PCR C2.1 and pPT-PCR C2.1 strains were mapped against their respective mitochondrial plasmid maps using bowtie 2.26 in single-end mode with the parameters no-unal -k 1. Read counts were generated using htseq-count.

### **3.5.10 Plasmid stability assay**

#### **3.5.10.1 Propagation of *E. coli* strains**

*E. coli* harboring either pTP-PCR C2.1 or pPT-TAR C1 [23] plasmids were inoculated from frozen strain stocks (note that these stocks were generated by transferring cloned mitochondrial DNA from yeast to *E. coli*, isolating single colonies on LB plates, and then grown overnight in liquid before freezing) overnight at  $37\text{ }^\circ\text{C}$  (225 RPM) in 5 mL of LB media supplemented with chloramphenicol ( $15\text{ }\mu\text{g mL}^{-1}$ ). The saturated overnight culture

was adjusted to an OD<sub>600</sub> of 0.1, and frozen strain stocks were generated (G0). Next, 1 µL of the adjusted culture was added to 50 mL of LB media supplemented with chloramphenicol (15 µg mL<sup>-1</sup>). Cultures were grown at 37 °C (225 RPM) to an OD<sub>600</sub> of ~3. Four repetitions (~60 generations) of diluting grown cultures to an OD<sub>600</sub> of 0.1 and passaging 1 µL of adjusted culture into 50 mL of LB media supplemented with chloramphenicol (15 µg mL<sup>-1</sup>) were performed. After four serial passages, frozen strain stocks of each bacterial strain adjusted to an OD<sub>600</sub> of 0.1 were generated to analyze plasmid stability (G60).

### **3.5.10.2 Analysis of descendant *E. coli* colonies**

Strain stocks of pTP-PCR C2.1 or pPT-TAR C1 from the start (G0) and end (G60) of propagation were thawed on ice for 20 min and then diluted 1:5000 with LB media in 1.5 mL microcentrifuge tubes. Next, 100 µL of each diluted culture was plated separately onto selective LB agar plates supplemented with chloramphenicol (15 µg mL<sup>-1</sup>) and grown at 37 °C for 24 h to obtain single colonies. Thirty single colonies of each construct were struck onto selective LB agar plates supplemented with chloramphenicol (15 µg mL<sup>-1</sup>) and grown for 12 h at 37 °C. Next, each streak was resuspended in a PCR tube containing 100 µL of TE buffer. The cell mixture was transferred to a Bio-Rad thermocycler and incubated at 95 °C for 15 min to lyse the cells. The cellular debris was pelleted to the bottom of the PCR tube using a microcentrifuge, and 1 µL of supernatant was used as a template for diagnostic MPX PCR. Two additional diagnostic primer sets (P 19–20F/R, listed in Supplementary Table C-1) were generated for this plasmid stability analysis. Primer pairs P 19–20F/R were designed to have an optimized melting temperature of 60 °C using the online tool Primer3 (<http://bioinfo.ut.ee/primer3-0.4.0/>). To test plasmid stability, primer sets P 19–24F/R generated 140-, 229-, 300-, 440-, 540-, and 606-bp amplicons, respectively. Then, 2 µL of the PCR products were loaded onto a 2% agarose (*w/v*) gel for electrophoresis and analyzed.

### 3.5.11 Statistical analyses

Statistical analyses were performed using Microsoft Excel spreadsheet software. Pair-wise comparisons were made using a Student's *t*-test with either equal or unequal variance based on the result of an F-test. The error bar shown represents the standard error of the mean.

## 3.6 References

1. Nelson DM, Tréguer P, Brzezinski MA, Leynaert A, and Quéguiner B. Production and dissolution of biogenic silica in the ocean: Revised global estimates, comparison with regional data and relationship to biogenic sedimentation. *Glob Biogeochem Cycles*. 1995;9:359–372. doi:10.1029/95GB01070
2. Tréguer P, Nelson DM, Van Bennekom AJ, DeMaster DJ, Leynaert A, and Quéguiner B. The silica balance in the world ocean: A reestimate. *Science*. 1995;268:375–379. doi:10.1126/science.268.5209.375
3. Pérez-Cabero M, Puchol V, Beltrán D, and Amorós P. *Thalassiosira pseudonana* diatom as biotemplate to produce a macroporous ordered carbon-rich material. *Carbon*. 2008;46:297–304. doi:10.1016/j.carbon.2007.11.017
4. Delalat B, Sheppard VC, Ghaemi SR, Rao S, Prestidge CA, McPhee G, et al. Targeted drug delivery using genetically engineered diatom biosilica. *Nat Commun*. 2015;6:1–11. doi:10.1038/ncomms9791
5. Armbrust EV, Berges JA, Bowler C, Green BR, Martinez D, Putnam NH, et al. The genome of the diatom *Thalassiosira pseudonana*: Ecology, evolution, and metabolism. *Science*. 2004;306:79–86. doi:10.1126/science.1101156
6. Oudot-Le Secq MP and Green BR. Complex repeat structures and novel features in the mitochondrial genomes of the diatoms *Phaeodactylum tricornutum* and *Thalassiosira pseudonana*. *Gene*. 2011;476:20–26. doi:10.1016/j.gene.2011.02.001
7. Oudot-Le Secq MP, Grimwood J, Shapiro H, Armbrust EV, Bowler C, and Green BR. Chloroplast genomes of the diatoms *Phaeodactylum tricornutum* and *Thalassiosira pseudonana*: Comparison with other plastid genomes of the red lineage. *Mol Genet Genomics*. 2007;277:427–439. doi:10.1007/s00438-006-0199-4

8. Karas BJ, Diner RE, Lefebvre SC, McQuaid J, Phillips APR, Noddings CM, et al. Designer diatom episomes delivered by bacterial conjugation. *Nat Commun.* 2015;6:1–10. doi:10.1038/ncomms7925
9. Poulsen N, Chesley PM, and Kröger N. Molecular genetic manipulation of the diatom *Thalassiosira pseudonana* (Bacillariophyceae). *J Phycol.* 2006;42:1059–1065. doi:10.1111/j.1529-8817.2006.00269.x
10. Hopes A, Nekrasov V, Kamoun S, and Mock T. Editing of the urease gene by CRISPR-Cas in the diatom *Thalassiosira pseudonana*. *Plant Methods.* 2016;12:1–12. doi:10.1186/s13007-016-0148-0
11. Trentacoste EM, Shrestha RP, Smith SR, Glé C, Hartmann AC, Hildebrand M, et al. Metabolic engineering of lipid catabolism increases microalgal lipid accumulation without compromising growth. *Proc Natl Acad Sci U.S.A.* 2013;110:19748–19753. doi:10.1073/pnas.1309299110
12. Tesson B, Lerch SJL, and Hildebrand M. Characterization of a new protein family associated with the silica deposition vesicle membrane enables genetic manipulation of diatom silica. *Sci Rep.* 2017;7:1–13. doi:10.1038/s41598-017-13613-8
13. Belshaw N, Grouneva I, Aram L, Gal A, Hopes A, and Mock T. Efficient gene replacement by CRISPR/Cas-mediated homologous recombination in the model diatom *Thalassiosira pseudonana*. *New Phytol.* 2022;1:438–452. doi:10.1111/nph.18587
14. Görlich S, Pawolski D, Zlotnikov I, and Kröger N. Control of biosilica morphology and mechanical performance by the conserved diatom gene *Silicanin-1*. *Commun Biol.* 2019;2:1–8. doi:10.1038/s42003-019-0436-0
15. Schober AF, Río Bártulos C, Bischoff A, Lepetit B, Gruber A, and Kroth PG. Organelle studies and proteome analyses of mitochondria and plastids fractions from the diatom *Thalassiosira pseudonana*. *Plant Cell Physiol.* 2019;60:1811–1828. doi:10.1038/s42003-019-0436-0
16. Avalos JL, Fink GR, and Stephanopoulos G. Compartmentalization of metabolic pathways in yeast mitochondria improves production of branched chain alcohols. *Nat Biotechnol.* 2017;31:1–10. doi:10.1038/nbt.2509
17. Bigger BW, Liao AY, Sergijenko A, and Coutelle C. Trial and error: How the unclonable human mitochondrial genome was cloned in yeast. *Pharm Res.* 2011;28:2863–2870. doi:10.1007/s11095-011-0527-1

18. Yoon YG and Koob MD. Efficient cloning and engineering of entire mitochondrial genomes in *Escherichia coli* and transfer into transcriptionally active mitochondria. *Nucleic Acids Res.* 2003;31:1407–1415. doi:10.1093/nar/gkg228
19. Gibson DG, Smith HO, Hutchison III CA, Venter JC, and Merryman C. Chemical synthesis of the mouse mitochondrial genome. *Nat Methods.* 2010;7:901–903. doi:10.1038/nmeth.1515
20. Gupta M and Hoo B. Entire maize chloroplast genome is stably maintained in a yeast artificial chromosome. *Plant Mol Biol.* 1991;17:361–369. doi:10.1007/BF00040631
21. Itaya M, Fujita K, Kuroki A, and Tsuge K. Bottom-up genome assembly using the *Bacillus subtilis* genome vector. *Nat Methods.* 2008;5:41–43. doi:10.1038/nmeth1143
22. O’Neill BM, Mikkelsen KL, Gutierrez NM, Cunningham JL, Wolff KL, Szyjka SJ, et al. An exogenous chloroplast genome for complex sequence manipulation in algae. *Nucleic Acids Res.* 2012;40:2782–2792. doi:10.1093/nar/gkr1008
23. Cochrane RR, Brumwell SL, Soltysiak MPM, Hamadache S, Davis JG, Wang J, et al. Rapid method for generating designer algal mitochondrial genomes. *Algal Res.* 2020;50:1–30. doi:10.1016/j.algal.2020.102014
24. Noskov VN, Karas BJ, Young L, Chuang R-Y, Gibson DG, Lin YC, et al. Assembly of large, high G+C bacterial DNA fragments in yeast. *ACS Synth Biol.* 2012;1:267–273. doi:10.1021/sb3000194
25. Benders GA, Noskov VN, Denisova EA, Lartigue C, Gibson DG, Assad-Garcia N, et al. Cloning whole bacterial genomes in yeast. *Nucleic Acids Res.* 2010;38:2558–2569. doi:10.1093/nar/gkq119
26. Karas BJ, Suzuki Y, and Weyman PD. Strategies for cloning and manipulating natural and synthetic chromosomes. *Chromosom Res.* 2015;23:57–68. doi:10.1007/s10577-014-9455-3
27. Karas BJ, Jablanovic J, Sun L, Ma L, Goldgof GM, Stam J, et al. Direct transfer of whole genomes from bacteria to yeast. *Nat Methods.* 2013;10:410–412. doi:10.1038/nmeth.2433
28. Karas BJ, Molparia B, Jablanovic J, Hermann WJ, Lin YC, Dupont CL, et al. Assembly of eukaryotic algal chromosomes in yeast. *J Biol Eng.* 2013;7:1–12. doi:10.1186/1754-1611-7-30

29. Yoon YG and Koob MD. Toward genetic transformation of mitochondria in mammalian cells using a recoded drug-resistant selection marker. *J Genet Genomics*. 2011;38:173–179. doi:10.1016/j.jgg.2011.03.005
30. Slattery SS, Diamond A, Wang H, Therrien JA, Lant JT, Jazey T, et al. An expanded plasmid-based genetic toolbox enables Cas9 genome editing and stable maintenance of synthetic pathways in *Phaeodactylum tricornutum*. *ACS Synth Biol*. 2018;7:328–338. doi:10.1021/acssynbio.7b00191
31. Brumwell SL, MacLeod MR, Huang T, Cochrane RR, Meaney RS, Zamani M, et al. Designer *Sinorhizobium meliloti* strains and multi-functional vectors enable direct inter-kingdom DNA transfer. *PLoS One*. 2019;14:e0206781. doi:10.1371/journal.pone.0206781
32. Sprouffske K and Wagner A. Growthcurver: An R package for obtaining interpretable metrics from microbial growth curves. *BMC Bioinformatics*. 2016;17:172. doi:10.1186/s12859-016-1016-7
33. Bolger AM, Lohse M, and Usadel B. Trimmomatic: A flexible trimmer for Illumina sequence data. *Bioinformatics*. 2014;30:2114–2120. doi:10.1093/bioinformatics/btu170
34. Langmead B and Salzberg SL. Fast gapped-read alignment with Bowtie 2. *Nat Methods*. 2012;9:357–359. doi:10.1038/nmeth.1923
35. Anders S, Pyl PT, and Huber W. HTSeq-A Python framework to work with high-throughput sequencing data. *Bioinformatics*. 2015;31:166–169. doi:10.1093/bioinformatics/btu638
36. Godiska R, Patterson M, Schoenfeld T, and Mead DA. Beyond pUC: Vectors for cloning unstable DNA. *Optim DNA Seq Process*. 2005;1:55–75.
37. Bierne H and Michel B. When replication forks stop. *Mol Microbiol*. 1994;13:17–23. doi:10.1111/j.1365-2958.1994.tb00398.x
38. Yoon YG and Koob MD. Selection by drug resistance proteins located in the mitochondria of mammalian cells. *Mitochondrion*. 2008;8:345–351. doi:10.1016/j.mito.2008.07.004
39. Rasala BA, Chao SS, Pier M, Barrera DJ, and Mayfield SP. Enhanced genetic tools for engineering multigene traits into green algae. *PLoS One*. 2014;9:e94028. doi:10.1371/journal.pone.0094028

40. Hu Z, Fan Z, Zhao Z, Chen J, and Li J. Stable expression of antibiotic-resistant gene *ble* from *Streptoalloteichus hindustanus* in the mitochondria of *Chlamydomonas reinhardtii*. PLoS One. 2012;7:e35542. doi:10.1371/journal.pone.0035542
41. Xie WH, Zhu CC, Zhang NS, Li DW, Yang WD, Liu JS, et al. Construction of novel chloroplast expression vector and development of an efficient transformation system for the diatom *Phaeodactylum tricornutum*. Mar Biotechnol. 2014;16:538–546. doi:10.1007/s10126-014-9570-3

## Chapter 4

### 4 Superior conjugative plasmids delivered by bacteria to diverse fungi

The work presented in this chapter is adapted from:

Cochrane, RR, Shrestha, A, Severo de Almeida, MM, Agyare-Tabbi, M, Brumwell, SL, Hamadache, S, Meaney, JS, Nucifora, DP, Say, HH, Sharma, J, Soltysiak, PM, Tong, C, Van Belois, K, Walker, EJM, Lachance, MA, Gloor, GB, Edgell, DR, Shapiro, RS, & Karas, BJ (2022). Superior conjugative plasmids delivered by bacteria to diverse fungi. BioDesign, 9802168.

#### 4.1 Introduction

The fungal kingdom is exquisitely diverse and home to countless species with profound impacts on ecological nutrient cycling, industrial manufacturing, and health and disease in humans, animals, and plants [1,2]. Yeast species are amongst the best-studied fungi and include the common yeast *S. cerevisiae*, which is a primary fermenter of beer, wine, and bread, and a ubiquitous eukaryotic model system. *S. cerevisiae* is also an important synthetic biology chassis for producing insulin, vaccine components, and other critical recombinant proteins [3]. The closely related *Saccharomyces boulardii* is a promising probiotic therapeutic, particularly in the context of obesity and type 2 diabetes [4,5]. Yeasts are also critical components of the human microbiota, including *Candida* species associated with vaginal yeast infections and invasive candidiasis [6], and *Malassezia* species with notable associations with Crohn's disease and pancreatic cancer [7, 8]. The skin-associated yeast *Candida auris* is an emerging fungal pathogen that can cause life-threatening infections and is highly refractory to antifungal drug treatment [9–11]. These diverse and critical roles in health, disease, and industrial manufacturing highlight the importance of studying and manipulating the biology of these key yeast species.

Given the diversity of yeast species and the breadth of niches they inhabit, there is a need to develop improved and innovative methods for DNA transformation in these



organisms. Genetic transformation techniques enable the manipulation of genomes of industrially important yeasts and further promote the ability to target, modify, or damage the genomes of fungal pathogens. Indeed, genetic-editing tools such as CRISPR have a promising role as novel antimicrobial agents due to their ability to specifically target pathogen-associated genes, leading to microbial death, growth inhibition, or targeted deletion of genes involved in antimicrobial resistance or virulence [12–18]. However, laboratory-based transformation protocols typically rely on chemical strategies to promote DNA uptake, which is not broadly applicable for manipulating yeasts in their native environments, such as those inhabiting the microbiome. One innovative strategy to promote the uptake of genetic material *in situ* is to exploit bacterial conjugation as a viable mechanism to transfer plasmids from bacteria to a recipient microbe via the bacterial type IV secretion system. Previous work has demonstrated the utility of bacterial conjugation for transferring plasmids, including those encoding CRISPR-based antimicrobials, between bacterial species, both *in vitro* [19,20] and *in vivo* in mouse microbiome models [21–23]. While bacterial conjugation typically occurs between bacterial species, cross-kingdom bacterial conjugation from bacteria to yeast and algae has been demonstrated [24–27]. Despite recently optimized protocols [28, 29], bacterial conjugation to yeast still suffers from a relatively low bacterial conjugation efficiency compared to prokaryotic recipients.

Thus, we sought to improve DNA transfer from bacteria to yeast by optimizing the genetic bacterial conjugation machinery of the pTA-Mob 2.0 plasmid [28]. This conjugative plasmid is composed of genetic elements required for plasmid maintenance and transfer [30,31]. Two regions, Tra1 and Tra2, are responsible for the transfer of plasmid DNA. Tra1 harbors the relaxase (TraH–J), primase (TraA–G), and leader (TraK–M) operons, which together coordinate the mobilization of the plasmid to the recipient [31]. The relaxase and leader operons encode the relaxosome, a protein complex essential for initial DNA processing during bacterial conjugation. Assembly of the protein complex (TraH–J) is initiated by TraJ binding to the 19-bp inverted repeat sequence in the *oriT* [32–34]. The interaction of TraI and TraJ, which TraH stabilizes, then orients the relaxase toward the nick-site [34]. After the formation of the relaxosome, TraI nicks and

covalently binds to the pDNA, ready for transfer to the recipient cell [35,36]. The binding of TraK to the *oriT* orients the pDNA into a more favorable position increasing the nicking reaction's efficiency [33,37]. TraC1, of the primase operon, is a DNA primase that co-transfers (along with single-stranded binding proteins) with the DNA to the recipient cell, where it is involved in restoring a double-stranded plasmid [38]. The primase operon also includes the TraG protein, which couples DNA processing by the relaxosome to DNA transfer by delivering the protein-DNA complex to the mating pair formation proteins [39,40]. The Tra2 region contains proteins (TrbB–L and TraF) required for mating pair formation, many of which are associated with the cell membrane. TrbC encodes a peptide responsible for forming the pilus. This peptide undergoes maturation by proteolytic cleavage followed by cyclization by TraF, resulting in rigid pili [41,42]. The pilus allows initial contact between the two cells and enables the transfer of single-stranded pDNA to the recipient cell.

Here, we developed and validated novel plasmids for improved bacterial conjugation efficiency between bacteria and diverse yeast species. We demonstrated that a cluster mutation in the relaxase operon, specifically in the *traJ* promoter, significantly improved DNA transfer from bacteria to *S. cerevisiae* and diverse yeasts, including the emerging pathogen *C. auris*. We generated improved, streamlined, and Golden Gate (GG) assembly-compatible plasmid derivatives of pTA-Mob 2.0 to enable facile insertion of custom genetic cassettes. Finally, we demonstrated that these designer conjugative plasmids can be used as a novel antifungal reagent with important applications for developing next-generation antifungal therapeutics.

## 4.2 Results

### 4.2.1 Development of streamlined conjugation plasmids

As a first step (Figure 4-1) toward creating an optimized and minimized conjugative plasmid for yeast, 55 single genes or small genetic regions were individually deleted from our previously established trans-kingdom conjugation plasmid, pTA-Mob 2.0 [28]

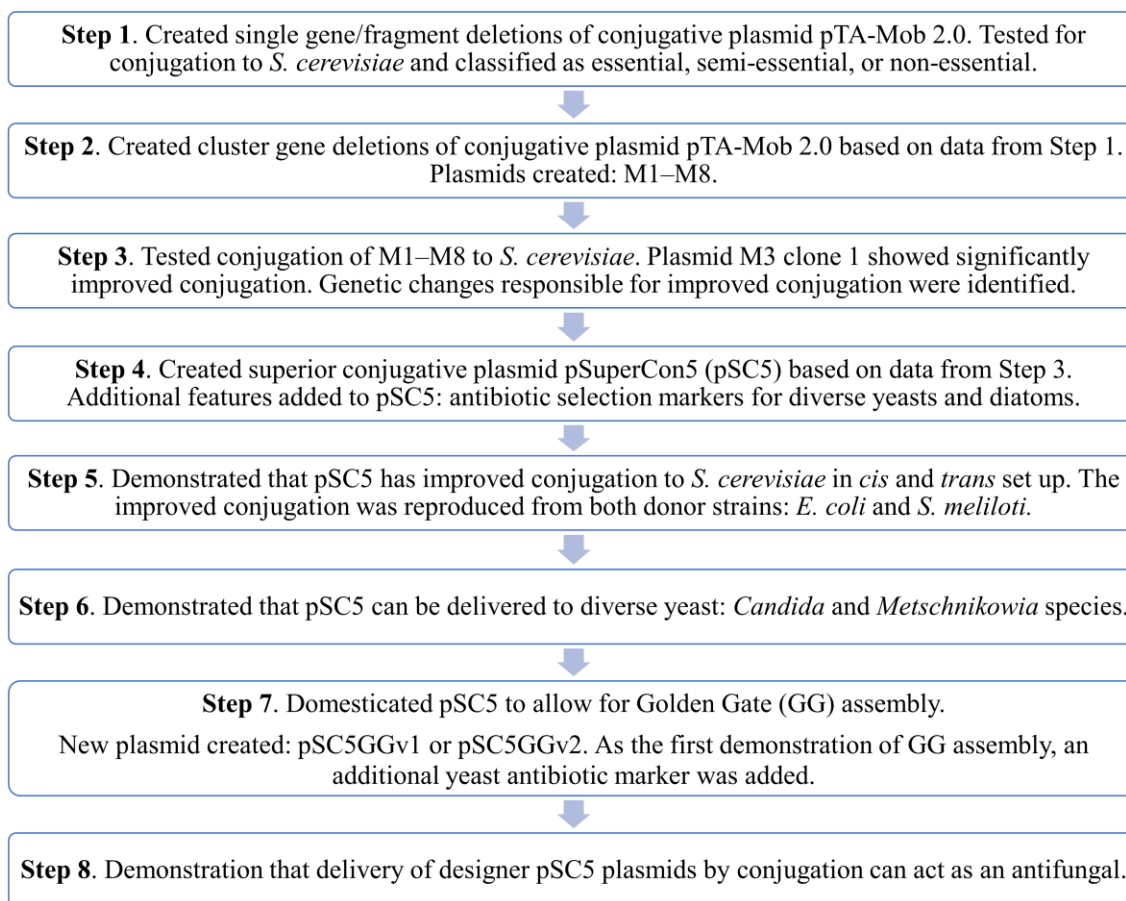


**Figure 4-1. Experimental Design.** The eight-step flowchart shows experiments and major findings described in this article.

(Supplemental Figure D-1, Supplemental Table D-1). To validate these plasmid variants, up to two clones of each were tested for bacterial conjugation from *E. coli* to *S. cerevisiae*, and the deletions were classified as essential (no bacterial conjugation), semi-essential (decreased bacterial conjugation), or non-essential (near wild-type bacterial conjugation) for bacteria-to-yeast conjugation (Supplemental Table D-3). Based on this data, four streamlined plasmids were created where clusters of non-essential genes were simultaneously removed (plasmids M1–M4, Table 4-1, Supplemental Table D-2). Plasmids M1–M4 were then conjugated from *E. coli* to *S. cerevisiae*, and we observed a significant increase in bacterial conjugation efficiency for plasmid M3 clone 1 (M3C1), monitored by yeast colony formation on selective media (Figure 4-2). Sequencing both M3 clones, M3C1 and M3C2, revealed multiple mutations in each clone, which are likely responsible for the increase in bacterial conjugation efficiency for M3C1 (Supplemental Table D-4).

To identify which mutations in M3C1 were responsible for the increased bacterial conjugation efficiency, we performed a fragment-swapping experiment between M3C1 and M3C2 to produce five hybrid plasmids M3C1\_F1–F5 (Figure 4-3). Each hybrid plasmid was created from four fragments amplified from M3C2 and one fragment from M3C1. The hybrid plasmid M3C1\_F4 (fragment 4 originated from M3C1) had the closest bacterial conjugation phenotype compared to M3C1 (Figure 4-3). There were two mutated regions in fragment 4 of M3C1: a cluster of mutations in the promoter of *traJ* and a single mutation in the open reading frame (ORF) of *traJ* (Supplemental Table D-4). To validate which mutation(s) contributed to the increased conjugative phenotype, the promoter or ORF *traJ* mutations were each individually introduced into pTA-Mob 2.0 and tested for relative bacterial conjugation phenotypes. Only the mutations in the promoter region of *traJ* improved bacterial conjugation to yeast (Figure 4-3). Additionally, we continued to minimize M3C1 by creating new plasmids with additional non-essential genes removed to obtain the plasmids M5–M8 (Figure 4-2). Each minimized plasmid of M5–M8 still produced more colonies when conjugated to yeast relative to the original pTA-Mob 2.0 plasmid (Figure 4-2).

**Table 4-1. Plasmids used in this study.** *aacC1* provides resistance to gentamicin; *cat* to chloramphenicol; *bla* to ampicillin; *y-nat* to nourseothricin in diverse yeast; *Sh ble* to zeocin in diverse yeasts. *HIS3* is required for the histidine biosynthesis; *URA3* for uracil biosynthesis; *TRP1* for tryptophan biosynthesis in *S. cerevisiae*. † - duplicated copy that is present in the plasmid backbone.

Plasmid	Plasmid Size (kbp)	<i>E. coli</i> Marker	Yeast Marker	Citation
<b>pTA-Mob 2.0</b>	57	<i>aacC1</i>	<i>HIS3/URA3</i>	Soltysiak <i>et al.</i> , 2019
<b>pAGE1.0</b>	18	<i>cat</i>	<i>HIS3</i>	Brumwell <i>et al.</i> , 2019
<b>pAGE2.0.T</b>	19	<i>cat</i>	<i>TRP1</i>	This Study
<b>pAGE2.0-i</b>	20	<i>cat</i>	<i>HIS3</i>	This Study
<b>pAGE2.0-iTraJ</b>	20	<i>cat</i>	<i>HIS3</i>	This Study
<b>pRS32</b>	11	<i>bla</i>	<i>Sh ble</i>	Shapiro <i>et al.</i> (unpublished)
<b>M1C1:</b> pTA-Mob 2.0 $\Delta trbO$ - <i>fiwA</i>	54	<i>aacC1</i>	<i>HIS3/URA3</i>	This Study
<b>M1C2:</b> pTA-Mob 2.0 $\Delta trbO$ - <i>fiwA</i>	54	<i>aacC1</i>	<i>HIS3/URA3</i>	This Study
<b>M2C5:</b> pTA-Mob 2.0 $\Delta klcA$ - <i>kleA</i>	53	<i>aacC1</i>	<i>HIS3/URA3</i>	This Study
<b>M3C1:</b> pTA-Mob 2.0 $\Delta istA$ - <i>traB</i>	52	<i>aacC1</i>	<i>HIS3</i>	This Study
<b>M3C2:</b> pTA-Mob 2.0 $\Delta istA$ - <i>traB</i>	52	<i>aacC1</i>	<i>HIS3</i>	This Study
<b>M4C16:</b> pTA-Mob 2.0 $\Delta istA$ - <i>traE</i>	46	<i>aacC1</i>	<i>HIS3</i>	This Study
<b>M4C19:</b> pTA-Mob 2.0 $\Delta istA$ - <i>traE</i>	46	<i>aacC1</i>	<i>HIS3</i>	This Study
<b>M5C1:</b> pTA-Mob 2.0 $\Delta trbN$ - <i>traE</i>	40	<i>aacC1</i>	<i>HIS3</i>	This Study
<b>M5C3:</b> pTA-Mob 2.0 $\Delta trbN$ - <i>traE</i>	40	<i>aacC1</i>	<i>HIS3</i>	This Study
<b>M6C2:</b> pTA-Mob 2.0 $\Delta trbN$ - <i>traE</i> , $\Delta klcA$ - <i>kleA</i>	35	<i>aacC1</i>	<i>HIS3</i>	This Study
<b>M6C4:</b> pTA-Mob 2.0 $\Delta trbN$ - <i>traE</i> , $\Delta klcA$ - <i>kleA</i>	35	<i>aacC1</i>	<i>HIS3</i>	This Study
<b>M7C2:</b> pTA-Mob 2.0 $\Delta trbN$ - <i>traE</i> , $\Delta trfA$ - <i>traJ</i> †	37	<i>aacC1</i>	<i>HIS3</i>	This Study
<b>M8C8:</b> pTA-Mob 2.0 $\Delta trbM$ - <i>traE</i> , $\Delta klcA$ - <i>kleA</i> , $\Delta trfA$ - <i>traJ</i> †	31	<i>aacC1</i>	<i>HIS3</i>	This Study
<b>M8C10:</b> pTA-Mob 2.0 $\Delta trbM$ - <i>traE</i> , $\Delta klcA$ - <i>kleA</i> , $\Delta trfA$ - <i>traJ</i> †	31	<i>aacC1</i>	<i>HIS3</i>	This Study
<b>M3C1_F1:</b> pTA-Mob 2.0 $\Delta istA$ - <i>traB</i>	52	<i>aacC1</i>	<i>HIS3</i>	This Study
<b>M3C1_F2:</b> pTA-Mob 2.0 $\Delta istA$ - <i>traB</i>	52	<i>aacC1</i>	<i>HIS3</i>	This Study
<b>M3C1_F3:</b> pTA-Mob 2.0 $\Delta istA$ - <i>traB</i>	52	<i>aacC1</i>	<i>HIS3</i>	This Study
<b>M3C1_F4:</b> pTA-Mob 2.0 $\Delta istA$ - <i>traB</i>	52	<i>aacC1</i>	<i>HIS3</i>	This Study
<b>M3C1_F5:</b> pTA-Mob 2.0 $\Delta istA$ - <i>traB</i>	52	<i>aacC1</i>	<i>HIS3</i>	This Study
<b>pTA-Mob 2.0 Tp</b>	56	<i>aacC1</i>	<i>HIS3/URA3</i>	This Study
<b>pTA-Mob 2.0 To</b>	56	<i>aacC1</i>	<i>HIS3/URA3</i>	This Study
<b>pSC5:</b> pTA-Mob 2.0 $\Delta istA$ - <i>traB</i>	56	<i>aacC1</i>	<i>HIS3/y-nat</i>	This Study
<b>pTA-Mob 2.1:</b> pTA-Mob 2.0 $\Delta traJ$ †	56	<i>aacC1</i>	<i>HIS3/URA3</i>	This Study
<b>pSC5.1:</b> pTA-Mob 2.0 $\Delta istA$ - <i>traB</i> , $\Delta traJ$ †	55	<i>aacC1</i>	<i>HIS3/y-nat</i>	This Study
<b>pSC5GGv1:</b> pTA-Mob 2.0 $\Delta istA$ - <i>traB</i> , + <i>mrfp</i>	57	<i>aacC1</i>	<i>HIS3/y-nat</i>	This Study
<b>pSC5GGv2:</b> pTA-Mob 2.0 $\Delta istA$ - <i>traB</i> , + <i>mrfp</i>	57	<i>aacC1</i>	<i>HIS3/y-nat</i>	This Study
<b>pSC5GGv1_ShBle:</b> pTA-Mob 2.0 $\Delta istA$ - <i>traB</i>	57	<i>aacC1</i>	<i>HIS3/y-nat/Sh ble</i>	This Study
<b>pSC5-toxic1:</b> pTA-Mob 2.0 $\Delta istA$ - <i>traB</i> , +ACL0117	59	<i>aacC1</i>	<i>HIS3/y-nat</i>	This Study
<b>pSC5-toxic2:</b> pTA-Mob 2.0 $\Delta istA$ - <i>traB</i> , +HindII	57	<i>aacC1</i>	<i>HIS3/y-nat</i>	This Study
<b>pSC5-toxic3:</b> pTA-Mob 2.0 $\Delta istA$ - <i>traB</i> , +HindII	57	<i>aacC1</i>	<i>HIS3/y-nat</i>	This Study

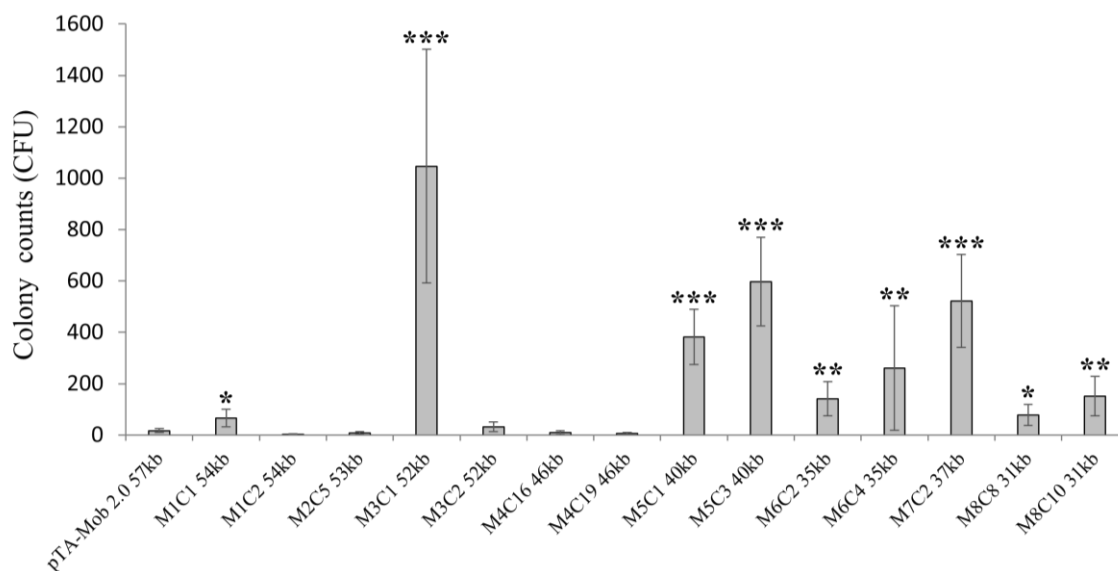


**Figure 4-2. Transfer of minimized plasmids from *E. coli* to *S. cerevisiae* via bacterial conjugation.** The conjugative plasmid, pTA-Mob 2.0, was used as a template to create the reduced versions M1–M4. M3C1 was used as a template to create M5–M8. When available, two clones of the same plasmid were tested (e.g., M1 C1 and C2). Error bars represent the  $\pm$  95% confidence interval (Student's *t*-test was used to carry out pairwise comparisons between pTA-Mob 2.0 (control) and minimized versions of pTA-Mob 2.0: \*  $p < 0.05$ , \*\*  $p < 0.01$ ; \*\*\*  $p < 0.001$ ).  $n = 9$  for all strains except  $n = 27$  for pTA-Mob 2.0.

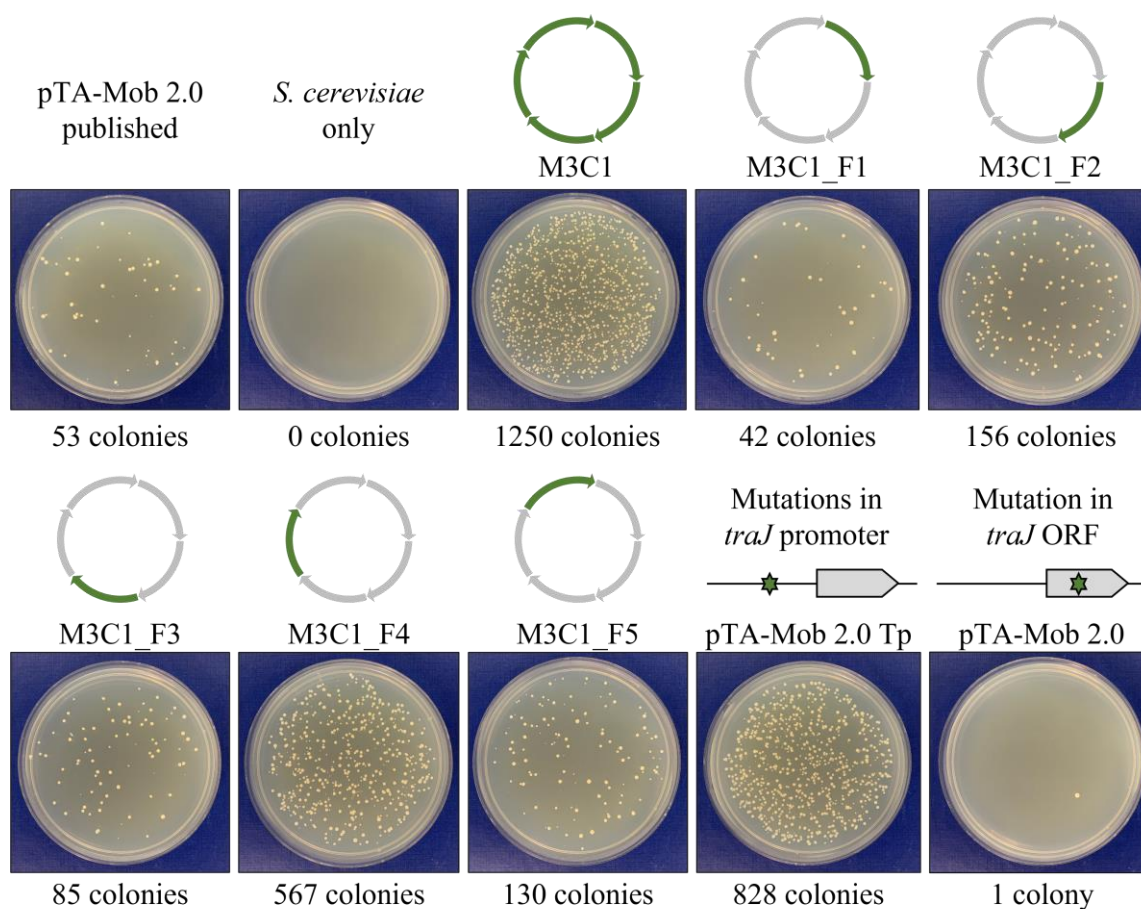


**Figure 4-3. Identification of mutations in M3C1 responsible for improved bacterial conjugation to *S. cerevisiae*.** *S. cerevisiae* transconjugant colony formation on agar plates containing synthetic complete media lacking histidine following bacterial conjugation of control: pTA-Mob 2.0, M3C1; hybrid: M3C1/M3C2; or mutated pTA-Mob 2.0 Tp/To plasmids from *E. coli*. Schematics above M3C1\_F1–F5 display the composition of each hybrid plasmid and which parent plasmid (M3C1/M3C2) fragments were PCR-amplified from. Green arrows represent fragments originating from M3C1, and grey arrows represent fragments from M3C2. In the schematic of *traJ*, green stars indicate mutations in pTA-Mob 2.0 Tp/To plasmids (Tp, a cluster of mutations; and To, a single mutation). Transconjugant colony counts are reported below the plate images.

#### 4.2.2 Creation of the superior conjugative plasmid pSC5

Based on the identified *traJ* promoter mutations, we created the pSC5 plasmid with additional genetic elements to deliver to diverse yeasts and diatoms. The pSC5 plasmid was built based on M3C1 and contained two copies of the nourseothricin resistance gene (*y-nat* and *d-nat*): one optimized for selection in diverse yeast and one for diatoms (Figure 4-4A). Bacterial conjugation efficiency for pSC5 from *E. coli* to *S. cerevisiae* was increased approximately 10- or 23-fold compared to pTA-Mob 2.0 when tested in *cis* (mobilizing itself) or *trans* (mobilizing another plasmid), respectively (Figure 4-4B, Supplemental Table D-5 & D-6). No significant difference in bacterial conjugation efficiency was observed when plasmids were transferred between *E. coli* strains (Figure 4-4B, Supplemental Table D-5 and D-6).

In order to more precisely evaluate the efficiency of bacteria-to-yeast conjugation, we performed additional experiments to monitor the effect of conjugation plasmid-containing *E. coli* on yeast viability. Cells from *E. coli*-to-yeast conjugation experiments were plated on non-selective yeast media supplemented with ampicillin to inhibit *E. coli* growth. More yeast colonies grew when pSC5 was used versus pTA-Mob 2.0 (Supplemental Table D-7), indicating that *E. coli* carrying pSC5 had reduced and/or fewer adverse effects on yeast when they are co-cultured. To determine if the same effect could be observed when different donor cells were used, we performed bacterial conjugation with *Sinorhizobium meliloti* as a donor, as it was previously shown to conjugate to yeast [25]. Similarly, a greater number of yeast colonies grew on non-selective plates when *S. meliloti* harboring pSC5 was used compared to pTA-Mob 2.0 (Supplemental Table D-8). In addition, a greater number of colonies on selective plates were observed following the bacterial conjugation of pSC5 from *S. meliloti* to *S. cerevisiae* compared to pTA-Mob 2.0 (Supplemental Figure D-2, Supplemental Table D-9).

Additional experiments will need to be performed to determine if there is a link between the increased number of yeast colonies on non-selective/selective plates and the



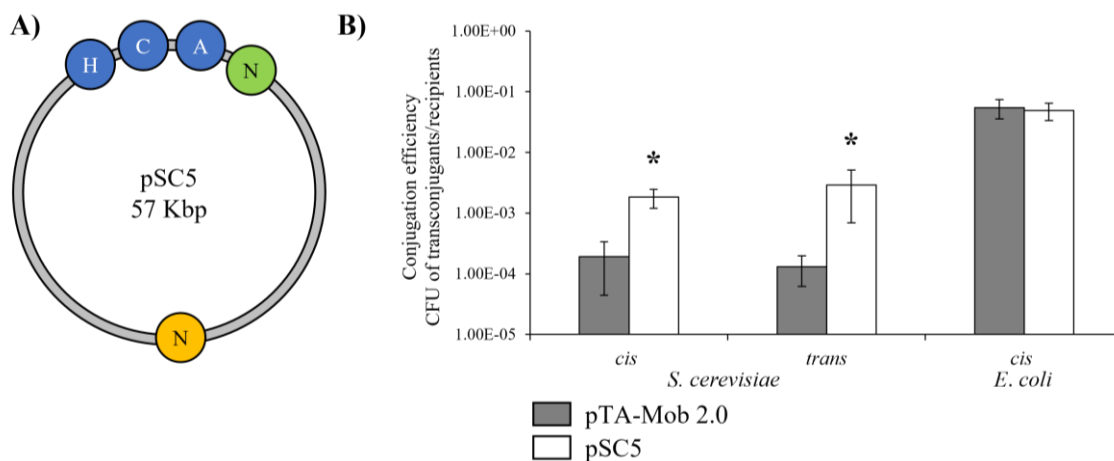


**Figure 4-4. Creation and analysis of the pSC5 conjugative plasmid.** **A)** Schematic of pSC5 plasmid map. N – Nourseothricin resistance gene encoded with the standard code for diatom (green) or the alternative yeast nuclear code for *Candida/Metschnikowia* (orange; Note – Also correctly translated in *S. cerevisiae*), HCA – *HIS3*, *CEN6*, and *ARSH4* for selection, replication, and maintenance in *S. cerevisiae*. **B)** Bacterial conjugation efficiency of pSC5 (white) compared to pTA-Mob 2.0 (grey) in either a *cis* or *trans* setup from *E. coli* to *S. cerevisiae* (left and middle), or from *E. coli* to *E. coli* in a *cis*-configuration (right). Bacterial conjugation efficiencies are graphed on a log<sub>10</sub> scale. Error bars represent the ± 95% confidence interval (Student's *t*-test: \*  $p < 0.05$ , \*\*  $p < 0.01$ , \*\*\*  $p < 0.001$ ).  $n = 3$  and  $n = 4$  for the *cis*- and *trans*-experiment in *S. cerevisiae*, respectively, and,  $n = 3$  for the *cis*-experiment in *E. coli*.

lower expression of *traJ* (Supplemental Figure D-3) in plasmids carrying the promoter mutation.

### 4.2.3 Bacterial conjugation to diverse yeast species

The significantly improved bacterial conjugation efficiency with the pSC5 plasmid suggests it may be effective for bacterial conjugation beyond a standard laboratory strain of *S. cerevisiae* and may have utility in transferring DNA from bacteria to diverse yeast species. To test the ability of pSC5 to transfer DNA to diverse yeast strains, we selected four *Metschnikowia* and six *Candida* species as conjugative recipients. Previously, we have demonstrated that small DNA fragments (*y-nat* selection marker) can be delivered to most of these species by electroporation [46]. Bacterial conjugation to these diverse yeasts was performed with the same protocol used for *S. cerevisiae*, modified to allow for selection on complete yeast media containing antibiotics. Transconjugant colonies were obtained for all species (Figure 4-5A, Supplemental Figures D-4, and D-5), and 1–8 transformant colonies for each species were genotyped by PCR for the presence of the *y-nat* marker. Of the 10 species tested, seven tested positive by PCR for the presence of the *y-nat* marker, suggesting successful bacterial conjugation had occurred (Supplemental Figure D-6). A plasmid rescue experiment, where total yeast DNA is electroporated into *E. coli*, was performed for selected colonies for each of the seven species, as well as *S. cerevisiae*. pSC5 plasmids from the seven yeast species were successfully recovered in *E. coli*; however, all except those recovered from *S. cerevisiae* showed rearrangements when diagnostic restriction enzyme digestion was performed (Figures 4-5B, C). Furthermore, only the plasmids recovered from *S. cerevisiae* were still able to conjugate (Supplemental Figure D-7).

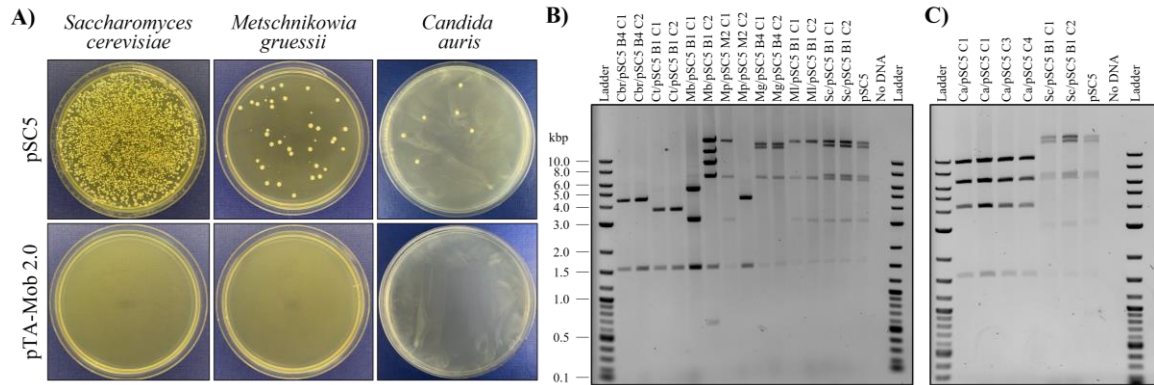


**Figure 4-5. Bacterial conjugation of pSC5 to wild yeast strains.** A) pSC5 conjugated to *S. cerevisiae* and the wild yeasts *M. gruessii* and *C. auris* on YPD plates supplemented with nourseothricin ( $100 \mu\text{g mL}^{-1}$ ). B, C) Diagnostic double restriction enzyme digestion (EcoRI-HF and AgeI-HF) of pSC5 rescued from yeast strains. The expected band sizes for pSC5 are 20,808-, 15,855-, 7314-, 6848-, 3189-, 1610-, and 6-bp. Cbr – *C. bromeliacearum*, Ct – *C. tolerans*, Mb – *M. borealis*, Mp – *M. pulcherrima*, Mg – *M. gruessii*, Ml – *M. lunata*, Sc – *S. cerevisiae*, and Ca – *C. auris*. Ladder: 2-log ladder.

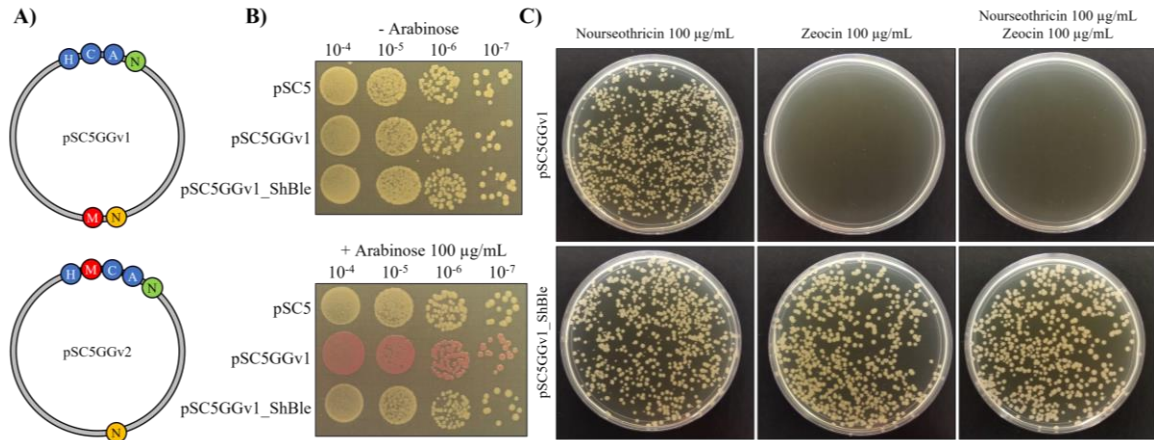


**Figure 4-6. Development of a pSC5 plasmid compatible with GG assembly.** **A)** Two versions of the pSC5 plasmid were created. Version 1 (pSC5GGv1) has the *mrfp* landing pad in the middle of the plasmid, and version 2 (pSC5GGv2) has the *mrfp* between the yeast elements *HIS3* and *CEN6-ARSH4*. **B)** Example of GG assembly to insert a gene of interest (*Sh ble*) into pSC5GGv1. pSC5 – original plasmid, pSC5GGv1 – domesticated plasmid, pSC5GGv1\_ShBle – a selected *E. coli* colony with *Sh ble* inserted grown on LB plates supplemented with gentamicin (40 µg mL<sup>-1</sup>). **C)** Bacterial conjugation of pSC5GGv1 and pSC5GGv1\_ShBle to *S. cerevisiae*.

#### 4.2.4 Domestication of pSC5 for Golden Gate assembly

Next, we sought to modify the pSC5 plasmid to make it readily amenable for cloning and easily incorporate any desired DNA fragment to facilitate downstream applications of bacterial-to-yeast conjugation. To this end, we eliminated existing BsaI restriction sites from pSC5 and created a single BsaI-based GG cloning-compatible site to enable efficient plasmid manipulation [48,49]. In addition, we incorporated a landing pad with monomeric Red Fluorescent Protein (*mrfp*) driven by an arabinose-inducible promoter (Figure 4-6A). In this modified plasmid, GG assembly can readily be used to replace the *mrfp* gene with any gene of interest, allowing for an easy visual screen for correct gene insertion events (white versus red bacterial colonies).

To validate this system, we inserted a second antibiotic marker (*Sh ble*) for yeast into pSC5GGv1 (Figure 4-6A) to create pSC5GGv1\_ShBle, which provides resistance to zeocin. White bacterial colonies were selected (Figure 4-6B) and genotyped with diagnostic MPX PCR and restriction digest (data not shown). These validated colonies were conjugated to *S. cerevisiae* and tested for survival on single or double antibiotic selection (Figure 4-6C). Successful transconjugants which received pSC5GGv1\_ShBle were able to grow on media supplemented with zeocin, nourseothricin, or both (Figure 4-6C).

#### 4.2.5 Proof of concept for bacterial conjugation-mediated delivery as an antifungal

To demonstrate that pSC5-based conjugative plasmids could be used as an antifungal, we developed a system where each donor *E. coli* strain carried two plasmids: a control plasmid (pAGE2.0.T), which can be selected on media lacking tryptophan, and either pSC5 or a pSC5-toxic plasmid, which can be selected on media lacking histidine (Figure 4-7A). We used GG assembly to create three pSC5-toxic plasmids, each carrying a gene that should be partially or fully toxic to yeast. To prevent toxicity in *E. coli*, in each toxic gene, we inserted a yeast *ACT1* intron [50]. Next, we cloned the *A. laidlawii* toxic gene [47] into pSC5GGv1 to generate pSC5-toxic1 or a *Haemophilus influenzae* HindII

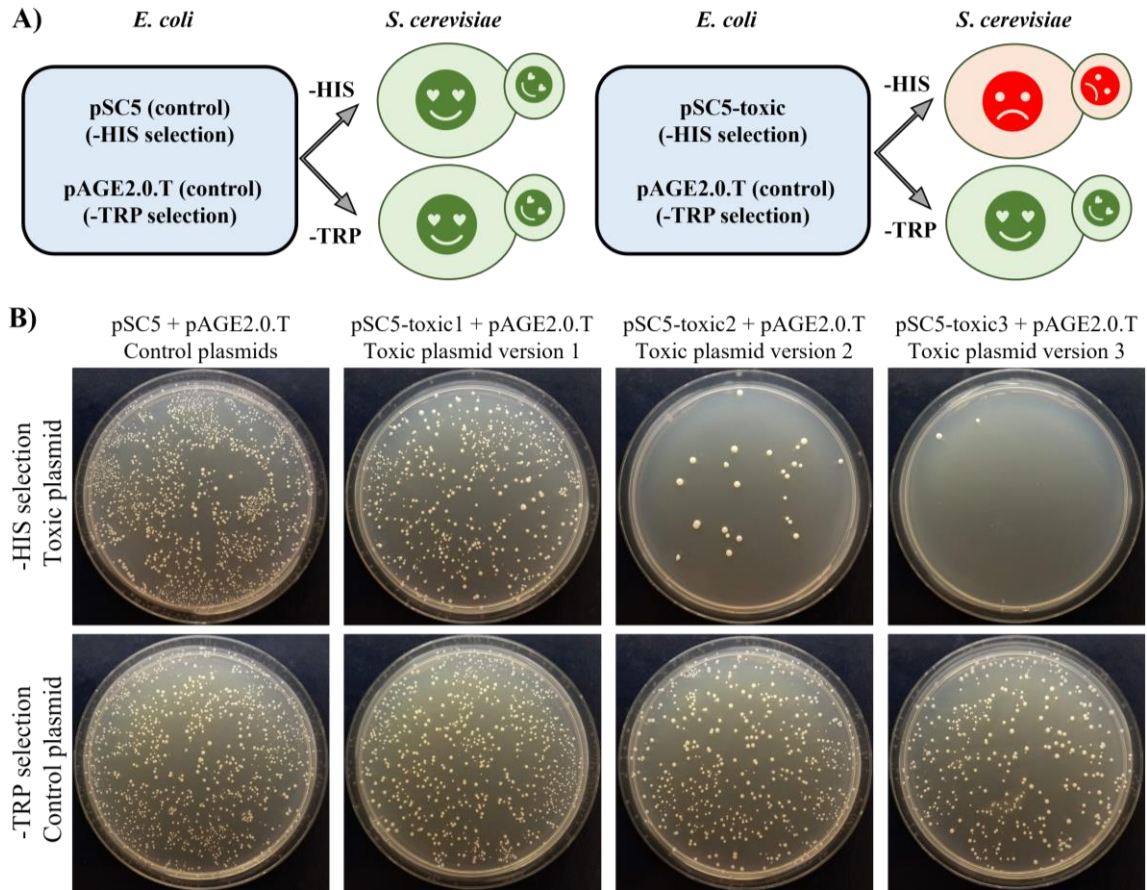


**Figure 4-7. Conjugation-based antifungal.** **A)** Diagram illustrating the predicted outcomes on *S. cerevisiae* colony formation following delivery of various plasmids via bacterial conjugation. The control strain (left) harboring pSC5 and pAGE2.0.T selected on synthetic complete media lacking either histidine or tryptophan will survive. Conversely, the experimental strain (right) harboring a pSC5-toxic plasmid and pAGE2.0.T, when selected on a synthetic complete media lacking histidine, will die. **B)** Assay for *S. cerevisiae* colony formation on -HIS or -TRP media following bacterial conjugation with three toxic plasmids. pSC5-toxic1 – partially toxic gene identified in *A. laidlawii* inserted in pSC5GGv1, pSC5-toxic2 – *H. influenzae* HindII restriction gene inserted in pSC5GGv1, pSC5-toxic3 – *H. influenzae* HindII restriction gene inserted in pSC5GGv2.

restriction enzyme gene into pSC5GGv1 and pSC5GGv2 to generate pSC5-toxic2 and pSC5-toxic3, respectively. The pSC5 and pSC5-toxic gene plasmids can act in *cis*, mobilizing themselves, and in *trans*, mobilizing the control plasmid pAGE2.0.T. Using a control *E. coli* strain carrying the plasmids pSC5 and pAGE2.0.T, we observed a similar colony number on both selection plates. For bacterial conjugation using the pSC5-toxic plasmids, substantially fewer colonies grew on media lacking histidine compared to pSC5. The most substantial difference in yeast colony formation was with donor *E. coli* carrying pSC5-toxic3 (Figure 4-7B, Supplemental Table D-10). This provides a proof of concept that bacteria-to-yeast conjugation can be used to deliver plasmid-based antifungals effectively.

### 4.3 Discussion

Bacterial conjugation-based techniques, such as the one described here, provide a unique and functional method to deliver plasmids between microbial species *in vitro* and *in vivo*. While there are innumerable possible applications for these systems, many have focused on using plasmid-encoded CRISPR-based genetic manipulation systems to modify the genomes of the recipient microbes [19,23,51]. Indeed, CRISPR-based gene targeting and manipulation systems offer a breadth of applications that can be paired with bacterial conjugation (or other methods of DNA delivery, such as phage transduction) to achieve desired manipulation of a target microbial population. The majority of this work to date has focused on bacterial species. For instance, CRISPR-based systems have been used to induce lethal DNA damage in key bacterial pathogens, including *E. coli*, *Staphylococcus aureus*, and *Clostridium difficile*, to effectively eradicate unwanted bacterial populations, including drug-resistant bacteria [13,14,52], and specific pathogenic species or subpopulations [13,16–19,53,54]. In addition to directly killing bacterial populations, CRISPR systems can also be applied to modify virulence determinants to erode microbial pathogenicity [53,55] or alter drug-resistance genes to restore antimicrobial susceptibilities [15,23,56–60]. To enable the application of these CRISPR systems *in vivo*, many have relied on bacterial conjugation or phage transduction to deliver the

relevant CRISPR components [13,17,21–23,61]. While this has been effective for delivery to bacterial strains, it has limited the applications in fungi, which lack well-established tools for bacterial conjugation or virus-based gene delivery [62,63].

To address the bottleneck of improving DNA delivery to yeast, we performed experiments to optimize the conjugative plasmid pTA-Mob 2.0 [28]. We first evaluated whether plasmid derivatives with targeted deletions of the conjugative plasmid could improve DNA transfer to *S. cerevisiae*. After testing 57 single-gene and four cluster-gene deletion plasmids, one with superior conjugative properties (M3C1) was identified. Sequence analysis of M3C1 revealed that in addition to the designed deletions, M3C1 had unintended mutations that were likely introduced during PCR amplification or plasmid assembly. The mutations responsible for improved bacterial conjugation to *S. cerevisiae* were narrowed down to the promoter region of *traJ* (Tp) using a fragment-swapping experiment. Following this discovery, five derivative plasmids of M3C1 were built containing the Tp mutation: four minimized versions (M5–M8) and pSC5 (containing selectable markers for diverse yeast species [46] and diatoms [24]). Each derivative plasmid of M3C1, including the smallest 31 kbp plasmid M8, outperformed the original 57 kbp pTA-Mob 2.0 plasmid when tested for DNA transfer to *S. cerevisiae*. Notably, using pSC5 compared to pTA-Mob 2.0, we observed an increase in bacterial conjugation to *S. cerevisiae* 10- or 23-fold in either a *cis* or *trans* setup, respectively. Yet, no increase in plasmid transfer was observed when pSC5 was conjugated between *E. coli* strains. This improved bacterial conjugation to *S. cerevisiae* could be partially explained by the increased *S. cerevisiae* viability during the co-culture bacterial conjugation step when plasmids harboring the Tp mutation are used. The same effect was observed when *S. meliloti* was used as a conjugative donor, suggesting the mechanism may be independent of the bacterial host. We also demonstrated that the Tp mutation results in a lower expression of the *traJ* gene. TraJ has been demonstrated as an essential conjugative protein that negatively autoregulates the expression of the relaxase operon [64]. Therefore, decreased expression of *traJ* could significantly affect the expression of all the conjugative machinery proteins. Further investigation will focus on resolving the link



between *traJ* downregulation and increased yeast viability or DNA transfer during the co-culture bacterial conjugation step.

The significantly improved pSC5 plasmid allowed DNA transfer to seven *Metschnikowia* and *Candida* yeast species, though relatively few colonies were obtained for each. One explanation for the low conjugative transfer could be that the *S. cerevisiae* centromere and the origin of replication were not functional in these yeasts. In such a case, the survival of these yeasts would only be possible if the conjugative plasmid was integrated into the yeast genome. Using a plasmid rescue experiment, we showed that plasmids could be recovered in *E. coli*, although none had the correct size or ability to conjugate. Since *E. coli* can assemble linear fragments into plasmids [65], it is most likely that some of the linear yeast fragments with integrated conjugative plasmids were assembled into plasmids in *E. coli*. Despite being unable to replicate as an episome in diverse yeasts, the improved conjugative plasmids, especially pSC5GGv1\_ShBle with two antibiotic-resistance genes, provide a great initial resource for DNA delivery. For applications where replicative plasmids are necessary for the yeast species of interest, species-specific origins of replication and centromeres must be identified and incorporated into the conjugative plasmid, as was done for *S. cerevisiae* [66,67].

Our improved conjugative plasmids hold promise as a novel antifungal. As a proof of concept, we cloned restriction nucleases onto the pSC5GGv2 plasmid and demonstrated that over 99% of yeast cells that receive the plasmid could be eliminated. However, additional improvements in the bacterial conjugation efficiency will need to be achieved before this technology can be used in antifungal treatments. In the future, our GG-compatible plasmids can be engineered with programmable systems such as CRISPR/Cas9 to target specific yeast strains. This coincides with the development and optimization of numerous CRISPR-based editing platforms optimized for diverse yeast species [68–72], including *Candida* pathogens [73]. Recent work has demonstrated the utility of CRISPR systems for modifying fungal genes involved in virulence [74–81] and antifungal drug resistance [74,77,82,83] in diverse *Candida* pathogens, and combining these CRISPR systems with this trans-kingdom bacterial conjugation system could facilitate the delivery of CRISPR to fungi in different environmental contexts.

## 4.4 Material and Methods

### 4.4.1 Experimental design

Experimental design is shown in Figure 4-1.

### 4.4.2 Microbial strains and growth conditions

*Saccharomyces cerevisiae* VL6–48 (ATCC MYA-3666: *MAT $\alpha$* , *his3- $\Delta$ 200*, *trp1- $\Delta$ 1*, *ura3-52*, *lys2*, *ade2-101*, *met14*, *psi*<sup>+</sup>, *cir*<sup>0</sup>) was grown in yeast media supplemented with ampicillin (100  $\mu\text{g mL}^{-1}$ ) as previously described in Section 2.4.1; or grown with selection on either: 1) yeast synthetic complete media lacking histidine supplemented with adenine hemi-sulfate, 2) yeast synthetic complete media lacking tryptophan, 3) 2 x YPDA supplemented with nourseothricin (100  $\mu\text{g mL}^{-1}$ ), or 4) 2 x YPDA supplemented with zeocin (100  $\mu\text{g mL}^{-1}$ ). Solid yeast media contained 2% agar. All yeast spheroplast preparation and transformations were performed as previously described in Section 2.4.5. *Escherichia coli* (Epi300, Lucigen) was grown as previously described in Section 2.4.1 supplemented with appropriate antibiotics (gentamicin (40  $\mu\text{g mL}^{-1}$ ) and chloramphenicol (15  $\mu\text{g mL}^{-1}$ )). Solid media contained 1.5% agar. For the transformation of *E. coli*, SOC media was used during the recovery time. Diverse yeasts, *Metschnikowia gruessii* (H53), *Metschnikowia pulcherrima* (CBS 5833), *Metschnikowia lunata* (BS 5946), *Metschnikowia borealis* (SUB 99-207.1), *C. auris*, *Candida tolerans* (UWOPS 98-117.5), *Candida bromeliacearum* (UNESP 00-103), *Candida pseudointermedia* (UWOPS 11-105.1), *Candida ubatubensis* (UNESP 01-247R), and *Candida* aff. *bentonensis* (UWOPS 00-168.1) were grown at 30 °C in 2 x YPDA (all diverse yeasts were obtained from Dr. Marc-Andre Lachance collection at Western University except *C. auris* came from <https://wwwn.cdc.gov/arisolatebank/>; accession number: SAMN05379609). *Sinorhizobium meliloti* (Rm4123 R<sup>-</sup>; obtained from Dr. Finan Lab, McMaster University) was grown at 30 °C in LBmc media (10 g L<sup>-1</sup> tryptone, 5 g L<sup>-1</sup> yeast extract, 5 g L<sup>-1</sup> NaCl, 0.301 g L<sup>-1</sup> MgSO<sub>4</sub>, and 0.277 g L<sup>-1</sup> anhydrous CaCl<sub>2</sub>) supplemented with appropriate

antibiotics (gentamicin 40  $\mu\text{g mL}^{-1}$  and streptomycin 100  $\mu\text{g mL}^{-1}$ ). Solid media contained 1.5% agar.

### 4.4.3 Plasmid construction

#### 4.4.3.1 PCR amplification

Plasmid fragments were amplified with GXL polymerase according to the manufacturer's instructions using annealing temperatures between 50 and 60 °C and 25–30 cycles.

#### 4.4.3.2 Plasmid assembly in yeast

Plasmids were assembled in yeast, as previously described [28]. Primers for deletion plasmids are listed in Supplemental Table D-1, and all primers and templates used to generate other plasmids are listed in Supplemental Table D-2: **(1) Single-gene/fragment deletion plasmids:** pTA-Mob 2.0 plasmid was used as a template. Each plasmid was created with nine standard fragments, as previously described [28], and two additional fragments designed as shown in Supplemental Figure D-1. **(2) Minimized plasmids (M1–8):** Eight minimized conjugative plasmids (M1–8) were designed based on the results obtained for the pTA-Mob 2.0 deletion plasmids. pTA-Mob 2.0 or M3C1 plasmid was used as a template for PCR fragments listed in Supplemental Table D-2. **(3) M3C1\_F1–F5 hybrid plasmids:** These plasmids were assembled by swapping the fragments between M3C1 and M3C2. **(4) pTA-Mob 2.0 Tp and pTA-Mob 2.0 To:** Primer-mediated mutagenesis was performed to introduce each mutation (Tp- in *traJ* promoter and To- in *traJ* ORF) into pTA-Mob 2.0. **(5) Superior conjugative plasmid (pSC5):** The pSC5 plasmid was derived from the M3C1 plasmid by the addition of two versions of the nourseothricin N-acetyltransferase (*nat*) gene, which provides resistance for the antibiotic nourseothricin. The first version was amplified from a plasmid pTA-Mob-NAT (unpublished, Karas lab), allowing selection in diatoms and referred to as d-*nat*; and the version was amplified from pGMO1 (unpublished, Karas lab), which

contained an alternative genetic code for selection in diverse yeasts as previously described [46] and referred to as *y-nat*. The remaining fragments of the pSC5 plasmid were amplified from M3C1, as previously described [28]. **(6) pTA-Mob 2.1/pSC5.1:** These two plasmids were created lacking the second copy of *traJ* located in the vector backbone. **(7) Domesticated pSC5 (pSC5GGv1/v2):** Two BsaI cut sites within the *fcpD* promoter and *traC1* ORF were removed from pSC5 using primer-mediated mutagenesis. A landing pad, consisting of an *mrfp* gene driven by an arabinose-inducible pBAD promoter and a terminator, was amplified from pAGE2.0-I using primers designed with new BsaI cut sites and homology either to directly downstream the native I-SceI restriction site (pSC5GGv1) or within the *HIS3/CEN6/ARSH4* element of the vector backbone (pSC5GGv2).

#### 4.4.3.3 Golden Gate assembly

(1) GG assembly. For GG assembly, 20 fmol of plasmid and insert were mixed in a 15  $\mu$ L reaction with 1.0  $\mu$ L T4 DNA ligase and 0.5  $\mu$ L BsaI-HF V2, using the following conditions: 10 cycles of 37 °C for 5 min and 16 °C for 10 min followed by incubation at 37 °C for 5 min, 80 °C for 10 min, and infinite hold at 12 °C. Primers are listed in Supplemental Table D-2. (2) pSC5GGv1\_ShBle. The zeocin resistance marker (*Sh ble*) cassette was amplified with flanking BsaI cut sites from pRS32 (unpublished, Shapiro Lab), and GG assembly was performed with pSC5GGv1. The primers used are listed in Supplemental Table D-2. (3) pSC5-toxic1, pSC5-toxic2, and pSC5-toxic3. Three versions of toxic plasmids were created to kill yeast cells, one with an *Acholeplasma laidlawii* toxic gene (ACL0117) [47] and two with the restriction enzyme HindII. The *A. laidlawii* and HindII cassettes contained an *ACT1* yeast intron, flanking BsaI cut sites, and either an *A. laidlawii* or HindII toxic gene. The *A. laidlawii* toxic gene cassette was amplified in three fragments: the *ACT1* yeast intron from *S. cerevisiae* VL6–48 and the toxic gene in two halves from *A. laidlawii* PG-8A with primers listed in Supplemental Table D-2. The *A. laidlawii* toxic gene cassette was constructed through a hierarchical GG assembly. First, the *ACT1* yeast intron and the second half of the *A. laidlawii* toxic

gene were assembled by GG assembly, and then 1  $\mu\text{L}$  of the product was used as a template for PCR amplification of the joined fragments. Next, GG assembly was performed with 20 fmol of the PCR product with the first half of the toxic gene, and the complete toxic gene cassette was PCR-amplified. The fully constructed cassette was then mixed with pSC5GGv1, and GG assembly was performed. The HindIII cassette split by the *ACT1* intron was flanked by the *URA3* promoter and terminator and was synthesized (BioMatik, Canada), then PCR-amplified and used in GG assembly with pSC5GGv1 or pSC5GGv2.

#### 4.4.4 Plasmid analysis

**Screening in yeast.** Following yeast assembly of the pTA-Mob 2.0 deletion plasmids, 20 individual yeast colonies were passed twice on agar plates containing synthetic complete media lacking histidine, and DNA was isolated and screened by MPX PCR using the Qiagen Multiplex Kit according to the Qiagen Multiplex PCR Handbook. For all other plasmids following yeast assembly, colonies were pooled rather than individually screened. **Transformation to *E. coli*.** Total DNA was isolated as previously described in Section 2.4.2.2. Isolated DNA (0.5–2  $\mu\text{L}$ ) was added to 40  $\mu\text{L}$  of *E. coli* electro-competent cells and electroporated using the Gene Pulser Xcell Electroporation System (2.5 kV voltage, 25  $\mu\text{F}$  capacitance, and 200  $\Omega$  resistance). Following a recovery in 1 mL of SOC media for 1 h at 37  $^{\circ}\text{C}$  (225 RPM), a 100–250  $\mu\text{L}$  aliquot of the transformants was plated on LB media supplemented with gentamicin (40  $\mu\text{g mL}^{-1}$ ). The cells transformed with GG-compatible plasmids (pSC5GGv1/v2, pSC5-toxic1, pSC5-toxic2, and pSC5-toxic3) were instead plated on LB plates containing gentamicin (40  $\mu\text{g mL}^{-1}$ ) and arabinose (100  $\mu\text{g mL}^{-1}$ ). **Screening in *E. coli*.** For GG-compatible plasmids, white colonies were screened for insertion of the cassette of interest by MPX PCR. For all other assembled plasmids, the transformed *E. coli* was pooled and conjugated to *S. cerevisiae*, the DNA was isolated, and transformed back to *E. coli* to focus screening on functional conjugative plasmids. Once in *E. coli*, all plasmids were genotypically screened using MPX PCR and restriction enzyme digest analysis. **Sequencing.** The plasmids, pTA-Mob

2.0 Tp/To, underwent Sanger DNA sequencing (London Regional Genomics Centre at Robarts Research Institute) to ensure the introduction of the correct mutations using the primers listed in Supplemental Table D-2. Selected plasmids were sequenced at CCIB DNA Core at Massachusetts General Hospital or the Western University sequencing facility.

#### 4.4.5 Bacterial conjugation

Both donor (*E. coli*) and recipient (*S. cerevisiae*) strains were prepared and frozen prior to bacterial conjugation experiments. For *E. coli* strains, saturated overnight cultures inoculated with a single colony were diluted to OD<sub>600</sub> of 0.1 in 50 mL of LB media supplemented with appropriate antibiotics (Table 4-1) and grown until an OD<sub>600</sub> of 1.0 was reached. The cells were pelleted (3000 x RCF, 15 min) in a 50 mL Falcon tube and resuspended in 500 µL ice-cold 10% glycerol. Then, 100 µL aliquots in Eppendorf tubes were frozen in a -80 °C ethanol bath and stored at -80 °C. For *S. cerevisiae* recipient strain preparation, a culture was started from a single colony and grown in 5 mL of 2 x YPDA media supplemented with ampicillin (100 µg mL<sup>-1</sup>) for 7 h. After, this culture was diluted in 50 mL of 2 x YPDA media supplemented with ampicillin (100 µg mL<sup>-1</sup>) and grown until an OD<sub>600</sub> of 3.0 was reached (~17 h). The cells were pelleted (3000 x RCF, 5 min) in a 50 mL Falcon tube and resuspended in 1 mL of ice-cold 10% glycerol. Then, 250 µL aliquots in Eppendorf tubes were frozen in a -80 °C ethanol bath and stored at -80 °C.

On the day of bacterial conjugation, conjugation plates (20 mL, 1.8% agar, 10% LB media, synthetic complete yeast media lacking histidine) were dried for 30 min. Aliquots of the donor (*E. coli*) and recipient (*S. cerevisiae*) strains were removed from the freezer and thawed on ice for approximately 20 min. Next, 50 µL of *S. cerevisiae* was added to the 100 µL of *E. coli* and mixed by gentle pipetting before being transferred to the plate and spread evenly. Alternatively, when the yeast toxic plasmids were being tested, 10 µL of the recipient *S. cerevisiae* strain was used. Once dried, the plates were incubated at 30 °C for 3 h, or 12 h when wild yeast strains were used as the recipient. The

plates were scraped with 2 mL of sterile double-distilled water (sddH<sub>2</sub>O), mixed by vortexing for 5 s, and 100  $\mu$ L plated on respective selection media (25 mL, 2% agar supplemented with ampicillin 100  $\mu$ g mL<sup>-1</sup>) listed in Table 4-1. In the case of wild yeast strains, they were plated on 1 x YPDA media supplemented with nourseothricin (100  $\mu$ g mL<sup>-1</sup>), and two technical replicates of each dilution (10<sup>0</sup>–10<sup>-1</sup>) were plated on selective plates. For experiments evaluating bacterial conjugation of pSC5 in *cis* and *trans*, dilution series of 10<sup>0</sup>–10<sup>-2</sup> were generated and plated on selective media while dilution series of 10<sup>-4</sup>–10<sup>-7</sup> were generated and plated on non-selective media (1 x YPDA supplemented with ampicillin 100  $\mu$ g mL<sup>-1</sup>); and two technical replicates were plated for each dilution.

#### **4.4.6 RNA isolation and quantitative reverse transcriptase-polymerase chain reaction**

For RNA isolation, each *E. coli* strain carrying either conjugative plasmid, pTA-Mob 2.1 or pSC5.1 were grown in LB media supplemented with gentamicin (40  $\mu$ g mL<sup>-1</sup>) overnight at 37 °C shaking at 225 RPM. In the morning, RNA was isolated as previously described in Section 3.5.8. Following DNase treatment with TURBO DNA-free Kit (Invitrogen), the RNA concentration and integrity were verified [43].

cDNA was prepared from 500 ng of RNA using the High-Capacity cDNA Reverse Transcription Kit (Applied Biosystems). Quantitative reverse transcriptase-polymerase chain reaction (qRT-PCR) was performed using six biological and three technical replicates on a ViiA7 system of QuantStudio Real-Time PCR System using the SYBR™ Select Master Mix under the following conditions: 50 °C for 2 mins, 95 °C for 2 mins followed by 40 cycles of: 95 °C for 1 s, 60 °C for 30 s. Expression levels were normalized against two reference genes (*rrsA* and *cysG*), as previously described [29]. Primer sequences used for the qRT-PCR expression analyses are listed in Supplemental Table D-2.

#### 4.4.7 Statistical analysis

The pairwise comparisons between groups were made using Student's *t*-test with either equal or unequal variance based on the result of an F-test. Data were expressed as either a  $\pm 95\%$  confidence interval, mean  $\pm$  standard error of the mean, or mean  $\pm$  standard deviation of at least three biological replicates. The tests were considered statistically significant when  $p < 0.05$  (\*),  $p < 0.01$  (\*\*), or  $p < 0.001$  (\*\*\*)).

## 4.5 References

1. Fisher MC, Gurr SJ, Cuomo CA, Blehert DS, Jin H, Stukenbrock EH, et al. Threats posed by the fungal kingdom to humans, wildlife, and agriculture. *MBio*. 2020;11:e00449-20. doi:10.1128/mBio.00449-20
2. Hyde KD, Xu J, Rapior S, Jeewon R, Lumyong S, Niego AGT, et al. The amazing potential of fungi: 50 ways we can exploit fungi industrially. *Fungal Divers*. 2019;97:1–136. doi:10.1007/s13225-019-00430-9
3. Parapouli M, Vasileiadis A, Afendra AS, and Hatziloukas E. *Saccharomyces cerevisiae* and its industrial applications. *AIMS Microbiol*. 2020;6:1–31. doi:10.3934/microbiol.2020001.
4. Edwards-Ingram L, Gitsham P, Burton N, Warhurst G, Clarke I, Hoyle D, et al. Genotypic and physiological characterization of *Saccharomyces boulardii*, the probiotic strain of *Saccharomyces cerevisiae*. *Appl Environ Microbiol*. 2007;73:2458–2467. doi:10.1128/AEM.02201-06
5. Everard A, Matamoros S, Geurts L, Delzenne NM, and Cani PD. *Saccharomyces boulardii* administration changes gut microbiota and reduces hepatic steatosis, low-grade inflammation, and fat mass in obese and type 2 diabetic db/db mice. *MBio*. 2014;5:e01011-14. doi:10.1128/mBio.01011-14
6. Pappas PG, Lionakis MS, Arendrup MC, Ostrosky-Zeichner L, and Kullberg BJ. Invasive candidiasis. *Nat Rev Dis Primers*. 2018;4:1–20. doi:10.1038/nrdp.2018.26
7. Limon JJ, Tang J, Li D, Wolf AJ, Michelsen KS, Funari V, et al. *Malassezia* is associated with Crohn's disease and exacerbates colitis in mouse models. *Cell Host Microbe*. 2019;25:377-388.e6. doi:10.1016/j.chom.2019.01.007



8. Aykut B, Pushalkar S, Chen R, Li Q, Abengozar R, Kim JI, et al. The fungal mycobiome promotes pancreatic oncogenesis via activation of MBL. *Nature*. 2019;574:264–267. doi:10.1038/s41586-019-1608-2
9. Proctor DM, Dangana T, Sexton DJ, Fukuda C, Yelin RD, Stanley M, et al. Integrated genomic, epidemiologic investigation of *Candida auris* skin colonization in a skilled nursing facility. *Nat Med*. 2021;27:1401–1409. doi:10.1038/s41591-021-01383-w
10. Du H, Bing J, Hu T, Ennis CL, Nobile CJ, and Huang G. *Candida auris*: Epidemiology, biology, antifungal resistance, and virulence. *PLoS Pathog*. 2020;16:e1008921. doi:10.1371/journal.ppat.1008921
11. Geddes-McAlister J and Shapiro RS. New pathogens, new tricks: Emerging, drug-resistant fungal pathogens and future prospects for antifungal therapeutics. *Ann N.Y. Acad Sci*. 2019;1435:57–78. doi:10.1111/nyas.13739
12. Palacios Araya D, Palmer KL, and Duerkop BA. CRISPR-based antimicrobials to obstruct antibiotic-resistant and pathogenic bacteria. *PLoS Pathog*. 2021;17:e1009672. doi:10.1371/journal.ppat.1009672
13. Citorik RJ, Mimee M, and Lu TK. Sequence-specific antimicrobials using efficiently delivered RNA-guided nucleases. *Nat Biotechnol*. 2014;32:1141–1145. doi:10.1038/nbt.3011
14. Kiga K, Tan XE, Ibarra-Chávez R, Watanabe S, Aiba Y, Sato'o Y, et al. Development of CRISPR-Cas13a-based antimicrobials capable of sequence specific killing of target bacteria. *Nat Commun*. 2020;11:2934. doi:10.1038/s41467-020-16731-6
15. Chavez A, Pruitt BW, Tuttle M, Shapiro RS, Cecchi RJ, Winston J, et al. Precise Cas9 targeting enables genomic mutation prevention. *Proc Natl Acad Sci U.S.A*. 2018;115:3669–3673. doi:10.1073/pnas.1718148115
16. Gomaa AA, Klumpe HE, Luo ML, Selle K, Barrangou R, and Beisel CL. Programmable removal of bacterial strains by use of genome-targeting CRISPR-Cas systems. *MBio*. 2014;5:e00928-13. doi:10.1128/mBio.00928-13
17. Selle K, Fletcher JR, Tuson H, Schmitt DS, McMillan L, Vridhambal GS, et al. *In vivo* targeting of *Clostridioides difficile* using phage-delivered CRISPR-Cas3 antimicrobials. *MBio*. 2020;11:e00019-20. doi:10.1128/mBio.00019-20
18. Bikard D, Euler CW, Jiang W, Nussenzweig PM, Goldberg GW, Duportet X, et al. Exploiting CRISPR-Cas nucleases to produce sequence-specific antimicrobials. *Nat Biotechnol*. 2014;32:1146–1150. doi:10.1038/nbt.3043

19. Hamilton TA, Pellegrino GM, Therrien JA, Ham DT, Bartlett PC, Karas BJ, et al. Efficient inter-species conjugative transfer of a CRISPR nuclease for targeted bacterial killing. *Nat Commun.* 2019;10:4544. doi:10.1038/s41467-019-12448-3
20. López-Igual R, Bernal-Bayard J, Rodríguez-Patón A, Ghigo JM, and Mazel D. Engineered toxin–intein antimicrobials can selectively target and kill antibiotic-resistant bacteria in mixed populations. *Nat Biotechnol.* 2019;37:755–760. doi:10.1038/s41587-019-0105-3
21. Neil K, Allard N, Roy P, Grenier F, Menendez A, Burrus V, et al. High-efficiency delivery of CRISPR-Cas9 by engineered probiotics enables precise microbiome editing. *Mol Syst Biol.* 2021;17:e10335. doi:10.15252/msb.202110335
22. Neil K, Allard N, Grenier F, Burrus V, and Rodrigue S. Highly efficient gene transfer in the mouse gut microbiota is enabled by the IncI<sub>2</sub> conjugative plasmid TP114. *Commun biology.* 2020;3:1–9. doi:10.1038/s42003-020-01253-0
23. Rodrigues M, McBride SW, Hullahalli K, Palmer KL, and Duerkop BA. Conjugative delivery of CRISPR-Cas9 for the selective depletion of antibiotic-resistant *enterococci*. *Antimicrob Agents Chemother.* 2019;63:e01454-19. doi:10.1128/AAC.01454-19
24. Karas BJ, Diner RE, Lefebvre SC, McQuaid J, Phillips APR, Noddings CM, et al. Designer diatom episomes delivered by bacterial conjugation. *Nat Commun.* 2015;6:6925. doi:10.1038/ncomms7925
25. Brumwell SL, MacLeod MR, Huang T, Cochrane RR, Meaney RS, Zamani M, et al. Designer *Sinorhizobium meliloti* strains and multi-functional vectors enable direct inter-kingdom DNA transfer. *PLoS One.* 2019;14:e0206781. doi:10.1371/journal.pone.0206781
26. Hayman GT and Bolen PL. Movement of shuttle plasmids from *Escherichia coli* into yeasts other than *Saccharomyces cerevisiae* using trans-kingdom conjugation. *Plasmid.* 1993;30:251–257. doi:10.1006/plas.1993.1056
27. Moriguchi K, Edahiro N, Yamamoto S, Tanaka K, Kurata N, and Suzuki K. Transkingdom genetic transfer from *Escherichia coli* to *Saccharomyces cerevisiae* as a simple gene introduction tool. *Appl Environ Microbiol.* 2013;79:4393–4400. doi:10.1128/AEM.00770-13
28. Soltysiak MPM, Meaney RS, Hamadache S, Janakirama P, Edgell DR, and Karas BJ. Trans-kingdom conjugation within solid media from *Escherichia coli* to *Saccharomyces cerevisiae*. *Int J Mol Sci.* 2019;20:5212. doi:10.3390/ijms20205212

29. Zoolkefli FIRM, Moriguchi K, Cho Y, Kiyokawa K, Yamamoto S, and Suzuki K. Isolation and analysis of donor chromosomal genes whose deficiency is responsible for accelerating bacterial and trans-kingdom conjugations by IncP1 T4SS machinery. *Front Microbiol.* 2021;12:971. doi:10.3389/fmicb.2021.620535
30. Norberg P, Bergström M, Jethava V, Dubhashi D, and Hermansson M. The IncP-1 plasmid backbone adapts to different host bacterial species and evolves through homologous recombination. *Nat Commun.* 2011;2:268. doi:10.1038/ncomms1267
31. Pansegrau W, Lanka E, Barth PT, Figurski DH, Guiney DG, Haas D, et al. Complete nucleotide sequence of Birmingham IncP $\alpha$  plasmids: Compilation and comparative analysis. *J Mol Biol.* 1994;239:623–663. doi:10.1006/jmbi.1994.1404
32. Ziegelin G, Fürste JP, and Lanka E. TraJ protein of plasmid RP4 binds to a 19-base pair invert sequence repetition within the transfer origin. *J Biol Chem.* 1989;264:11989–11994. doi:10.1016/S0021-9258(18)80164-8
33. Fürste JP, Pansegrau W, Ziegelin G, Kröger M, and Lanka E. Conjugative transfer of promiscuous IncP plasmids: Interaction of plasmid-encoded products with the transfer origin. *Proc Natl Acad Sci U.S.A.* 1989;86:1771–1775. doi:10.1073/pnas.86.6.1771
34. Pansegrau W, Balzer D, Kruff V, Lurz R, and Lanka E. *In vitro* assembly of relaxosomes at the transfer origin of plasmid RP4. *Proc Natl Acad Sci U.S.A.* 1990;87:6555–6559. doi:10.1073/pnas.87.17.6555
35. Pansegrau W, Schröder W, and Lanka E. Relaxase (TraI) of IncP alpha plasmid RP4 catalyzes a site-specific cleaving-joining reaction of single-stranded DNA. *Proc Natl Acad Sci U.S.A.* 1993;90:2925–2929. doi:10.1073/pnas.90.7.2925
36. Pansegrau W and Lanka E. Mechanisms of initiation and termination reactions in conjugative DNA processing: Independence of tight substrate binding and catalytic activity of relaxase (TraI) of IncP $\alpha$  plasmid RP4. *J Biol Chem.* 1996;271:13068–13076. doi:10.1074/jbc.271.22.13068
37. Ziegelin G, Pansegrau W, Lurz R, and Lanka E. TraK protein of conjugative plasmid RP4 forms a specialized nucleoprotein complex with the transfer origin. *J Biol Chem.* 1992;267:17279–17286. doi:10.1016/S0021-9258(18)41923-0
38. Rees CE and Wilkins BM. Protein transfer into the recipient cell during bacterial conjugation: Studies with F and RP4. *Mol Microbiol.* 1990;4:1199–1205. doi:10.1111/j.1365-2958.1990.tb00695.x
39. Cabezón E, Sastre JI, and de la Cruz F. Genetic evidence of a coupling role for the TraG protein family in bacterial conjugation. *Mol Gen Genet.* 1997;254:400–406. doi:10.1007/s004380050432

40. Grahn AM, Haase J, Bamford DH, and Lanka E. Components of the RP4 conjugative transfer apparatus form an envelope structure bridging inner and outer membranes of donor cells: Implications for related macromolecule transport systems. *J Bacteriol.* 2000;182:1564–1574. doi:10.1128/JB.182.6.1564-1574.2000
41. Eisenbrandt R, Kalkum M, Lurz R, and Lanka E. Maturation of IncP pilin precursors resembles the catalytic dyad-like mechanism of leader peptidases. *J Bacteriol.* 2000;182:6751–6761. doi:10.1128/JB.182.23.6751-6761.2000
42. Eisenbrandt R, Kalkum M, Lai EM, Lurz R, Kado CI, and Lanka E. Conjugative pili of IncP plasmids, and the Ti plasmid T pilus are composed of cyclic subunits. *J Biol Chem.* 1999;274:22548–22555. doi:10.1074/jbc.274.32.22548
43. Cochrane RR, Brumwell SL, Shrestha A, Giguere DJ, Hamadache S, Gloor GB, et al. Cloning of *Thalassiosira pseudonana*'s mitochondrial genome in *Saccharomyces cerevisiae* and *Escherichia coli*. *Biology.* 2020;9:358. doi:10.3390/biology9110358
44. Karas BJ, Jablanovic J, Irvine E, Sun L, Ma L, Weyman PD, et al. Transferring whole genomes from bacteria to yeast spheroplasts using entire bacterial cells to reduce DNA shearing. *Nat Protoc.* 2014;9:743–750. doi:10.1038/nprot.2014.045
45. Cochrane RR, Brumwell SL, Soltysiak MPM, Hamadache S, Davis JG, Wang J, et al. Rapid method for generating designer algal mitochondrial genomes. *Algal Res.* 2020;50:102014. doi:10.1016/j.algal.2020.102014
46. Gordon ZB, Soltysiak MPM, Leichthammer C, Therrien JA, Meaney RS, Lauzon C, et al. Development of a transformation method for *Metschnikowia borealis* and other CUG-Serine yeasts. *Genes.* 2019;10:78. doi:10.3390/genes10020078
47. Karas BJ, Tagwerker C, Yonemoto IT, Hutchison III CA, and Smith HO. Cloning the *Acholeplasma laidlawii* PG-8A genome in *Saccharomyces cerevisiae* as a yeast centromeric plasmid. *ACS Synth Biol.* 2012;1:22–28. doi:10.1021/sb200013j
48. Marillonnet S and Grütznert R. Synthetic DNA assembly using Golden Gate cloning and the hierarchical modular cloning pipeline. *Curr Protoc Mol Biol.* 2020;130:e115. doi:10.1002/cpmb.115
49. Engler C, Kandzia R, and Marillonnet S. A one pot, one step, precision cloning method with high throughput capability. *PLoS One.* 2008;3:e3647. doi:10.1371/journal.pone.0003647
50. Ng R and Abelson J. Isolation and sequence of the gene for actin in *Saccharomyces cerevisiae*. *Proc Natl Acad Sci U.S.A.* 1980;77:3912–3916. doi:10.1073/pnas.77.7.3912

51. Ruotsalainen P, Penttinen R, Mattila S, and Jalasvuori M. Midbiotics: Conjugative plasmids for genetic engineering of natural gut flora. *Gut Microbes*. 2019;10:643–653. doi:10.1080/19490976.2019.1591136
52. Hullahalli K, Rodrigues M, and Palmer KL. Exploiting CRISPR-Cas to manipulate *Enterococcus faecalis* populations. *Elife*. 2017;6:e26664. doi:10.7554/eLife.26664
53. Ram G, Ross HF, Novick RP, Rodriguez-Pagan I, and Jiang D. Conversion of *staphylococcal* pathogenicity islands to CRISPR-carrying antibacterial agents that cure infections in mice. *Nat Biotechnol*. 2018;36:971–976. doi:10.1038/nbt.4203
54. Lam KN, Spanogiannopoulos P, Soto-Perez P, Alexander M, Nalley MJ, Bisanz JE, et al. Phage-delivered CRISPR-Cas9 for strain-specific depletion and genomic deletions in the gut microbiome. *Cell Rep*. 2021;37:109930. doi:10.1016/j.celrep.2021.109930
55. Vercoe RB, Chang JT, Dy RL, Taylor C, Gristwood T, Clulow JS, et al. Cytotoxic chromosomal targeting by CRISPR/Cas systems can reshape bacterial genomes and expel or remodel pathogenicity islands. *PLoS Genet*. 2013;9:e1003454. doi:10.1371/journal.pgen.1003454
56. Kim JS, Cho DH, Park M, Chung WJ, Shin D, Ko KS, et al. CRISPR/Cas9-mediated re-sensitization of antibiotic-resistant *Escherichia coli* harboring extended-spectrum  $\beta$ -lactamases. *J Microbiol Biotechnol*. 2016;26:394–401. doi:10.4014/jmb.1508.08080
57. Wang P, He D, Li B, Guo Y, Wang W, Luo X, et al. Eliminating mcr-1-harboring plasmids in clinical isolates using the CRISPR/Cas9 system. *J Antimicrob Chemother*. 2019;74:2559–2565. doi:10.1093/jac/dkz246
58. Valderrama JA, Kulkarni SS, Nizet V, and Bier E. A bacterial gene-drive system efficiently edits and inactivates a high copy number antibiotic resistance locus. *Nat Commun*. 2019;10:1–8. doi:10.1038/s41467-019-13649-6
59. Wang K and Nicholaou M. Suppression of antimicrobial resistance in MRSA using CRISPR-dCas9. *Clin Lab Sci*. 2017;30:207–213. doi:10.29074/ascls.30.4.207
60. Li Q, Zhao P, Li L, Zhao H, Shi L, and Tian P. Engineering a CRISPR interference system to repress a class 1 integron in *Escherichia coli*. *Antimicrob Agents Chemother*. 2020;64:e01789-19. doi:10.1128/AAC.01789-19
61. Park JY, Moon BY, Park JW, Thornton JA, Park YH, and Seo KS. Genetic engineering of a temperate phage-based delivery system for CRISPR/Cas9 antimicrobials against *Staphylococcus aureus*. *Sci Rep*. 2017;7:44929. doi:10.1038/srep44929

62. Gietz RD and Woods RA. Genetic transformation of yeast. *Biotechniques*. 2001;30:816–20, 822–6, 828 passim. doi:10.2144/01304rv02
63. Martín JF. Fungal transformation: From protoplasts to targeted recombination systems. In: *Genetic Transformation Systems in Fungi, Volume 1 2015* (pp 3–18). Springer, Cham. doi:10.1007/978-3-319-10142-2\_1
64. Zatyka M, Jagura-Burdzy G, and Thomas CM. Regulation of transfer genes of promiscuous IncP alpha plasmid RK2: Repression of Tra1 region transcription both by relaxosome proteins and by the Tra2 regulator TrbA. *Microbiology*. 1994;140:2981–2990. doi:10.1099/13500872-140-11-2981
65. Kostylev M, Otwell AE, Richardson RE, and Suzuki Y. Cloning should be simple: *Escherichia coli* DH5 $\alpha$ -mediated assembly of multiple DNA fragments with short end homologies. *PLoS One*. 2015;10:e0137466. doi:10.1371/journal.pone.0137466
66. Stinchcomb DT, Struhl K, and Davis RW. Isolation and characterisation of a yeast chromosomal replicator. *Nature*. 1979;282:39–43. doi:10.1038/282039a0
67. Clarke L and Carbon J. Isolation of a yeast centromere and construction of functional small circular chromosomes. *Nature*. 1980;287:504–509. doi:10.1038/287504a0
68. Cai P, Gao J, and Zhou Y. CRISPR-mediated genome editing in non-conventional yeasts for biotechnological applications. *Microb Cell Fact*. 2019;18:63. doi:10.1186/s12934-019-1112-2
69. Morio F, Lombardi L, and Butler G. The CRISPR toolbox in medical mycology: State of the art and perspectives. *PLoS Pathog*. 2020;16:e1008201. doi:10.1371/journal.ppat.1008201
70. Raschmanová H, Weninger A, Glieder A, Kovar K, and Vogl T. Implementing CRISPR-Cas technologies in conventional and non-conventional yeasts: Current state and future prospects. *Biotechnol Adv*. 2018;36:641–665. doi:10.1016/j.biotechadv.2018.01.006
71. Stovicek V, Holkenbrink C, and Borodina I. CRISPR/Cas system for yeast genome engineering: Advances and applications. *FEMS Yeast Res*. 2017;17:fox030. doi:10.1093/femsyr/fox030
72. Shan L, Dai Z, and Wang Q. Advances and opportunities of CRISPR/Cas technology in bioengineering non-conventional yeasts. *Front Bioeng Biotechnol*. 2021;9:765396. doi:10.3389/fbioe.2021.765396

73. Uthayakumar D, Sharma J, Wensing L, and Shapiro RS. CRISPR-based genetic manipulation of *Candida* species: Historical perspectives and current approaches. *Front Genome Ed.* 2021;2:606281. doi:10.3389/fgeed.2020.606281
74. Vyas VK, Barrasa MI, and Fink GR. A *Candida albicans* CRISPR system permits genetic engineering of essential genes and gene families. *Sci Adv.* 2015;1:e1500248. doi:10.1126/sciadv.1500248
75. Enkler L, Richer D, Marchand AL, Ferrandon D, and Jossinet F. Genome engineering in the yeast pathogen *Candida glabrata* using the CRISPR-Cas9 system. *Sci Rep.* 2016;6:35766. doi:10.1038/srep35766
76. Rosiana S, Zhang L, Kim GH, Revtovich AV, Uthayakumar D, Sukumaran A, et al. Comprehensive genetic analysis of adhesin proteins and their role in virulence of *Candida albicans*. *Genetics.* 2021;217:iyab003. doi:10.1093/genetics/iyab003
77. Shapiro RS, Chavez A, Porter CBM, Hamblin M, Kaas CS, DiCarlo JE, et al. A CRISPR-Cas9-based gene drive platform for genetic interaction analysis in *Candida albicans*. *Nat Microbiol.* 2018;3:73–82. doi:10.1038/s41564-017-0043-0
78. Zoppo M, Luca MD, Villarreal SN, Poma N, Barrasa MI, Bottai D, et al. A CRISPR/Cas9-based strategy to simultaneously inactivate the entire ALS gene family in *Candida orthopsilosis*. *Future Microbiol.* 2019;14:1383–1396. doi:10.2217/fmb-2019-0168
79. Santana DJ and O’Meara TR. Forward and reverse genetic dissection of morphogenesis identifies filament-competent *Candida auris* strains. *Nat Commun.* 2021;12:1–13. doi:10.1038/s41467-021-27545-5
80. Huang MY, Woolford CA, May G, McManus CJ, and Mitchell AP. Circuit diversification in a biofilm regulatory network. *PLoS Pathog.* 2019;15:e1007787. doi:10.1371/journal.ppat.1007787
81. Min K, Biermann A, Hogan DA, and Konopka JB. Genetic analysis of NDT80 family transcription factors in *Candida albicans* using new CRISPR-Cas9 approaches. *mSphere.* 2018;3:e00545-18. doi:10.1128/mSphere.00545-18
82. Wensing L, Sharma J, Uthayakumar D, Proteau Y, Chavez A, and Shapiro RS. A CRISPR interference platform for efficient genetic repression in *Candida albicans*. *mSphere.* 2019;4:e00002-19. doi:10.1128/mSphere.00002-19
83. Ennis CL, Hernday AD, and Nobile CJ. A markerless CRISPR-mediated system for genome editing in *Candida auris* reveals a conserved role for Cas5 in the caspofungin response. *Microbiol Spectr.* 2021;9:e0182021. doi:10.1128/Spectrum.01820-21

## Chapter 5

### 5 General Discussion

The development of WGE for mitochondria could enable the study of the origins of eukaryotes, progress treatments for mitochondrial diseases in humans, and produce superlative eukaryotes for industry. However, bottlenecks to a synthetic biology approach for whole mitochondrial genome engineering exist, including the need for standardized genetic engineering methods and inept DNA delivery efficiencies to eukaryotes. This thesis begins to address these limitations by presenting protocols for rapidly engineering diatom mitochondrial genomes and genetic tools for improved DNA delivery to eukaryotes. The whole mitochondrial genome engineering method enables the inexpensive and rapid generation of derivative mitochondrial genomes. The superior conjugative plasmid, pSC5, improves bacterial conjugation to eukaryotes and provides an amenable system for engineering efforts, such as redirecting DNA delivery from the nucleus to the mitochondria. Additionally, its increased bacterial conjugation efficiency offers an initial tool for DNA delivery to diverse yeasts relevant to medicine and industry. The technologies presented represent the initial steps toward whole mitochondrial genome engineering that have important implications in future basic scientific research, medicines, and biotechnologies.

#### 5.1 Design-build-test: Mitochondrial genome cloning and engineering

Efficient mitochondrial genome engineering efforts require cloned genomes for template DNA to modify and standardized protocols to create variant mitochondrial genomes reproducibly. The mitochondrial genomes of two diatoms, *P. tricornutum* and *T. pseudonana*, were cloned in *S. cerevisiae* and *E. coli* using PCR-based and TAR cloning methods. The cloning was efficient for both species despite differences in the characteristics of the mitochondrial DNA, such as size, type of repetitive elements, and G+C% content. Although both cloning methods were successful, each has advantages



and limitations. The TAR cloning method directly captures an endogenous mitochondrial genome but is labor-intensive, time-consuming, and inefficient relative to the PCR-based method. However, this method produced a *bona fide* mitochondrial template for optimizing a rapid and efficient PCR-based engineering protocol. The PCR-based engineering protocol can be applied to any species with sequencing data and is currently cheaper than DNA synthesis. It is adaptable and can produce many genetic modifications, including single nucleotide polymorphisms, insertions, deletions, addition and removal of selection markers, and introduction of entire biosynthetic pathways. For instance, the first designed modification of *P. tricornutum* and *T. pseudonana*'s mitochondrial genomes included the removal of repetitive DNA regions that further simplified PCR amplification for future iterations of genome engineering. However, PCR-based cloning and engineering methods can inadvertently introduce mutations or be incapable of amplifying large repetitive sequences.

The PCR-based engineering protocol requires approximately ten days; however, each cycle introduces ~1–2 mutations per 20 kbp of sequence (Tables 2-2 and 3-2). This mutation rate is significant because mitochondrial genomes are generally small and compact, which increases the likelihood that a mutation could impact endogenous genetic structures vital to its function. Prior to delivery experiments, modified genomes should be sequenced to identify any mutations, which can then be individually corrected or screened out. In the future, the PCR-based engineering method could be replaced with a GG assembly method [1] to increase the genetic tractability of derivative mitochondrial genomes while maintaining the flexibility of PCR-based modifications.

## **5.2 Mitochondrial plasmid stability and host burden**

Faithful maintenance of cloned mitochondrial genomes (i.e., plasmids) in host organisms is crucial for downstream experimentation. After successfully cloning two diatom mitochondrial genomes in *S. cerevisiae* and *E. coli*, their plasmid stability and host burden were examined. Often shared genetic elements, aberrant gene expression, or repetitive sequences can cause cellular dysregulation, host burden, and plasmid instability

[2–9]. Mitochondrial plasmids posed no observable host burden in either host species despite RNA sequencing in *E. coli* detecting gene expression from both diatom mitochondrial genomes (Supplemental Tables C-3 and C-4). Host burden was observed via reduced end-point culture density of all plasmids maintained at a high copy number in *E. coli* (Figures 3-2B and 3-3G, H). Although maintaining problematic plasmids at a high copy number is generally poor practice, it is excellent at amplifying low-level host burden or plasmid instability to identify troublesome regions.

Despite minimal host burden, *T. pseudonana*'s mitochondrial plasmid had detectable instability, likely due to its repetitive elements. Both diatom mitochondrial genomes contain segregated repetitive elements but of different types. Specifically, *P. tricornutum* contains 35.5 kbp of direct repeats, whereas *T. pseudonana* contains 4.8 kbp of inverted repeats [10]. The mutated *T. pseudonana* mitochondrial plasmids were sequenced, and large deletions were observed in proximity to the inverted repeat regions implicating their involvement. Repetitive DNA sequences in mitochondrial genomes are essential for interactions with nucleoproteins, proper genome segregation during cellular division, and often contain replication origins [11]. However, plasmids containing inverted repeats within bacterial hosts are troublesome and unstable [8,9] because they can produce secondary structures and cause replication fork stalling, increasing the likelihood of recombination events [5–8]. Alternatively, these problematic plasmids can be stably maintained in eukaryotic hosts [12–14] and transferred to bacteria temporarily for high-yield DNA isolation or mitochondrial DNA delivery experiments. Notably, the mutation frequency of *T. pseudonana*'s cloned mitochondrial genome is sufficiently low that it would not hinder potential delivery experiments provided DNA is screened following propagation in *E. coli*.

### 5.3 Improving bacterial conjugation

Bacterial conjugation delivers DNA to diverse cell types but with highly variable efficiencies between species [15–18]. For example, bacterial conjugation between Gram-negative bacteria is highly efficient and delivers DNA to 10–30% of possible recipient

cells, whereas bacterial conjugation to eukaryotes, such as *S. cerevisiae*, ranges from  $10^5$ – $10^7$  transconjugants per recipient cell [15,16,19]. While conjugative plasmids can deliver DNA to diverse cell types, if transferred to a eukaryotic host in nature, they would only persist transiently because they lack the eukaryotic genetic elements required for their maintenance, replication, and selection [15]. Therefore, our group and others have adapted conjugative plasmids for various cell types by adding eukaryotic genetic elements for algal [16,18], fungal [15–17,19,20], plant [15], and mammalian cells [15,21,22]. However, bacterial conjugation efficiencies to eukaryotic hosts using these engineered conjugative plasmids remain drastically lower relative to their bacterial counterparts. In eukaryotes, continued propagation of each plasmid can only occur vertically, inherited by direct genetic descendants of recipient cells. Whereas, in bacterial hosts, following plasmid transfer to a recipient cell, that cell can then become a donor and continue the propagation of the plasmid horizontally to other potential recipient cells. Without a selection pressure to acquire, maintain and transfer conjugative plasmids, these systems cannot naturally evolve for efficient transfer to eukaryotes, and therefore, many conjugative systems could likely be optimized using a synthetic biology approach to massively increase the efficiency of DNA delivery to various species.

Multiple factors have been examined to improve bacterial conjugation efficiency to yeast, such as optimizing protocol parameters [19], engineering the genetic background of donor cells [23], and assaying modifications made to conjugative plasmids [15]. For instance, bacterial conjugation efficiency can differ by orders of magnitude by adjusting the donor-to-recipient cell ratio [19]. Others have assayed the Keio *E. coli* knockout library and identified donor chromosomal gene deficiencies that improve bacterial conjugation to *S. cerevisiae* [23]. Future research could investigate potential yeast gene deficiencies that could make *S. cerevisiae* an improved recipient by screening the Yeast Knockout (YKO) Collection. Here, a deletion plasmid library of pTA-Mob 2.0 was created to improve DNA delivery to yeast and begin generating the resources necessary for adapting and optimizing bacterial conjugation to different cell types and subcellular localizations. The bacterial conjugation efficiency to yeast of each deletion plasmid in the library was assessed, and the data generated was used to create various

streamlined conjugative plasmids by combining multiple non-essential deletions. This series of conjugative plasmids drastically reduced in size led to the identification of the highly transmissible conjugative plasmid, pSC5.

### 5.3.1 Improved bacterial conjugation efficiency to eukaryotes

Efficiency of DNA delivery is one of the most significant limitations of any genetic engineering effort in synthetic biology. The engineered plasmid pSC5 improves bacterial conjugation ~23-fold to *S. cerevisiae* with no significant effect on conjugation between bacteria. Improved bacterial conjugation to yeast was linked to a cluster mutation in the *traJ* promoter region of M3C1, which was identified using a plasmid fragment-swapping experiment, that was subsequently incorporated into pSC5 (Figure 4-3). TraJ is an essential conjugative protein with multiple functions. It is a negative autoregulatory transcription factor that partly controls the expression of the relaxase operon [24], is a member of the relaxosome protein complex that binds the *oriT*, and orients the relaxase protein, TraI, to the plasmid nick site [15,25–28]. qRT-PCR revealed reduced *traJ* mRNA in *E. coli* harboring pSC5.1 compared to pTA-MOB 2.1, but what effect this has on all the mobilization proteins under its regulation is yet to be determined.

Increased transconjugant yield was also found using an alternative bacterial host, *S. meliloti*, suggesting that improved bacterial conjugation to yeast was donor independent. Furthermore, regardless of donor bacterial species, some proportion of the increased bacterial conjugation efficiency in pSC5 resulted from reduced co-culture toxicity to the recipient, *S. cerevisiae*, when the *traJ* promoter region was mutated. Future research should seek to minimize the host burden and toxicities associated with bacterial conjugation on both host and recipient cells to maximize the efficiency of DNA delivery. This could be achieved partially by streamlining conjugative plasmids (Table 4-1; Figure 4-2) and creating inducible conjugative systems to reduce and temporally control the metabolic costs and toxicities of bacterial conjugation.

Many eukaryotic organisms with industrial potential, including unconventional yeasts, are overlooked because they lack genetic tools or DNA delivery methods. Unconventional yeasts are of interest to industry for their unique contributions to the fermentation process, bioremediation qualities, and production of industrial ethanol, foodstuffs, and probiotics [29–31]. Other species can act as opportunistic pathogenic yeasts (e.g., *Candida* – candidiasis), which are a growing concern in medicine [32–35]. *Candida auris* is an emerging *Candida* pathogen attracting attention because of its resistance to multiple conventional antifungal drugs [34,35]. pSC5 was shown to deliver DNA to unconventional yeast species that were previously unreported to have undergone bacterial conjugation. We repurposed pSC5 as a novel antifungal by loading the plasmid with different genes toxic to yeasts [36,37] and demonstrated that 99% of yeast that received the plasmid during bacterial conjugation were no longer viable. While for *S. cerevisiae*, bacterial conjugation efficiencies of  $1 \times 10^{-3}$ – $10^{-4}$  transconjugants per recipient cell are bordering satisfactory for developing a novel therapeutic (Figure 4-4). The need for continued improvement is highlighted by drastically lower bacterial conjugation efficiencies for unconventional yeasts, such as *Metschnikowia*, range between  $1 \times 10^{-6}$ – $10^{-7}$  transconjugants per recipient cell, which at its current state would have a negligible impact (Supplemental Figure D-5). Despite still being too early for an efficacious antifungal treatment, pSC5 is still an excellent tool for initial DNA delivery efforts in unconventional yeasts and as a starting point for engineering efforts to attenuate DNA delivery to the mitochondria.

### **5.3.2 Modulating bacterial conjugation specificity for mitochondrial DNA-delivery**

Two approaches have been proposed for mitochondrial transformation using bacterial conjugation: 1) intra-cellular bacterial conjugation and 2) engineering conjugative proteins with mitochondrial localization signals [38,39]. In either scenario, bacterial conjugation is performed under suboptimal conditions. For instance, the non-standard conditions of cytosolic bacterial conjugation and the engineering of mobilization proteins likely reduce the efficiency of DNA transfer. pSC5 is a strong candidate conjugative

plasmid for either approach because its improved DNA delivery to yeast could mitigate the anticipated reduction to bacterial conjugation efficiencies. Additionally, it is a highly malleable and engineerable system, which we have demonstrated in our lab by using pSC5's parent plasmid pTA-Mob 2.0 to generate streamlined plasmids (Figure 4-2) and plasmid libraries (Supplemental Tables D-1, and D-3), complement gene knockouts in *trans*, and perform bacterial conjugation with an engineered relaxase harboring an N-terminal nuclear localization signal (unpublished, Karas lab). In any case, modulation of bacterial conjugation for mitochondrial transformation will require a highly efficient starter plasmid because of the trade-off between bacterial conjugation efficiency and specificity.

Previously it has been shown that *E. coli* can be engineered to evade vacuolar degradation [40] and successfully conjugate in the cytosol of a eukaryotic cell to another bacteria [41]. It has also been demonstrated that bacterial conjugation can successfully transform isolated mitochondria [42]. These two findings suggest that cell fusion and bacterial conjugation could be combined to generate a novel method of DNA delivery to the mitochondria. Intracellular mitochondrial DNA delivery by bacterial conjugation is an attractive alternative method because bacterial conjugation has evolved for efficient delivery between bacteria, not eukaryotes. This bias may enhance the specificity of DNA delivery to the “bacteria-like” mitochondria rather than the nuclear membrane. Furthermore, the pilus could directly interact with the mitochondrial membranes during cytosolic bacterial conjugation bypassing the mitochondrial transport machinery entirely. It was found that mutations in the *traJ* promoter region increased yeast recipient cell viability (Supplemental Tables D-7 and D-8). Future research into this approach for mitochondrial transformation may benefit from low-toxicity donor strains for intracellular bacterial conjugation, such as those harboring pSC5.

The other bacterial conjugation-based approach for mitochondrial DNA delivery is the engineering of key mobilization protein machinery with the addition of mitochondrial localization signals. Multiple conjugative proteins, which have been reported to interact and co-translocate with pDNA to the recipient cytoplasm, could be engineered with mitochondrial localization signals and tested. These include primase

(TraC), relaxase (TraI), recombinase (RecA), and single-stranded binding proteins (SSBs) [15,43–45]. However, engineering any conjugative mobilization protein will likely diminish its function [15]. For example, relaxase is a complex protein responsible for 1) recognizing and nicking the *oriT*, 2) covalently binding the plasmid DNA, 3) co-translocating with DNA from donor to recipient cell, 4) scanning incoming single-stranded DNA, 5) nicking the incoming strand, and 6) re-circularizing the single-stranded DNA after transfer [15,46–48]. The hope is that engineering mobilization proteins with a mitochondrial localization signal will redirect DNA delivery from the nucleus to the mitochondria. However, superior conjugative systems will be crucial to offset the decreased efficacy of DNA transfer caused by modifying any key mobilization proteins with mitochondrial localization signals.

## 5.4 Whole mitochondrial genome engineering

Whole mitochondrial genome engineering is the cumulation of standardized genome engineering protocols and mitochondrial transformation methods. While the number of mitochondrial genomes cloned and protocols for engineering them has steadily increased, novel methods of DNA delivery have been stagnant [49]. Mitochondrial transformation of single-celled eukaryotes has been exclusively performed by biolistic bombardment (i.e., gene gun delivery), a destructive method that mechanically punctures cell membranes, leaving the vast majority of cells unviable. Only *S. cerevisiae* [50–54], *C. reinhardtii* [54–58], and *C. glabrata* [59] have successfully undergone mitochondrial transformation procedures. Each species transformed has a linear mitochondrial genome, recoverable respiratory deficient mutants, and cell walls reflecting the traits and conditions enabling successful transformation using biolistic-mediated DNA delivery [51,54,60]. Alternative methods, such as electroporation, have been attempted, which are effective on isolated mitochondria but render the mitochondria permanently inactivated in whole-cell experiments [38,42,61,62]. Highly efficient, generalizable, and less destructive DNA delivery methods are needed to transform the mitochondria of diverse eukaryotes and to enable whole mitochondrial genome delivery. Bacterial conjugation is

a promising alternative method that occurs entirely *in vivo*, is highly engineerable, and is indiscriminate in DNA delivery that could be used for diverse cell types and subcellular localizations.

## 5.5 Conclusion

The future of synthetic biology is complete genetic control of cellular systems, which has been demonstrated in prokaryotes and begun for eukaryotes. However, in eukaryotes, WGE is limited to the nucleus and requires developing the same tools for the mitochondria. This thesis presents methods to rapidly engineer mitochondrial genomes and an improved conjugative plasmid for DNA delivery to eukaryotes. The mitochondrial genome engineering platform presented in Chapters 2 and 3 offers an alternative method to DNA synthesis for deriving designer mitochondrial genomes. The method is inexpensive and rapid, requiring 10-14 days. It is efficient, requires minimal screening, and is adaptable for introducing diverse mutations. The mitochondrial genomes cloned as plasmids were generally stable and non-toxic despite detectable low-level mRNA expression in *E. coli*. These findings support the feasibility of engineering these diatom's mitochondrial genomes comprising the design-build phases of the DBT cycle. Nevertheless, it still requires the development of efficient methods of mitochondrial transformation in these diatom species.

The study presented in Chapter 4 improved the efficiency of DNA delivery by bacterial conjugation to eukaryotes. The deletion plasmid library of pTA-Mob 2.0 characterized the essentiality of 55 genes for bacterial conjugation of IncP $\alpha$  plasmids to yeast. Notably, a mutation in the *traJ* promoter region linked to improved bacterial conjugation offers researchers an excellent tool for initial DNA-delivery experiments, especially to yeasts with previously no reports of DNA transformation. It also highlights a critical role in the regulation of the *traJ* gene and the entire relaxosome operon, inciting investigation into its relationship to the eukaryotic recipient cells and associated co-culture toxicities. Future research should continue to improve the efficiency of bacterial conjugation to eukaryotic recipients and attempt to adapt this process for targeted DNA



delivery to diverse eukaryotes and specific subcellular localizations using superior conjugative plasmids. I found that adding an N-terminal yeast nuclear localization signal to pTA-Mob 2.0's relaxase (TraI) decreased the performance of bacterial conjugation 100–1000-fold. It will be for future researchers to use the improved conjugative plasmid, pSC5, to modify the specificity of this conjugative system for mitochondrial DNA delivery and expand mitochondrial transformation methods to additional species.

Finally, the progression towards a completed DBT cycle critical for synthetic biology will enable efficient production and delivery of designer mitochondrial genomes to an increasing number of eukaryotic hosts. Currently, biolistic-mediated gene gun delivery enables mitochondrial transformation for *S. cerevisiae*, *C. glabrata*, and *C. reinhardtii*. The installation of designer mitochondrial genomes could be attempted immediately using *S. cerevisiae* to determine the feasibility and current limitations preventing the installation of completely designer mitochondrial genomes. The state of the field is a nearly complete DBT test cycle for mitochondrial genomes of *S. cerevisiae* and *C. reinhardtii*. In order to expand the number of transformable organisms, selection markers and mitochondrial phenotypic knockouts must be characterized for adequately controlled experiments. It will then be possible to compare the biolistic-mediated gene gun delivery method of mitochondrial transformation to promising alternative methods being generated, such as bacterial conjugation. Once WGE tools for mitochondria are generated, genome-scale variation in the mitochondria can be studied, pathways that produce essential medicines or lucrative products for industry can be introduced, and these tools can be applied to additional chassis organisms.

## 5.6 References

1. Engler C, Gruetzner R, Kandzia R, and Marillonnet S. Golden Gate shuffling: A one-pot DNA shuffling method based on type II restriction enzymes. *PLoS One*. 2009;4:e5553. doi:10.1371/journal.pone.0005553
2. Mita S, Monnat RJ, and Loeb LA. Direct selection of mutations in the human mitochondrial tRNA<sup>Thr</sup> gene: Reversion of an 'uncloneable' phenotype. *Mutat Res Mol Mech Mutagen*. 1988;199:183–190. doi:10.1016/0027-5107(88)90244-8

3. Silva F, Queiroz JA, and Domingues FC. Evaluating metabolic stress and plasmid stability in plasmid DNA production by *Escherichia coli*. *Biotechnol Adv*. 2012;30:691–708. doi:10.1016/j.biotechadv.2011.12.005
4. Kearsey SE, Flanagan JG, and Craig IW. Cloning of mouse mitochondrial DNA in *E. coli* affects bacterial viability. *Gene*. 1980;12:249–255. doi:10.1016/0378-1119(80)90107-9
5. Pearson CE, Zorbas H, Price GB, and Zannis-Hadjopoulos M. Inverted repeats, stem-loops, and cruciforms: Significance for initiation of DNA replication. *J Cell Biochem*. 1996;63:1–22. doi:10.1002/(SICI)1097-4644(199610)63:1<1::AID-JCB1>3.0.CO;2-3
6. Bierne H and Michel B. When replication forks stop. *Mol Microbiol*. 1994;13:17–23. doi:10.1111/j.1365-2958.1994.tb00398.x
7. Voineagu I, Narayanan V, Lobachev KS, and Mirkin SM. Replication stalling at unstable inverted repeats: Interplay between DNA hairpins and fork stabilizing proteins. *Proc Natl Acad Sci*. 2008;105:9936–9941. doi:10.1073/pnas.0804510105
8. Kaushal S and Freudenreich CH. The role of fork stalling and DNA structures in causing chromosome fragility. *Genes Chromosom Cancer*. 2019;58:270–283. doi:10.1002/gcc.22721
9. Godiska R, Patterson M, Schoenfeld T, and Mead DA. Beyond pUC: Vectors for cloning unstable DNA. *Optim DNA Seq Process*. 2005;1:55–76.
10. Oudot-Le Secq M-P and Green BR. Complex repeat structures and novel features in the mitochondrial genomes of the diatoms *Phaeodactylum tricornutum* and *Thalassiosira pseudonana*. *Gene*. 2011;476:20–26. doi:10.1016/j.gene.2011.02.001
11. Kuroiwa T, Nishida K, Yoshida Y, Fujiwara T, Mori T, Kuroiwa H, et al. Structure, function and evolution of the mitochondrial division apparatus. *Biochim Biophys Acta Mol Cell Res*. 2006;1763:510–521. doi:10.1016/j.bbamcr.2006.03.007
12. Bigger B, Tolmachov O, Collombet J-M, and Coutelle C. Introduction of chloramphenicol resistance into the modified mouse mitochondrial genome: Cloning of unstable sequences by passage through yeast. *Anal Biochem*. 2000;277:236–242. doi:10.1006/abio.1999.4382

13. Bigger BW, Liao A-Y, Sergijenko A, and Coutelle C. Trial and error: How the unclonable human mitochondrial genome was cloned in yeast. *Pharm Res.* 2011;28:2863–2870. doi:10.1007/s11095-011-0527-1
14. Karas BJ, Suzuki Y, and Weyman PD. Strategies for cloning and manipulating natural and synthetic chromosomes. *Chromosom Res.* 2015;23:57–68. doi:10.1007/s10577-014-9455-3
15. Waters VL. Conjugative transfer in the dissemination of beta-lactam and aminoglycoside resistance. *Front Biosci.* 1999;4:d433-56. doi:10.2741/Waters
16. Brumwell SL, MacLeod MR, Huang T, Cochrane RR, Meaney RS, Zamani M, et al. Designer *Sinorhizobium meliloti* strains and multi-functional vectors enable direct inter-kingdom DNA transfer. *PLoS One.* 2019;14:e0206781. doi:10.1371/journal.pone.0206781
17. Hayman GT and Bolen PL. Movement of shuttle plasmids from *Escherichia coli* into yeasts other than *Saccharomyces cerevisiae* using trans-kingdom conjugation. *Plasmid.* 1993;30:251–257. doi:10.1006/plas.1993.1056
18. Karas BJ, Diner RE, Lefebvre SC, McQuaid J, Phillips APR, Noddings CM, et al. Designer diatom episomes delivered by bacterial conjugation. *Nat Commun.* 2015;6:6925. doi:10.1038/ncomms7925
19. Heinemann JA and Sprague GF. Bacterial conjugative plasmids mobilize DNA transfer between bacteria and yeast. *Nature.* 1989;340:205–209. doi:10.1038/340205a0
20. Piers KL, Heath JD, Liang X, Stephens KM, and Nester EW. *Agrobacterium tumefaciens*-mediated transformation of yeast. *Proc Natl Acad Sci.* 1996;93:1613–1618. doi:10.1073/pnas.93.4.1613
21. Waters VL. Conjugation between bacterial and mammalian cells. *Nat Genet.* 2001;29:375–376. doi:10.1038/ng779
22. Kunik T, Tzfira T, Kapulnik Y, Gafni Y, Dingwall C, and Citovsky V. Genetic transformation of HeLa cells by *Agrobacterium*. *Proc Natl Acad Sci.* 2001;98:1871–1876. doi:10.1073/pnas.98.4.1871
23. Zoolkefli FIRM, Moriguchi K, Cho Y, Kiyokawa K, Yamamoto S, and Suzuki K. Isolation and analysis of donor chromosomal genes whose deficiency is responsible for accelerating bacterial and trans-kingdom conjugations by IncP1 T4SS machinery. *Front Microbiol.* 2021;12:620535. doi:10.3389/fmicb.2021.620535

24. Zatyka M, Jagura-Burdzy G, and Thomas CM. Regulation of transfer genes of promiscuous IncP $\alpha$  plasmid RK2: Repression of TraI region transcription both by relaxosome proteins and by the Tra2 regulator TrbA. *Microbiology*. 1994;140:2981–2990. doi:10.1099/13500872-140-11-2981
25. Ziegelin G, Fürste JP, and Lanka E. TraJ protein of plasmid RP4 binds to a 19-base pair invert sequence repetition within the transfer origin. *J Biol Chem*. 1989;264:11989–11994. doi:10.1016/S0021-9258(18)80164-8
26. Fürste JP, Pansegrau W, Ziegelin G, Kröger M, and Lanka E. Conjugative transfer of promiscuous IncP plasmids: Interaction of plasmid-encoded products with the transfer origin. *Proc Natl Acad Sci*. 1989;86:1771–1775. doi:10.1073/pnas.86.6.1771
27. Pansegrau W, Balzer D, Kruff V, Lurz R, and Lanka E. *In vitro* assembly of relaxosomes at the transfer origin of plasmid RP4. *Proc Natl Acad Sci*. 1990;87:6555–6559. doi:10.1073/pnas.87.17.6555
28. Pansegrau W and Lanka E. Mechanisms of initiation and termination reactions in conjugative DNA processing: Independence of tight substrate binding and catalytic activity of relaxase (TraI) of IncP $\alpha$  plasmid RP4. *J Biol Chem*. 1996;271:13068–13076. doi:10.1074/jbc.271.22.13068
29. Hyde KD, Xu J, Rapior S, Jeewon R, Lumyong S, Niego AGT, et al. The amazing potential of fungi: 50 ways we can exploit fungi industrially. *Fungal Divers*. 2019;97:1–136. doi:10.1007/s13225-019-00430-9
30. Parapouli M, Vasileiadi A, Afendra A-S, and Hatziloukas E. *Saccharomyces cerevisiae* and its industrial applications. *AIMS Microbiol*. 2020;6:1–31. doi:10.3934/microbiol.2020001
31. Segal-Kischinevzky C, Romero-Aguilar L, Alcaraz LD, López-Ortiz G, Martínez-Castillo B, Torres-Ramírez N, et al. Yeasts inhabiting extreme environments and their biotechnological applications. *Microorganisms*. 2022;10:794. doi:10.3390/microorganisms10040794
32. Fisher MC, Gurr SJ, Cuomo CA, Blehert DS, Jin H, Stukenbrock EH, et al. Threats posed by the fungal kingdom to humans, wildlife, and agriculture. *MBio*. 2020;11:e00449-20. doi:10.1128/mBio.00449-20
33. Pappas PG, Lionakis MS, Arendrup MC, Ostrosky-Zeichner L, and Kullberg BJ. Invasive candidiasis. *Nat Rev Dis Prim*. 2018;4:1–20. doi:10.1038/nrdp.2018.26
34. Geddes-McAlister J and Shapiro RS. New pathogens, new tricks: Emerging, drug-resistant fungal pathogens and future prospects for antifungal therapeutics. *Ann N.Y. Acad Sci*. 2019;1435:57–78. doi:10.1111/nyas.13739

35. Du H, Bing J, Hu T, Ennis CL, Nobile CJ, and Huang G. *Candida auris*: Epidemiology, biology, antifungal resistance, and virulence. *PLOS Pathog.* 2020;16:e1008921. doi:10.1371/journal.ppat.1008921
36. Smith HO and Welcox KW. A restriction enzyme from *Hemophilus influenzae*: I. Purification and general properties. *J Mol Biol.* 1970;51:379–391. doi:10.1016/0022-2836(70)90149-X
37. Karas BJ, Tagwerker C, Yonemoto IT, Hutchison CA, and Smith HO. Cloning the *Acholeplasma laidlawii* PG-8A genome in *Saccharomyces cerevisiae* as a yeast centromeric plasmid. *ACS Synth Biol.* 2012;1:22–28. doi:10.1021/sb200013j
38. Yoon YG, Koob MD, and Yoo YH. Re-engineering the mitochondrial genomes in mammalian cells. *Anat Cell Biol.* 2010;43:97–109. doi:10.5115/acb.2010.43.2.97
39. Pallen MJ. Time to recognise that mitochondria are bacteria? *Trends Microbiol.* 2011;19:58–64. doi:10.1016/j.tim.2010.11.001
40. Yoon YG and Koob MD. Nonreplicating intracellular bacterial vector for conjugative DNA transfer into mitochondria. *Pharm Res.* 2012;29:1040–1045. doi:10.1007/s11095-012-0701-0
41. Lim YM, de Groof AJC, Bhattacharjee MK, Figurski DH, and Schon EA. Bacterial conjugation in the cytoplasm of mouse cells. *Infect Immun.* 2008;76:5110–5119. doi:10.1128/IAI.00445-08
42. Yoon YG and Koob MD. Transformation of isolated mammalian mitochondria by bacterial conjugation. *Nucleic Acids Res.* 2005;33:e139–e139. doi:10.1093/nar/gni140
43. Pansegrau W and Lanka E. Enzymology of DNA transfer by conjugative mechanisms. *Prog Nucleic Acid Res Mol Biol.* 1996;54:197–251. doi:10.1016/S0079-6603(08)60364-5
44. del Solar G, Giraldo R, Ruiz-Echevarría MJ, Espinosa M, and Díaz-Orejas R. Replication and control of circular bacterial plasmids. *Microbiol Mol Biol Rev.* 1998;62:434–464. doi:10.1128/MMBR.62.2.434-464.1998
45. Rees CED and Wilkins BM. Protein transfer into the recipient cell during bacterial conjugation: Studies with F and RP4. *Mol Microbiol.* 1990;4:1199–1205. doi:10.1111/j.1365-2958.1990.tb00695.x
46. Pansegrau W, Schröder W, and Lanka E. Concerted action of three distinct domains in the DNA cleaving-joining reaction catalyzed by relaxase (TraI) of conjugative plasmid RP4. *J Biol Chem.* 1994;269:2782–2789. doi:10.1016/S0021-9258(17)42011-4

47. Balzer D, Pansegrau W, and Lanka E. Essential motifs of relaxase (TraI) and TraG proteins involved in conjugative transfer of plasmid RP4. *J Bacteriol.* 1994;176:4285–4295. doi:10.1128/jb.176.14.4285-4295.1994
48. Pansegrau W, Schröder W, and Lanka E. Relaxase (TraI) of IncPα plasmid RP4 catalyzes a site-specific cleaving-joining reaction of single-stranded DNA. *Proc Natl Acad Sci.* 1993;90:2925–2929. doi:10.1073/pnas.90.7.2925
49. Lightowers RN. Mitochondrial transformation: Time for concerted action. *EMBO Rep.* 2011;12:480–481. doi:10.1038/embor.2011.93
50. Cohen JS and Fox TD. Expression of green fluorescent protein from a recoded gene inserted into *Saccharomyces cerevisiae* mitochondrial DNA. *Mitochondrion.* 2001;1:181–189. doi:10.1016/S1567-7249(01)00012-5
51. Bonnefoy N and Fox TD. Directed alteration of *Saccharomyces cerevisiae* mitochondrial DNA by biolistic transformation and homologous recombination. In *Methods molecular biology*; 2007; Vol. 372, pp. 153–166 ISBN 6176321972.
52. Johnston SA, Anziano PQ, Shark K, Sanford JC, and Butow RA. Mitochondrial transformation in yeast by bombardment with microprojectiles. *Science.* 1988;240:1538–1541. doi:10.1126/science.2836954
53. Fox TD, Sanford JC, and McMullin TW. Plasmids can stably transform yeast mitochondria lacking endogenous mtDNA. *Proc Natl Acad Sci.* 1988;85:7288–7292. doi:10.1073/pnas.85.19.7288
54. Bonnefoy N and Remacle C. Biolistic transformation of *Chlamydomonas reinhardtii* and *Saccharomyces cerevisiae* mitochondria. *Methods Mol Biol.* 2022:1–19.
55. Hu Z, Zhao Z, Wu Z, Fan Z, Chen J, Wu J, et al. Successful expression of heterologous *egfp* gene in the mitochondria of a photosynthetic eukaryote *Chlamydomonas reinhardtii*. *Mitochondrion.* 2011;11:716–721. doi:10.1016/j.mito.2011.05.012
56. Randolph-Anderson BL, Boynton JE, Gillham NW, Harris EH, Johnson AM, Dorthu M-P, et al. Further characterization of the respiratory deficient *dum-1* mutation of *Chlamydomonas reinhardtii* and its use as a recipient for mitochondrial transformation. *Mol Gen Genet MGG.* 1993;236:235–244. doi:10.1007/BF00277118
57. Remacle C, Cardol P, Coosemans N, Gaisne M, and Bonnefoy N. High-efficiency biolistic transformation of *Chlamydomonas* mitochondria can be used to insert mutations in complex I genes. *Proc Natl Acad Sci.* 2006;103:4771–4776. doi:10.1073/pnas.0509501103

58. Hu Z, Fan Z, Zhao Z, Chen J, and Li J. Stable expression of antibiotic-resistant gene *ble* from *Streptoalloteichus hindustanus* in the mitochondria of *Chlamydomonas reinhardtii*. PLoS One. 2012;7:e35542. doi:10.1371/journal.pone.0035542
59. Zhou J, Liu L, and Chen J. Mitochondrial DNA heteroplasmy in *Candida glabrata* after mitochondrial transformation. Eukaryot Cell. 2010;9:806–814. doi:10.1128/EC.00349-09
60. Yamasaki T, Kurokawa S, Watanabe KI, Ikuta K, and Ohama T. Shared molecular characteristics of successfully transformed mitochondrial genomes in *Chlamydomonas reinhardtii*. Plant Mol Biol. 2005;58:515–527. doi:10.1007/s11103-005-7081-3
61. Collombet J-M, Wheeler VC, Vogel F, and Coutelle C. Introduction of plasmid DNA into isolated mitochondria by electroporation: A novel approach toward gene correction for mitochondrial disorders. J Biol Chem. 1997;272:5342–5347. doi:10.1074/jbc.272.8.5342
62. Yoon YG and Koob MD. Efficient cloning and engineering of entire mitochondrial genomes in *Escherichia coli* and transfer into transcriptionally active mitochondria. Nucleic Acids Res. 2003;31:1407–1415. doi:10.1093/nar/gkg228

## Appendices

### Appendix A: Copyright Permissions

Written permission is not required from the journals of Algal Research (<https://www.elsevier.com/about/policies/copyright>), Biology (<https://www.elsevier.com/about/policies/copyright>), or BioDesign Research (<https://spj.science.org/page/research/for-authors#copyright-and-licensing>) for use of these publications. Use of these publications as part of my written thesis for academic purposes is permitted under the Creative Commons Act (<https://creativecommons.org/licenses/by-nc/4.0/legalcode>).



## Permission for Chapter 2

### Author rights

The below table explains the rights that authors have when they publish with Elsevier, for authors who choose to publish either open access or subscription. These apply to the corresponding author and all co-authors.

Author rights in Elsevier's proprietary journals	Published open access	Published subscription
Retain patent and trademark rights	√	√
Retain the rights to use their research data freely without any restriction	√	√
Receive proper attribution and credit for their published work	√	√
Re-use their own material in new works without permission or payment (with full acknowledgement of the original article): 1. Extend an article to book length 2. Include an article in a subsequent compilation of their own work 3. Re-use portions, excerpts, and their own figures or tables in other works.	√	√
Use and share their works for scholarly purposes (with full acknowledgement of the original article): 1. In their own classroom teaching. Electronic and physical distribution of copies is permitted 2. If an author is speaking at a conference, they can present the article and distribute copies to the attendees 3. Distribute the article, including by email, to their students and to research colleagues who they know for their personal use 4. Share and publicize the article via Share Links, which offers 50 days' free access for anyone, without signup or registration 5. Include in a thesis or dissertation (provided this is not published commercially) 6. Share copies of their article privately as part of an invitation-only work group on commercial sites with which the publisher has a hosting agreement	√	√
Publicly share the preprint on any website or repository at any time.	√	√
Publicly share the accepted manuscript on non-commercial sites	√	√ using a CC BY-NC-ND license and usually only after an embargo period (see <a href="#">Sharing Policy</a> for more information)
Publicly share the final published article	√ in line with the author's choice of end user license	×
Retain copyright	√	×

## Permission for Chapter 3



### MDPI Open Access Information and Policy

All articles published by MDPI are made immediately available worldwide under an open access license. This means:

- everyone has free and unlimited access to the full-text of *all* articles published in MDPI journals;
- everyone is free to re-use the published material if proper accreditation/citation of the original publication is given;
- open access publication is supported by the authors' institutes or research funding agencies by payment of a comparatively low **Article Processing Charge (APC)** for accepted articles.

#### Permissions

No special permission is required to reuse all or part of article published by MDPI, including figures and tables. For articles published under an open access Creative Common CC BY license, any part of the article may be reused without permission provided that the original article is clearly cited. Reuse of an article does not imply endorsement by the authors or MDPI.

## Permission for Chapter 4



### Copyright And Licensing

*Research* content is Open Access, published under a [Creative Commons Attribution License \(CC BY\)](#) on a continuous basis. This means that content is freely available to all readers upon publication and content is published as soon as production is complete. Science and Technology Review Publishing House holds an exclusive license to the content, the author(s) hold copyright and retain the right to publish. Visit our [FAQ page](#) for information on re-use.

## Appendix B: Supplemental Information for Chapter 2

### B.1 Supplemental Tables

**Table B-1. List of primers used to amplify and screen *Phaeodactylum tricornutum*'s mitochondrial genome.**

Name	Primers	Length (bp)
<b>Amplification of <i>P. tricornutum</i>'s mitochondrial genome: pPT-PCR</b>		
Homology regions to the pAGE3.0 plasmid are highlighted		
Fragment 1	BK141F – ctgttacacgttgactgggacaaaatggtttattgaagg BK141R – ttggaataaaaagggttcgaaccttgaatgatcgtaccaa	5217
Fragment 2	BK142F – ttatttaacaaaatgcctcttggggttctatgatca BK142R – actagtcgttaaatggttagttggttttaataagc	5190
Fragment 3	BK143F – tggctcgggtaaaagacctacctggagtaaaatcatcta BK143R – gttttccaaaagatggggcgcatgtttttccatttta	5197
Fragment 4	BK144F – gtgtaaatctatgaaaaattattgaaatcaaaattacga BK144R – tccatgtttataaaaatattgaatgttcagattttt	5175
Fragment 5	BK145F – cccagtttcatttttggctccaatcaaatgctgtaaa BK250R – cgacaagcagcagcgagatcccacatcaagctagatcgcgcgcggcggaagctcccaaaaagatgacaaaacc	2815
Fragment 6	BK251F – ttctgtaaatcgggttgcatttttagggaagcttcgccgcgcgcgcatcactagcttgattgggatctcgc BK88R – aagcctgaccgagagcaatcccgcagcttcaagtggtgatgctcctatgtgtaagtcaccaatgactcaacgatt	9124
Fragment 7	BK88F – aatcgttgagtgcaatgggacttacacatagacaccatcacaccactgaagactcgggattgctctcggcaagctt BK245R – tcccccccgcctaaggaacttgctgtaaaagcgtgaaaagcgcgacgcgacgcctctgctcctgctcgggtgatgta	8571
Fragment 8	BK247F – tcgagctgtaagtacatcaccgacgagaagcgaagacgatcgcgacgcctttcacgcttttacgaccaagtttcctta BK146R – cttcacgaaaattcaatttcgctgagtttctgctggaga	5655
Fragment 9	BK147F – gctgacgcctgccagtgctgcaagattaaaggaaaggggt BK147R – agtaagcacgcgcaaaaaaaggtagaactggttaggagat	5299
Fragment 10	BK148F – tagcttttcgctccgaaaccaagatgtttttttcatic BK140R – cccaacactattaaattctcaactttgtttacaggatt	9264
<b>Amplification of TAR cloning capture vector: pPT-TAR</b>		
Homology regions to the pAGE3.0 plasmid are highlighted		
Fragment 1	BK92R – ttgcatttttggcgcttcttattctagtatagcacctgccatagcgcgcgcccatacactgatactagcttgattgg BK88R – aagcctgaccgagagcaatcccgcagcttcaagtggtgatgctcctatgtgtaagtcaccaatgactcaacgatt	9142
Fragment 2	BK88F – aatcgttgagtgcaatgggacttacacatagacaccatcacaccactgaagactcgggattgctctcggcaagctt BK93F – gacagtgaaggtctttataaggcttattgctttaggcggcgaactcctccgctcgcgacgatacgtcttgcctgctcgt	8581
<b>Diagnostic MPX PCR primers</b>		
Amplicon 1	BK901F – tattgcatcaggcacagag BK901R – gcccaaaagcataggtgcat	265
Amplicon 2	BK902F – aaagctgcaaggcagttgat BK902R – agccaaaaaggtttcgatt	171
Amplicon 3	BK903F – ggcagaaaagctgagcctaa BK903R – cctatggtgcaaggcattt	224
Amplicon 4	BK904F – ttcatgttggctccaatc BK904R – cagttcaggttcgggatgt	334
Amplicon 5	BK905F – gttctgtttcggcgatta BK905R – aacacagaccgacaccttcc	405
Amplicon 6	BK906F – acgttttgcagtaccctgg BK906R – accataagtcacgggaatc	507

**Table B-2. List of mutations identified in cloned *P. tricornutum* mitochondrial genomes.** Plasmids containing the cloned genomes were sequenced using an Illumina MiSeq and mapped to their respective reference sequences by the CCIB DNA Core Facility at Massachusetts General Hospital. Mutations were identified using Geneious version 2020.0 created by Biomatters. Positions are based on residue numbering beginning with the first base in Fragment 1 of the result sequence and counting towards Fragment 2 (see Figure 3-1A). Published sequence: expected sequence as designed by combining published sequence for the *P. tricornutum* mitochondrial genome [1] and based on plasmid pAGE3.0 [2] according to the respective cloning strategy.

Position	Mutation	Location	Effect
<b>pPT-PCR C1   Reference: Published sequence</b>			
8002	G > T	<i>mt-rps2</i>	Arg <sub>114</sub> > Ile
15,327	C > A	<i>mt-rpl2</i>	Gln <sub>35</sub> > Lys
16,259	1-bp insertion	<i>mt-rps19</i>	Frameshift
18,073	C > A	<i>mt-atp9</i>	Leu <sub>42</sub> > Met
22,687	G > A	<i>mt-cob</i> terminator	Unknown
22,714–22,871	158-bp insertion	<i>mt-cob</i> terminator	Unknown
34,783	129-bp deletion	Vector backbone (intergenic)	No effect
57,408	G > T	Intergenic	No effect
59,856	C > T	<i>mt-cox1</i>	Thr <sub>245</sub> > Ile
<b>pPT-PCR C2   Reference: Published sequence</b>			
159	1-bp deletion	<i>mt-cox1</i> intron	Unknown
17,214	G > T	<i>mt-rps3</i>	Met <sub>310</sub> > Ile
27,716	G > T	Vector backbone ( <i>S. meliloti</i> repA2B2C2)	Ala <sub>135</sub> > Glu
42,554	G > T	<i>mt-nad5</i>	Glu <sub>595</sub> > STOP
56,559	T > C	<i>mt-nad7</i>	Ile <sub>191</sub> > Thr
<b>pPT-PCR C2-1   Reference: pPT-PCR C2</b>			
1197	C > T	<i>mt-cox1</i> intron	Unknown
1473	C > T	<i>mt-cox1</i> intron	Unknown
12,811	G > A	<i>mt-nad1</i>	Asp <sub>295</sub> > Asn
27,716	T > G	Vector backbone ( <i>S. meliloti</i> repA2B2C2)	Glu <sub>135</sub> > Ala
55,673	G > A	<i>mt-cox2</i>	Val <sub>195</sub> > Ile
<b>pPT-PCR C2-2   Reference: pPT-PCR C2</b>			
27,716	T > G	Vector backbone ( <i>S. meliloti</i> repA2B2C2)	Glu <sub>135</sub> > Ala
<b>pPT-TAR C1   Reference: Published sequence</b>			
17,871	C > A	<i>mt-cox3</i>	Gly <sub>215</sub> > Gly
<b>pPT-TAR C2   Reference: Published sequence</b>			
8415	C > A	Vector backbone ( <i>S. cerevisiae</i> ARSH4)	No effect
17,906	C > A	<i>mt-cox3</i>	Gly <sub>215</sub> > Gly
46,055	3847-bp deletion	Repeat region	Effect unknown.
46,182	8004-bp deletion	Repeat region	
46,235	T > C	Repeat region	
46,246	403-bp deletion	Repeat region	Note: Mutations detected in repetitive region are likely due to sequencing errors.
46,300	A > G	Repeat region	
46,304	C > T	Repeat region	
46,442	G > A	Repeat region	
46,536	G > A	Repeat region	
46,851	8165-bp deletion	Repeat region	
46,927	7906-bp deletion	Repeat region	
47,185	497-bp deletion	Repeat region	
47,757	3601-bp deletion	Repeat region	
47,891	C > T	Repeat region	
47,913	413-bp deletion	Repeat region	

## Appendix C: Supplemental Information for Chapter 3

### C.1 Supplemental Figures

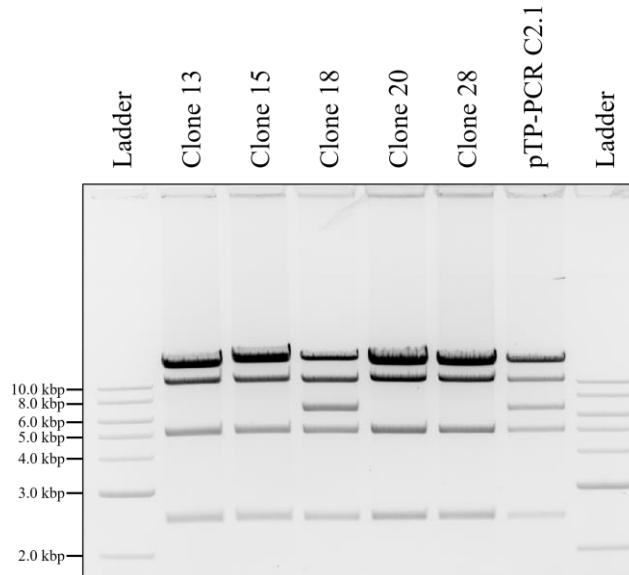


**Figure C-1. PvuI restriction digest analysis of mutated mitochondrial genomes from the plasmid stability assay.** pTP-PCR C2.1 (control) and five mutated clones (see Figure 3-4B) were analyzed. Band sizes of 6-, 2454-, 4863-, 6262-, 12,869-, 15,404-, and 15,749-bp are expected. Notes: 1 – Mutated pTP-PCR C2.1 genomes 13, 15, 20, and 28 show an incorrect restriction pattern confirming the result from the MPX PCR experiment (Figure 3-4B); 2 – The 6 bp band is not visible in this gel.

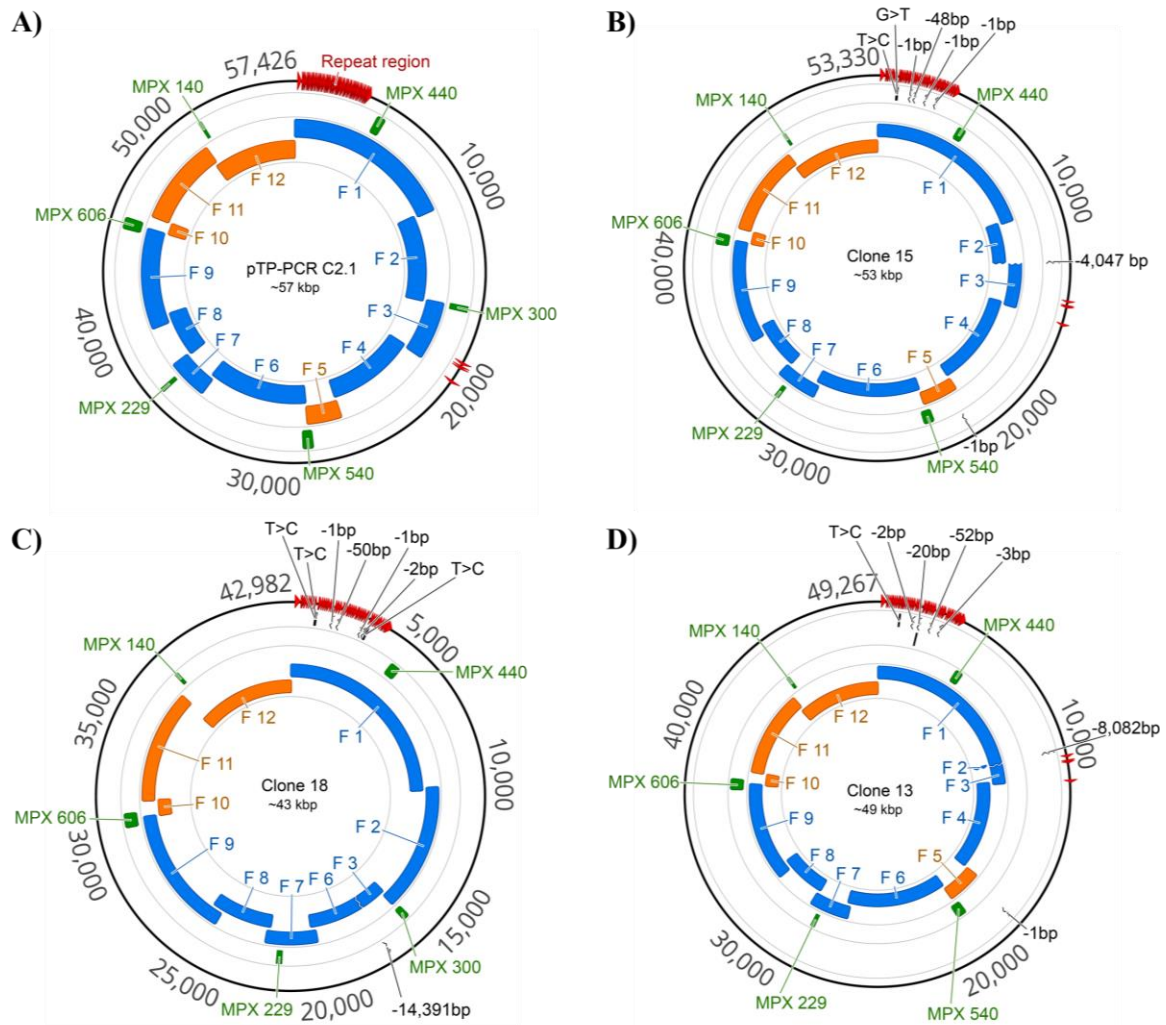


**Figure C-2. Sequencing analysis of three mutated pTP-PCR C2.1 clones from the plasmid stability assay.** **A)** Plasmid map of the reference sequence, pTP-PCR C2.1, prior to genome stability assay (Figure 3-4) experiment. **B–D)** Plasmid maps of clones 13, 15, and 18 with mutations identified after next-generation sequencing displayed. For all plasmid maps, the relative sizes and positions of the mitochondrial genome fragments (blue), plasmid backbone fragments (orange), and repetitive sequences (red) are shown. The six MPX PCR amplicons used for diagnostic screening and their sizes in bp are indicated (green). These images were generated using Geneious version 2020.2.4, created by Biomatters. Notes: 1 – in both **B)** and **D)** a deletion in fragments 2 and 3 resulted in the absent 300 bp MPX amplicon; 2 – in **C)** a deletion spanning fragments 3–6 resulted in the absent 540 bp MPX amplicon.

## C.2 Supplemental Tables

**Table C-1. List of primers used to amplify and screen *Thalassiosira pseudonana*'s mitochondrial genome.**

Name	Primers	Length (bp)
<b>Original amplification of the full <i>T. pseudonana</i> mitochondrial genome (pTP-PCR C1/2 – Design 1)</b>		
Fragment 1	P1F – ttccattagttgcagtcactccgtttgtttggcgcgcctcagcaacagggtacaacc P1R – agcgttaaaaagttaaaaaatagcgtatataaattatg	10,735
Fragment 2	P2F – tatctatacaattttgcttcagtaacattttat P2R – aaaagaattgcctgtattttaactacaattatagaaa	6092
Fragment 3	P3F – aatctaaaaactctacttaaaaaactaattcaaat P3R – ataaaaataaaagtaagctgtcttaagctgttcggc	3610
Fragment 4	P4F – caggaaatgtcaattttgttttaaaaacaagtttaccactaatctattatagaagata P4R – ggctcgaacagctcgtactcttaggaccgttatagttacgtaaaagtataaattctaa	6274
Fragment 5	P5F – tgaccaagatataaaaacttttagaattataaacatttactgaactataacggctctaa P5R – ttaaatgttaaaactgagctgttaaaagtttgaccatctataaccctgtatccc	2152
Fragment 6	P6F – tcgtttcatcagttacgctagggataacagggtatataagatgtcaaaaactttaaacg P6R – ttccttcacaacacgaagcaaaatttaataacataagattataggataatttag	7035
Fragment 7	P7F – aaaatataacatttaccacttctagtgatattctgg P7R – atttgatgagctctggttaaaacttttaaacattgc	2512
Fragment 8	P8F – tggttacgatactttgataaaaaaaatcggaggatgga P8R – cgatttattgataagcaacgagattgtaaaatggccac	3250
Fragment 9	P9F – ccatactattgaatgttcgagttataaaatgccaaaagtaactagtttagtca P9R – cgtataatgaccccgaagcagggttagcagcggaaagatcagggcagttcagattaa	6216
Fragment 10	P10F – cataaaaacagttcaaaataaactgaactgcctcagatcttcctcgcataaccct P10R – catagacggccgaccccgagggcaaccagctcgcgatcgcgatcgtctgccc	859
Fragment 11	P11F – agtaccatccgagcgaagcaagacgatcgcgagctggtgccctcgccc P11R – ccatctgctcatcaccagctcgaaccagaacgataatccttctgtaagtgcag	5367
Fragment 12	P12F – tgaccaggagctgctactgaggcagcactgagatcctccctcttctactgac P12R – aagtaagttataaactggtgtaccctgtgctcggagcgcgcaaaccaaacgccc	5870
<b>Amplification of the <i>T. pseudonana</i> reduced mitochondrial genome (pTP-PCR C3/4 – Design 2)</b>		
Fragment 1	P2F – tatctatacaattttgcttcagtaacattttat P2R – aaaagaattgcctgtattttaactacaattatagaaa	6092
Fragment 2	P3F – aatctaaaaactctacttaaaaaactaattcaaat P3R – ataaaaataaaagtaagctgtcttaagctgttcggc	3610
Fragment 3	P4F – caggaaatgtcaattttgttttaaaaacaagtttaccactaatctattatagaagata P13R – tcgttaaaagtttgaccattaaagtgtataaattctaa	6254
Fragment 4	P13F – taataatcaatgatttttaaaactataaacgtt P6R – ttccttcacaacacgaagcaaaatttaataacataagattataggataatttag	7174
Fragment 5	P17F – ataaaattacgaaaaagtaactaccatcctgctgct P8R – cgatttattgataagcaacgagattgtaaaatggccac	5417
Fragment 6	P14F – ccatactattgaatgttcgagttataaattgccaa P14R – cctaaaagacatagcagcgaacacgagcagatatacccaatcaagctagatcgttaagctgtatagcttgata	6372
Fragment 7	P15F – cgagaataaataatattgcttttattctcttcaagctatacaagcttaactgatactgctgattggatc P15R – aagcttgacagcagacaaatcccgagctcagtgctgctgtatgttaagcaccatgcaactcaacgatt	9136
Fragment 8	P16F – aatcgttgatgcatgctgacttacatagacaccatcacaccactgaagactcgggattgctcggcgaagctt P16R – cctaaaaaaattttgagaataagtaattatgctttgctgtattatcaaaaacgatcctcctgctgctg	8441
Fragment 9	P18F – gaggcactcagctgtaagtacatcaccagcagcaagcgaagcagatcgttttgataaaaacgatcaaaagactaa P1R – agcgttaaaaagttaaaaatagcgtatataaattatg	6810
<b>Final amplification of the <i>T. pseudonana</i> mitochondrial genome (pTP-PCR Design 1)</b>		
Fragment 1	P25F – aaaaatgcattgggaaaaaggttaaaattaccccaacgaaa P25R – gtagaataaaggctggtgattgccacagttttgct	5138
Fragment 2	P26F – gtaaccaagtatgacgtcccaattgcgagattacctac P26R – cgttttttaaaactctgcaatttactgcaaaagcaaca	5244
Fragment 3	P27F – ttgtatgctgctcttatttaaacactttgcggttt P27R – cgtcactccagatcgcgcttctctgctcctctg	5230
Fragment 4	P28F – taaaaagccctaaatccagctgaacgctggttatag P28R – gcttaagtagactgaactactgacctacgcttatcagg	6884
Fragment 5	P29F – gagggcatcttttatataataaattcccaacctcaa P29R – atgtacggggcgtgtgtacaaaagcaagctacgtattca	5959
Fragment 6	P30F – tcttagtccgattgaaagctgcaactcgtttacatgaag P30R – ttaagctatagcttcaatgctgaatgattgaaagagg	5107



Fragment 7	P31F – aatagt gaaaattatgttttc gaaaattctacagcaggt P31R – tgttgtaaacattatgtatattctttgtttgctcattg	5948
Fragment 8	P32F – attgaategttttacatgetccaggaatgtcaatttgt P32R – atattatatttattgtaaatattggatttccagcta	5391
Fragment 9	P33F – aatttagcttcgaaataaacgctaagcctt gaaaagata P33R – agttgtctttctggaaatgccatttggctagtttttag	5888
Fragment 10	P34F – tacacaaaagggaaagttaacatttctgaacaatgcaaa P34R – catttactcatgattttgggtagattctgtgataa	6155
Fragment 11	P35F – agccataatctgttaaaatagctttaaattgagtggt P35R – tatgatatgatagaacattataaacggctgaaagaggta	4289
<b><i>T. pseudonana</i> diagnostic MPX PCR primers</b>		
Amplicon 1	P19F – gctcacgacatcagtttgc P19R – tgctggcttttcaagttcct	140
Amplicon 2	P20F – gcttaattcacgcttattgaaaa P20R – atggcttgaaggacatcca	229
Amplicon 3	P21F – agttaaatctatagaaaatgcaaatagttattaacagt P21R – aaaatagaatctttgaaaaagtttctcctgaagttttaga	300
Amplicon 4	P22F – agttttaattttttgtctgctattgtttatttttagc P22R – cacctaaactaatgggtctaaaaatataatgataagctc	440
Amplicon 5 (only +IR)	P23F – tggctaccctgtggaacacctatctgtattaacgaagc P23R – gttttgggaacaggaagtcattgttcaaatcacattatt	540
Amplicon 6 (only +IR)	P24F – ggtcataagccatattcagtagaatataaatgfactat P24R – agccggccagcctcgagagcaggattcccgttgagcacc	606

**Table C-2. List of mutations identified in cloned *T. pseudonana* mitochondrial genomes by next-generation sequencing.**

Position	Mutation	Location/Gene	Effect
<b>pTP-PCR C1.1 (Reference: pTP-PCR Design 1)</b>			
888	A > G	Repeat region	Unknown
902	G > A	Repeat region	Unknown
1000	A > G	Repeat region	Unknown
1587	28-bp deletion	Repeat region	Unknown
1879	28-bp deletion	Repeat region	Unknown
1880	G > C	Repeat region	Unknown
2112	9-bp deletion	Repeat region	Unknown
2890	19-bp deletion	Repeat region	Unknown
2968	T > C	Repeat region	Unknown
3032	19-bp deletion	Repeat region	Unknown
3221	A > G	Repeat region	Unknown
3623	T > C	Repeat region	Unknown
9841	G > A	<i>rrnS</i>	Unknown
21,950	G > T	<i>rps12</i>	Val <sub>87</sub> > Phe
22,337	2-bp deletion	<i>rps7</i>	Frameshift
22,433	1-bp deletion	<i>rps7</i>	Frameshift
22,716	C > A	<i>rpl14</i>	Gln <sub>44</sub> > Lys
25,274	G > A	<i>tatC</i>	Thr <sub>56</sub> > Ile
30,179	1-bp deletion	<i>rps19</i>	Frameshift
33,603	T > C	<i>nad11</i>	Leu <sub>373</sub> > Ser
35,514	G > A	<i>trnS(gct)</i>	Unknown
42,462	G > A	<i>orf718 (cox1 intron)</i>	No effect
46,617	2-bp deletion	Vector backbone (intergenic)	No effect
56,480	G > A	Vector backbone (intergenic)	No effect
<b>pTP-PCR C2.1 (Reference: pTP-PCR Design 1)</b>			
848	A > G	Repeat region	Unknown
862	G > A	Repeat region	Unknown
960	A > G	Repeat region	Unknown
1549	26-bp deletion	Repeat region	Unknown
1843	27-bp deletion	Repeat region	Unknown
1843	G > C	Repeat region	Unknown
2074	89-bp deletion	Repeat region	Unknown
2385	31-bp deletion	Repeat region	Unknown
2743	17-bp deletion	Repeat region	Unknown
2822	T > C	Repeat region	Unknown
2886	17-bp deletion	Repeat region	Unknown
3077	A > G	Repeat region	Unknown
3479	T > C	Repeat region	Unknown
9697	G > A	<i>rrnS</i>	Unknown
11,838	1-bp deletion	<i>cox3</i>	Frameshift
22,763	C > T	<i>rpl14</i>	Pro <sub>107</sub> > Ser
27,402	1-bp insertion	Intergenic	No effect
29,153	1-bp deletion	<i>rpl2</i>	Frameshift
34,681	1-bp deletion	Intergenic	No effect
41,218	G > A	<i>orf718 (cox1 intron)</i>	Pro <sub>388</sub> > Ser
44,615	G > A	<i>nad5</i>	No effect
46,475	2-bp deletion	Vector backbone (intergenic)	No effect
49,206	1-bp insertion	Vector backbone (intergenic)	No effect

<b>pTP-PCR C3.1 (Reference: pTP-PCR Design 2)</b>			
1846	1-bp deletion	Vector backbone ( <i>S. meliloti repA2B2C2</i> )	Frameshift
7209	G > T	Vector backbone ( <i>E. coli repE</i> )	Pro <sub>103</sub> > Ser
21,050	1-bp insertion	<i>rrnL</i>	Unknown
23,484	G > A	<i>rrnS</i>	Unknown
24,048	G > A	<i>nad6</i>	Met <sub>142</sub> > Ile
24,115	T > A	<i>nad6</i>	Leu <sub>165</sub> > Met
34,435	C > G	<i>rps4</i>	Ile <sub>162</sub> > Met
35,699	1-bp deletion	<i>rps12</i>	Frameshift
39,198	1-bp deletion	Intergenic	No effect
40,103	1-bp deletion	<i>rps11</i>	Frameshift
45,855	1-bp insertion	<i>nad11</i>	Frameshift
46,604	10,890-bp deletion	Several coding regions	Unknown
<b>pTP-PCR C4.1 (Reference: pTP-PCR Design 2)</b>			
7-8	AC > TA	Vector backbone (intergenic)	No effect
748	C > T	Vector backbone ( <i>nat</i> )	Pro <sub>50</sub> > Leu
2513	C > T	Vector backbone ( <i>S. meliloti repA2B2C2</i> )	Arg <sub>176</sub> > His
11,179	G > A	Vector backbone ( <i>E. coli parB</i> )	No effect
11,228	C > A	Vector backbone ( <i>E. coli parB</i> )	Ala <sub>146</sub> > Asp
18,322	1-bp deletion	<i>atp6</i>	Frameshift
23,483	G > A	<i>rrnS</i>	Unknown
25,862	C > T	<i>cox3</i>	No effect
33,411	5-bp deletion	Intergenic	No effect
41,950	C > T	<i>rps3</i>	Ser <sub>64</sub> > Leu
42,081	1-bp deletion	<i>rps3</i>	Frameshift
46,598	G > A	Intergenic	No effect

**Table C-3. Count of raw RNA sequencing reads for strains with either the pPT-PCR C2.1 genome or plasmid backbone alone (pPtGE31).** Raw counts were enumerated by mapping against the appropriate reference and counted using HTSeq using –nonunique all mode. Three biological replicates were performed (repA, repB, repC) for each condition. Genes regions were counted for the features.

Gene	pPtGE31 repA	pPtGE31 repB	pPtGE31 repC	pPT-PCR C2.1 repA	pPT-PCR C2.1 repB	pPT-PCR C2.1 repC
<i>cat</i>	2224	4737	3625	3395	4988	6646
<i>atp6</i>	0	0	0	13	6	18
<i>atp8</i>	0	0	0	0	0	0
<i>atp9</i>	0	0	0	0	0	0
<i>cob</i>	0	0	0	51	82	133
<i>cox1</i>	0	0	0	1417	1576	3028
<i>cox2</i>	0	0	0	4	6	23
<i>cox3</i>	0	0	0	12	15	23
<i>nad1</i>	0	0	0	7	9	11
<i>nad11-a</i>	0	0	0	2	6	7
<i>nad11-b</i>	0	0	0	8	8	10
<i>nad2</i>	0	0	0	25	54	51
<i>nad3</i>	0	0	0	1	0	3
<i>nad4</i>	0	0	0	8	10	27
<i>nad4L</i>	0	0	0	0	0	0
<i>nad5</i>	0	0	0	11	17	17
<i>nad6</i>	0	0	0	9	4	17
<i>nad7</i>	0	0	0	29	32	52
<i>nad9-rps14</i>	0	0	0	4	7	11
<i>rRNA 1.1</i>	0	0	0	8	19	22
<i>rRNA 1.2</i>	0	0	0	81	99	165
<i>rRNA 1.3</i>	0	0	0	6	7	12
<i>rRNA 1.4</i>	0	0	0	38	78	145
<i>rpl14</i>	0	0	0	2	2	1
<i>rpl16</i>	0	0	0	0	2	3
<i>rpl2</i>	0	0	0	2	0	3
<i>rpl5</i>	0	0	0	0	0	0
<i>rpl6</i>	0	0	0	0	2	3
<i>rps10</i>	0	0	0	1	0	3
<i>rps11</i>	0	0	0	0	0	4
<i>rps12</i>	0	0	0	0	1	1
<i>rps13</i>	0	0	0	1	0	0
<i>rps19</i>	0	0	0	1	0	4

---

<i>rps2</i>	0	0	0	0	1	2
<i>rps3</i>	0	0	0	2	2	5
<i>rps4</i>	0	0	0	0	1	7
<i>rps7</i>	0	0	0	1	1	2
<i>rps8</i>	0	0	0	1	0	5
<i>tatC</i>	0	0	0	11	9	38
<i>trnA(ugc)</i>	0	0	0	1	0	0
<i>trnC(gca)</i>	0	0	0	0	1	0
<i>trnD(guc)</i>	0	0	0	0	0	0
<i>trnE(uuc)</i>	0	0	0	19	33	42
<i>trnF(gaa)</i>	0	0	0	1	0	4
<i>trnG(gcc)</i>	0	0	0	0	0	0
<i>trnH(gug)</i>	0	0	0	0	0	0
<i>trnI(cau)</i>	0	0	0	2	0	0
<i>trnI(gau)</i>	0	0	0	2	5	6
<i>trnK(uuu)</i>	0	0	0	0	0	0
<i>trnL(uaa)</i>	0	0	0	0	0	0
<i>trnL(uag)</i>	0	0	0	0	0	1
<i>trnM(cau)</i>	0	0	0	16	26	48
<i>trnM(cau)</i>	0	0	0	1	2	14
<i>trnN(guu)</i>	0	0	0	1	0	1
<i>trnP(ugg)</i>	0	0	0	0	0	0
<i>trnQ(uug)</i>	0	0	0	9	5	14
<i>trnR(ucg)</i>	0	0	0	0	0	1
<i>trnR(ucu)</i>	0	0	0	0	1	5
<i>trnS(gct)</i>	0	0	0	6	15	32
<i>trnS(tga)</i>	0	0	0	0	0	0
<i>trnV(uac)</i>	0	0	0	54	81	121
<i>trnW(cca)</i>	0	0	0	0	0	0
<i>trnY(gua)</i>	0	0	0	0	0	2

---

**Table C-4. Count of raw RNA sequencing reads for strains with either the pTP-PCR C2.1 genome or plasmid backbone alone (pPtGE31).** Raw counts were enumerated by mapping against the appropriate reference and counted using HTSeq using –nonunique all mode. Three biological replicates were performed (repA, repB, repC) for each condition. Genes regions were counted for the features.

Genes	pPtGE31 repA	pPtGE31 repB	pPtGE31 repC	pTP-PCR C2.1 repA	pTP-PCR C2.1 repB	pTP-PCR C2.1 repC
<i>cat</i>	2224	4737	3625	1856	1439	4337
<i>atp6</i>	0	0	0	0	0	1
<i>atp8</i>	0	0	0	0	0	0
<i>atp9</i>	0	0	0	0	0	1
<i>cob</i>	0	0	0	10	3	13
<i>cox1</i>	0	0	0	427	463	914
<i>orf718</i>	0	0	0	402	438	883
<i>cox2</i>	0	0	0	2	0	3
<i>cox3</i>	0	0	0	11	12	27
<i>nad1</i>	0	0	0	2	0	2
<i>nad11</i>	0	0	0	2	0	2
<i>nad2</i>	0	0	0	0	1	1
<i>nad3</i>	0	0	0	1	0	1
<i>nad4</i>	0	0	0	1	0	3
<i>nad4L</i>	0	0	0	0	0	0
<i>nad5</i>	0	0	0	5	2	5
<i>nad6</i>	0	0	0	1	0	6
<i>nad7</i>	0	0	0	46	27	38
<i>nad9</i>	0	0	0	0	0	0
<i>rpl14</i>	0	0	0	0	0	6
<i>rpl16</i>	0	0	0	0	5	1
<i>rpl2</i>	0	0	0	1	12	8
<i>rpl5</i>	0	0	0	0	0	1
<i>rpl6</i>	0	0	0	0	0	0
<i>rps10</i>	0	0	0	0	0	0
<i>rps11</i>	0	0	0	0	0	0
<i>rps12</i>	0	0	0	4	0	0
<i>rps13</i>	0	0	0	1	0	1
<i>rps14</i>	0	0	0	0	0	0
<i>rps19</i>	0	0	0	1	9	3
<i>rps2</i>	0	0	0	0	0	0
<i>rps3</i>	0	0	0	1	0	0
<i>rps4</i>	0	0	0	0	0	0

---

<i>rps7</i>	0	0	0	0	0	1
<i>rps8</i>	0	0	0	0	0	0
<i>rrnS</i>	0	0	0	23	17	36
<i>rrnL</i>	0	0	0	70	46	112
<i>tatC</i>	0	0	0	2	0	1
<i>trnA(ugc)</i>	0	0	0	1	0	0
<i>trnC(gca)</i>	0	0	0	0	0	0
<i>trnD(guc)</i>	0	0	0	0	0	0
<i>trnE(uuc)</i>	0	0	0	0	0	2
<i>trnF(gaa)</i>	0	0	0	0	0	0
<i>trnG(gcc)</i>	0	0	0	0	0	1
<i>trnH(gug)</i>	0	0	0	0	0	0
<i>trnI(cau)</i>	0	0	0	2	0	0
<i>trnI(gau)</i>	0	0	0	0	0	0
<i>trnK(uuu)</i>	0	0	0	0	0	1
<i>trnL(uaa)</i>	0	0	0	0	0	0
<i>trnL(uag)</i>	0	0	0	1	0	0
<i>trnM(cau)</i>	0	0	0	7	4	15
<i>trnN(guu)</i>	0	0	0	1	0	0
<i>trnP(ugg)</i>	0	0	0	0	0	0
<i>trnQ(uug)</i>	0	0	0	0	0	1
<i>trnR(ucg)</i>	0	0	0	0	0	1
<i>trnR(ucu)</i>	0	0	0	0	0	0
<i>trnS(gct)</i>	0	0	0	1	0	2
<i>trnS(tga)</i>	0	0	0	1	0	0
<i>trnV(uac)</i>	0	0	0	0	0	1
<i>trnW(cca)</i>	0	0	0	1	0	1
<i>trnW(uca)</i>	0	0	0	0	0	1
<i>trnY(gua)</i>	0	0	0	0	0	0

---

### C.3 Supplemental Notes

**Note C-1. Determination of outliers in the calculation of doubling time for *E. coli* strains.** The median of the dataset was calculated, as well as the lower (Q1) and upper (Q3) quartiles representing the data points at which 25% of the data falls below and above, respectively. The interquartile range ( $IQR = Q3 - Q1$ ) that indicates the boundaries of non-outlier data points was then calculated. Next, the inner fence of the dataset was found by multiplying IQR by 1.5, then subtracting that value from Q1 and adding it to Q3. Any point outside the inner fence is considered a minor outlier. The outer fence of the dataset was found by multiplying IQR by 3, then subtracting that value from Q1 and adding it to Q3. Any data point outside the outer fence is considered a major outlier. Here, we have only omitted major outliers from our determination of td.



## Appendix D: Supplemental Information for Chapter 4

### D.1 Supplemental Figures

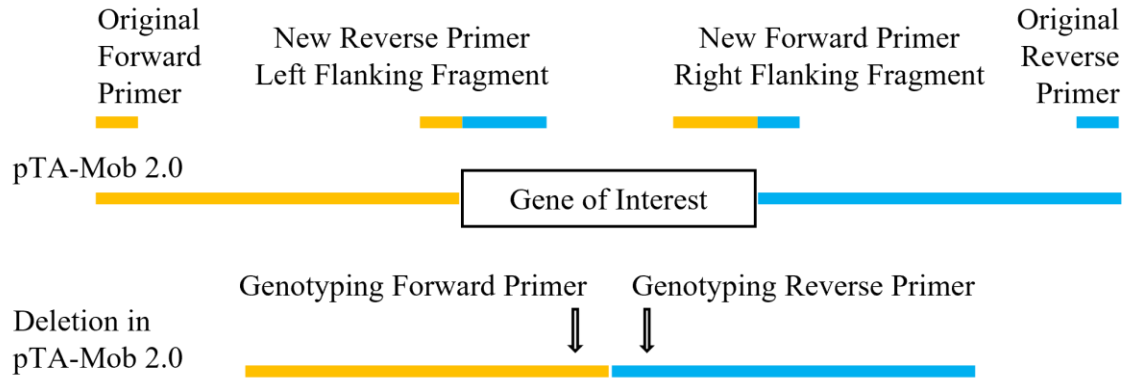


**Figure D-1. Deletion plasmid assembly strategy.** Each deletion plasmid was assembled from nine standard fragments as described in (Soltysiak et al. 2019) and two modified fragments amplified with original forward primer and new reverse primer, and new forward primer and original reverse primer. After assembly, each deletion was genotyped by MPX PCR.

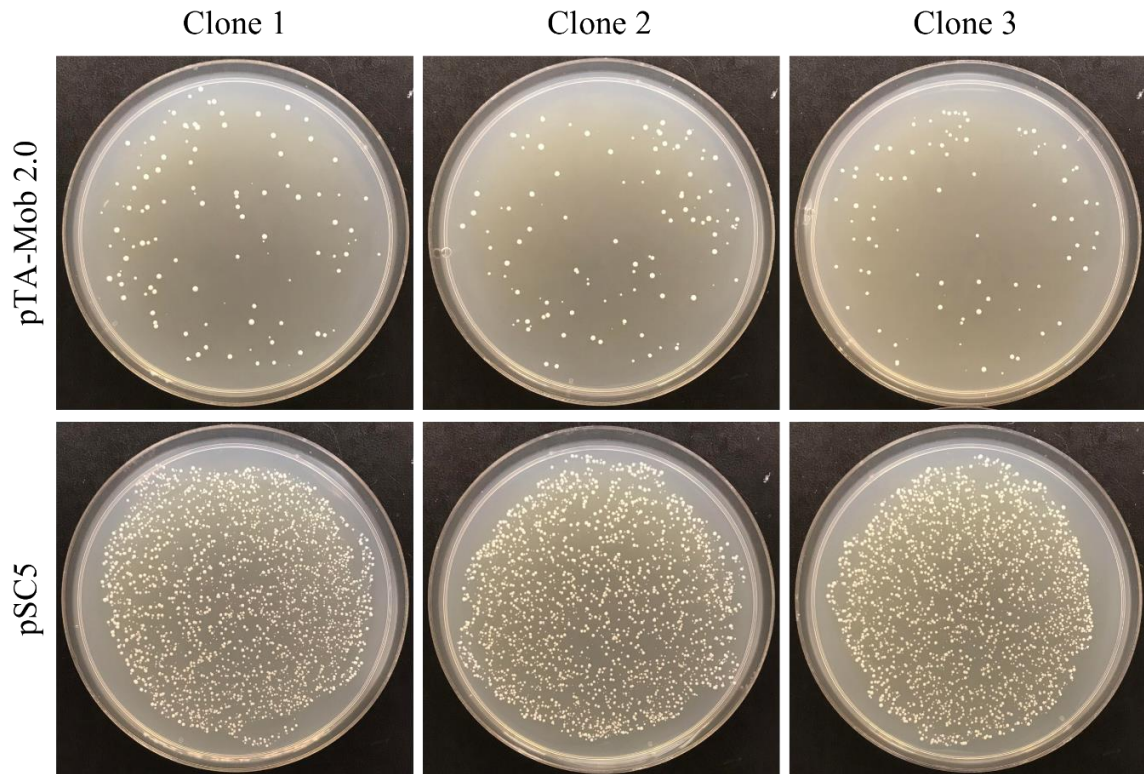


**Figure D-2. Bacterial conjugation from *S. meliloti* to *S. cerevisiae*.** Representative plates of yeast transconjugants following bacterial conjugation from three *S. meliloti* clones harboring either pTA-Mob 2.0 or pSC5, plated on synthetic complete media lacking histidine supplemented with ampicillin ( $100 \mu\text{g mL}^{-1}$ ).

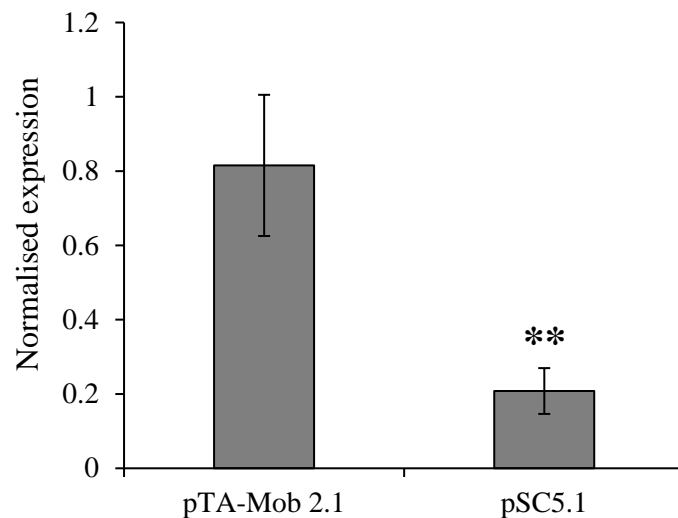


**Figure D-3. Quantitative real-time polymerase chain reaction (qRT-PCR) of *traJ* expression.** *traJ* mRNA expression in *E. coli* harboring the conjugative plasmids pTA-Mob 2.1 and pSC5.1 by qRT-PCR. The mean  $\pm$  SE is given for six biological replicates normalized to the reference genes *rrsA* and *cysG*. Student's *t*-test was used to compare pTA-Mob 2.1 and pSC5.1, and asterisks denote the significant difference between the pairwise comparison (\*,  $p < 0.05$ ; \*\*,  $p < 0.01$ ).

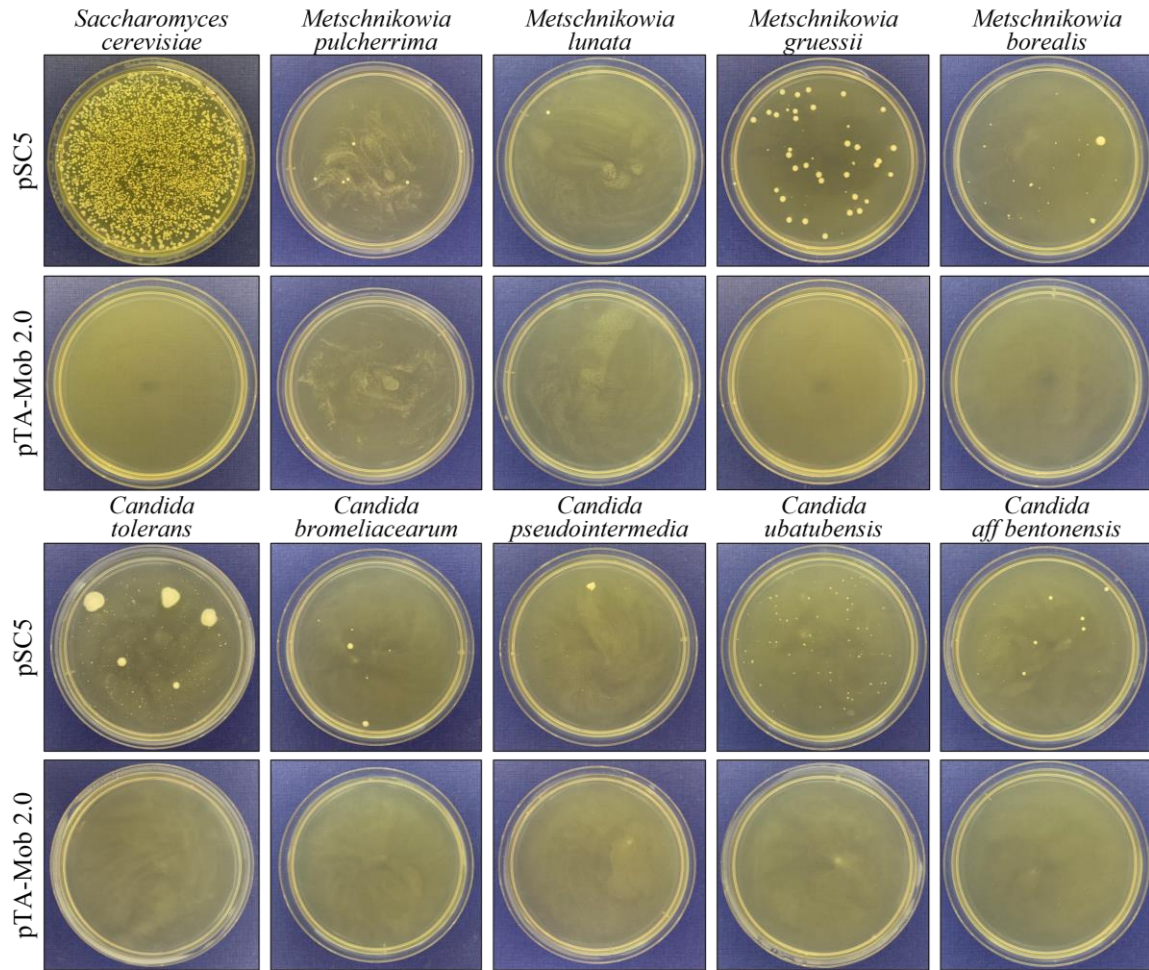


**Figure D-4. Bacterial conjugation from *E. coli* to diverse yeast species.**

Representative plates of yeast transconjugants following bacterial conjugation from *E. coli* harboring either pSC5 or pTA-Mob 2.0, plated on YPAD media supplemented with nourseothricin ( $100 \mu\text{g mL}^{-1}$ ) and ampicillin ( $100 \mu\text{g mL}^{-1}$ ).

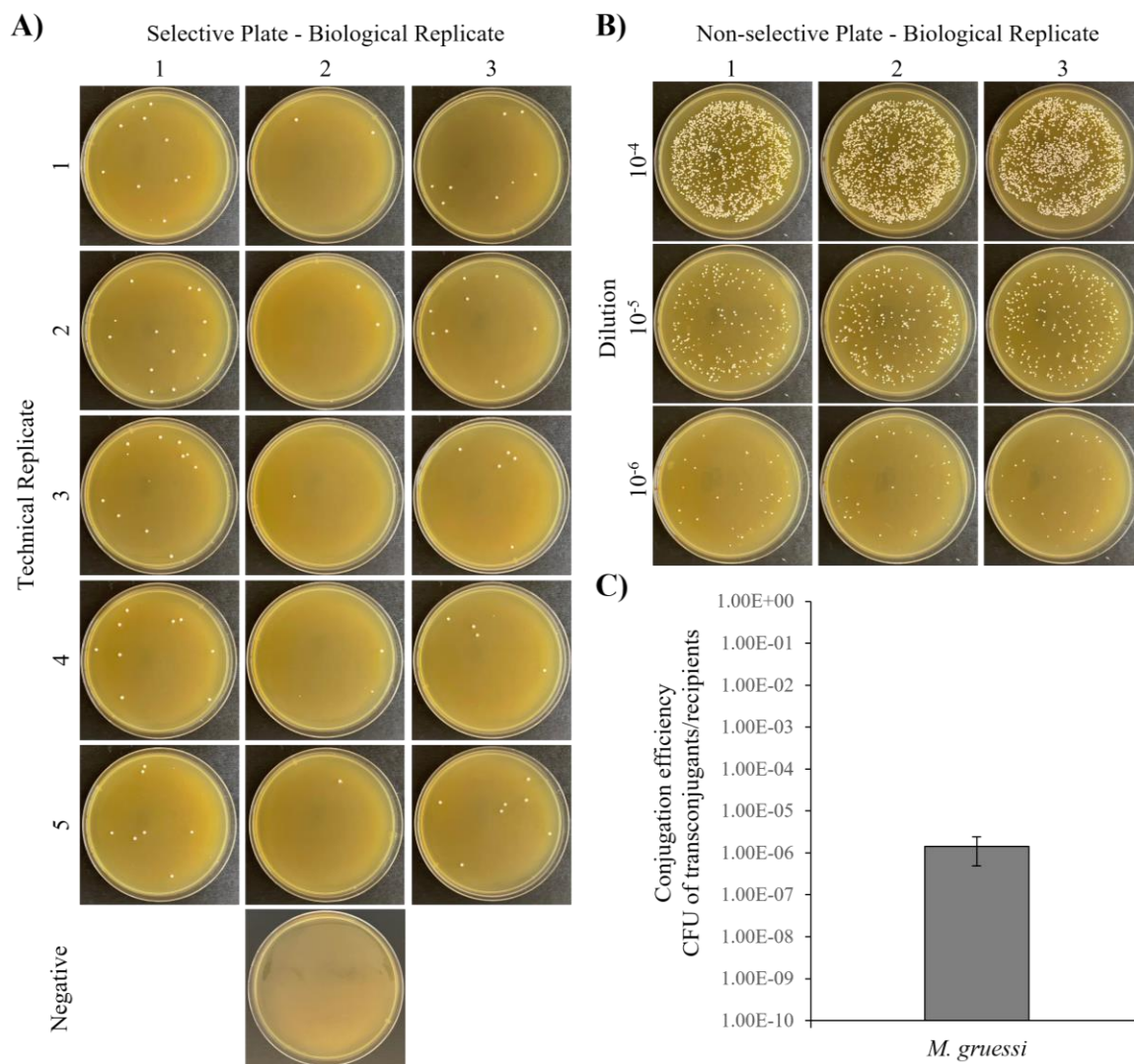


**Figure D-5. Bacterial conjugation efficiency of pSC5 to *Metschnikowia gruessi*.** **A)** Three replicates of *M. gruessi* transconjugants plated on five YPDA plates supplemented with nourseothricin ( $100 \mu\text{g mL}^{-1}$ ) and ampicillin ( $100 \mu\text{g mL}^{-1}$ ). **B)** Dilution series ( $10^{-3}$ – $10^{-5}$ ) of *M. gruessi* plated on YPDA plates supplemented with ampicillin ( $100 \mu\text{g mL}^{-1}$ ). **C)** Average bacterial conjugation efficiency of *M. gruessi* represents the mean  $\pm$  standard deviation for three biological replicates.



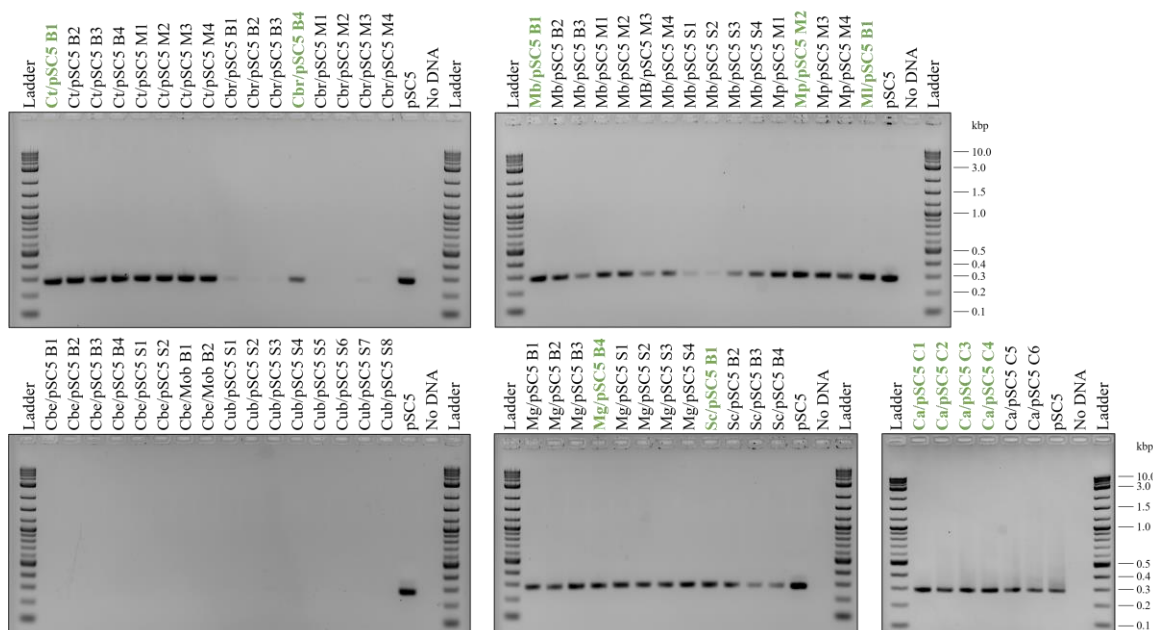


**Figure D-6. Genotyping transconjugants of diverse yeast species.** Genotyping of diverse yeast strains following bacterial conjugation with *E. coli* harboring pSC5. MPX PCR was performed to amplify the nourseothricin resistance gene of amplicon size 283-bp. Ct – *Candida tolerans*, Cbr – *Candida bromeliacearum*, Mb – *Metschnikowia borealis*, Mp – *Metschnikowia pulcherrima*, Ml – *Metschnikowia lunata*, Cbe – *Candida* aff. *bentonensis*, Cub – *Candida ubatubensis*, Mg – *Metschnikowia gruessi*, Sc – *Saccharomyces cerevisiae*, Ca – *Candida auris*, B – big colony, M – medium colony, and S – small colony. Clones highlighted in green were further analyzed with restriction enzyme digest and a phenotypic bacterial conjugation screen (Figure 4-5, Supplemental Figure D-7). Ladder – NEB 2-log ladder.

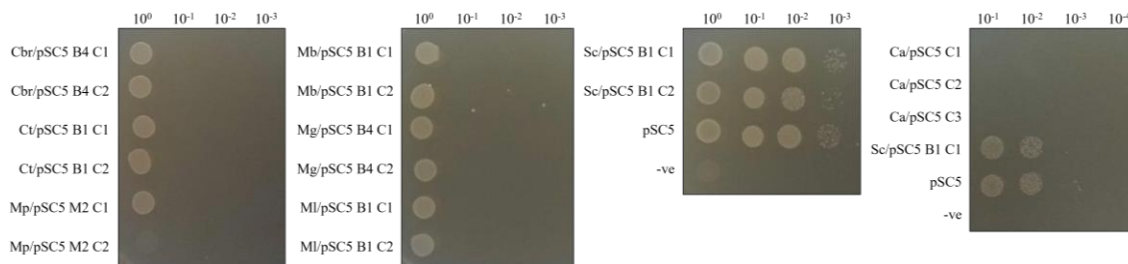


**Figure D-7. Phenotypic bacterial conjugation screen (*E. coli* to *E. coli*) of recovered transconjugant plasmids from diverse yeast species.** Selected recovered pSC5 plasmids from diverse yeast and *S. cerevisiae* were transformed into *E. coli* and tested for bacterial conjugation to *E. coli* harboring pAGE1.0. Transconjugant *E. coli* were spot plated on LB plates supplemented with chloramphenicol ( $30 \mu\text{g mL}^{-1}$ ) and gentamicin ( $60 \mu\text{g mL}^{-1}$ ). Ct – *Candida tolerans*, Cbr – *Candida bromeliacearum*, Cbe – *Candida bentonensis*, Cub – *Candida ubatubensis*, Mb – *Metschnikowia borealis*, Mp – *Metschnikowia pulcherrima*, Ml – *Metschnikowia lunata*, Mg – *Metschnikowia gruessi*, Sc – *S. cerevisiae*, Ca – *Candida auris*, B – Big colony, M – Medium colony, -ve – Negative (*S. cerevisiae* only).





40	8	36,149-36,190	F - cteggcttgcctgcte R - gtaaccaaggctcagaat	488	<i>traX</i> (36,149-36,190) <i>traI</i> (33,954-36,152) & <i>traJ</i> (36,187-36,558)	tcgctctctgatggagcgcataggggagctgtggcaagctctccctcggcggagcgaagctcatgagggcgtgtcccgccggggcagagccttgcgaagcaegtcccatg
41	8	36,187-36,558	F - gegaagtcctctctgat R - gctcttggcagtcctctc	333	<i>traI</i> (36,187-36,558) & <i>traX</i> (36,149-36,190)	aatcaegcgcacccccggccgttttagcgctcaaaaagccgttgcgaantctgagcttctgtgtatcaacggcgtcgaantcgcgaegcgttttttagcgtctaaag
42	8	36,796-37,199	F - tcgctataatgacccgaag R - gttgcgcgagtttaattgct	338	<i>traK</i> (36,796-37,200)	atgcagaaataactgaactgagggagcagcggagacgatggcgaatactacatggtccccgcttccctcaaacatgtaatttgcctatgctctcgtctccctc
43	8	37,201-37,921	F - aacggggaggtcaagtct R - tgaatgctcaggtcagc	335	<i>traL</i> (37,200-37,925)	caectcaaccaacagcgaacaaaaggatcactgtaaatgagcagcagattgaaga
44	8	37,926-38,359	F - ggcgaagctttagcagat R - tgcacaagaagccagctaa	312	<i>traM</i> (37,922-38,359)	cgccctgttgaacagctcagcggcggcgtctatgaatcgcagagcgcagatgaa
45	8	38,411-39,758	F - ggcgaagtaataagagaca R - tgcgaaaagcaccctatg	348	<i>upf5.4</i> (38,412-39,758)	gcagatgaaaagcccgcttgcggcgttttttgcggagcgcctcccttttagccg
46	8/9	40,292-41,218	F - ttgtctcgtctgacaaat R - acctgcccgttaagtcgaaa	305	<i>kfrA</i> (40,292-41,218)	ttgtctcattatttagtaactgcgttctctctcctcctacagactcctgttgg
47	9	41,932-42,444	F - ggatagcttgaacatcagga R - acccgacaagctgaaaag	295	<i>korF</i> (41,941-42,444)	ggtaagatattattctaccaatccggagcacaactgataaataaacgcagitt
48	9	44,843-45,793	F - ttggtgaacatagcggtag R - gttcagacagcctcatca	313	<i>klaC</i> (44,843-45,796)	cttgcacaacagagcggcttcttctcgcagtcattctcgtctcctttagag
49	9/10	45,793-46,875	F - ctgctcgtcgaatgctgat R - gctcatcacaaccagaaca	392	<i>klaB</i> (45,793-46,929) & <i>klaC</i> (44,843-45,796)	ccagccctacgtggcgaacaaactggtttgtgtgcatgtagcagacataggg
50	10	46,947-47,720	F - catgtgaaagcagcatag R - ttcgatggatgttgccttg	317	<i>klaA</i> (46,947-47,720)	aacagcagacagcccaagccctatcgtcctcgcagcacaacacacagctgtt
51	10	47,843-48,157	F - gacagctctgagggatc R - ggtactgaccgacacact	332	<i>klaF1</i> (47,843-48,157) & <i>klaF2</i> (47,843-48,013)	tgcgtcttttcaagcgttctcagcggcgttctccgctgctcagaccctcggctgg
52	10	47,839-48,013	F - caanaactcctcctcaatc R - ttgagcaatgccaagcag	318	<i>klaF1</i> (47,843-48,157)	ccctcgaanaagcaataaccaccgcgggggtatcagacggcgggagaacccatg
53	10	48,185-48,508	F - ctccgattgaccagtagc R - aagtaaccaagtggtcag	341	<i>klaE</i> (48,185-48,508)	ggaggctcaagaagcggccctcaaggagcttgccttcaagctctgaaagcctc
54	10	48,620-48,838	F - cncgctcgaactgataa R - aatgctattgcccagagc	319	<i>klaD</i> (48,620-48,838)	ctgtcttgcaattgacccaagcgtcggaggtcgaagcagggccctcaagagct
55	10	48,854-49,084	F - ctgacccactgttgcatt R - cagggaaaaggtgtttcaa	324	<i>klaC</i> (48,854-49,084)	atcgatcagcggcccggaanaactcggcgcctaccatccctcggctgaggt
56	10	49,237-49,452	F - gctctcggcaatgacatc R - actgtccaccagcagatc	338	<i>klaB</i> (49,237-49,452)	ggcgaattccggccgtcactgcagccagggatgatggatgacccccgattct
57	10	49,501-49,734	F - ggctaaggctgaaatgga R - actttacccaaggagagag	336	<i>klaA</i> (49,501-49,734)	agtcaccctctctactctactatcccccggcggattgctccctgtaatt
						gcccgtatagctcccaactcaaltaccggagcccaatcgcgccagggatgatgca
						gagcgtcactgcttgaanaacccctcctcgtcgcagcgcctatctcttgagaga
						ggcccgtacgtcggcctctcaagagatagggccttgcagccaggggaaggt
						ctcttgagagagccaccgtgagcggcctcgttccggggttgcctccgttgg
						ggcacttcgccagctcagcaaccggagatcaaccggcgaacggcccgctacg

**Table D-2. List of primers used to amplify the assembly fragments and genotype the plasmids created in Chapter 4.**

Fragment	Primer	Primer sequence (5' to 3')	Expected size (bp)	Template
<b>M1</b>				
F1	F	tgccgccgcgcatggtcgtaatgggaccgatagcccg	5782	pTA-Mob 2.0
	R	ttaacctactccttggttccggggatctcgcgactc		
F2	F	atcgaagagaagcaggacga	6373	pTA-Mob 2.0
	R	tgctggtccatgaagatgaa		
F3	F	tcgagctgatgttgacgac	6137	pTA-Mob 2.0
	R	ggacttgaggttctctgct		
F4	F	gtggacattggttcagcaa	3693	pTA-Mob 2.0
	R	gcgagaacctactaaggagaactagagcgtacgtgcttcgaaccactcggaggacgggt		
F5	F	aaccgtccctccagtggttcgaagcacgtacgtctagttctccttagtaggttctcgc	3476	pTA-Mob 2.0
	R	aagcgtgaatgatcccaag		
F6	F	gagcaatggatagccgatgt	6206	pTA-Mob 2.0
	R	aagcgtgaatgatcccaag		
F7	F	tgtaacgcttcccgttagtc	6295	pTA-Mob 2.0
	R	cattgcaaagcactgatgt		
F8	F	gatccgctcctgaactctg	6259	pTA-Mob 2.0
	R	aggcccttccaatgaat		
F9	F	ttcttgaatgcggggcgtcctggtgagcgtagtcaccg	6000	pTA-Mob 2.0
	R	cgttcccgcctgccctgattggcccgtgacgaccgct		
F10	F	aatgttgcaaagcgtacag	5745	pTA-Mob 2.0
	R	agccctcccgtatcgtagt		
<b>M2</b>				
F1	F	tgccgccgcgcatggtcgtaatgggaccgatagcccg	5782	pTA-Mob 2.0
	R	ttaacctactccttggttccggggatctcgcgactc		
F2	F	atcgaagagaagcaggacga	6373	pTA-Mob 2.0
	R	tgctggtccatgaagatgaa		
F3	F	tcgagctgatgttgacgac	6137	pTA-Mob 2.0
	R	ggacttgaggttctctgct		
F4	F	ggaccagcgcagtcaccatcaacggcctgatgagcgcc	6000	pTA-Mob 2.0
	R	atcggcgtgaagcccaacaggccca		
F5	F	gtggacattggttcagcaa	6273	pTA-Mob 2.0
	R	agctcatgcatcaacaagc		
F6	F	gagcaatggatagccgatgt	6206	pTA-Mob 2.0
	R	aagcgtgaatgatcccaag		
F7	F	tgtaacgcttcccgttagtc	6295	pTA-Mob 2.0
	R	cattgcaaagcactgatgt		
F8	F	gatccgctcctgaactctg	6259	pTA-Mob 2.0
	R	aggcccttccaatgaat		
F9	F	ttcttgaatgcggggcgtcctgg	4224	pTA-Mob 2.0
	R	tgaacacgcatcccggtgagggtcaagcagcggcaagagacgaaagccgggttccggg		
F10	F	ccggaaaccgggcttctctcttgcgctgcttgacctccacggcgatgcgtgtca	2664	pTA-Mob 2.0
	R	agccctcccgtatcgtagt		
<b>M3</b>				
F1	F	tgccgccgcgcatggtcgtaatgggaccgatagcccg	5782	pTA-Mob 2.0
	R	ttaacctactccttggttccggggatctcgcgactc		
F2	F	atcgaagagaagcaggacga	6373	pTA-Mob 2.0
	R	tgctggtccatgaagatgaa		
F3	F	tcgagctgatgttgacgac	6137	pTA-Mob 2.0
	R	ggacttgaggttctctgct		
F4	F	ggaccagcgcagtcaccatcaacggcctgatgagcgcc	6000	pTA-Mob 2.0
	R	atcggcgtgaagcccaacaggccca		
F5	F	gtggacattggttcagcaa	3693	pTA-Mob 2.0
	R	gcgagaacctactaaggagaactagagcgtacgtgcttcgaaccactcggaggacgggt		
F6	F	aaccgtccctccagtggttcgaagcacgtacgtctagttctccttagtaggttctcgc	3476	pTA-Mob 2.0
	R	aagcgtgaatgatcccaag		
F7	F	tgtaacgcttcccgttagtc	6295	pTA-Mob 2.0
	R	cattgcaaagcactgatgt		
F8	F	gatccgctcctgaactctg	6259	pTA-Mob 2.0
	R	aggcccttccaatgaat		
F9	F	ttcttgaatgcggggcgtcctggtgagcgtagtcaccg	6000	pTA-Mob 2.0
	R	cgttcccgcctgccctgattggcccgtgacgaccgct		
F10	F	aatgttgcaaagcgtacag	5745	pTA-Mob 2.0
	R	agccctcccgtatcgtagt		
<b>M4</b>				
F1	F	tgccgccgcgcatggtcgtaatgggaccgatagcccg	5782	pTA-Mob 2.0
	R	ttaacctactccttggttccggggatctcgcgactc		
F2	F	atcgaagagaagcaggacga	6373	pTA-Mob 2.0
	R	tgctggtccatgaagatgaa		
F3	F	tcgagctgatgttgacgac	6137	pTA-Mob 2.0
	R	ggacttgaggttctctgct		

F4	F	ggaccaggcgcagtcaccatcaacggcctgatgagcgc	6000	pTA-Mob 2.0
	R	atggcgtgaagccaacaggccca		
F5	F	gtggacattggttcagcaa	3476	pTA-Mob 2.0
	R	ggttctgacctgtgagggtaggggatatacgtgctcgaaccactcggaggacggtt		
F6	F	aaccgtccctccgagtggttcgaagcacgtatataccctaccctaccaggctcagaacc	3655	pTA-Mob 2.0
	R	tgtaacgcttccggtagtc		
F7	F	gatccgctcctgaactctg	6259	pTA-Mob 2.0
	R	aggcccttccaatgaat		
F8	F	ttcttgaatgcgcggcgtcctggtgagcgtagtcaccg	6000	pTA-Mob 2.0
	R	cgttcccctgcccctgattggcccctgacgaccgct		
F9	F	aatgttccaaggcgtacg	5745	pTA-Mob 2.0
	R	agccctcccgtatcgtatt		
<b>M5</b>				
F1	F	tgccgcgcgcgatggtcgtaatgggaccgatagcccgt	11,593	M3C1
	R	tgctggtccatgaagatgaa		
F2	F	tcgagctgatggttgcagac	8884	M3C1
	R	tcacagcccgttctgacctggtgagggtaggggatatacgtatcccctcccctacc		
F3	F	ggtaaaggaggggatagcgatataccctaccctaccaggctcagaaccggcctgatga	3675	M3C1
	R	cattgcaaaagcactgatgt		
F4	F	gatccgctcctgaactctg	6253	M3C1
	R	aggcccttccaatgaat		
F5	F	ttcttgaatgcgcggcgtcctggtgagcgtagtcaccg	10,447	M3C1
	R	agccctcccgtatcgtatt		
<b>M6</b>				
F1	F	aaaacaaaagcccgaaccggccttctctcttgcgcgggggtgatcctccggtt	12,900	M3C1
	R	tgctggtccatgaagatgaa		
F2	F	tcgagctgatggttgcagac	11,800	M3C1
	R	tcacagcccgttctgacctggtgagggtaggggatatacgtatcccctcccctacc		
F3	F	ggtaaaggaggggatagcgatataccctaccctaccaggctcagaaccggcctgatga	3675	M3C1
	R	cattgcaaaagcactgatgt		
F4	F	gatccgctcctgaactctg	6253	M3C1
	R	aggcccttccaatgaat		
F5	F	ttcttgaatgcgcggcgtcctggtgagcgtagtcaccg	4262	M3C1
	R	gggcacttcccaggtcagcaaccggagatcaaccggcggcaagagacgaaagccc		
<b>M7</b>				
F1	F	tgccgcgcgcgatggtcgtaatgggaccgatagcccgt	5132	M3C1
	R	tgccccgcgtgagtcggggcaatcccgaaggagggtgaccgcttcccctcatctgta		
F2	F	ctggccgctaccggcgtaacagatgaggcaagcgtcaccctccttgcgggattg	3819	M3C1
	R	tgctggtccatgaagatgaa		
F3	F	tcgagctgatggttgcagac	8884	M3C1
	R	tcacagcccgttctgacctggtgagggtaggggatatacgtatcccctcccctacc		
F4	F	ggtaaaggaggggatagcgatataccctaccctaccaggctcagaaccggcctgatga	3675	M3C1
	R	cattgcaaaagcactgatgt		
F5	F	gatccgctcctgaactctg	6253	M3C1
	R	aggcccttccaatgaat		
F6	F	ttcttgaatgcgcggcgtcctggtgagcgtagtcaccg	10,447	M3C1
	R	agccctcccgtatcgtatt		
<b>M8</b>				
F1	F	aaaacaaaagcccgaaccggccttctctcttgcgcgggggtgatcctccggtt	6610	M3C1
	R	tgccccgcgtgagtcggggcaatcccgaaggagggtgaccgcttcccctcatctgta		
F2	F	ctggccgctaccggcgtaacagatgaggcaagcgtcaccctccttgcgggattg	11,686	M3C1
	R	tgacctggtgagggtaggggatatacgtatcccctcccggctgtagctcctaagagtc		
F3	F	agcccgcccaatcctgaacgactcttagagctacgaccggggaggggatagcgatatac	3710	M3C1
	R	cattgcaaaagcactgatgt		
F4	F	gatccgctcctgaactctg	6253	M3C1
	R	aggcccttccaatgaat		
F5	F	ttcttgaatgcgcggcgtcctggtgagcgtagtcaccg	4262	M3C1
	R	gggcacttcccaggtcagcaaccggagatcaaccggcggcaagagacgaaagccc		
<b>M3C1_F1</b>				
F1	F	tgccgcgcgcgatggtcgtaatgggaccgatagcccgt	11,593	M3C1
	R	tgctggtccatgaagatgaa		
F2	F	tcgagctgatggttgcagac	11,800	M3C2
	R	atggcgtgaagccaacaggccca		
F3	F	gtggacattggttcagcaa	6500	M3C2
	R	aagcgtgaatgatcccaag		
F4	F	tgtaacgcttccggtagtc	11,797	M3C2
	R	aggcccttccaatgaat		
F5	F	ttcttgaatgcgcggcgtcctggtgagcgtagtcaccg	10,447	M3C2
	R	agccctcccgtatcgtatt		
<b>M3C1_F2</b>				
F1	F	tgccgcgcgcgatggtcgtaatgggaccgatagcccgt	11,593	M3C2
	R	tgctggtccatgaagatgaa		
F2	F	tcgagctgatggttgcagac	11,800	M3C1
	R	atggcgtgaagccaacaggccca		
F3	F	gtggacattggttcagcaa	6500	M3C2
	R	aagcgtgaatgatcccaag		
F4	F	tgtaacgcttccggtagtc	11,797	M3C2
	R	aggcccttccaatgaat		

F5	R	aggcccttgccaatgaat	10,447	M3C2
	F	ttctttgaatgcgcgggcgtcctggtgagcgtagtcagc		
	R	agccctcccgtatcgtagtt		
<b>M3C1_F3</b>				
F1	F	tgccgccgcgcgcatggtcgtaatgggaccgatagcccgt	11,593	M3C2
F2	R	tgctgtccatgaagatgaa	11,800	M3C2
	F	tcgagctgatgttgacgac		
F3	R	atggcgtgaagcccaacagggccca	6500	M3C1
	F	gtggacattggttcagcaa		
F4	R	aagcgtgaatgatcccaag	11,797	M3C2
	F	tgtaacgcttcccgtagtc		
F5	R	aggcccttgccaatgaat	10,447	M3C2
	F	ttctttgaatgcgcgggcgtcctggtgagcgtagtcagc		
	R	agccctcccgtatcgtagtt		
<b>M3C1_F4</b>				
F1	F	tgccgccgcgcgcatggtcgtaatgggaccgatagcccgt	11,593	M3C2
F2	R	tgctgtccatgaagatgaa	11,800	M3C2
	F	tcgagctgatgttgacgac		
F3	R	atggcgtgaagcccaacagggccca	6500	M3C2
	F	gtggacattggttcagcaa		
F4	R	aagcgtgaatgatcccaag	11,797	M3C1
	F	tgtaacgcttcccgtagtc		
F5	R	aggcccttgccaatgaat	10,447	M3C2
	F	ttctttgaatgcgcgggcgtcctggtgagcgtagtcagc		
	R	agccctcccgtatcgtagtt		
<b>M3C1_F5</b>				
F1	F	tgccgccgcgcgcatggtcgtaatgggaccgatagcccgt	11,593	M3C2
F2	R	tgctgtccatgaagatgaa	11,800	M3C2
	F	tcgagctgatgttgacgac		
F3	R	atggcgtgaagcccaacagggccca	6500	M3C2
	F	gtggacattggttcagcaa		
F4	R	aagcgtgaatgatcccaag	11,797	M3C2
	F	tgtaacgcttcccgtagtc		
F5	R	aggcccttgccaatgaat	10,447	M3C1
	F	ttctttgaatgcgcgggcgtcctggtgagcgtagtcagc		
	R	agccctcccgtatcgtagtt		
<b>pTA-Mob 2.0 Tp</b>				
F1	F	tgccgccgcgcgcatggtcgtaatgggaccgatagcccgt	5752	pTA-Mob 2.0
F2	R	tttaacctacttcttggttccggggatctcgcgactc	6374	pTA-Mob 2.0
	F	atcgaagagaagcaggacga		
F3	R	tgctgtccatgaagatgaa	6137	pTA-Mob2.0
	F	tcgagctgatgttgacgac		
F4	R	ggacttgaggttgcctgct	6000	pTA-Mob 2.0
	F	ggaccagcgcgagtcaccatcaacggcctgatgagcgcc		
F5	R	atggcgtgaagcccaacagggccca	6273	pTA-Mob 2.0
	F	gtggacattggttcagcaa		
F6	R	agctcatgcatcacaacagc	6206	pTA-Mob 2.0
	F	gagcaatggatagccgatgt		
F7	R	aagcgtgaatgatcccaag	6295	pTA-Mob 2.0
	F	tgtaacgcttcccgtagtc		
F8a	R	cattgcaaaagcactgatgt	1881	pTA-Mob 2.0
	F	gatccgctccttgaactctg		
F8b	R	atccaagcgctcagccgagggcaagcgatggctgatgaaaccaagccaaccaggaagg	4435	pTA-Mob 2.0
	F	ccttctggttgcttggtttcacagccatccgcttgcctcggctgacgcccgttgat		
F9	R	aggcccttgccaatgaat	6000	pTA-Mob 2.0
	F	ttctttgaatgcgcgggcgtcctggtgagcgtagtcagc		
F10	R	cgttcccgcctcccctgattggcccgtgatgaccgct	5745	pTA-Mob 2.0
	F	aatgttgcaaggcgtatcag		
R		agccctcccgtatcgtagtt		
<b>pTA-Mob 2.0 To</b>				
F1	F	tgccgccgcgcgcatggtcgtaatgggaccgatagcccgt	5752	pTA-Mob 2.0
F2	R	tttaacctacttcttggttccggggatctcgcgactc	6374	pTA-Mob 2.0
	F	atcgaagagaagcaggacga		
F3	R	tgctgtccatgaagatgaa	6137	pTA-Mob2.0
	F	tcgagctgatgttgacgac		
F4	R	ggacttgaggttgcctgct	6000	pTA-Mob 2.0
	F	ggaccagcgcgagtcaccatcaacggcctgatgagcgcc		
F5	R	atggcgtgaagcccaacagggccca	6273	pTA-Mob 2.0
	F	gtggacattggttcagcaa		
F6	R	agctcatgcatcacaacagc	6206	pTA-Mob 2.0
	F	gagcaatggatagccgatgt		
F7	R	aagcgtgaatgatcccaag	6295	pTA-Mob 2.0
	F	tgtaacgcttcccgtagtc		
F8a	R	cattgcaaaagcactgatgt	1821	pTA-Mob 2.0
	F	gatccgctccttgaactctg		
F8b	R	gcagcccacctcaaggttactgccttcagacgaacgaagagcgattgaggaanaagg	4526	pTA-Mob 2.0
	F	tagccgacagctcatgccggccgccgcccctttctcaatcgtctcttctgctct		
R		aggcccttgccaatgaat		

F9	F	ttcttgaatgcgcccgtcctggtgagcgtatgccagc	6000	pTA-Mob 2.0
	R	cgttcccgcctgcccctgattggcccgtgatcgaccgct		
F10	F	aatgttgcaagcgcacag	5745	pTA-Mob 2.0
	R	agccctcccgtatcgtagt		
<b>Sequencing primers to check mutations in <i>traJ</i> region</b>				
F1	F	gtttcagcagcccagc		
	R	cgctgcataaccctgcttcg		
<b>pSC5</b>				
F1	F	tgcccccgcgcgatggtcgtaatggaccgatagccct	7280	pTA-Mob 2.0-NAT
	R	tttaacctactccttgggtccggggatctcgcgactc		
F2	F	atcgaagagaagcaggacga	6373	M3C1
	R	tgctgtccatgaagatgaa		
F3	F	tcgagctgatgttgacgac	11,800	M3C1
	R	atcggcgtgaagcccaacaggccca		
F4	F	gtggacattggtttcagcaa	3692	M3C1
	R	caagcattgggtccgtatcaacctgaccgtctcgaaccactcggaggacggtt		
F5	F	aaaccgtccctccagtggtcgaagcagcgtcatggtatagacggaaccaatgctt	2573	pGMO1
	R	aggagaactagagcgtaatccctgtatccctcaaacacccttcaatgggttcga		
F6	F	cattgaaagggtttgttagggataacagggttaattacgctctagtctccttagtagt	3477	M3C1
	R	aagcgtgaatgatcccaag		
F7	F	tgtaacgtctcccgtatgc	11,797	M3C1
	R	aggcccttcccaatgaa		
F8	F	ttcttgaatgcgcccgtcctggtgagcgtatgccagc	10,447	M3C1
	R	cgttcccgcctgcccctgattggcccgtgatcgaccgct		
F9	F	aatgttgcaagcgcacag	5745	MV3C1
	R	agccctcccgtatcgtagt		
<b>pSC5GGv1</b>				
F1	F	tgcccccgcgcgatggtcgtaatggaccgatagccct	6112	pSC5
	R	taattagcattttccttattctgttgcagatctctccttgcaggttcaacaact		
F2	F	aagatctcgacaacagaataaagcgaaaaatgctaataatgcactaacctcaggccct	7196	pSC5
		(To domesticate BsaI site)		
	R	tgctgtccatgaagatgaa		
F3	F	tcgagctgatgttgacgac	6137	pSC5
	R	ggacttgaggttgcctgct		
F4	F	ggaccagcgcagtcaccatcaacgcctgatgagcgc	6000	pSC5
	R	atcggcgtgaagcccaacaggccca		
F5	F	gtggacattggtttcagcaa	11,926	pSC5
	R	caatgtctgatcaaatggacaattggtttctgctcattaccctgttaccctaca		
F6	F	acctcgggtggccttctcgtttataggtctcatgcttacgctctagtctccttag	1187	pSC5
	R	cgaattgaaacggaggcgcacaagaaggcgcagaagtcgggtctctacgtcggccacctc		
F7	F	cgactctcgccttctgtcgcctccttcaattcgggtctcttgcctccatga	8239	pSC5
		(To domesticate BsaI site)		
	R	cattgcaaaagcactgatgt		
F8	F	gatccctcctgaactctg	6256	pSC5
	R	aggcccttcccaatgaa		
F9	F	aatgttgcaagcgcacag	4928	pSC5
	R	agccctcccgtatcgtagt		
F10	F	attgaaagggtttgtaggataacagggttaagtagaccaagaaccaattgtccatat	1276	pAGE2.0-i
		(To amplify <i>mrfp</i> Gene)		
	R	gagaacctactaaggagaactagagcgtaaagcgtgagacctataaacgcagaaggccca		
		(To amplify <i>mrfp</i> Gene)		
<b><i>Sh ble</i> fragment for GG assembly</b>				
<i>Sh ble</i> gene	F	ggtctcagtaataatcaagcttg	1063	pRS32 (From Shapiro lab)
	R	taggtctcaagcaactggatggcg		
<b>HindIII fragment for GG assembly</b>				
HindIII toxic gene	F	ggtctcagtaagcgcgccttggcagacaatccatcgcgtccgccatctccagcagc	1618	pUC57 HindIII plasmid (Synthesized vector)
	R	ggtctcagattatcttcttctcctgcaagtttttctctgcaagttgggtaagaata		
<b><i>A. laidlawii</i> (Al) toxic gene fragments for GG assembly</b>				
1 <sup>st</sup> half of Al toxic gene	F	ggtctcagtaagtaagcttggcatgttcataatagatggttaacagatcattataaag	2072	<i>A. laidlawii</i> strain PG-8A DNA
	R	ggtctcatagtcattaatacctggagcgttaatttactctatgtctcctcaaggctt		
<i>ACT1</i> intron	F	ggtctcaactgatgttctagccttgcaccatcccatttaactgtaagaagaattgca	327	<i>S. cerevisiae</i> total DNA
	R	ggtctcactaaacataatataatagcaacaaaaagaatgaagcaatcgtatttagacatg		
2 <sup>nd</sup> half of Al toxic gene	F	ggtctcattagtctaatgaagtttacttaataattacgcttcaataatggttactg	1061	<i>A. laidlawii</i> strain PG-8A DNA
	R	ggtctcaagcaggaccataagaatccgaaaaacttaatactgtcccaaatgttaata		
<b>Genotyping <i>nat</i> marker</b>				
<i>nat</i> gene	F	tccagttgatccaccattga	283	
	R	caaccacaatgaccagcac		
<b>pSC5GGv2</b>				
F1	F	tgcccccgcgcgatggtcgtaatggaccgatagccct	4235	pSC5GGv1
	R	atatggacaattgttcttctgctcattacatatataacacatgatataatcgtatgc		
F2	F	tggccttctcgtttataggtctcatgctatacctaatgagtcagtaagtatgta	3149	pSC5GGv1
	R	tttaacctactccttgggtccggggatctcgcgactc		
F3	F	taggagtcgggttgaacgt	6177	pSC5GGv1
	R	tgctgtccatgaagatgaa		
F4	F	tcgagctgatgttgacgac	6137	pSC5GGv1
	R	ggacttgaggttgcctgct		
F5	F	ggaccagcgcagtcaccatcaacgcctgatgagcgc	6000	pSC5GGv1

F6	R	atcggcgtgaagcccaacaggcca	6300	pSC5GGv1
	F	gtggacattggtttcagcaa		
F7	R	aggagaactagagcgttaattaccctgttatccctacaaacaccttcaatgggcttcca	3512	pSC5GGv1
	F	cattgaaagggtgttttagggataaacagggttaattacgctctagtctcttagtaggt		
F8	R	aagcgtaatgatcccaag	6295	pSC5GGv1
	F	tgtaacgctcccggtagtc		
F9	R	cattgcaaaagcactgatgt	6253	pSC5GGv1
	F	gatccgctcctgaactctg		
F10	R	aggcccttccaatgaat	6000	pSC5GGv1
	F	ttctttgaatgcggcgctcctggtgagcgtatccagc		
F11	R	cgttcccgcctgcccctgattggcccgtgatcgaccgt	4928	pSC5GGv1
	F	aatgttgcaagcgcgatcag		
F12	R	agccctcccgtatcgtatt	1276	pAGE2.0-i
	F	gcatacgtatatacatgtgtatataatgtaagagaccaagaaccaattgtccatat (To amplify <i>mrfp</i> gene)		
	R	tacatactactgacatcataggtatacagcatgagacataaacgcagaaggcca (To amplify <i>mrfp</i> gene)		
<b>pTA-Mob 2.1</b>				
F1	F	tgccccgcgcgatggtcgttaatgggaccgatagcccgt	5259	pTA-Mob 2.0
	R	gggagatctgctggccaacgttccaaccgactcctaccggccagcctcgcagagca		
F2	F	gcggtgctcaacgggaatcctgctctgcgaggctgcccggtaggagtgcggttgaacgt	6177	pTA-Mob 2.0
	R	tgctggtccatgaagatgaa		
F3	F	tcgagctgatgttgacgac	6137	pTA-Mob 2.0
	R	ggacttgaggttgcctctgct		
F4	F	ggaccagcgcagtcaccatcaacggcctgatgagcgcc	6000	pTA-Mob 2.0
	R	atcggcgtgaagcccaacaggcca		
F5	F	gtggacattggtttcagcaa	6289	pTA-Mob 2.0
	R	agctcatgcatcaaacagc		
F6	F	gagcaatggatagccgatgt	6204	pTA-Mob 2.0
	R	aagcgtaatgatcccaag		
F7	F	tgtaacgctcccggtagtc	6295	pTA-Mob 2.0
	R	cattgcaaaagcactgatgt		
F8	F	gatccgctcctgaactctg	6256	pTA-Mob 2.0
	R	aggcccttccaatgaat		
F9	F	ttctttgaatgcggcgctcctggtgagcgtatccagc	6000	pTA-Mob 2.0
	R	cgttcccgcctgcccctgattggcccgtgatcgaccgt		
F10	F	aatgttgcaagcgcgatcag	4928	pTA-Mob 2.0
	R	agccctcccgtatcgtatt		
<b>pSC5.1</b>				
F1	F	tgccccgcgcgatggtcgttaatgggaccgatagcccgt	6757	pSC5
	R	cacgcgacaagcagcagcagatataccaatcaagctagtcggccagcctcgcagagca		
F2	F	gcggtgctcaacgggaatcctgctctgcgaggctgcccggtaggagtgcggttgaacgt	6177	pSC5
	R	tgctggtccatgaagatgaa		
F3	F	tcgagctgatgttgacgac	6137	pSC5
	R	ggacttgaggttgcctctgct		
F4	F	ggaccagcgcagtcaccatcaacggcctgatgagcgcc	6000	pSC5
	R	atcggcgtgaagcccaacaggcca		
F5	F	gtggacattggtttcagcaa	9812	pSC5
	R	aagcgtaatgatcccaag		
F6	F	tgtaacgctcccggtagtc	6295	pSC5
	R	cattgcaaaagcactgatgt		
F7	F	gatccgctcctgaactctg	6256	pSC5
	R	aggcccttccaatgaat		
F8	F	ttctttgaatgcggcgctcctggtgagcgtatccagc	10,549	pSC5
	R	agccctcccgtatcgtatt		
<b>qRT-PCR primers</b>				
<i>rrsA</i> gene	F	ctcttgccatcgatgtgccca	106	pTA-Mob 2.1 and pSC5.1 cDNA
	R	ccagtggtgctgcatcctctca		
<i>cysG</i> gene	F	ttgtcggcggtggtgatgtc	136	pTA-Mob 2.1 and pSC5.1 cDNA
	R	atcgggtgaacttggaataaacg		
<i>traJ</i> gene	F	acgaccccgtgatttttag	109	pTA-Mob 2.1 and pSC5.1 cDNA
	R	gccttcagacgaacgaaga		

**Table D-3. Bacterial conjugation phenotype of each plasmid in the pTA-Mob 2.0 deletion plasmid library.** Bacterial conjugation phenotypes of pTA-Mob 2.0 deletion strains are displayed as the ratio of deletion plasmid transconjugants relative to pTA-Mob 2.0 transconjugants. All clones were tested using 1 biological and 3 technical replicates, except for deletion plasmid 32 C2\*, where 6 biological and 1–3 technical replicates were used. Additional replicas were performed for plasmid 32 C2\* due to the high variations in the initial experiments. Deletions were categorized as either non-essential (green; 0.51–5.98), semi-essential (light-green; 0.06–0.50), or essential (red & orange; 0–0.05) based on their bacterial conjugation ratio. Contradictory results for clones for the same genes could be due to mutations introduced during the PCR fragment amplification or yeast assembly. N/D: Not done.

Deletion plasmid	Clone name	Ratio for clone 1	Ratio for clone 2
1	C1, C2	0.36	1.04
2	C1, C5	1.25	0.00
3	C2, C3	1.90	0.00
4	C2, C3	0.00	0.00
5	C1, C2	0.00	0.00
6	C2, C3	0.00	0.00
7	C2, C3	0.00	0.00
8	C4, C5	0.00	0.00
9	C2, C8	0.00	0.00
10	C2, C2.1	0.00	0.00
11	C2, C3	0.00	0.00
12	C2, C5	0.00	0.00
13	C4, C5	0.00	0.00
14	C1, C2	2.37	3.60
15	C1, C5	0.00	0.00
16	C1, C5	3.09	0.01
17	C2, C3	N/D	0.12
18	C2, C3	1.31	1.11
19	C4, C5	N/D	0.15
20	C2, C3	0.54	0.39
21	C4, C5	0.31	0.98
22	C2, C3	0.53	0.64
23	C1, C2	0.51	0.46
24	C3, C16	0.63	1.03
25	C1, C2.1	N/D	N/D
26	C2.2, C3	0.52	1.39
27	C1, C2	2.06	0.11
28	C2	N/D	0.34
29	C2, C5	0.98	0.00
30	C6, C7	4.36	1.22
31	C1, C2	0.57	1.47
32	C1, C2*	0.75	5.98*
33	C3, C6	0.20	0.24
34	C1, C3	0.00	0.51
35	C1.1, C6	0.33	1.09
36	C1, C2	0.00	0.00
37	C2	0.00	N/D
38	C2, C3	0.00	0.00
39	C2, C8	0.00	0.24
40	C1, C5	0.00	0.00
41	C5, C7	0.00	0.00
42	C2, C4	N/D	0.00
43	C2, C4	0.00	0.00
44	C3, C5	0.00	0.00
45	C9, C10	0.00	0.04
46	C1.1, C10	0.00	0.22
47	C1, C5	0.65	1.49
48	C1	0.05	N/D
49	C1, C5	0.32	0.41
50	C4, C5	0.39	0.67
51	C3, C5	N/D	N/D
52	C1, C2	1.81	0.61
53	C2	N/D	0.69
54	C1, C2	0.00	0.00
55	C1, C5	0.43	0.41
56	C2, C3	0.46	0.60
57	C1, C5	0.65	1.03

**Table D-4. Whole plasmid sequencing of minimal conjugative plasmid 3 (M3C1 and M3C2).** Mutations in M3C1 and M3C2 were identified by next-generation sequencing and aligned to the reference sequence: pTA-Mob 2.0. Nucleotide numbering begins at the forward primer of Fragment 1. Note: The 4912 bp deletion in M3C1 and M3C2 was removed intentionally.

Plasmid	Fragment	Plasmid position	Nucleotide mutation	Amino acid mutation	Gene
M3C1	1	3342	1 bp insertion (T)		
M3C1	2	14,111	G <sub>731</sub> > T	Arg <sub>244</sub> > Leu	<i>trbF</i>
M3C1	2	20,676	G <sub>505</sub> > T	Asp <sub>169</sub> > Tyr	<i>trbN</i>
M3C1	3	25,788	C <sub>138</sub> > A		
M3C1	3	26,489	4,912 bp Deletion		<i>URA3</i>
M3C1	4	37,156	T <sub>77</sub> > G	Glu <sub>26</sub> > Ala	<i>traJ</i>
M3C1	4	37,242–37,246	GAATT > CTCGG		
M3C2	3	25,787	C <sub>138</sub> > A		<i>parE</i>
M3C2	3	26,488	4,912 bp Deletion		<i>URA3</i>
M3C2	4	37,458	G > T		
M3C2	5	48,347	A <sub>47</sub> > G	Leu <sub>16</sub> > Ser	<i>klaA</i>



**Table D-5. *Cis*- and *trans*-bacterial conjugations of pSC5. *S. cerevisiae* transconjugant concentrations following bacterial conjugation of pSC5 compared to pTA-Mob 2.0 in either *cis*- (self-transmissible) or *trans*- (mobilization of a secondary plasmid – pAGE2.0.T) and *E. coli* transconjugant concentrations following bacterial conjugation of pSC5 compared to pTA-Mob 2.0 in *cis*- from *E. coli* (Figure 4-4). Results are shown as colony-forming units per mL (CFU mL<sup>-1</sup>) for four biological replicates, each with two technical replicates.**

Configuration	Plasmid	Rep 1 (CFU mL <sup>-1</sup> )	Rep 2 (CFU mL <sup>-1</sup> )	Rep 3 (CFU mL <sup>-1</sup> )	Rep 4 (CFU mL <sup>-1</sup> )	Average (CFU mL <sup>-1</sup> )
<i>Cis</i> ( <i>S. cerevisiae</i> )	pTA-Mob 2.0	3.1 x 10 <sup>3</sup>	4.2 x 10 <sup>3</sup>	3.6 x 10 <sup>3</sup>	3.8 x 10 <sup>3</sup>	3.7 x 10 <sup>3</sup>
	pSC5	1.9 x 10 <sup>6</sup>	1.3 x 10 <sup>5</sup>	1.3 x 10 <sup>5</sup>	1.0 x 10 <sup>5</sup>	1.4 x 10 <sup>5</sup>
<i>Trans</i> ( <i>S. cerevisiae</i> )	pTA-Mob 2.0	6.6 x 10 <sup>2</sup>	5.7 x 10 <sup>2</sup>	1.3 x 10 <sup>3</sup>	2.8 x 10 <sup>3</sup>	1.3 x 10 <sup>3</sup>
	pSC5	5.3 x 10 <sup>4</sup>	8.3 x 10 <sup>4</sup>	8.5 x 10 <sup>4</sup>	6.2 x 10 <sup>4</sup>	7.1 x 10 <sup>4</sup>
<i>Cis</i> ( <i>E. coli</i> )	pTA-Mob 2.0	2.2 x 10 <sup>6</sup>	1.0 x 10 <sup>6</sup>	2.2 x 10 <sup>6</sup>	2.7 x 10 <sup>6</sup>	2.1 x 10 <sup>6</sup>
	pSC5	1.0 x 10 <sup>6</sup>	1.4 x 10 <sup>6</sup>	1.0 x 10 <sup>6</sup>	1.2 x 10 <sup>6</sup>	1.2 x 10 <sup>6</sup>

**Table D-6. Recipient yeast cell concentrations used in bacterial conjugation experiments of Figure 4-3.** The concentration of *S. cerevisiae* recipient cultures formed on the non-selective plate (1 x YPAD supplemented with ampicillin 100  $\mu\text{g mL}^{-1}$ ) following the bacterial conjugation of pSC5 and pTA-Mob 2.0 in *cis*- and *trans*-configuration. Concentrations are presented as colony-forming units per mL (CFU  $\text{mL}^{-1}$ ) for four biological replicates, each with two technical replicates.

Configuration	Plasmid	Rep 1 (CFU $\text{mL}^{-1}$ )	Rep 2 (CFU $\text{mL}^{-1}$ )	Rep 3 (CFU $\text{mL}^{-1}$ )	Rep 4 (CFU $\text{mL}^{-1}$ )	Average (CFU $\text{mL}^{-1}$ )
<i>Cis</i>	pTA-Mob 2.0	$1.3 \times 10^7$	$1.5 \times 10^7$	$3.9 \times 10^7$	$4.7 \times 10^7$	$2.9 \times 10^7$
	pSC5	$6.7 \times 10^7$	$6.9 \times 10^7$	$1.1 \times 10^8$	$1.1 \times 10^8$	$9.1 \times 10^7$
<i>Trans</i>	pTA-Mob 2.0	$8.0 \times 10^6$	$4.0 \times 10^6$	$4.3 \times 10^7$	$3.7 \times 10^7$	$2.3 \times 10^7$
	pSC5	$1.2 \times 10^7$	$1.5 \times 10^7$	$9.5 \times 10^7$	$9.3 \times 10^7$	$5.4 \times 10^7$

**Table D-7. *S. cerevisiae* cell viability following bacterial conjugation with different *E. coli* strains.** *S. cerevisiae* cell concentrations obtained by hemocytometer (all cells) or plating on non-selective plates (1 x YPAD supplemented with ampicillin 100  $\mu\text{g mL}^{-1}$ ; live cells) following a 3 h incubation at 30 °C alone or with *E. coli* either harboring no plasmid, pTA-Mob 2.0, or pSC5.

Donor Recipient	Hemocytometer cell count (cells $\text{mL}^{-1}$ )	Colony count (CFU $\text{mL}^{-1}$ )	
		Technical replicas	Average
Donor: no <i>E. coli</i> Recipient: <i>S. cerevisiae</i>	5.08 x 10 <sup>8</sup>	2.01 x 10 <sup>8</sup>	2.08 x 10 <sup>8</sup>
		2.27 x 10 <sup>8</sup>	
		1.97 x 10 <sup>8</sup>	
Donor: <i>E. coli</i> Epi300 Recipient: <i>S. cerevisiae</i>	6.14 x 10 <sup>8</sup>	2.05 x 10 <sup>8</sup>	2.19 x 10 <sup>8</sup>
		2.37 x 10 <sup>8</sup>	
		2.15 x 10 <sup>8</sup>	
Donor: <i>E. coli</i> Epi300 with pTA-Mob 2.0 Recipient: <i>S. cerevisiae</i>	2.56 x 10 <sup>8</sup>	1.4 x 10 <sup>7</sup>	1.63 x 10 <sup>7</sup>
		1.0 x 10 <sup>7</sup>	
		2.5 x 10 <sup>7</sup>	
Donor: <i>E. coli</i> Epi300 with pSC5 Recipient: <i>S. cerevisiae</i>	4.06 x 10 <sup>8</sup>	1.41 x 10 <sup>8</sup>	1.44 x 10 <sup>8</sup>
		1.45 x 10 <sup>8</sup>	
		1.47 x 10 <sup>8</sup>	

**Table D-8. *S. cerevisiae* cell viability following bacterial conjugation with different *S. meliloti* strains.** *S. cerevisiae* cell counts by hemocytometer (all cells) or plating on non-selective plates (1 x YPAD supplemented with ampicillin 100  $\mu\text{g mL}^{-1}$ ; live cells) following a 3 h incubation at 30 °C alone or with *S. meliloti* either harboring pTA-Mob 2.0 or pSC5.

Donor Recipient	Hemocytometer cell count (cells mL <sup>-1</sup> )		Colony count (CFU mL <sup>-1</sup> )	
	Biological replicas	Average	Biological replicas	Average
Donor: no <i>S. meliloti</i> Recipient: <i>S. cerevisiae</i>	3.04 x 10 <sup>8</sup>	3.04 x 10 <sup>8</sup>	1.27 x 10 <sup>8</sup>	1.27 x 10 <sup>8</sup>
Donor: <i>S. meliloti</i> Rm4126 R <sup>-</sup> with pTA-Mob 2.0 Recipient: <i>S. cerevisiae</i>	3.16 x 10 <sup>8</sup>	3.07 x 10 <sup>8</sup>	9.70 x 10 <sup>7</sup>	8.47 x 10 <sup>7</sup>
	3.48 x 10 <sup>8</sup>		1.10 x 10 <sup>8</sup>	
	2.58 x 10 <sup>8</sup>		4.70 x 10 <sup>7</sup>	
Donor: <i>S. meliloti</i> Rm4126 R <sup>-</sup> with pSC5 Recipient: <i>S. cerevisiae</i>	3.84 x 10 <sup>8</sup>	4.11 x 10 <sup>8</sup>	1.85 x 10 <sup>8</sup>	1.60 x 10 <sup>8</sup>
	4.52 x 10 <sup>8</sup>		1.67 x 10 <sup>8</sup>	
	3.98 x 10 <sup>8</sup>		1.27 x 10 <sup>8</sup>	

**Table D-9. *S. cerevisiae* transconjugant colony count following bacterial conjugation with *S. meliloti*.** Colony counts of *S. cerevisiae* transconjugant re-suspension (2 mL) following bacterial conjugation with three biological replicates of *S. meliloti* (Rm4126) harboring either pTA-Mob 2.0 or pSC5, plated on synthetic complete yeast media lacking histidine supplemented with ampicillin ( $100 \mu\text{g mL}^{-1}$ ) (Supplemental Figure D-2).

Plasmid	Colony count (CFU)			
	100 $\mu\text{L}$		50 $\mu\text{L}$	
	Replicate 1	Replicate 2	Replicate 1	Replicate 2
pTA-Mob 2.0 #1	114	147	53	68
pTA-Mob 2.0 #2	108	123	34	54
pTA-Mob 2.0 #3	92	87	46	39
pSC5 #1	2514	1044	1341	546
pSC5 #2	2399	2145	1254	1159
pSC5 #3	2504	572	1220	260

**Table D-10. Yeast transconjugant colony counts for the bacterial conjugation-based antifungal experiment (Figure 4-7).** *S. cerevisiae* transconjugant colony counts following bacterial conjugation with *E. coli* harboring pAGE2.0.T and either pSC5, pSC5-toxic1, pSC5-toxic2, or pSC5-toxic3. Note: Colonies were counted from plating 100  $\mu$ L of undiluted (1x) and diluted (10x) yeast transconjugant re-suspension (2 mL) on synthetic complete yeast media lacking either histidine (*HIS3*) or tryptophan (*TRP1*). Colonies were counted manually. tmtc – too many to count; Rep – replicate.

Plasmid	Yeast selection marker (CFU)								Ratio <i>HIS3/TRP1</i>	
	<i>HIS3</i>				<i>TRP1</i>					
	Rep 1	Rep 2	Rep 3	Average	Rep 1	Rep 2	Rep 3	Average		
1 x	pSC5	tmtc	tmtc	592	592.0	tmtc	tmtc	302	302.0	1.960
	pSC5-toxic1	tmtc	tmtc	230	230.0	tmtc	tmtc	264	264.0	0.871
	pSC5-toxic2	25	17	5	15.7	594	tmtc	169	381.5	0.041
	pSC5-toxic3	2	1	0	1.0	428	tmtc	188	308.0	0.003
10 x	pSC5	208	436	55	233	174	262	33	156.3	1.490
	pSC5-toxic1	62	105	27	64.7	107	149	23	93	0.695
	pSC5-toxic2	4	1	0	1.7	66	72	18	52	0.032
	pSC5-toxic3	0	0	0	0	50	107	17	58	0

### D.3 Supplemental Notes

**Note D-1. Bacterial conjugation from *E. coli* to *E. coli* – cis-configuration.** *E. coli*, donor and recipient strains, were prepared as in Section 4.4.5, except the donor strains were resuspended in 5 mL of ice-cold 10% glycerol, and 500  $\mu$ L aliquots were prepared in 1.5 mL Eppendorf tubes. To assess the bacterial conjugation of pSC5 between bacteria, two donor strains of *E. coli* harboring either pSC5 or pTA-Mob 2.0 and an *E. coli* recipient strain harboring pAGE1.0 (chloramphenicol 15  $\mu$ g mL<sup>-1</sup>; [Brumwell et al. 2019](#); Table 1) were prepared and stored in the -80 °C freezer. On the day of the bacterial conjugation, conjugation plates (20 mL, LB media with 1.5% agar) were prepared, and tubes containing the *E. coli* strains were removed from the freezer and thawed on ice. Once thawed, 10  $\mu$ L of the donor *E. coli* strain was added to 100  $\mu$ L of the recipient *E. coli* strain and mixed by pipetting prior to being transferred to the plate and spread evenly. Plates were incubated at 30 °C for 90 min and then were scraped with 1.5 mL of ddH<sub>2</sub>O and mixed thoroughly by vortexing for 5 s. A dilution series (10<sup>-1</sup>–10<sup>-8</sup>) was created in a 96-well plate, and 100  $\mu$ L of dilutions 10<sup>-1</sup>–10<sup>-4</sup> were plated on selection plates (25 mL, LB media with 1.5% agar supplemented with chloramphenicol 15  $\mu$ g mL<sup>-1</sup> and gentamicin 40  $\mu$ g mL<sup>-1</sup>). On non-selective plates (LB media with 1.5% agar supplemented with chloramphenicol 15  $\mu$ g mL<sup>-1</sup>), 100  $\mu$ L of dilutions 10<sup>-1</sup>–10<sup>-8</sup> were plated. Plates were incubated at 37°C overnight, and the following morning the colonies were counted, and bacterial conjugation efficiency was calculated (transconjugant CFU / recipient CFU).

**Note D-2. Bacterial conjugation from *S. meliloti* to *S. cerevisiae* – cis-configuration.** *S. meliloti* was prepared similarly to *E. coli*; overnight cultures of a single colony were diluted to OD<sub>600</sub> of 0.1 in 50 mL of LB media with appropriate antibiotics (streptomycin 100  $\mu$ g mL<sup>-1</sup> and gentamicin 40  $\mu$ g mL<sup>-1</sup>) and grown until an OD<sub>600</sub> of 1.0 was achieved. On the day of bacterial conjugation, the conjugation plates (20 mL, synthetic complete yeast media lacking histidine 1.8% agar and 10% LBmc media) were made, and the *S. meliloti* and *S. cerevisiae* cells were thawed on ice for ~20 min. Once thawed, 50  $\mu$ L of *S.*

*cerevisiae* was added to 100  $\mu\text{L}$  of *S. meliloti* and mixed by gentle pipetting before being transferred to the plate and spread evenly. The plates were incubated at 30°C for 3 h. Next, the plates were scraped with 2 mL of  $\text{sddH}_2\text{O}$  and mixed thoroughly by vortexing for 5 s. For each bacterial conjugation, 3 biological replicates and 1 technical replicate were used, and 100  $\mu\text{L}$  of each dilution ( $10^0$ – $10^{-1}$ ) for each sample was plated on selection plates (25 mL, synthetic complete yeast media lacking histidine, 2% agar, supplemented with ampicillin (100  $\mu\text{g mL}^{-1}$ )). The plates were incubated at 30 °C, scored after 4 days, and bacterial conjugation efficiency was calculated.

**Note D-3. Bacterial conjugation from *E. coli* to *S. cerevisiae* – *cis*- and *trans*-configuration.** To assess bacterial conjugation of pSC5 to *S. cerevisiae* in *cis*-orientation, two donor strains of *E. coli* harboring either pSC5 or pTA-Mob 2.0 (gentamycin 40  $\mu\text{g mL}^{-1}$ ) were prepared as in Section 4.4.5, and in *trans*-orientation two donor strains of *E. coli* harboring either pSC5 and pAGE2.0.T or pTA-Mob 2.0 and pAGE2.0.T (gentamycin 40  $\mu\text{g mL}^{-1}$  and chloramphenicol 15  $\mu\text{g mL}^{-1}$ ) were prepared as in Section 4.4.5 and all stored in the -80°C freezer. On the day of bacterial conjugation, the conjugation plates (*cis* – 20 mL, synthetic complete yeast media lacking histidine 1.8% agar and 10% LB media; *trans* – 20 mL, synthetic complete yeast media lacking tryptophan 1.8% agar and 10% LB media) were prepared, and the *E. coli* and *S. cerevisiae* cells were thawed on the ice for ~20 min. Once thawed, 50  $\mu\text{L}$  of *S. cerevisiae* was added into the *E. coli* tube containing 100  $\mu\text{L}$  of cells and mixed by pipetting before being transferred to the plate and spread evenly. The plates were incubated at 30 °C for 3 h. Next, the plates were scraped with 2 mL of  $\text{sddH}_2\text{O}$  and mixed thoroughly by vortexing for 5 s. A dilution series ( $10^0$ – $10^{-7}$ ) was generated, and two technical replicates of 100  $\mu\text{L}$  for dilutions  $10^0$  –  $10^{-4}$  were plated on selection plates (*cis* – 25 mL, synthetic complete yeast media lacking histidine 2% agar supplemented with ampicillin (100  $\mu\text{g mL}^{-1}$ ); *trans* – 25 mL, synthetic complete yeast media lacking tryptophan 2% agar supplemented with ampicillin (100  $\mu\text{g mL}^{-1}$ )); and two technical replicates of 100  $\mu\text{L}$  for dilutions for each sample ( $10^{-4}$ – $10^{-7}$ ) were plated on non-selective plates (25 mL, 1 x YPDA supplemented with ampicillin



(100  $\mu\text{g mL}^{-1}$ ). The plates were incubated at 30°C, scored after 4 days, and bacterial conjugation efficiency was calculated.

**Note D-4. Bacterial conjugation from *E. coli* to diverse yeast and transconjugant analysis.** Bacterial conjugation proceeded as described in Section 4.4.5, except once dried, the conjugation plates were incubated at 30°C for 12 h, and selection plates were incubated at 30°C for 3 days before the number of colonies was counted. The plasmid was isolated from selected diverse yeast transconjugants to test the recovery of the pSC5 plasmid. The recovered plasmids were transformed into *E. coli* by electroporation and re-conjugated back from *E. coli* to diverse yeast species following the protocol in Section 4.4.5, except on selective plates, cells were spot plated rather than spread on full plates. After bacterial conjugation, cells were scraped with 2 mL of sddH<sub>2</sub>O. These cells were serially diluted in 96-well plates, and 5  $\mu\text{L}$  of different dilutions ( $10^0$ – $10^{-4}$ ) were spot plated in 1 x YPDA media supplemented with nourseothricin (100  $\mu\text{g mL}^{-1}$ ).

**Note D-5. Bacterial conjugation-based kill assay in *S. cerevisiae*.** To assess yeast killing facilitated by bacterial conjugation, three donor *E. coli* strains harboring pAGE2.0.T and either pSC5-toxic1, pSC5-toxic2, or pSC5-toxic3 (gentamicin 40  $\mu\text{g mL}^{-1}$  and chloramphenicol 15  $\mu\text{g mL}^{-1}$ ) and the recipient *S. cerevisiae* were prepared as in Section 4.4.5 and stored in the -80°C freezer. On the day of bacterial conjugation, the conjugation plates (20 mL, synthetic complete yeast media lacking histidine 1.8% agar and 10% LB media) were made, and the *E. coli* and *S. cerevisiae* cells were thawed on ice for ~20 min. Once thawed, 10  $\mu\text{L}$  of *S. cerevisiae* was added into the *E. coli* tube containing 100  $\mu\text{L}$  of cells and mixed by pipetting before being transferred to the plate and spread evenly. The plates were incubated at 30°C for 3 h. Next, the plates were scraped with 2 mL of sddH<sub>2</sub>O and mixed thoroughly by vortexing for 5 s. For each bacterial conjugation, 4 biological replicates and 1 technical replicate were used, and 100  $\mu\text{L}$  of each dilution ( $10^0$  –  $10^{-1}$ ) for each sample was plated on both selective plates (25 mL, synthetic complete yeast media lacking histidine and synthetic complete yeast media lacking tryptophan, 2% agar, supplemented with ampicillin (100  $\mu\text{g mL}^{-1}$ ). The plates

were incubated at 30°C, colonies were scored after 4 days, and killing efficiency (CFU on synthetic complete yeast media lacking histidine / CFU on synthetic complete yeast media lacking tryptophan) was calculated.

## Curriculum Vitae

# RYAN COCHRANE

Department of Biochemistry  
University of Western Ontario

PhD Candidate  
London, Ontario N6A 5C1

### EDUCATION

<b>PhD Candidate</b> , Biochemistry University of Western Ontario, London, ON	2017 – Present
<b>Bachelor of Medical Sciences</b> , Honors Specialization in Interdisciplinary Medical Sciences University of Western Ontario, London, ON	2012 – 2017

### SCHOLARSHIPS AND AWARDS

NSF RCN Travel Award, Build-A-Cell Workshop #8	\$800	2022
The Canadian Graduate Scholarship – Doctoral (CGS-D)	\$105,000	2021
Ontario Graduate Scholarship	\$15,000	2020
NSF RCN Travel Award, SynCell2020	\$750	2020
NSF RCN Travel Award, Build-A-Cell Workshop #6	\$400	2020
Harold B. Stewart Memorial Lecture and Research Showcase, 2 <sup>nd</sup> Place Poster Presentation	\$20	2018
Symposium on Synthetic Biology 2.0, 2 <sup>nd</sup> Place Poster Presentation	\$150	2017
The Western Scholarship of Excellence	\$2000	2013

### PUBLICATIONS

**Cochrane, R.R.**, Shrestha, A., Severo de Almeida, MM, Agyare-Tabbi, M, Brumwell, SL, ... Karas, BJ (2022). Superior conjugative plasmids delivered by bacteria to diverse fungi. *BioDesign*, 9802168.

**Cochrane, R.R.**, Brumwell, S.L., Shrestha, A., Giguere, D.J., Hamadache, S., Gloor, G.B., Edgell, D.R. and Karas, B.J. (2020) Cloning of *Thalassiosira pseudonana*'s mitochondrial genome in *Saccharomyces cerevisiae* and *Escherichia coli*. *Biology*, 9(11), 358.

**Cochrane, R.R.**, Brumwell, S.L., Soltysiak, M.P., Hamadache, S., Davis, J.G., ... Karas, B.J. (2020) Rapid method for generating designer algal mitochondrial genomes. *Algal Research*, 50, 102014.

Brumwell, S.L., MacLeod M.R., Huang T., **Cochrane R.R.**, Meaney R.S., ... Karas, B.J. (2019) Designer *Sinorhizobium meliloti* strains and multi-functional vectors enable direct inter-kingdom DNA transfer. *PLoS ONE* 14(6): e0206781.

## PRESENTATIONS

The cloning and engineering of diatom mitochondrial genomes in yeast and bacteria. Molecular Life of Diatoms 6, Virtual Meeting. July, 2021 (Poster/Talk).

The cloning and engineering of diatom mitochondrial genomes in yeast and bacteria. Phycological Society of America (PSA), Virtual Meeting. July, 2021 (Poster/Talk).

Rapid method for generating designer algal mitochondrial genomes. International Conference on Engineering Synthetic Cells and Organelles, Virtual Meeting. May, 2021 (Poster).

Development of methods for the generation and delivery of designer algal mitochondrial genomes. Graduate Research Symposium, University of Western Ontario, London, ON, Canada. May, 2020 (Talk).

Rapid for generating designer algal mitochondrial genomes. Build-A-Cell Workshop #6, Mountain View, CA, USA. January, 2020 (Poster).

Development of whole mitochondrial genome transformation for the introduction of multiple simultaneous genetic modifications in *Phaeodactylum tricorutum*. Synthetic Biology Symposium 4.0, Waterloo, ON, Canada. May, 2019 (Poster/Talk).

Development of methods for the generation and delivery of designer algal mitochondrial genomes. London Health Research Day, London, ON, Canada. April, 2019 (Poster).

Development of synthetic organelle genomes for commercial and scientific use. Canadian Algal Workshop, Toronto, ON, Canada. February, 2019 (Poster).

Development of synthetic organelle genomes for commercial and scientific use. Western Synthetic Biology Symposium 3.0, London, ON, Canada. July, 2018 (Poster).

Development of synthetic organelle genomes for commercial and scientific use. London Health Research Day, London, ON, Canada. May, 2018 (Poster).

Development of synthetic organelle genomes for commercial and scientific use. Harold B. Stewart Memorial Lecture and Research Showcase, London, ON, Canada. January, 2018 (Poster).

Development of synthetic organelle genomes for commercial and scientific use.  
Symposium on Synthetic Biology 2.0, London, ON, Canada. July, 2017 (Poster).

## TEACHING AND MENTORING EXPERIENCE

### Teaching Assistantship, University of Western Ontario

Biochemistry 3386B: Clinical Biochemistry	2020
Biochemistry 3381A: Biological Macromolecules	2019
Biochemistry 2280A: Biochemistry and Molecular Biology	2019
Biochemistry 3381A: Biological Macromolecules	2018
Biology 1002B: Biology for Science II	2018

### Undergraduate Mentorship, University of Western Ontario

Anya Zomer	Volunteer	2021 – 2022
Emily Carvalhais	4 <sup>th</sup> year Biochemistry thesis student	2021 – 2022
Samir Hamadache	4 <sup>th</sup> year Biochemistry thesis student	2018 – 2019
Jennifer Davis	3 <sup>rd</sup> year Biochemistry thesis student	2018 – 2019
Daniel Tsyplenkov	4 <sup>th</sup> year Biochemistry thesis student	2017 – 2018
Samuel Tholl	Volunteer	2018 – 2020
Kaitlyn Dan	Volunteer	2018 – 2019
Jiayi Wang	Volunteer	2018 – 2019
SynBio Hacks Case Competition		2018
Air Forman, Angelo Empleo, and Ayushi Bhatt		
Western Synthetic Biology Research Program (WSBR)		2017 – 2019

## LEADERSHIP AND EXTRACURRICULAR ACTIVITIES

Canadian Medical Hall of Fame, Brand Ambassador (London, ON),	2022 – Present
National Scholarship Application Committee, Reviewer (UWO),	2022
InterACT, Mentor (London, ON),	2020 – Present
RotarACT, VP of Community Events (London, ON)	2020 – 2021
Forest City SynBio Steering Committee, Member (London, ON),	2019 – 2021
Biochemistry Graduate Student Association, Chair (UWO),	2019 – 2021
Biochemistry Graduate Student Association, Member (UWO),	2018 – 2019
Be-Al-U-Can-B, Volunteer (UWO),	2017 – 2020
Raising Hope, Volunteer (UWO),	2017 – 2020
Retiring with Strong Minds, Volunteer (UWO),	2017 – 2018

## RELEVANT WORK EXPERIENCE

Volunteer January – September 2017  
Dr. David Edgell's Lab, University of Western Ontario, London, ON, Canada.

Research Lab Assistant May – September 2015  
Dr. Jeremy McNeil's Lab, University of Western Ontario, London, ON, Canada.